Technology Collaboration Programme by IEA

IEAGHG

Geological Storage of CO_2: Seal Integrity Review

Technical Report 2024-06
September 2024

IEA Greenhouse Gas R&D Programme

About the IEA Greenhouse Gas R&D Programme

Leading the way to net zero with advanced CCS research. IEAGHG are at the forefront of cutting-edge carbon, capture and storage (CCS) research. We advance technology that reduces carbon emissions and accelerates the deployment of CCS projects by improving processes, reducing costs, and overcoming barriers. Our authoritative research is peer-reviewed and widely used by governments and industry worldwide. As CCS technology specialists, we regularly input to organisations such as the IPCC and UNFCCC, contributing to the global net-zero transition.

About the International Energy Agency

The International Energy Agency (IEA), an autonomous agency, was established in November 1974. Its primary mandate is twofold: to promote energy security amongst its member countries through collective response to physical disruptions in oil supply, and provide authoritative research and analysis on ways to ensure reliable, affordable and clean energy. The IEA created Technology Collaboration Programmes (TCPs) to further facilitate international collaboration on energy related topics.

CONTACT DETAILS

Tel: +44 (0)1242 802911
E-mail: mail@ieaghg.org
Internet: www.ieaghg.org

Address: IEAGHG, Pure Offices,
Cheltenham Office Park, Hatherley Lane,
Cheltenham, GL51 6SH, UK

Citation

The report should be cited in the literature as follows: IEAGHG, "Geological Storage of CO_2: Seal Integrity Review", 2024-06, September 2024, doi.org/10.62849/2024-06.

Acknowledgements

This report describes work undertaken by CO2CRC on behalf of IEAGHG. The principal researchers were:

- David Bason
- Hadi Nourollah
- Simone de Morton
- Max Watson
- Genna Petho
- Ivan Maffeis
- Micheal Rieger
- Geoff O'Brien

To ensure the quality and technical integrity of the research undertaken by IEAGHG each study is managed by an appointed IEAGHG manager. The report is also reviewed by a panel of independent technical experts before its release.

The IEAGHG manager for this report was: Nicola Clarke

The expert reviewers for this report were:

- Elin Skurtveit, *NGI*
- Jamie Andrews, *Equinor*
- Alex Bump, *BEG*
- Colm Pierce, *CASP*
- Owain Tucker, *Shell*
- Simon Shoulders, *BP*
- Jonathan Hodgkinson, *BP*
- Reza Majidi, *BP*
- Callum Leighton, *BP*

GEOLOGICAL STORAGE OF CO_2: SEAL INTEGRITY REVIEW

(IEA/CON/23/294)

CCS is a well proven technology and can demonstrably safely store carbon dioxide CO_2. The success of geological sequestration of CO_2 depends on the permanent containment of the injected CO_2 in the storage formation at depth. Prior to CO_2 injection commencing, the storage formation and the sealing capacity of the caprock overlying the formation are exhaustively studied to confirm suitability. This includes establishing the boundaries of the reservoir, which provide an effective seal to prevent leaking to either the surface or to adjacent geological formations

This comprehensive seal integrity review, undertaken by CO2CRC on behalf of IEAGHG, provides a detailed, updated exploration of the critical aspects of seal potential in the context of the geological storage of CO_2. The review focuses on developments in this field since 2011. It highlights the importance of seals in ensuring the containment of CO_2 and the considerations involved in predicting the long-term impact of CO_2 interactions with seal formations.

In a well-characterised storage site the chance of leakage to the atmosphere is negligible. The primary reason for this low risk is that it is very difficult to extract CO_2 once it is in the subsurface. For example, in a saline aquifer the CO_2 becomes trapped in tiny pore spaces in the rock and dissolves in saline water making it almost immobile. Accordingly, reversal of the CO_2 to the atmosphere will be rare and unusual given the purpose of a well-managed site is to prevent such emissions. To ensure this, throughout the period of injection and for many years after injection ceases, the CO_2 is carefully monitored to ensure any undesired events are detected early so that effective remedial action is promptly taken.

Key Messages

- The study reviewed the regulatory frameworks in four of the most mature jurisdictions. As demonstrated in these examples, jurisdictions should include a robust legislative framework to govern reservoir seals and permanent CO_2 storage. These should be regularly updated as technological advances occur. This will also help project developers/operators, who must comply with the requirements, to stay up-to-date with best practice
- CO_2 may be contained in a variety of geological settings ‘plays’, including a conventional reservoir/seal pair, composite seals or utilising residual or mineral trapping.
- In the rare instance of leakage, shear failure at the caprock/storage unit interface or fault reactivation poses the primary risk for leakage (not accounting for leakage risk along legacy wells).
- Many methods to characterise and evaluate seal integrity rely on access to core samples and well testing, which can be site-specific and localised. Best practice assessments will consider a wide range of sources and use other datasets for a regional approach.
- The long-term impacts of CO_2 on seal formations are evaluated and show largely positive results indicating that re-precipitation of minerals may enhance seal potential. In some cases alteration of cements may impact geomechanical properties.
- The impact of pressure on seals at a local scale needs to be paired with basin scale understanding of the regional stress field, the extent of the seal and potential interaction

with adjacent geological CO_2 storage projects. This is an area that and requires further research and understanding.

- CO_2 controlled release experiments require representative test data and are thus much slower to undertake than running numerical models on faults, however they offer valuable learnings. There are still scale-up challenges in transferring such learnings to commercial projects at greater depths.

Background to the Study

As Carbon Capture and Storage (CCS) is implemented to meet climate goals CO_2 storage sites will need to extend beyond well-characterised hydrocarbon plays and into extensive saline aquifers where there is potentially less data to evaluate not only reservoir quality but also seal integrity. In the absence of a hydrocarbon column, verifying seals (both caprock formations and faults) in a saline formation is more challenging. Even in depleted oil and gas reservoirs, there are seal integrity considerations that require rigorous assessment.

One of the key objectives of this work is to provide an up-to-date, definitive, 'go-to' report that summarises seal qualities and how to characterise them where there is a lack of data, especially for deep saline formations. Stakeholders must be convinced that designated primary seals, and the overburden, are effective barriers to CO_2 migration over periods that equate to timescales that give effective climate mitigation, i.e. 1000s of years. The significance of site-specific conditions needs to be explained in terms that all stakeholders can understand including regulators and local communities.

Scope of Work

This study is a focused, integrated review of the advances made in seal integrity over the last decade, building on an IEAGHG report (by Kaldi et al) published in 2011 on Caprocks Systems for the Geological Storage of CO_2[1].

The approach of the report layout is as follows: Sections 2 and 3 provide the context to set the scene for the report with an introduction to the concept of containment and the various risk mechanisms that may contribute to the loss of containment. The concept of a storage complex is introduced, with a discussion on recent advances in thinking around composite seals in addition to the conventional understanding of sequestering CO_2 within a structural trap under an impermeable seal. The report then comprises the following sections:

Section 4: Seal Potential is explored, comprising three elements of seal capacity, integrity, and character, discussed in detail with up-to-date research that pertains to these concepts.

Section 5: Long-Term Impact of CO_2 on Seal Formations, which includes a literature review including the rate of migration and reactivity of CO_2 with seal units.

Section 6: Risk Assessment for CO_2 Containment, current qualitative and semi-quantitative risk assessment techniques are discussed with application to commercial-scale CO_2 storage projects.

Section 7: Methods to Characterise and Evaluate Seal Integrity, including data gathering and new laboratory or well/borehole-log-based analysis techniques.

Section 8: Modelling of Faults and Fractures for CO_2 Flow, recent advances in simulations.

Section 9: Large-scale Geomechanical Modelling.

[1] IEAGHG, "Caprock Systems for CO2 Geological Storage", 2011-01

Section 10: Monitoring Technologies, the available methods for monitoring or inferring seal integrity in large-scale or pilot CO_2 storage systems are reviewed as monitoring, measurement and verification planning is a key component in assessing containment and conformance of a CO_2 storage project.

Section 11: International Regulatory Framework – CO_2 Seals, the relevant regulatory and policy measures for CO_2 storage development and approvals and how these measures pertain to reservoir seals and the permanency of CO_2 storage are discussed in the final section of the report.

The report concludes with a set of Conclusions and Recommendations. The appendices contain a primer on the commonly used method of mercury injection capillary pressure (MICP) with an MICP Database, and a table of monitoring technologies.

The study is intended to be a point of reference for technical professionals, as well as regulators and community stakeholders, to assess whether a prospective storage site demonstrates the required characteristics to contain CO_2 within the required timescales to be an effective solution for mitigating climate change.

Findings of the Study

The report first introduces the common elements of the geological CO_2 storage (GCS) system in a sedimentary basin. With CO_2 storage planned within a storage unit, i.e. the interval the CO_2 is intended to remain underlying a barrier, such as a top seal, sealing fault or less conventionally a composite seal. Secondary seals may also be utilised. Potential pathways or events that could lead to CO_2 migrating out of the Storage Complex are referred to as risk mechanisms, with the majority related to seal integrity. Note that leakage along legacy wells is outside of the scope of this review (Figure 1).

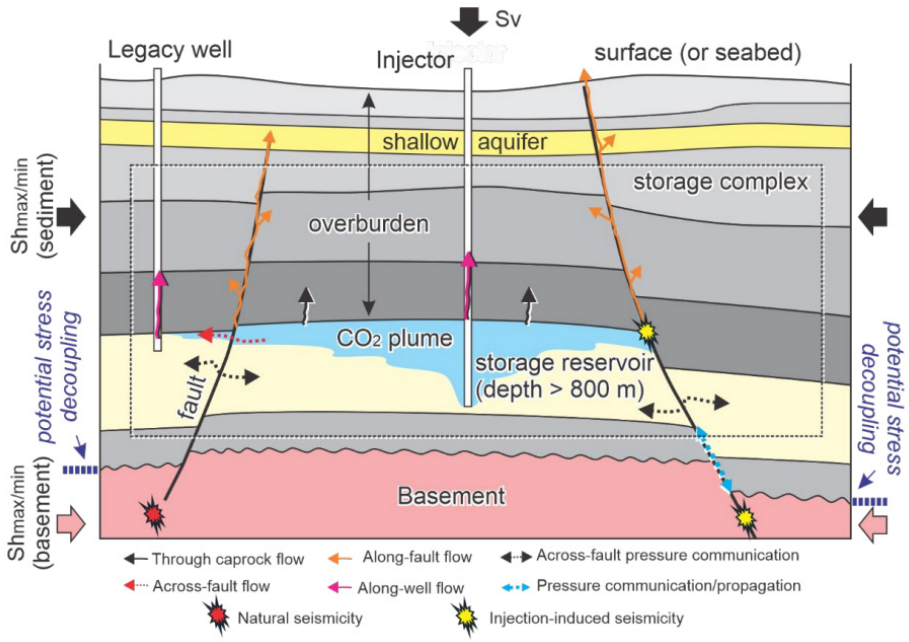

Figure 1: GCS Storage System and Risk Mechanisms[2]

[2] Wu, L., Skurtveit, E., Thompson, N., Michie, E. A. H., Fossen, H., Braathen, A., Fisher, Q., Lidstone, A., & Bostrøm, B. (2022). Containment Risk Assessment and Management of CO_2 Storage on the Horda Platform. *SSRN Electronic Journal*. https://doi.org/10.2139/ssrn.4272132

The following storage plays can be considered for the geological containment of CO_2: closure storage or membrane seals, whereby low permeable rocks act as a barrier to the upward buoyant migration of CO_2 resulting in the retention of CO_2 within a storage formation; composite seals, which broaden the scope of evaluating different storage sites e.g. as planned at the South West Hub Project in Western Australia; and mineral trapping, e.g. such as in basalts like in the Carbfix projects, whereby the complete dissolution of CO_2 removes the need for a caprock as the gas is no longer buoyant. The study focuses on the effectiveness of effective geological barriers, i.e. a seal.

Seal Potential

In a traditional GCS storage play, a geological structure is overlain by a competent seal that enables a buoyant column of CO_2 to be retained. Properties of an effective seal include low permeability, high capillary entry pressure, sufficient thickness and lateral extent, and chemical stability. Capillary (membrane) seals are a 'nice-to-have' for GCS but not necessarily critical when considering the timescales relevant for CO_2 storage.

The seal potential is a collective descriptor that encompasses:

- Seal Capacity: CO_2 leakage through the seal.
- Seal Geometry or Character: the areal extent of the seal, thickness and internal heterogeneity
- Seal Integrity: the propensity of the caprock to fail in a brittle sense or its ductile behaviour.

Many lithologies can serve as effective seals in CO_2 storage, with shale being the most abundant (50% of all sedimentary rocks) and common lithology as a seal, and although porous, are very impermeable. Evaporites are less common but are the principal seal for more than half the world's largest oil reservoirs and their plasticity helps maintain their integrity as a seal over time. Carbonate lithologies vary depending on how they were deposited, the diagenetic processes and hydrodynamic conditions, which, in turn, affect their ability to act as a seal primarily by impacting porosity and permeability. They can show higher entry capillary pressure making them excellent membrane seals but are more likely to develop fractures and faults resulting in a loss of seal integrity. Chalk can act as an effective seal if porosity is reduced through diagenesis and fractures are sealed by mineral precipitation. Coals have also been shown to have good sealing properties with low porosity and with CO_2 adsorption onto the coal surface.

Table 1: Examples of Primary Seals for GCS Projects and Developments

Project/Region	Operational	Onshore/Offshore	Primary Seal Formation	Primary Seal Description	Reference
Sleipner	Yes	Offshore	Nordland	Shale	(Springer & Lindgren, 2006)
Snøhvit	Yes	Offshore	Nordmela	Shale	(Gao, 2013)
Quest	Yes	Onshore	Deadwood Formation	Shale	(Rock et al., 2017)
Gorgon CCS	Yes	Onshore	Barrow Group	Shale	(Trupp et al., 2021)
South West Hub	Yes (Pilot)	Onshore	Lesueur	Interbedded sand and shale	(Langhi et al., 2021)
Aurora	No	Offshore	Drake and Burton	Shale	(Rahman, Fawad,

					Jahren, et al., 2022)
Endurance	No	Offshore	Rot	Layered evaporites and mudstones	(BP, 2022)
Acorn CCS	No	Offshore	Rodby & Lista	Shale	(Worden et al., 2020)
Hamilton CCS	No	Offshore	Mercia	Mudstone	(Gamboa et al., 2019)
CarbonNet	No	Offshore	Latrobe Group ("T2")	Intraformational coals and shales	(Hoffman, 2018)
Regional seal for largest oil/gas fields (Ghawar)	No	Onshore	Hith and Arab	Layered evaporites	(Boehm et al., 2023)

Seal capacity estimates should never be made in isolation, and should include the broader regional picture of how basin-scale processes might impact seal integrity. For example, evaluate future interaction of multiple large GCS projects within the same sedimentary basin. Thematic examples of basin-scale processes are presented from the Gippsland and Bonaparte basins, Australia.

In terms of seal assessment broadly two containment issues may arise, tensile fractures which may result in rapid migration from the storage unit and slow breakthrough where CO_2 enters the overlying, low permeable unit and is controlled by multi-phase (Darcy) flow in porous media.

Containment of CO_2 is not limited to the traditional definition of seal capacity, which is grounded in the capillary threshold pressure concept and column height calculations from petroleum prospecting and a broader discussion is necessary and reflected in this report.

Recent laboratory measurements for CO_2 breakthrough pressures were discussed e.g. Espinoza and Santamarina (2017)[3] using a variety of sediments and Skurtveit et al (2012)[4] using shale samples from the Draupne Formation in the North Sea.

Capillary pressure is introduced with a review of recent research into wettability and interfacial tension (IFT), two of the key inputs for calculating capillary pressure. The literature review resulted in a large variation in wettability (7- 92°) for CO_2/quartz/water (or brine) systems. Other important conclusions were that $scCO_2$ (supercritical CO_2) behaves significantly differently than gaseous CO_2 in terms of wettability. Since the preparation of this report three new studies, conducted independently, show that $scCO_2$/brine against a variety of subsurface mineralogies is water-wet and remains water-wet in all typical storage conditions[5][6][7].

[3] Espinoza, D. N., & Santamarina, J. C. (2017). CO2 breakthrough—Caprock sealing efficiency and integrity for carbon geological storage. *International Journal of Greenhouse Gas Control*, *66*, 218-229.
[4] Skurtveit, E., Aker, E., Soldal, M., Angeli, M., & Wang, Z. (2012). Experimental investigation of CO2 breakthrough and flow mechanisms in shale. *Petroleum Geoscience* 2012;; 18 (1): 3–15.
5 Awad MM, Espinoza DN. (2024) Mudrock wettability at pressure and temperature conditions for CO2 geological storage. International Journal of Greenhouse Gas Control. 135:104160. https://doi.org/10.1016/j.ijggc.2024.104160
6 Carmago AP, Jusufi A, Lee AGK, Kopli J, Morris JF, Giovambattista N. (2024) Water and Carbon Dioxide Capillary Bridges in Nanoscale Slit Pores: Effects of Temperature, Pressure, and Salt Concentration on the Water Contact Angle. Langmuir. 2024 accepted.
7 Tapriyal D, Haeri F, Crandall D, Horn W, Lun L, Lee A, Goodman A. (2024) CO2 wetting properties on reservoir caprock conducted at conditions targeted for commercial scale CO2 storage. Geophysical Research Letters. Accepted. DOI: 10.1029/2024GL109123

There is a lack of wettability information for important minerals that are not publicly available, including anhydrite, siderite, and halite[8]. In general, salinity can affect the IFT of reservoir fluids, with an increase in salinity the solubility of CO_2 in brine decreases, leading to changes in brine density and IFT. Brine type only has a limited influence on CO_2-brine IFT.

Should capillary threshold pressure be exceeded, it is not a given that substantial loss of containment should follow. Invasion percolation (drainage) through low permeability, porous media (i.e. a homogenous unfractured seal) progresses extremely slowly. An example of the quanta of leakage rates if percolation across the seal is given[3].

Seal integrity is explored including in-situ stress, which can be contributed to by a complex set of mechanisms generated over geological time. Maximum horizontal stress can be estimated from formation integrity testing (FIT), leak-off testing (LOT) or extended leak-off testing (XLOT). A recent study detailed the characterisation of the in-situ stresses on the Horda platform related to the Northern Lights project and provides an example of the types of data that may be gathered as part of site characterisation[9]. Equinor has also recently published a study that quantifies the relationship of in-situ stress versus depth and pore pressure with a focus primarily on the Norwegian Continental Shelf [10].

There are three types of rock failure: compression, tension, and shear. A recent review of the geomechanical challenges associated with GCS identified the geomechanical mechanisms that may result in CO_2 migration out of a storage complex[11]. A recent review of caprock integrity in depleted hydrocarbon reservoirs highlighted that mechanical rock properties for caprocks are less readily available than the highly characterised flow units[12]. A summary of the caprock properties from a selection of pilot GCS sites globally is provided in Table 2, it highlights the measured rock mechanical data (Young's modulus (E), Poisson's ratio and Unconfined Compressive Strength (UCS)) that is publicly available at the pilot sites.

[8] Iglauer, S., Pentland, C. H., & Busch, A. (2015). CO2 wettability of seal and reservoir rocks and the implications for carbon geo-sequestration. *Water Resources Research*, *51*(1), 729-774.
[9] Thompson, N., Andrews, J. S., Wu, L., & Meneguolo, R. (2022). Characterization of the in-situ stress on the Horda platform – A study from the Northern Lights Eos well. *International Journal of Greenhouse Gas Control*, *114*, 103580.
[10] Thompson, N., Andrews, J. S., Reitan, H., & Teixeira Rodrigues, N. E. (2022). Data Mining of In-Situ Stress Database Towards Development of Regional and Global Stress Trends and Pore Pressure Relationships. SPE Norway Subsurface Conference
[11] Song, Y., Jun, S., Na, Y., Kim, K., Jang, Y., & Wang, J. (2023). Geomechanical challenges during geological CO2 storage: A review. *Chemical Engineering Journal*, *456*, 140968.
[12] Paluszny, A., Graham, C. C., Daniels, K. A., Tsaparli, V., Xenias, D., Salimzadeh, S., Whitmarsh, L., Harrington, J. F., & Zimmerman, R. W. (2020). Caprock integrity and public perception studies of carbon storage in depleted hydrocarbon reservoirs. *International Journal of Greenhouse Gas Control*, *98*, 103057.

Table 2: Caprock integrity data for GCS in depleted hydrocarbon reservoir projects[12]

Project/ Region	Storage Site	Age	Primary Seal	Thickness (m)	Porosity (%)	Permeability (m^2)	E (GPa)	Poisson (:)	UCS (MPa)
Snøhvit	Snøhvit Field	Mid Jurassic	Nordmela Fm.	60–105, 62–200	13	$1–23\times10^{-15}$	-	-	-
Heletz	Heletz-Kokhav	Lower Cretaceous	Rewaha shale	23–54	6-10	1×10^{-18}	0.3-8	0.4	-
K12-B	Leman Gas Field	Late Carboniferous-Permian	Upper Permian Zechstein anhydrite, halite evaporites	550	-	-	-	-	-
Schwarze Pumpe	Ketzin	Upper Triassic	Claystone	165	-	-	-	-	-
Lacq	Rousse Gas Field	Jurassic	Flysch Sequence (clay and marl)	> 2000	-	-	-	-	-
In Salah	Krechba Gas Field	Carboniferous	Carboniferous Visean mudstone	900–950	1	1×10^{-14}	-	-	-
Otway International Test Centre	Naylor Field	Late Cretaceous (91–89.5 Ma	Belfast Mudstone (89–82 Ma)	280	<15	$<1\times10^{-15}$	8-16	0.3	9970–14,830
ROAD	P18-4 depleted reservoir	Triassic	Solingen, Rot, Muschelkalk and Keuper Fm., Upper Germanic Trias Grp	200	-	-	26	0.3	-
Peterhead	Goldeneye Field	Cretaceous	Carrack Fm.	40–100	6	1×10^{-20}	20	0.15	-
Barendrecht	Barendrecht	Triassic	Claystone	90	-	-	-	-	-
Hunterston	East Irish Sea Hamilton	Triassic	Sandy mudstones and halite, Mercia Mudstone Grp. Leyland Fm.	< 594	20-40	-	-	-	-
Edmonton, Alberta	QUEST	Cambrian	Middle Cambrian shale (Deadwood Formation)	50	-	-	-	-	-

Long-Term Impact on CO_2 of Seal Formations

It is important to assess the long-term containment capability of the seal. Accurate predictions of the precise impact of CO_2 on seals over the timescales required for permanent sequestration are challenging. However, understanding the underlying processes can inform plans to reduce containment of risk to as low as reasonably practicable and to design appropriate monitoring plans. An improved understanding of top seal behaviour can be achieved through laboratory studies, modelling, and analysis of natural analogues with an emphasis on acquiring high-quality core samples.

Geochemical reactions in sealing mechanisms are an important consideration for long-term containment and the geomechanical integrity of the top and fault seals. Seal permeability severely hampers the ability for geochemical reactions with CO_2 and reduces the importance of this process in site characterisation. Diffusion is not thought to present a leakage process of significance in most cases, and the rate of diffusion into the seal will be the determining factor for CO_2 mineral trapping reactions.

In a reservoir system containing reactive minerals, the decrease in pH caused by CO_2 dissolution is buffered by reactions. The mineralogy of the seal is important to understand as certain clays, carbonates, and other minerals, if present, are susceptible to dissolution. However, the low permeability of the seal and pH buffering reduces the rate of reactions.

Some simplified geochemical modelling supported with laboratory work of the CO_2 transport process and the CO_2–brine–rock reaction into top seals, has occurred, mostly for shale top seals. There is limited knowledge of thermodynamics and reaction kinetics in seal lithologies and much variance in the rates of reaction. Many researchers suggest that in the long term, the sealing capacity of top seals is enhanced due to geochemical processes (dissolution then precipitation of minerals)[13,14]. Certainly, the reaction of acidic CO_2-rich fluids on the seal is likely to be slow and of limited penetration and can be advantageous or disadvantageous to containment.

In addition to changes in mineralogy resulting from dissolution and precipitation reactions, the impact on geomechanics must be considered. Alteration of cements may affect the overall cohesion of the rock. Weakening or strengthening of the cementing materials can influence the rock's strength. Further chemical changes can also cause the top seal to undergo swelling or shrinkage. Some minerals may expand or contract upon hydration or dehydration (at the reservoir-seal interface) respectively, which can induce stress within the rock and potentially impact its integrity.

Many natural CO_2 and CO_2-rich hydrocarbon accumulations have been identified and studied (e.g. the NACENT project, Europe; the NACS project, USA; Jiangsu Basin, China; Green River, USA and a natural analogues study in Australia) to improve the understanding of CO_2 storage. These and other studies provided rich information on the CO_2 storage processes within the reservoir, yet there is limited data and samples from the seal rock itself.

Risk Assessment for CO_2 Containment

Seal evaluation is a crucial element in the risk profile for a CO_2 storage site, making the assessment of risk essential. Risk assessment requires appropriate uncertainty management and should be undertaken early in order to develop appropriate risk management strategies. The

[13] Yang, G., Ma, X., Feng, T., Yu, Y., Yin, S., Huang, M., & Wang, Y. (2020). Geochemical modelling of the evolution of caprock sealing capacity at the Shenhua CCS demonstration project. *Minerals*, *10*(11), 1009.
[14] Gherardi, F., Xu, T., & Pruess, K. (2007). Numerical modeling of self-limiting and self-enhancing caprock alteration induced by CO2 storage in a depleted gas reservoir. *Chemical Geology*, *244*(1-2), 103-129.

monitoring and verification plans at a site need regular reviews during the injection and post-injection phases, and modifications made as necessary.

Qualitative and semi-quantitative risk assessment techniques exist applicable to GCS projects. Qualitative methods rely on qualitative judgements and subjective analysis (e.g. risk matrix or risk bow-ties). Whereas, although semi-quantitative methods can be more challenging early in a project's development process, they encourage integrated multi-disciplinary analysis (IMDA) critical for effective risk analysis of complex systems such as GCS storage sites. The following applications of qualitative and semi-quantitative risk assessment tools have been discussed:

- Risk matrix and risk bow-tie methods e.g. Peterhead CCS by Shell; Shenhua CCS Project in China, the Northern Lights Aurora Storage Site; Quest by Shell;
- The semi-quantitative risk method (Risk Identification and Strategy using Quantitative Evaluation) RISQUE tool developed by (Bowden, 2011)[15] and applied to multiple sites in Australia, the In Selah project and the Weyburn-Midale project;
- An example of a semi-quantitative risk assessment tool is also described – the National Risk Assessment Partnership Open-Source Integrated Assessment Model (NRAP-Open-IAM)[16] which has been applied to the Quest project to complement the bow-tie assessment to demonstrate the integration of qualitative and semi-quantitative risk assessments in a storage project[17].

Risk mitigation via active and passive pressure management (APM/PPM) is included in the section on risk assessment. An active pressure management system involves extracting brine to the surface, whereas a passive pressure management system utilises wells with a shallower formation open to flow to relieve pressure. By limiting the build-up of pore-pressure several risks can be managed including those associated with seal integrity. To be effective both the uncertainties of the CO_2 storage and water disposal aspects need to be characterised. The Gorgon CCS project is the only commercial-scale project that has deployed APM to date.

Methods to Characterise and Evaluate Seal Integrity

Regulatory frameworks need to ensure the safe and effective deployment of CCS technology, including regulations for the long-term monitoring and maintenance of CO+ storage sites. The study reviewed the frameworks in four of the most mature jurisdictions. For each jurisdiction the requirements that pertain specifically to storage complex seals are outlined.

For example, in Australian Federal waters, GCS appraisal programs must consider acquiring data demonstrating that the *"confining zones of the storage formation constitute an effective and sound sealing mechanism"*. This may involve quantification of the range of porosity and permeability of the seal; the reactivity of rock types with the proposed GHG storage substance in both the reservoir and seal rocks; and the local stress regime, fracture gradients, fault stability and the geomechanical response of the storage formation to injection. Hence, conventional coring programs will likely be more extensive, and expanded logging (e.g. FMI), or in-situ testing (e.g. ELOT) programs may be required.

[15] Bowden, A. R., Lane, M.R., Martin, J.H. (2011). *Triple Bottom Line Risk Management – Enhancing Profit, Environmental Performance and Community Benefit*. Wiley and Sons, New York.
[16] Vasylkivska, V., Dilmore, R., Lackey, G., Zhang, Y., King, S., Bacon, D., Chen, B., Mansoor, K., & Harp, D. (2021). NRAP-Open-IAM: A Flexible Open-Source Integrated-Assessment-Model for Geologic Carbon Storage Risk Assessment and Management. *Environmental Modelling & Software*, *143*, 105114.
[17] Brown, C., Lackey, G., Schwartz, B., Dean, M., Dilmore, R., Blanke, H., O'Brien, S., Rowe, C. (2022). Integrating Qualitative and Quantitative Risk Assessment Methods for Carbon Storage: A Case Study for the Quest Carbon Capture and Storage Facility. 16th Greenhouse Gas Control Technologies Conference, Lyon

To characterise the seal integrity the following methods may be employed and developments in these fields are the focus of this section. Targeted log acquisition or well testing, e.g. petrophysical logs, image logs, extended leak-off testing, diagnostic fracture injection testing, micro-frac; and laboratory testing of samples, e.g. tri-axial testing and imaging studies.

Detailed stress field characterisation using image logs for GCS projects were discussed, including examples of when formation micro resistivity imaging (FMI) has been applied to not only provide sedimentary, textural, and structural detail but also to provide an improved understanding of the distribution of insoluble material within a seal providing an understanding of potential migration pathways through the caprock (e.g. In Salah, Frio and UK examples). FMI or other image log tools can be combined with other logging tools or regional data such as seismicity data to help characterise the stress field and stress-induced features. Seismicity data sets can also provide valuable insights into stress and strain distribution at a regional scale, but caution should be applied when extrapolating small-magnitude earthquakes to larger-scale tectonic processes.

Non-destructive digital core analysis techniques μCT (X-ray micro-computed tomography) and SEM (Scanning Electron Microscope) are helpful to characterise prospective seals at multiple scales and on a variety of sample sizes (e.g. cuttings or sidewall cores). The advantages and disadvantages of selecting sidewall core and cuttings are discussed. Core imaging studies can help identify coring-induced fractures from natural fractures.

An emerging field of research lies where pore-scale imaging techniques are combined with computational approaches to create a numerical representation of the pore spaces and upscaled to form pore physics inputs (e.g. capillary pressure and relative permeability curves) for flow simulation. The demand on computational requirements makes upscaling these techniques a challenge at present.

Three general approaches for calculating a brittleness index in caprocks are: mineral-based; log-based and elastic-based. The best practice, as recommended by a top seal assessment for the Northern Lights project[10] is to consider all data sources (petrophysical logs, laboratory testing and geophysical-derived inputs) rather than rely on a single approach. Limitations to these brittleness index methods include how these methods indicate lithology rather than rock failure and a more accurate prediction of a rock's propensity to fracture can be achieved by undertaking a fracability evaluation[18]. If the fracability index is then integrated with information regarding the in-situ stress state and the existence of natural fractures, this would result in a more comprehensive assessment.

The preparation, sealing, sampling and testing of cores are outlined and these are crucial steps in geomechanical analysis to maintain the integrity and representative nature of core samples. Particularly true when clay minerals are present in significant percentages.

Triaxial testing determines critical mechanical properties of reservoirs and seals by subjecting samples to controlled stress conditions to understand how these rocks behave under the pressure and stress pathways experienced during CO_2 injection and storage. A testing program of mechanical experiments for the EOS well of the Northern Lights Project[19] helps demonstrate the range of geomechanical testing that should be considered for a storage project.

Modelling of Faults and Fractures for CO_2 Flow

[18] Jin, X., Shah, S. N., Roegiers, J.-C., & Zhang, B. (2015). An integrated petrophysics and geomechanics approach for fracability evaluation in shale reservoirs. *SPE Journal*, *20*(03), 518-526.
[19] Barnhoorn, A. S., B.P; Chandra, D. (2022). *Rheology data overview for study sites*. https://www.sharp-storage-act.eu/publications--results/

The presence or creation of faults and fractures may provide a conduit for the migration of injected CO_2 into shallower formations or to the surface or water column. For this reason the modelling of properties of flow across faults is common practice in reservoir simulation and the study of possible flow along/up the fault is an active area of research for CO_2 storage.

The description and numerical reproduction of fault seal and fault flow properties are the focus of a growing body of literature with most of the research considering it appropriate to adopt the conceptual model of a fault as a barrier for across flow and conduit along flow, arising from simplified core-damage zone architecture. This is mainly valid for faults in the subsurface unaffected by structural complexity.

Presented here are two approaches to numerical modelling. Firstly, a fault as a quasi-vertical channel in the model grid that has been refined to account for the size and orientation of the fault. This might be appropriate if the fault is present within an extensive aquifer system and the size of the fault exceeds the width of the fault-fracture system. Secondly, two main zones of the fault are described: the core zone, characterised by low permeability and barrier/baffling to flow; and the fractured damage zone, which typically has a higher vertical permeability that provides a conduit for vertical flow of CO_2. This might be required if the storage formation is characterised as a closed aquifer system of finite extent.

The mineralogy of the host rock influences the architecture of the fault and therefore the preferred model. The vertical conduit model can be representative where relatively soft formations (e.g., sandstones or shales) result in less extensive fracture zones with lower fracture density and possibly 'selfheal'. Whereas the core-damage zone model would be the preferred approach in carbonate formations that are characterised by high stiffness and can give rise to an extensive fracture network with vertical permeabilities of more than a Darcy.

If faults are identified as a critical risk to CO_2 containment, focused data acquisition may reduce uncertainty in the flow properties of the fault. Also valuable in the evaluation is the discretisation of the volumes in the damage zones as the linear density and consequent permeability usually decreases with distance from the core.

A site characterisation should also look beyond the characterisation of the fault in the storage formation and seal and consider any shallower formations to which the CO_2 (or brine) may migrate as the storage formation, fault and shallower formations may establish a comprehensive flow system. The magnitude of leakage may be strongly impacted by the presence of one or more thief zones at shallower intervals – as seen in the DETECT project from the Green River site, USA examples[20] [21].

Simulations for the two fault modelling techniques as dominantly presented in the literature were performed with a traditional approach to discretisation and gridding. A structured grid with refinement in the fault zone accounts for fault size, geometry, and possible local heterogeneities. Whereas an effective upscaling of flow properties in the fault zone is possible using a relatively coarse grid, mainly for representing the fractured damage zones.

Recent advanced numerical techniques using unstructured grids for modelling subsurface formations can be effectively applied to simulate fault scenarios and can be implemented to characterise the geometry, particularly formation discontinuities like wells or faults.

[20] Dean, M., Snippe, J., Busch, A., Fink, R., Hursyt, S., Lidstone, A., Claes, H., Forbes Inskip, N., Rizzo, R., Phillips, T., Doster, F., Geiger, S., March, R., Kubeyev, A., Kampman, N. and Bisdom, K. (2020). *Final report of the DETECT project.*

[21] Snippe, J., Kampman, N., Bisdom, K., Tambach, T., March, R., Maier, C., Phillips, T., Inskip, N. F., Doster, F., & Busch, A. (2022). Modelling of long-term along-fault flow of CO2 from a natural reservoir. *International Journal of Greenhouse Gas Control*, *118*, 103666.

Unstructured gridding can help resolve issues when the communication between grid blocks is unrelated to geological layering, such as faults. When large grids are employed for extended durations (10s-100s of years) there are computational implications and the efficient asynchronous simulation solution can be valuable in this instance.

CO_2 controlled release experiments are discussed[22] [23] and it is acknowledged that it takes longer to acquire representative experimental CO_2 storage test data than it does to develop simulation-driven workflows. These experiments are, however, valuable to test monitoring technologies, but with multiple 'scale-up' challenges in transferring the learnings to commercial scale projects at greater depths and site-specific structural and geological settings.

Large-scale Geomechanical Modelling

Reservoir simulation is becoming more widespread as computational performance improves, resulting in a trend of increasingly more complex reservoir (or total "storage system") models. Whilst not all problems require the practising subsurface geoscientist or engineer to utilise numerical simulation, there are undoubtedly problems that require the interaction between fluid flow and heat transfer (i.e., conventional reservoir simulation) with induced stresses within the reservoir, caprock, over-, under-, and side burden (i.e., geomechanical modelling).

In this section of the report- the fundamentals of the creation of a geomechanical model have been outlined, from a simple 1D mechanical earth model approach to expansive and computationally intensive coupled 3D modelling that captures the hydraulic, mechanical, thermal and chemical behaviours of the storage complex and overburden.

Examples of modelling for GCS are presented that cover key themes, including recent literature examples that convey aspects including the vertical extent of the modelling domain, the considerations of coupling hydraulic and mechanical models, tensile and shear failure of a GCS seal based on both continuum and discrete fracture network methodologies; and an example of a CO_2 injection well placement methodology that simultaneously assess both injected volumes and geomechanical failure.

Finally, a limited number of hydraulic-mechanical-chemical (HMC) modelling case studies exist in the public domain pertaining to the assessment of cap rock integrity. A recent literature review of geo-mechanical-chemical impacts comprehensively describes the complexity of this topic and highlights several research gaps. In the modelling domain, further work should focus on developing guiding principles for when the interaction of geochemical and geomechanical effects needs to be considered for GCS, which would benefit both technical professionals and regulators.

Monitoring Technologies

All CCS projects face unique as well as common problems. Thus, there is no 'silver bullet' for seal integrity monitoring and historical monitoring, measurement and verification (MMV) plans have deployed multiple complementary technologies with MMV deployments becoming more focused of late. Accordingly, regulators and project proponents should avoid the assumption that because a technology was used in one project it should be used in another. A

[22] Michael, K., Avijegon, A., Ricard, L., Myers, M., Tertyshnikov, K., Pevzner, R., Strand, J., Hortle, A., Stalker, L., Pervukhina, M., Harris, B., Feitz, A., Pejcic, B., Larcher, A., Rachakonda, P., Freifeld, B., Woitt, M., Langhi, L., Dance, T., . . . Seyyedi, M. (2020). A controlled CO2 release experiment in a fault zone at the In-Situ Laboratory in Western Australia. *International Journal of Greenhouse Gas Control*, *99*, 103100.

[23] Tenthorey, E., Feitz, A., Knackstedt, M., Dewhurst, D.N., Watson, M. (2022). The Otway CCS Fault Injection Experiment: Fault Analysis. 16th Greenhouse Gas Control Technologies Conference (GHGT-16), Lyon.

review (IEAGHG, 2020)[24] of monitoring technologies is included in the appendices, to avoid duplication of effort this section provides additional insight into technologies applicable for monitoring seal integrity and value of information (VOI) assessments. Well-bore integrity technologies are out with the scope of the report.

Fibre optics offer several advantages including the distribution of data acquisition and longevity. DAS (Distributed Acoustic Sensing) and DTS (distributed temperature sensing) have been deployed as part of monitoring programs at large-scale GCS projects (e.g. Aquistore, Quest, Otway), though DSS (distributed strain sensing) has only been tested at pilot sites (in Canada, Korea, Japan and Otway). More of the more novel applications of seismic monitoring have been examined, e.g. overburden time shifts in 4D seismic head waves in active seismic monitoring[25] and monitoring for CO_2 leakage (e.g. the Lacq-Rousse site, France) and micro-seismicity detection (e.g. Weyburn, Quest, In Salah, Otway) using passive seismic monitoring.

Surface deformation monitoring, for example, tiltmeters (e.g. Aquistore) and InSAR (e.g. In Salah, Quest and Gorgon) do not directly measure changes in the storage complex seal(s), except by inference. Combining surface deformation monitoring technologies with distributed strain monitoring of the overburden may offer valuable inputs to help calibrate hydraulic-mechanical models for GCS.

Value of Information (VOI) is commonly applied in the oil and gas industry to support decision making and similar principles can be applied to the design of CO_2 storage monitoring programmes. Fundamental principles include relevance, material – i.e. the information may change a decision and economics. VOI has been applied to assess the likelihood of leakage into a groundwater source[26]; machine learning techniques have been used to estimate the VOI of a 4D seismic assessment of the Utsira saline aquifer and determine the optimal time to stop CO_2 injections into the reservoir[27] and an example from the geothermal sector.

Gorgon CCS illustrates how multiple monitoring technologies have been deployed to help characterise the link between CO_2 injection, pressure distribution and geomechanical changes so that risks can be actively managed. Downhole pressure and temperature monitoring, 4D seismic, InSAR surface deformation monitoring, injection profile surveys, vertical seismic profiles (VSP), saturation logging and passive micro-seismic monitoring arrays help to calibrate not only the dynamic modelling but also the geomechanical models[28].

International Regulatory Frameworks

Successful deployment of GCS on a global scale hinges on establishing comprehensive and effective regulatory regimes. Table 3 summarises the regulatory status for reservoir seal definition. The report goes into detail on the key legislative frameworks that regulate GCS

[24] IEAGHG (2020) Monitoring and modelling of CO2 storage: the potential for improving the cost-benefit ratio of reducing risk 2020-01

[25] Anyosa, S., Bunting, S., Eidsvik, J., Romdhane, A., & Bergmo, P. (2021). Assessing the value of seismic monitoring of CO2 storage using simulations and statistical analysis. *International Journal of Greenhouse Gas Control*, *105*, 103219

[26] Trainor-Guitton, W., Ramirez, A., Yang, X., Mansoor, K., Sun, Y., & Carroll, S. A. (2013). Value of information methodology for assessing the ability of electrical resistivity to detect co2/brine leakage into a shallow aquifer. *International Journal of Greenhouse Gas Control*, *18*, 103-113.

[27] Tadjer, A., Hong, A., & Bratvold, R. B. (2021). A sequential decision and data analytics framework for maximizing value and reliability of CO2 storage monitoring. *Journal of Natural Gas Science and Engineering*, *96*, 104298

[28] Haynes, A., Jager, K., Maekivi, J., Scoby-Smith, L., & Shawcross, T. (2023). Integration of the comprehensive Gorgon CO2 surveillance program for history matching of the Dupuy reservoir model. *The APPEA Journal*, *63*, S386-S390.

activities with a particular focus on policy and regulatory measures as they relate to reservoir seals and the permanency of CO_2 storage for the EU, Australia, USA, and Canada.

Table 3 – A summary of the regulatory status for reservoir seal definition

Jurisdiction	Regulatory Status		Regulatory Clarity Regarding Seal Integrity
	Legislation/ Regulations	Guidance Documents	
European Union*			
United States (Onshore)*			
United States (Offshore)			
Australia (Offshore)*			
Canada (Onshore)*			
Brazil (Offshore)			
Malaysia (Country-wide)			
Malaysia (State of Sarawak)			
Indonesia			
Thailand			

* Detailed discussion provided in this report

In-place

Under development/development required

Awaiting framework

Despite the varied and intricate nature of CCS regulations across these jurisdictions, they all include a robust legislative framework to govern reservoir seals and permanent CO_2 storage. These standards ensure the effectiveness and security of CCS deployments by highlighting the importance of seal integrity and storage permanence. Additionally, the legislation acknowledges the necessity for adaptability, encouraging updates to regulatory requirements as technological advancements emerge. Therefore, CCS project proponents must stay up-to-date on the latest legislative and regulatory developments within their jurisdiction to guarantee legislative compliance.

Conclusions

The study presents a comprehensive review of defining and assessing seal integrity, from initial concepts, latest research, assessing risk, modelling faults and fractures and creating larger geomechanical models, selecting appropriate monitoring technologies and understanding how regulations vary across jurisdictions to cover CO_2 containment and seal integrity.

The primary risk mechanisms for leakage, not accounting for legacy wells, includes tensile failure through the caprock, shear failure at the caprock/storage unit interface or due to fault reactivation and rock deformation.

CO_2 may be contained in other plays beyond a 'conventional' reservoir-seal pair, and a site with a composite seal may also contain CO_2 within satisfactory timescales, or utilising residual or mineral trapping.

The long-term impact of CO_2 on different formations is discussed including the rate of migration and reactivity of CO_2 with seal formations. Predicting the exact impact over thousands of years is challenging. Geochemical processes can be advantageous with re-precipitation of minerals decreasing the permeability or disadvantageous due to dissolution and is dependent on the availability of cations and evolving chemical conditions. The speed of these reactions is strongly dependent on the flow of CO_2 and acidified formation waters, which is hampered by very low permeability.

Insights into recent developments in laboratory or log-based analysis techniques are presented, including methods for calculating the brittleness index, imaging techniques, log-based characterisation of top seals and faults and a recent example of formation micro-resistivity imaging role in seal assessment. Small scale and local techniques need to be paired with basin scale understanding of the regional stress field, extent of the seal, and potential interaction with adjacent GCS projects.

A literature review of the most recent advancements in modelling CO_2 migration along or near a fault has been undertaken, including research performed as part of the DETECT project and advanced gridding and numerical solution techniques. Control release CO_2 experiments are also discussed.

From a legislative perspective, fully understanding and evaluating the seal is as important as understanding the storage formation, and understanding the connection between the reservoir and seal is critical especially when applying for permits to ensure they comply with regulatory requirements.

This comprehensive seal integrity review provides a detailed, updated exploration of the critical aspects of seal potential in the context of the geological storage of CO_2. Highlighting the importance of seals in ensuring the containment of CO_2 and the challenges of predicting the long-term impact of CO_2 interactions with seal formations.

Expert Review

Nine expert reviewers from six organisations initially reviewed the first draft of this document, and two reviewers completed a second review. The manuscript received detailed and extensive comments, drew on the reviewer's expertise and helped shape and refine the second draft.

It was recognised that the authors had compiled a useful, well-organised and well-researched report spanning a wide range of topics, with well-addressed studies from Australia. It was thought to be a good starting point for someone looking for more detailed references on specific topics and with useful compilations in the appendices. However, with a view that a range of readership might access the report, there were recommendations to tighten up the structure, provide more context, give summaries at the beginning of sections with key insights, elaborate further on a range of topics, and expand the use of examples and references. The conclusions needed to be strengthened with room to provide more opinion throughout the report as well as the final summary and recommendations should be added. All these recommended additions have now been incorporated.

Context to the document was seen as critical to several reviewers requiring consistency of terms used, introduction to the anatomy of a storage site, definition of leakage and pathways, and the requirement of a seal to provide containment of CO_2 for thousands of years (not millennia) with

no emissions to the surface or water supplies. There was a request also from several reviewers to employ a greater use of natural analogues in the discussion to demonstrate that geological seals can retain CO_2 for geologic time; geochemical impacts are cm to m scale in thickness and have not demonstrably shown to compromise seal integrity and that known CO_2 leakage occurs via faults, fractures and wells – not across seals. Additional analogues include reference to column height databases. Context was felt as critical to accurate risk assessment and that appropriate risk was communicated – and that we expect success.

It was felt that although capillary pressure seals are important with regard to geological time, it is less critical for timescales appropriate for the geological storage of CO_2. Another reviewer echoed these sentiments, whereby petroleum-type seals work for CCS, but the goal of sequestration means that we could inject under flat-lying seals (like Sleipner, Decatur or Quest) and minimize the column height and buoyancy pressure on the seal. We can also take advantage of local capillary trapping, residual trapping, dissolution and distributed buoyant traps to minimize that fraction of mobile CO_2, and thus maximize the security. The discussion of mineral trapping is a step in the right direction, but the reviewer suggests a more complete discussion, including other trapping mechanisms and the general idea of selecting storage sites that minimize buoyancy pressure and the chance for leakage, regardless of the seal.

Other suggested additions to the technical discussion included the thermal stability of the seal due to the temperature alteration and injection of CO_2. Gaps also were highlighted with regard to research on the controls on wettability, interfacial tension and other factors related to capillarity in CO_2-brine systems. These have now been addressed.

Lastly, a thorough review and rewrite process was undertaken to improve the report's structure, clarity and readability. Following the second review, reworking and additional material were added, notably in sections 4.2 (Seal Capacity), 4.5 (Basin scale processes), chapter 9 (Large scale geomechanical modelling) and chapter 10 (Monitoring technologies).

Recommendations

The following recommendations are proposed by the study:

- More laboratory studies are desired for various seal types, e.g., assessing the sealing properties of multiple minerals, including dolomite, anhydrite, siderite, and halite.
- Though the permeability of seals is the limiting factor, more knowledge of geochemical reaction kinetics and how they relate to changes in flow properties, as well as the geomechanical properties of seals, still needs to be obtained. An improved understanding of top seal behaviour can be achieved through laboratory studies, modelling, and analysis of natural analogues. To conduct these studies, obtaining high-quality samples of seals is essential for investigating the chemical and geomechanical properties. A set of recommendations/guidelines for preserving the core from potential sealing units would be valuable to ensure that opportunities are noticed. There may be a need for the relevant authorities to require data collection as a supplement to planned data collection in conventional oil and gas exploration wells. Such additional data can provide information about areas' further potential for large-scale storage of CO_2. Collecting additional data can reduce the uncertainty of a future CO_2 storage facility and may offer the potential for significant savings by avoiding a future dedicated CO_2 storage verification well.
- There are numerous proposed methods for modelling CO_2 migration through faults, but more experimental data is needed to underpin or support one method over another. Several CO_2-controlled release experiments have been discussed in this report, noting that “scale-up” challenges remain when attempting to transfer the learnings to

commercial-scale GCS projects. A "post-mortem" of what was learned from these experiments should be undertaken when these experiments are completed. This review should also attempt to collate any key insights from other projects that seek to address scale-up challenges for fault leakage (e.g. the DETECT project).

- Future studies should focus on creating a framework of the "fit-for-purpose" approaches for undertaking hydraulic-mechanical-thermal (HMT) simulations at the various stages of assessment for regional or site-specific GCS. This framework should include the key model framing decisions that need to be made (e.g. vertical and lateral extent, coupling method, etc). Further, a limited number of hydraulic-mechanical-chemical (HMC) modelling case studies in the public domain also pertain to assessing cap rock integrity. Future work should focus on developing guiding principles for when the interaction of geochemical and geomechanical effects needs to be considered for GCS, which would benefit both technical professionals and regulators.
- The reality should be reinforced that we expect successful containment in GCS by undertaking effective site characterisation. A comparison between the extensive risk assessment frameworks proposed for GCS and those currently required in the oil and gas industry would be valuable. There is a danger that higher standards will be set for "proving" containment in GCS than have been established in the oil and gas industry without due cause.
- As highlighted in the report, in petroleum systems a seal is considered effective if it retains large, mobile hydrocarbon accumulations over geological timeframes. By contrast, for GCS the nature of the trapping and sealing mechanisms, as well as the long-term seal integrity are paramount for geostorage to be achieved over geological timeframes.
- Outside of dedicated research groups and those at the forefront of the industry, most of the discussion for GCS focuses on CO_2 containment under an aquitard. However, the containment options are much larger for CCS as geostorage of CO_2 can be applied under a broader suite of seals and trapping mechanisms. Future engagements with the public, regulators and other stakeholders should explain this so that it is understood that the size of the opportunity for emissions abatement using geological storage of CO_2 is communicated effectively.
- There are gaps in the research of the impact of multiple large scale GCS projects within the same sedimentary basin on elevating pressure and the impact on seal capacity.

CO2CRC
Building a low emissions future

Geological Storage of CO_2: Seal Integrity Review

IEAGHG R&D Programme (IEA/CON/23/294)

David Bason[1], Dr. Hadi Nourollah[1], Dr. Simone de Morton[1], Dr. Max Watson[1], Genna Petho[1], Ivan Maffeis[1], Michael Rieger[1], Dr. Geoff O'Brien[1]

June 2024, CO2CRC Report No: RPT23-6595 (Rev2)

[1]CO2CRC Ltd

CO2CRC
Level 3, 289 Wellington Parade South
East Melbourne, Victoria 3002
PO Box 24121, Melbourne
Victoria 3001
www.co2crc.com.au

Bason, D, et al., 2024. Geological Storage of CO_2: Seal Integrity Review (IEA/CON/23/294). CO2CRC Ltd, Melbourne, Australia, CO2CRC Publication Number RPT23-6595.

Executive Summary

Geological carbon sequestration (GCS) is a proven and increasingly cost-effective technology that can permanently remove CO_2 from the atmosphere. Following the CO_2 capture step, which can be from a number of emission sources, including natural gas processing, power generation and industrial processes such as cement and steel production, the CO_2 is compressed, transported by pipeline or ships, and then injected deep (>800 m sub-surface or -seafloor) underground into suitable storage reservoirs.

A key component of a robust storage system is the presence of largely to completely impermeable sealing units, which prevent the unexpected migration of the sub-surface CO_2 plume out of the storage site, vertically, laterally, or via a combination of both. Assessing the seals' veracity– the containment component of the storage system - is essential to gaining regulatory sanction for any geological carbon storage project. Demonstrating containment through a project's lifecycle also represents a vital aspect of the Monitoring and Verification programs undertaken to assess the migration of CO_2 plumes in the sub-surface.

This report provides a comprehensive review of recent advancements in the evaluation, modelling, and monitoring of top and fault seal integrity for GCS sites. Understanding the parameters that define an effective seal for CO2 storage is crucial to ensuring the safe, secure, and permanent storage of CO_2.

This report examines various sealing scenarios that ensure the long-term stability and permanence of GCS. It investigates the concept of seal potential, a collective descriptor that encompasses seal capacity, seal geometry and seal integrity. Determining seal potential can be complex, particularly when considering the long-term impact of CO_2 on various sealing lithologies, and consequently, this report examines research regarding the long-term impact of CO_2 on the integrity of seals. This includes a thorough investigation of evidence of deterioration or enhancement from laboratory-based experimental work and modelling, focusing on the potential extent and probability of seal integrity deterioration.

Risk assessment is critical throughout the lifecycle of a geological carbon storage project, particularly because many potential pathways for CO_2 leakage involve vertical migration through the seal. Therefore, evaluating the seal is a vital component of the risk profile for a GCS site. Various methods for characterising and evaluating seal integrity are examined, including qualitative and quantitative assessment methods and various risk mitigation approaches.

Understanding the geomechanical behaviour of caprocks and reservoirs is another key parameter to understanding overall seal integrity. The fundamentals of geomechanical modelling are therefore examined, including the identification of risks associated with poro-elastic stress coupling and the repressurisation of (depleted) hydrocarbon reservoirs. The report leverages past research and supplements it with additional data to ensure a robust analysis of both single and multi-fracture systems.

Monitoring is a critical activity throughout the lifespan of a GCS project and continues to be essential even after the project's completion. The report analyses the performance of different monitoring technologies currently deployed at large-scale GCS sites, including pressure monitoring, fibre optics, seismic, electromagnetics and surface deformation techniques.

The simulation of CO_2 migration along faults and through fractures is another important aspect examined in this report. By utilising current numerical approaches and validating these models through controlled release experiments and high-resolution seismic and resistivity surveys, the report provides best practice guidelines for modelling CO_2 migration in faulted regions.

Finally, the legislative and regulatory requirements for GCS significantly impact a project's efficient and timely implementation. Over the past decade, regulations for CO_2 geological storage have been developed across various jurisdictions, reflecting the multifaceted nature of GCS. Understanding these diverse regulatory approaches is crucial, and so this report examines the manner in which various jurisdictions define a "seal," in other words, what the various regulatory requirements for "seals" across these jurisdictions are.

Contents

1. Introduction

1.1 Overview

In 2011, the IEAGHG released a report, Caprock Systems for the Geological Storage of CO_2 (Kaldi, 2011), providing a high-level overview of issues related to caprocks. The study defined seal potential (including seal capacity, seal geometry and seal integrity) and discussed many of the fundamental aspects of geomechanics, hydrodynamics, geochemical interactions with seals and the available monitoring techniques. This current study builds on the previous research, specifically on seal integrity and recent developments in this field since 2011.

The objective of the present study is to provide an updated point of reference for technical professionals, regulators, and community stakeholders to assess whether a prospective storage site demonstrates the required characteristics to contain CO_2 within the required timescales to be an effective solution for mitigating climate change (in the order of millennia). It provides a comprehensive review of recent advancements in the evaluation, modelling and monitoring of top and fault seal integrity for carbon GCS sites and is aligned with the objectives outlined by the IEAGHG technical specification document "IEA/CON/23/289". The focus of GCS has evolved substantially over the last 15 -20 years.

Previously, the predominant focus for GCS was on CO_2 storage within depleted oil and gas fields, a storage environment that was rich in data and understanding, especially in terms of fluid and gas production from the reservoir units. Hydrocarbon production results in the depressurisation (i.e. deflation) of the reservoir system. In contrast, the injection of CO_2 as part of geological carbon storage results in the repressurisation of the reservoir (with a different fluid – CO_2) and the reinflation of the overlying sealing units. This inflation of the seals is not well understood and could potentially result in issues with seal integrity. Consequently, a more aggressive roll-out of GCS projects utilising depleted hydrocarbon fields needs to consider the sealing units in detail, a key difference to the reservoir-centric approaches used in hydrocarbon development.

Similarly, it has become apparent over the last 15-20 years that it will be necessary for project proponents to target all available, viable storage sites (to meet emission reduction targets), hence the global focus on GCS within saline aquifer formations. This type of storage play is generally much larger but also much more poorly characterised than depleted fields, and the GCS projects will target deep saline formations with seals that have not been previously assessed for their hydrocarbon retention capacity. Seal assessment in such situations is vitally important but also challenging.

In the present review, the challenges of assessing seal integrity in both depleted fields and saline aquifer storage systems are reviewed.

1.2 Uniqueness of Seals for GCS

The 2005 IPCC Special Report on CCS (Metz, 2005) found that the fraction of CO_2 retained in appropriately selected and managed storage sites is very likely to exceed 99% over 100 years and is likely to exceed 99% over 1000 years. This is consistent with a report from the Zero Emissions Platform (ZEP) published in 2019, which states that for a typical North Sea storage site, over 99.99% of injected CO_2 is expected to remain stored deep underground for at least 500 years (Hoydalsvik et al., 2021). Fundamentally, the industry expects successful containment. Nevertheless, detailed technical studies are required on a site-by-site basis to effectively characterise and provide assurance of containment.

Containment requirements for GCS are not the same as in petroleum. In petroleum, a seal is considered effective if it retains large, mobile accumulations of hydrocarbon over geological timeframes. This is fundamentally different from the objectives of GCS.

Petroleum-type seals are effective for GCS, but the objective and timeframes for CO_2 sequestration mean that alternative sealing concepts may be considered (e.g. Sleipner, Decatur, Quest) that minimise the column height and buoyancy pressure on the seal.

In addition to storage within a structure under a capillary seal (closure storage), there are various other trapping mechanisms that can create an effective seal. Residual, solubility and mineral trapping are the most prevalent in literature. However, other forms of trapping, such as local capillary trapping (Saadatpoor et al., 2010) or distributed buoyant traps can minimise that fraction of mobile CO_2 and thus maximise security.

An effective seal for GCS is simply a state of nature that enables a certain mass/volume of CO_2 to be retained within the defined boundaries (both lateral and vertical) of the storage complex for a prescribed period.

1.3 Report Structure

This report provides some overall context to the topic of GCS seals, including the concept of containment and the various risk mechanisms that may contribute to loss of containment (section 2). The concept of a storage complex is also introduced. Next, recent research into alternative opportunities for the GCS, such as composite seals, is discussed. These alternative sealing concepts represent an important distinction from the perhaps more traditional view of sequestering CO_2 within a structural trap under a capillary seal.

The remainder of the report is structured as follows:

Seal Potential (section 4)

Background on the definition of seal potential is provided, and the three elements of seal potential (seal capacity, seal integrity and seal character are discussed in more detail, as well as any new models, theories, experiments, or studies that pertain to these concepts.

Long-term Impact of CO_2 on Seals (section 5)

This section of the report also discusses the findings from a literature review identifying the long-term impact of CO_2 on caprock or seal unit lithologies, especially the rate of migration and reactivity of CO_2 with seal units.

Risk Assessment (section 6)

The current risk assessment methodologies for assessing CO_2 containment are outlined, including a discussion of both qualitative and quantitative risk assessment techniques, as well as applications of these risk assessment techniques to commercial-scale CO_2 storage projects.

Methods to Evaluate Seal Integrity (sections 7, 8, 9 and 10)

After the completion of a risk assessment, the natural next step thereafter is to identify opportunities to eliminate, substitute and/or mitigate the identified risks where possible through (i) data gathering, (ii) modelling, and (iii) deployment of monitoring technologies.

- The results of data gathering and new laboratory or well/borehole-log-based analysis techniques pertaining to seal integrity over the past decade are presented in section 7.
- Advances in the modelling domain, specifically large-scale reservoir-geomechanical simulations for CO_2 storage, are reported in the literature (section 9), as well as recent advances in the simulation of CO_2 flow along faults and fractures (section 8).

- Monitoring, measurement, and verification (MMV) planning is a key component in assessing the containment and conformance of a CO_2 storage project. Therefore, the different available methods for monitoring or inferring seal integrity in large-scale or pilot CO_2 storage systems are also reviewed (section 10).

International Regulatory Frameworks – CO_2 Seals (section 11)

In addition to technological challenges, there are also social and regulatory challenges associated with CO_2 storage. Public acceptance of GCS is crucial for its successful implementation, and concerns over potential leakage and environmental impacts must be addressed. Regulatory frameworks also need to be developed to ensure the safe and effective deployment of GCS, including regulations for the long-term monitoring and maintenance of CO_2 storage sites. The relevant regulatory and policy measures for CO_2 storage development and approvals around the globe, and how these measures pertain to reservoir seals and the permanency of CO_2 storage are discussed in the final section of this report.

Throughout this report, we have attempted to use consistent terminology where possible to describe various aspects that, when combined, describe a GCS storage complex. However, please note that the terminology varies across jurisdictions and even amongst academics and CO_2 storage practitioners.

2. GCS Containment, Risk Mechanisms and Nomenclature

In this report, various subsurface elements of a GCS system are frequently referenced. A storage unit(s) (illustrated in light yellow in Figure 1) is the geological interval(s) in which the CO_2 is intended to remain. In general, GCS projects consider the storage of CO_2 at depths of around 800 m or greater (depending on geothermal gradient) to take advantage of the substantial increase in density at these prevailing temperatures and pressures, thereby using the pore space in the storage unit more effectively.

A top seal (dark grey) overlies the storage unit and is a barrier to flow, acting to prevent buoyant CO_2 from migrating (primarily upwards). A GCS project may rely on a primary seal, but other secondary seals can also be utilised as part of an intended CO_2 storage play. A caprock, which is a term inherited from the oil and gas industry, prevents the upward or lateral migration of hydrocarbons. For GCS, an effective seal is not necessarily a single lithological unit and can, for example, be a 'confining system'.

A caprock can be utilised as part of a CO_2 storage play but it is not necessary for a caprock to be present for GCS if a sealing mechanism has been identified.

Other elements of the GCS system include the overburden, which is defined as the entire rock between the storage system and the surface or seabed, the underburden, and the basement (pink), which is typically of metamorphic or igneous origin.

The *Storage Site* is defined in the EU Directive (2009/31/EC) as *a "defined volume area within a geological formation used for the geological storage of CO_2 and associated surface and injection facilities".* Further, a *Storage Complex* includes the storage site but also "*any surrounding geological domain which can have an effect on overall storage integrity and security; that is, secondary containment formations".*

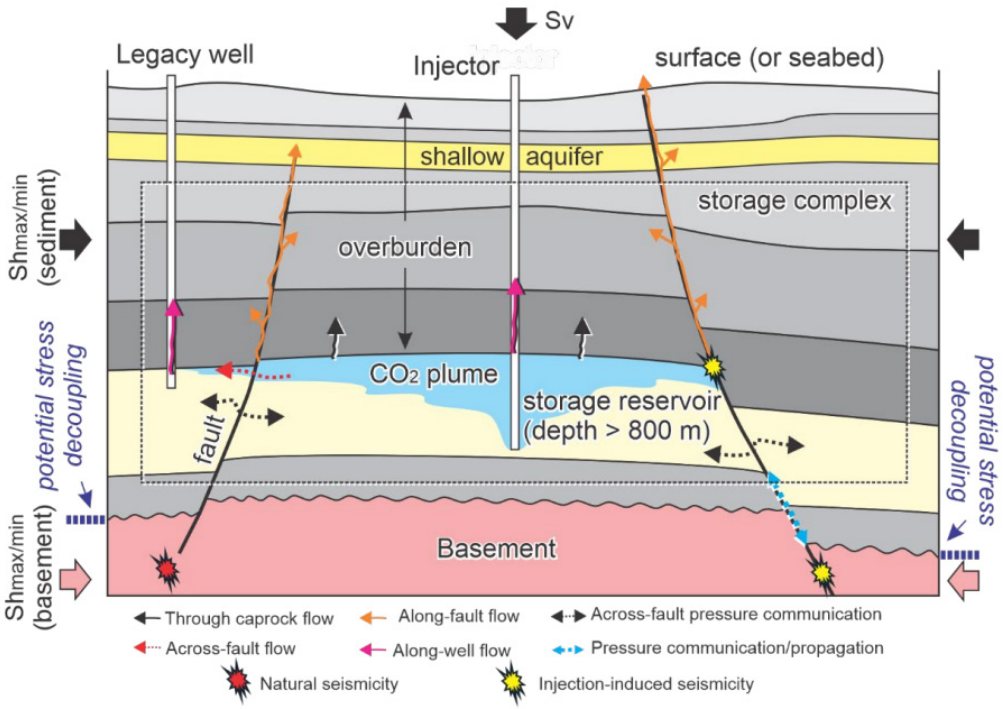

Figure 1: GCS Storage System and Risk Mechanisms (Wu et al., 2022)

In this report, leakage is defined as positive evidence that anthropogenic CO_2 is not contained within the prescribed storage complex. By containment we generally refer to CO_2 (at quantities that can be measured or inferred) remaining within the storage complex, which is defined through permitting in both a lateral and vertical domain. However, we acknowledge that containment risk in GCS is not limited to only CO_2 and that brine displacement and other pore fluids should also be considered in some settings (e.g., protection of USDWs in the onshore US). Importantly, though we adopt this terminology, it is critical to highlight that in many cases, vertical migration of CO_2 out of a storage complex does not imply that it will be released into the atmosphere or into the water column.

Similarly, in some jurisdictions, other terminology exists. For example, in Australian Commonwealth waters, the term *Storage Formation* has been defined. A Storage Formation is not equivalent to a geological formation. Indeed, CO_2 may migrate laterally, remaining within the same geological formation and causing no deleterious impact but still be considered a loss of containment. Several definitions from various jurisdictions are presented in Table 1.

Table 1: GCS definitions and terminology

Confining Layer/Zone/Strata/System	
Class VI Wells (USA Onshore)	A geologic formation, group of formations, or part of a formation stratigraphically overlying the injection zone(s) that acts as a barrier to fluid movement
Storage Formation/Complex/Unit/Reservoir, Injection Zone	
CCS Directive Article 3 (Europe)	The storage site and surrounding geological domain which can have an effect on overall storage integrity and security; that is, secondary containment formations
OPGGSA (Australia)	A part of a geological formation, where that part is suitable, with or without engineering enhancements, for the permanent storage of a GHG substance
Class VI Wells (USA Onshore)	Injection zone means a geologic formation, group of formations, or part of a formation that is of sufficient areal extent, thickness, porosity, and permeability to receive carbon dioxide through a well or wells associated with a geological sequestration project
Leakage	
CCS Directive Article 3 (Europe)	Any release of CO_2 from the storage complex
Containment	
SPE SRMS Guidelines	Part of the subsurface assessment that controls movement of stored CO_2 within a specific area. Necessary criteria for estimating and identifying storable quantities. A projected timeframe (e.g., 1000 years) should be stated with the assessment.

The potential pathways or events that can lead to CO_2 migrating out of a Storage Complex are referred to as risk mechanisms. These risk mechanisms are, at a high level, common to all CO_2 storage sites, with varying degrees of likelihood for the event occurring.

Some of the potential risk mechanisms for CO_2 migration out of the storage complex are identified in Figure 1 and are described in more detail in Table 2. The majority of the mechanisms relate to seal integrity, which is the primary focus of this report, including the potential for seal failure due to natural processes, such as earthquakes and fault reactivation, the existence or creation of natural fractures in the seal (Zappone et al., 2021) and the long-term stability of seals under conditions of elevated CO_2 pressure and thermal effects (Busch, 2009). Note that this study that well leakage via legacy wells is outside the scope of this study.

Table 2: Description of Typical Risk Mechanisms

Risk Mechanism	Related to Seal Integrity?	Description
Seal geometry	Yes	CO_2 leakage beyond the top seal due to insufficient lateral extent and/or thickness of the seal over the storage area
Seal capacity	Yes	CO_2 leakage through the top seal enables vertical migration of CO_2 outside of the primary storage unit.
Seal degradation	Yes	CO_2 exposure over time causes geochemical degradation of the primary seal, resulting in CO_2 leakage through new stratigraphic pathways in the primary seal
Induced fracturing through the seal	Yes	CO_2 injection exceeds the fracture limits of seal rock, causing the growth of new vertical fracture pathways through the primary seal and leakage of CO_2.
Juxtaposition failure	Yes	CO_2 loss may occur through across fault leakage if injection interval sands are incorrectly interpreted to have a sufficient juxtaposition seal for CO_2 along the storage system's bounding faults.
Natural seismicity	Yes	Natural seismicity, such as earthquakes (unrelated to the project activities) within the limits of the storage system, could cause the reactivation of key faults and CO_2 loss above the top seal. However, this is anticipated to be uncommon. There are no documented cases to date of natural seismicity causing seal leakage from CO_2 storage or hydrocarbon reservoirs
Induced seismicity	Yes	Seismic activity caused by human/external activity (e.g., CO_2 injection), forming new leakage pathways.
Well leakage	Yes	Degradation of wellbore materials, or the absence or degradation of plugs and cement, creates a CO_2 leakage pathway – primarily into the above zone but potentially to shallower potable water aquifers and the surface environment. Loss can occur in abandoned, suspended, shut-in, monitoring and injection wells. Well leakage is outside the scope of this study but may pose the highest risk for containment in many GCS projects.

Reactivation of faults	Yes	CO_2 injection causes changes in stress and subsequent reactivation of existing faults, which causes new leakage pathways. Risk relates to seal integrity if the reactivated leakage pathway penetrates the seal.
Migration Direction	No	CO_2 migrates outside of the permit area due to processes unidentified previously, such as preferential migration pathways, exceeding the capacity of structural closure, ineffective filling, active hydrodynamics, etc.

3. GCS Storage Plays

As highlighted in previous sections, sealing requirements in GCS differ from those in petroleum and therefore, various GCS storage plays can be considered. This section discusses the various scenarios.

Closure Storage

In structural trapping, impermeable (or low permeability) rocks such as shales and mudstones, anhydrite, halite, or tight carbonates (discussed in section 4.1) act as a barrier to the upward buoyant migration of CO_2, resulting in the retention of CO_2 within a storage formation (Iglauer et al., 2015).

The CO_2 'fate' plot (Figure 2) will be familiar to many readers. The plot illustrates the trapping contribution of various mechanisms (structural and stratigraphic, residual, solubility, and mineral trapping) as a function of time. However, various authors have reported that the plot is not representative of the various trapping mechanisms in a temporal sense.

As an example, (Snippe & Tucker, 2014) conducted reservoir simulation studies using hydro-geochemically-coupled modelling tools (i.e. PHREEQ coupling, refer to section 9.1.8) to investigate the contribution of various trapping mechanisms for CO_2 storage in both a depleted gas field and a dipping saline aquifer in settings that are considered to be realistic for large-scale GCS projects. The authors concluded that the structural setting (open versus closed) was the key driver for the fate of the free CO_2. The free CO_2 phase evolved much more rapidly into the other fates (residually trapped, dissolved or mineralised) in the open structural setting than within a closed structure (Figure 3).

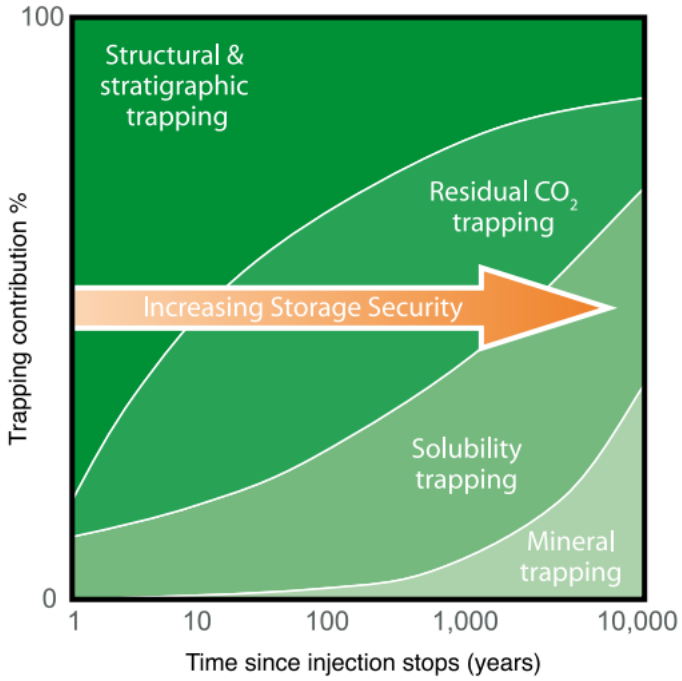

Figure 2: Storage security depends on a combination of physical and geochemical trapping (Metz, 2005)

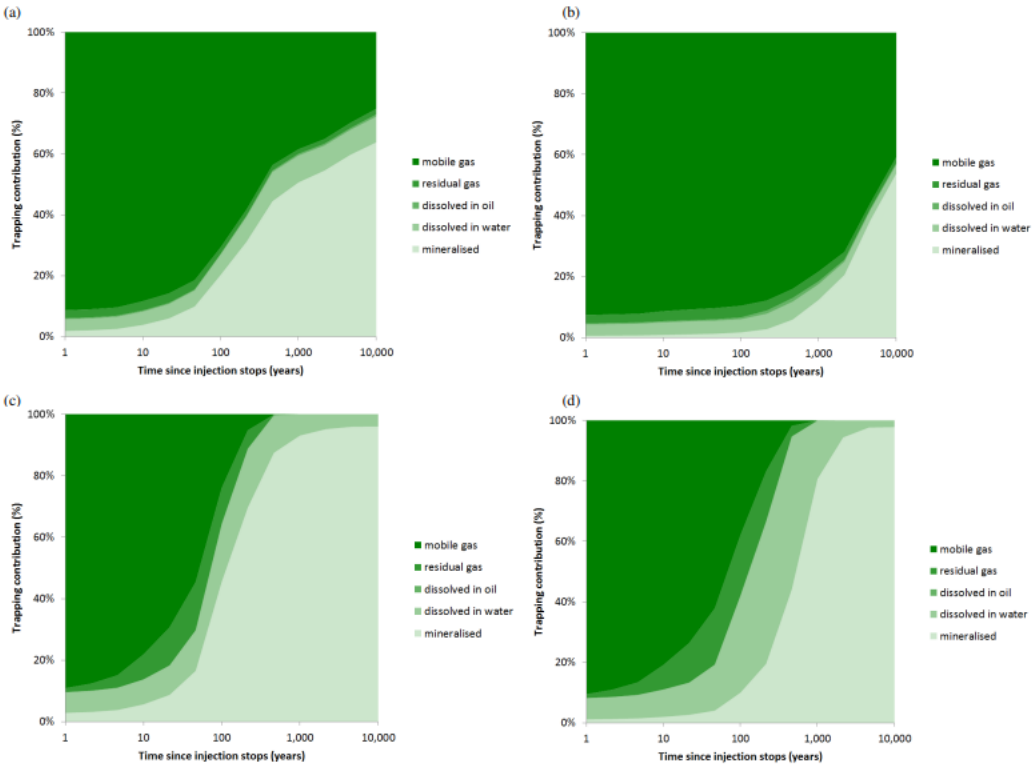

Figure 3: CO_2 fate plots for different structural settings and geochemical assumptions. (a) A depleted gas field without dawsonite; (b) A depleted gas field with slow kinetics including dawsonite; (c) A dipping saline aquifer without dawsonite; (d) A dipping saline aquifer with slow kinetics including dawsonite.

Composite Seals

In residual trapping, pore-scale capillary forces counteract the buoyancy forces, and therefore, CO_2 becomes immobile (when CO_2 dissolution is not considered).

Recent research has articulated the concept of composite seals as an alternative target for GCS therefore broadening the solution space pertaining to the evaluation of different storage sites (Bump et al., 2023). Composite seals are described as a confining system in which the lateral extensiveness of the confining elements is not defined; instead, containment relies on barriers that create a tortuous path for the CO_2 thereby enhancing dissolution (solubility) and residual trapping (Bump et al., 2023). The study illustrates the concept through laboratory experiments and numerical simulations using data from Southern Louisana Miocene deltaic deposits.

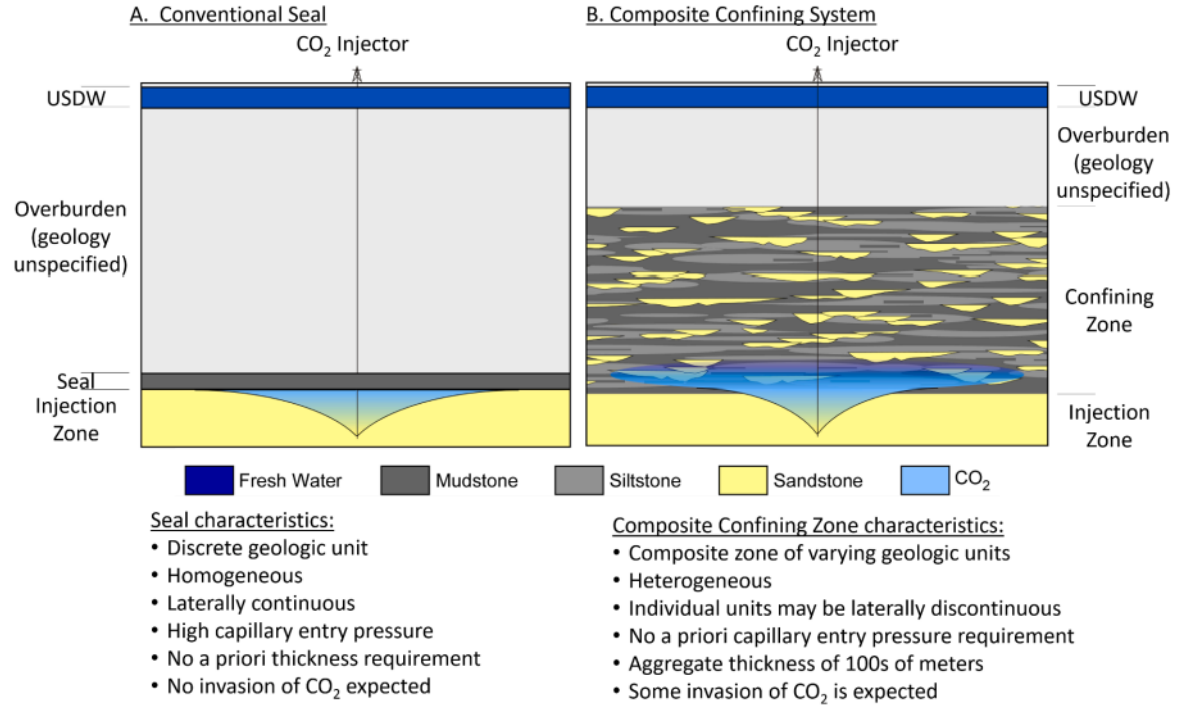

Figure 4: Conceptual example of a composite confining system (Bump et al., 2023)

Another example of a CO_2 project currently under evaluation that does not include a "conventional" seal is the proposed South West Hub Project in Western Australia. The proposed geological storage concept is to sequester industrially generated CO_2 deep underground in the Lesueur Sandstone formation.

The project is still in the research phase, with an estimated storage injection rate of 800,000 tonnes per annum to be injected over a 30-year period (Stalker et al., 2013). Under the currently proposed migration-assisted trapping concept, residual trapping through the thick sequence of interbedded sand and shale sediments of the ~1500 m thick Lower and Upper Lesueur formation will play a key role in preventing vertical migration out of the storage complex, particularly because the overlying Eneabba formation is expected to be thin and not laterally extensive and therefore plays a limited role in structural trapping (Stalker et al., 2013).

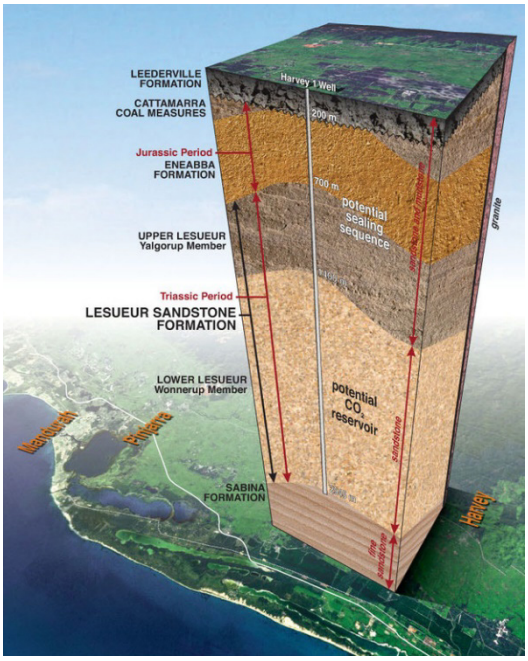

Figure 5: South West Hub GCS Concept (Government of Western Australia: Department of Mines, 2023)

Mineral Trapping

Non-closure storage provides the opportunity for a larger proportion of the injected CO_2 to be dissolved into the formation water, and therefore, it is more prone to mineralisation trapping than in a closure store (as there is more CO_2 in solution to mineralise). In this type of GCS play, the composition of the host formation is important; though there would likely be limited mineralisation in a very clean siliciclastic formation, more can occur in a carbonate storage reservoir (e.g., Weyburn).

The typical IPCC illustration of trapping mechanisms for GCS indicates that mineral trapping does not make a material contribution to trapping in the near term after CO_2 injection has ceased (Figure 6, left image). The IPCC model for GCS focuses on trapping mechanisms within sedimentary basins, which are primarily composed of sedimentary rocks with a clastic origin. Mineralisation can occur on a much shorter timescale for GCS sites utilising carbonate or igneous storage formations.

GCS projects that are seeking to exploit this rapid mineralisation of CO_2 are the Carbfix projects (Iceland) and the Wallula pilot project (USA). At Carbfix and Wallula, CO_2 is injected into natural basalt reservoirs.

Typically, minerals that are highly reactive to CO_2 contain magnesium, calcium, and/or iron. Basalt, for example, may contain pyroxene or olivine minerals. The carbonation reaction then involves the dissolution of CO_2 in water to form carbonic acid (H_2CO_3), which then reacts with the mineral surface to release metal cations (e.g., Mg^{2+}, Ca^{2+}, Fe^{2+}) and form less reactive carbonate minerals (e.g., magnesium carbonate, calcium carbonate, iron carbonate) (Rasool & Ahmad, 2023).

At the Wallula pilot project, some CO_2 mineralisation had occurred within 24 months, though free-phase CO_2 was still present at the top of the reservoir and held in place by an impermeable flow core caprock (McGrail et al., 2017).

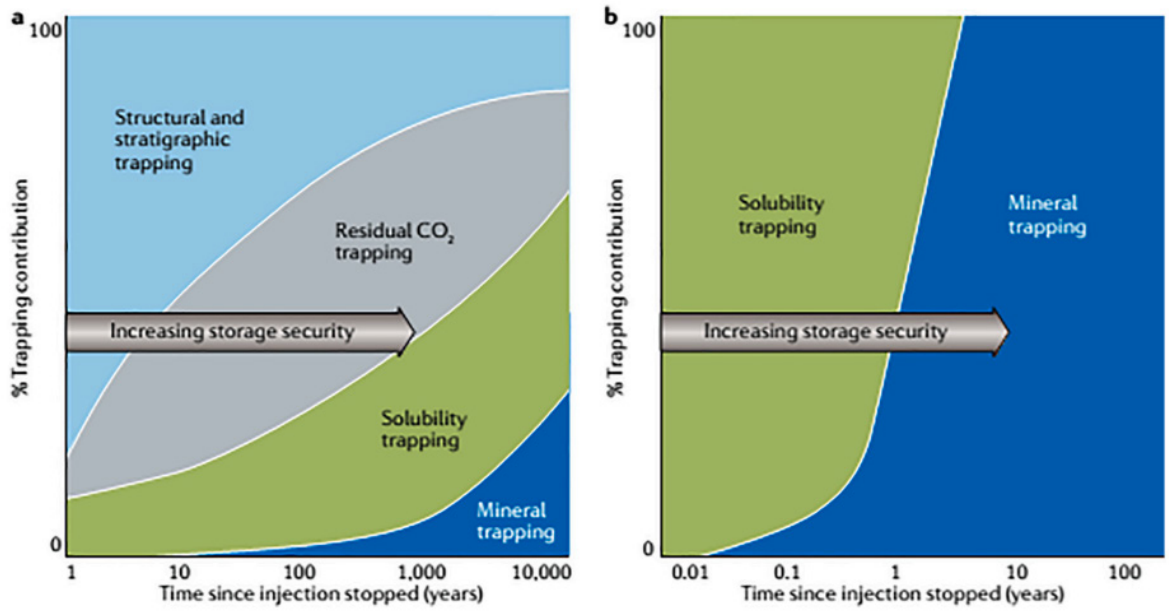

Figure 6: Comparison of CO_2 trapping mechanisms in sedimentary basins (left) (modified after IPCC, 2005) and basalts with mineral carbonation trapping (right) (Snæbjörnsdóttir et al, 2022, modified from Snæbjörnsdóttir et al, 2017)

Conversely, at the Carbfix2 project CO_2 is dissolved in water via mixing at a depth of approximately 750 m before it is injected into an aquifer at depths between 1900 and 2200 m (Gunnarsson et al., 2018). In this example, the complete dissolution of the CO_2 removes the need for a caprock, as the gas is no longer buoyant (Rosenqvist et al., 2023). Monitoring of the CO_2 mineralisation processes is achieved using chemical tracers, fluid sampling in dedicated monitoring wells and soil flux measurements (Carbfix). The key to containment is demonstrating that the carbonated water is retained in the subsurface until the CO_2 has been scavenged from the water.

4. Seal Potential

In GCS, the success of permanently storing CO_2 in geological formations relies on the presence of effective geological barriers. Seals act as crucial components in ensuring the long-term containment of CO_2, preventing upward, lateral, or downward migration and subsequent migration into areas outside the storage unit.

The "traditional" GCS storage play is effectively a geological structure (e.g. an anticline) overlain with a competent seal that enables a buoyant column of CO_2 to be retained. Capillary (membrane) seals are a "nice-to-have" for GCS but not necessarily critical when the timeframes for CO_2 storage are considered.

In 2011, the IEAGHG released a report, Caprock Systems for the Geological Storage of CO_2 (Kaldi, 2011), providing a high-level overview of issues related to caprocks. The study defined seal potential, including the concepts of seal capacity, seal geometry and seal integrity)

Seal potential is a collective descriptor that encompasses:

i) **Seal Capacity**: CO_2 leakage through the seal.

ii) **Seal Geometry**: the areal extent of the seal (lateral continuity) and thickness.

iii) **Seal Integrity**: the propensity of the caprock to fail in a brittle sense or its ductile behaviour.

For **seal capacity,** however**,** it should not be assumed that once the capillary threshold pressure is exceeded, there will be a substantial loss of containment from the storage formation. When flow across a membrane seal is established, i.e. a continuous phase of CO_2 exists, the flow rate is controlled by the permeability and thickness of the seal, as well as the differential pressure across it (Darcy flow), and this will be very low due (i.e. nanoDarcy) permeability and a low relative permeability effect.

Similarly, **seal geometry** may be more appropriately referred to as **seal character,** and the definition extended to include the geometry/extent, thickness, and internal heterogeneity of the seal.

The determination of sealing potential in geological formations, particularly in shale units, can be a complex and non-trivial task. Generally, the petroleum and mining industries have not prioritised coring the reservoir seal/caprock as the primary driver has been to obtain samples of the reservoir itself, although coring of shales may have been performed when wanting to characterize shale strength (UCS, HCS) to optimize drilling of deviated wells in petroleum fields. Moreover, coring shales are often challenging and may result in low recovery rates, and the condition of the sampled interval may be disturbed in the coring process. As a result, petrophysical well-log analysis is a more commonly employed method for collecting data on shale formations. However, such data collection methods may not always provide a complete understanding of the sealing potential of the shale unit.

4.1 Seal Lithologies

In recent years, there has been a body of research investigating the behaviour of CO_2 within different lithologies, including well-cemented sandstones, certain limestones, argillaceous clay-rich mud rocks, and shales and evaporates.

Fundamental properties of an effective seal include low permeability, high capillary entry pressure, sufficient thickness and lateral extent, and chemical stability. A seal's ability to prevent CO_2 leakage depends on its ability to resist stresses that may be imposed on it over greenhouse gas removal timeframes. Understanding the lithological and structural characteristics of seals in different geological settings is essential to ensuring the success of CO_2 storage projects.

There are several properties, including porosity and permeability, that when combined with various conceptual models, are used to describe seals. These properties should always be considered in combination with other factors, such as lithology, thickness, depth of burial, potential heterogeneity, etc., to provide an improved understanding of the sealing properties.

Many lithologies can serve as effective seals in CO_2 storage, including less common lithologies such as chalks, coals and evaporites. A summary of the various sealing lithologies for current and future CO_2 storage projects is provided in Table 3. Many of these seals would be classified as a Sneider type A seal or higher (refer to Table 20).

Table 3: Examples of Primary Seals for GCS Projects and Developments

Project/Region	Operational	Onshore/Offshore	Primary Seal Formation	Primary Seal Description	Reference
Sleipner	Yes	Offshore	Nordland	Shale	(Springer & Lindgren, 2006)
Snøhvit	Yes	Offshore	Nordmela	Shale	(Gao, 2013)
Quest	Yes	Onshore	Deadwood Formation	Shale	(Rock et al., 2017)
Gorgon CCS	Yes	Onshore	Barrow Group	Shale	(Trupp et al., 2021)
South West Hub	Yes (Pilot)	Onshore	Lesueur	Interbedded sand and shale	(Langhi et al., 2021)
Aurora	No	Offshore	Drake and Burton	Shale	(Rahman, Fawad, Jahren, et al., 2022)
Endurance	No	Offshore	Rot	Layered evaporites and mudstones	(BP, 2022)
Acorn CCS	No	Offshore	Rodby & Lista	Shale	(Worden et al., 2020)
Hamilton CCS	No	Offshore	Mercia	Mudstone	(Gamboa et al., 2019)
CarbonNet	No	Offshore	Latrobe Group (“T2”)	Intraformational coals and shales	(Hoffman, 2018)
Regional seal for largest oil/gas fields (Ghawar)	No	Onshore	Hith and Arab	Layered evaporites	(Boehm et al., 2023)

Shale and Mudstone

Shales comprise a major part (more than 50%) of sedimentary rocks (Boggs, 2009; Johnston & Christensen, 1995). They are the most common seal lithology in CO_2 Storage. Mudstones form when very fine-grained sediments settle through the water column in low-energy environments, such as lakes and lagoons or in deepwater settings. They are composed predominantly of very fine quartz grains and clay minerals and can contain minor components of a variety of other minerals and organic materials. The distinction between mud, mudstone and shale is a function of the depth of burial – muds are clay and quartz-rich sediments, lithified mud is mudstone, and shale is a fissile mudstone (Aplin & Macquaker, 2011). The very fine grain size of mudstone and shales results in small pore space connectivity (pore throats), meaning mudstone and shales can have relatively high porosity but very low permeability (Aplin & Moore, 2016). Burial further impacts the porosity and permeability of mudstones, with compaction reducing both pore space (porosity) and pore throat size (permeability) (Aplin & Moore, 2016). The Lower Cretaceous Rodby Shale, which is a seal for the Acorn CCS project, has a mean porosity of approximately 14%, a mean permeability of 263 nD (2.58×10^{-19} m^2) (Worden et al., 2020).

The low permeability of shales and mudstones restricts fluid flow, making them a robust sealing lithology (Aplin & Macquaker, 2011; Boggs, 2009; Krushin, 1997). Despite their widespread existence, measurements of the geomechanical, hydraulic and elastic properties of shale can prove challenging (Sarout & Guéguen, 2008). This is the result of the relatively porous nature of shale, combined with its extremely low permeability, suggesting a limited connected pore space and, thus, a violation of the assumptions of the Gassmann fluid substitution (Josh et al., 2012). Gassmann fluid substitution (Gassmann, 1951) assumes connectivity of the porous space, independence of the shear moduli of the rock and homogeneity of the rock.

The presence of clay minerals in mudstones and shales significantly impacts both their porosity and permeability (Josh et al., 2012). Clay mineral content in shales can vary widely, ranging from 25%-70% (Hornby et al., 1994; Sarout and Guéguen, 2008). The principal clay minerals in mudstones and shales are phyllosilicates, including illite, muscovite, kaolinite, chlorite and smectite. Phyllosilicates are a class of minerals characterised by their sheet-like structure. During the deposition of mudstones, clay minerals settle out of suspension within the water column, tending to align preferentially on their flat sides. Subsequent compaction and diagenesis processes further enhance this preferred orientation.

The composition of shale significantly influences its properties. Shales with a substantial amount of organic material, known as 'organic shales,' are typically prolific sources of petroleum. In contrast, shales that are rich in carbonate minerals are referred to as carbonate shales, while those with a high content of silicates like feldspar and quartz are known as silicate shales. Additional data from unconventional reservoir characterisation of shale/mudrocks can be leveraged to reduce gaps in knowledge on how various lithologies respond to changes in pressure and stress.

Evaporites

In contrast to mudstones and shales, evaporites make up less than 2% of the world's sedimentary rocks (Warren & Warren, 2016). Despite their sparsity, evaporites serve as the principal seal for more than half of the world's largest oil reservoirs, demonstrating that evaporites can retain large columns of buoyant fluid including CO_2 (Bump et al., 2023; Warren & Warren, 2016). Evaporites are sedimentary rocks formed by the precipitation of minerals from evaporating water, typically in arid and semi-arid settings where evaporation exceeds precipitation (Warren & Warren, 2016). Evaporite deposits encompass an array of minerals, among which evaporite salts such as anhydrite ($CaSO_4$) are a common seal lithology for both hydrocarbon reservoirs and geologic carbon storage projects (e.g. Quest) (Hangx et al., 2014; Kirkham et al., 2022). Evaporitic carbonates, notably calcium carbonate ($CaCO_3$) and dolomite ($CaMg(CO_3)_2$) often occur in association with anhydrite seals. Evaporite salts tend to precipitate from highly concentrated brines found in environments such as supratidal flats and sabkhas, whereas evaporitic carbonates begin to precipitate in the early stages of brine concentration in seawater or lake settings (Warren & Warren, 2016). As both anhydrite and dolomite develop in similar depositional settings they often occur as reservoir-seal pairs (Sneider et al., 1997). In contrast to anhydrite, diagenetic processes acting on dolomite can enhance porosity and permeability, making it an excellent reservoir rock (Sarg, 2001). Evaporites such as anhydrites are distinguished by their

tightly bonded crystalline structures, which lead to elevated capillary pressures and consequent impermeability (Rezaeyan et al., 2015). Furthermore, the plasticity of anhydrite and other evaporite minerals over geological timescales enables them to undergo plastic deformation under pressure, unlike other lithologies that may fracture (Kirkham et al., 2022). This characteristic helps maintain their integrity as seals through time.

Due to the similarities in depositional settings, evaporites occur as lateral facies equivalents to carbonate and dolomite (Sarg, 2001). This results in vertical and lateral facies transition between these lithologies and subsequent heterogeneities in the porosity and permeability of evaporite seals (Sarg, 2001). Core studies of high-capacity anhydrite layer seals in dolomitic reservoirs from the St Andres Formation in New Mexico have been undertaken (Sneider et al., 1997)(Figure 7). Porous zones (within the St Andres Fm) lose porosity and permeability where dolomite grades into anhydrite (Pitt & Scott, 1981). Pinch-out of permeability may occur by less permeable limestone interfingering with more permeable dolomite. This observation happens regionally, moving from south to north, and is visible in the cored interval of Figure 7. Anhydrite zones, if unfractured, rank among the highest-grade seals on Sneider's scale (Table 20).

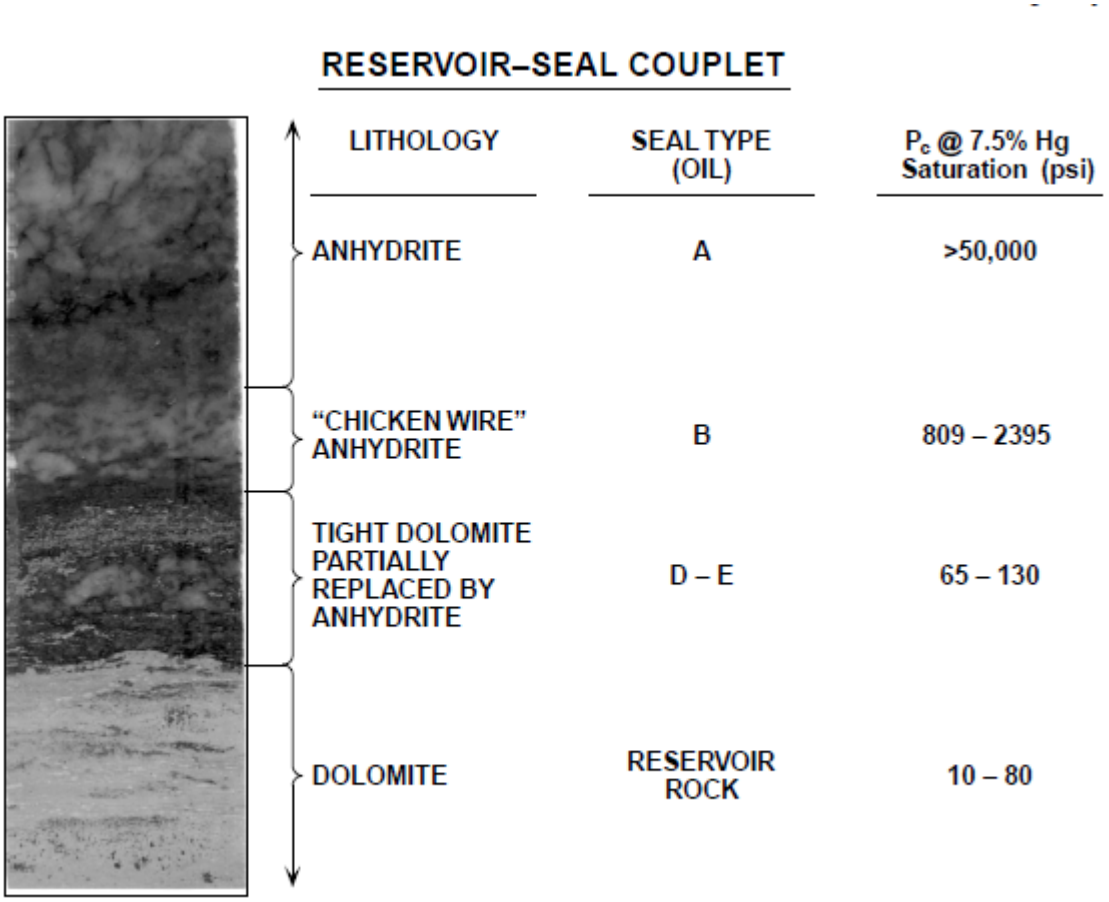

Figure 7: Core section from St Andres formation (Pitt & Scott, 1981)

Carbonates

The ability of carbonate rocks to act as a seal is dependent on several factors, including the environment of deposition, diagenetic processes, and hydrodynamic conditions. Carbonates are typically categorised by their dominant components: the matrix, grains, and cement (Tucker & Wright, 2009). The matrix of limestone consists of microcrystalline calcite called micrite and is the main constituent of marl, along with some clay and other organic minerals (Tucker & Wright, 2009). Marls form in a variety of freshwater and marine

depositional environments where clay and carbonate particles settle out of suspension and accumulate. The fine-grained composition of marls contributes to their relatively low permeability, enabling them to function effectively as a seal (Dávila et al., 2016).

The primary porosity of carbonate rocks, controlled predominately by grain type and matrix, can undergo substantial alteration due to dissolution and early diagenetic processes (Tucker & Wright, 2009). As carbonate grains dissolve, calcite cement often precipitates, filling in the adjacent primary pores. This leads to the formation of tightly cemented carbonate rock, marked by distinct moldic porosity and reduced permeability. Carbonate rocks that contain microporosity or unconnected vugs can act as "subtle seals" (porous barriers to hydrocarbon migration) (Dolson et al., 2018). Subtle seals may contain mobile water and may have porosities exceeding those in the reservoir but a lower permeability and higher capillary pressure due to smaller pore-throat size.

Dolomitization can vary in its impact on porosity, either enhancing or diminishing it and subsequently turning a carbonate from a potential reservoir into a seal. The precipitation of dolomite crystals within the pores of carbonate rock can occlude pore space and decrease the size of the pore throats, thus reducing permeability. When dolomitization occurs in a carbonate overlying a lithology that is more porous and permeable, the resulting dolomite layer can serve as an effective barrier, preventing fluid flow from the reservoir below and providing local and intra-formation seals (Lynch & Trollope, 2001; S. Zhang et al., 2022). Research from the Otway International Test Centre (Australia) has concluded that the precipitation of dolomite within the pore space of the Paaratte Formation has effectively inhibited CO_2 flow locally. The dolomitic rocks were generally modelled as discs that precipitated above good-quality reservoir units (beach sands and channels) (Jenkins et al., 2017).

Chalk is a fine-grained carbonate rock primarily consisting of coccoliths, which are the calcite plates from microscopic marine algae, typically deposited in deepwater settings (Tucker & Wright, 2009). The overburden pressure, the degree of natural fracturing, and diagenetic alterations, such as cementation and compaction, all play crucial roles in defining the permeability and porosity of chalk deposits (Bonto et al., 2021) Under certain conditions when porosity is reduced through diagenetic processes, or if the fractures are sealed by mineral precipitation, chalk can act as an effective seal (Bonto et al., 2021).

In many instances, carbonates are geomechanically harder. Rock strength refers to the ability to withstand stress without deforming, whilst brittleness is a measure of a rock's tendency to fracture rather than deform plastically when stressed. High strength in rocks often correlates with brittleness, but high-strength rocks will not fracture unless the stresses exceed their tensile or shear strength. Therefore, harder rocks, such as carbonates, are more resistant to deformation. However, when deformation occurs, they are more likely to deform in a brittle failure mode.

Alternative Lithologies

Recent studies have also explored the use of alternative lithologies as seals for CO_2 storage. Coal, for example, has been shown to have good sealing properties due to its high organic content and low porosity (Hoffman, 2018). The CO_2 is adsorbed onto the coal surface, creating an effective seal to prevent the CO_2 from leaking. While shale remains the most common seal lithology in CO_2 storage, alternative lithologies offer potential options for sites where shale is not present or may not be suitable for storage. It is important to note that each lithology has its own unique characteristics and requires careful evaluation on a site-by-site basis to ensure its suitability for CO_2 storage.

4.2 Seal Capacity

In the context of GCS seal assessment, it is important to distinguish between two possible containment issues. The first is related to seal integrity, for example, the creation of tensile fractures, which may result in rapid migration from the storage unit (refer to section 4.4). The second is the slow breakthrough, where CO_2 enters the shallower, low-permeability unit above and is controlled by multi-phase (Darcy) flow in porous media.

An aquitard, or confining unit, is a low-permeability unit that can store groundwater and transmit it slowly from one aquifer to another. Indeed, when discussing the concept of slow vertical migration of CO_2 it is appropriate to picture GCS seals as a stacked series of aquitards and (open or confined) aquifers. At each point along the potential migration pathway, as long as flow remains under the conditions for porous media, the ability of the CO_2 to migrate will continue to decrease when an aquitard is encountered. This reduction in migration comes from various factors, including residual trapping of CO_2, which decreases the column height of the CO_2 and hence the buoyancy forces, as well as the continued dissolution of the CO_2 at each point in the migration pathway and any geochemical exchange that occurs with each aquitard.

The absolute permeability, water saturation, and viscosity control the advective transport of CO_2 after breakthrough (Pentland et al., 2011). For typical percolating saturations $_sCO_2 < 0.3$, the Corey-Brook equation predicts a relative permeability $krCO_2 < 0.32 = 0.09$ (Peters, 2012). Even if a relatively high CO_2 saturation in an aquitard was established, the relative permeability end-point may be quite low. (Benson, 2013) published the results of a study into relative permeability for multi-phase flow in CO_2 storage. The low end-point values that are reported in the literature may be due to current experimental limitations (the unfavourable mobility ratio and high interfacial tension between CO_2/brine result in capillary pressures needed to achieve high CO_2 saturations in the cores) but could also be due to rock heterogeneity (channelling and bypassing).

The concept of seal capacity has been used historically applied for GCS to calculate the column height of CO_2 that can be supported by capillary pressure (Kaldi, 2011). Seal capacity is directly related to the pore throat size, connectivity of pore throats, wettability, and interfacial tension. In this report, we do not limit the discussion on containment to this traditional definition of seal capacity, which is grounded in the capillary threshold pressure concept and column height calculations from petroleum prospecting.

Importantly, it should not be assumed that there is a substantial loss of containment from the storage formation once the capillary threshold pressure is exceeded. Invasion percolation (drainage) through low-permeability, porous media (i.e., a homogenous unfractured seal) progresses extremely slowly, with a low relative permeability of supercritical CO_2 to brine. Capillary entry pressure gets fluid into the seal, but the pressure required to move fluid through the full thickness of a seal and into an overlying permeable unit is quite different.

In this section, the concept of capillary pressure is introduced, as well as the key inputs required to calculate capillary pressure. A primer on the commonly used mercury porosimetry method, including its limitations, is provided in Appendix A-1 and A-2.

CO_2 Breakthrough Pressure

(Espinoza & Santamarina, 2017) studied the breakthrough pressure for several homogenous specimens of various sediments (e.g., fine sand, calcium carbonate and kaolinite). In this study, rather than using the MICP method, the breakthrough pressures for the prepared specimens were measured using an apparatus that enabled constant vertical stress to be applied and the continuous measurement of pressure and flow rate using transducers. Importantly, the authors concluded that the Laplace equation overpredicts the capillary breakthrough pressure when the mean pore size is used as CO_2 invades along percolating paths made of the larger pores (Espinoza & Santamarina, 2017).

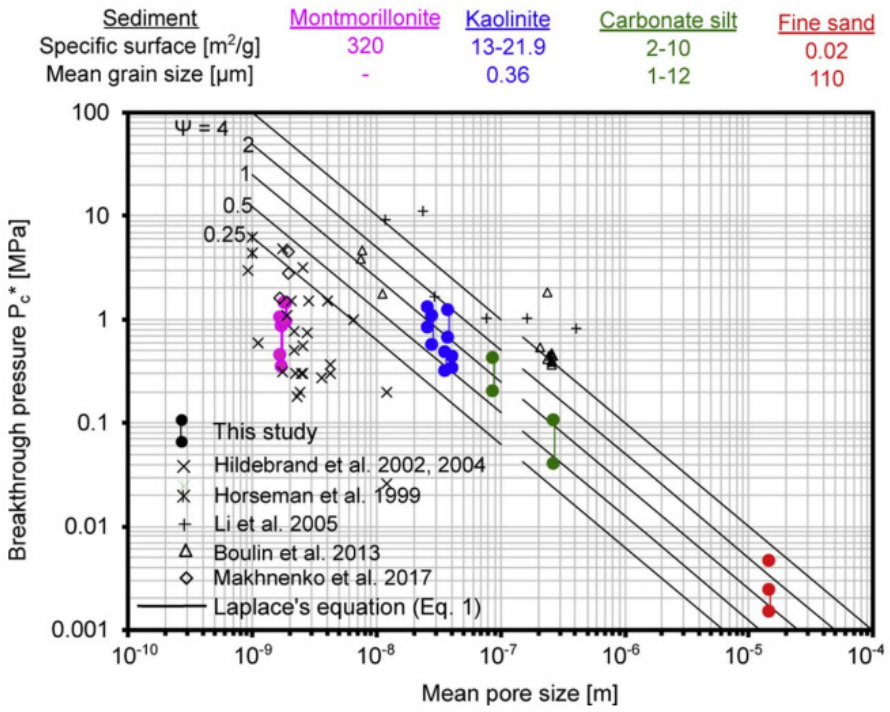

Figure 8: Mean pore size versus breakthrough pressure (Espinoza & Santamarina, 2017)

Post-Breakthrough Advective Flow

Leakage will be advection-controlled once percolation takes place at most storage sites being considered *(Espinoza & Santamarina, 2017)*. Advection, the transfer of heat or matter by the flow of a fluid, can be estimated using the Darcy equation:

$$q_{CO2}^{adv} = \frac{k k_{CO2}^{r} \rho_{CO2}}{\mu_{CO2}} \frac{(\Delta P - \rho_{CO2} g t_h)}{t_h}$$

$$q_{CO2}^{adv} = \ advection\ mass\ flow\ rate, k = absolute\ permeability, k_{CO2}^{r} = \ CO_2\ relative\ permeability$$

$$\rho_{CO2} = density\ of\ CO_2, \mu_{CO2} = viscocity\ of\ CO_2, \Delta P = pressure\ gradient\ , t_h = seal\ thickness\ , g = acceleration\ due\ to\ gravity$$

Indeed, it is valuable to put the advective post-breakthrough flow of CO_2 into context by applying typical values for sealing lithologies in GCS. A range of mass flux rates as a function of seal permeability and thickness to illustrate the concept are presented in Table 4. Several assumptions underpin the calculated values, but it is readily apparent that the numbers are very small.

In this discussion, we have deliberately avoided explicitly prescribing an “acceptable” leakage rate from a storage complex. In our opinion, any metric should be site-specific and focus on the extent to which CO_2 leakage would have an adverse impact, e.g., on safety and the environment. More details on risk assessment methodologies are provided in section 6.

Table 4: Mass flow rates, post-breakthrough advective flow. Assuming k^r_{CO2} = 0.09, μ_{CO2} = 1e-04 Pa.s, ρ_{CO2}= 700 kg/m^3, ΔP = 1 MPa, g = 9.81 ms^{-2}

Seal Permeability (nD)	q^{adv}_{CO2}(Tonnes/m^2/year) for seal thickness (m)		
	1	10	100
1	2.0e-5	1.9e-6	6.5e-8
10	2.0e-4	1.9e-5	6.5e-7
100	2.0e-3	1.9e-4	6.5e-6
1000	2.0e-2	1.9e-3	6.5e-5

Combining Porous and Fractured Media Flow

Effective pressure was also the focus of a separate experimental investigation on CO_2 breakthrough and flow mechanisms in shale (Skurtveit et al., 2012). In this study, breakthrough mechanisms for scCO_2 using shale samples from the Draupne Formation in the North Sea were evaluated. Effective pressure conditions are an important consideration for breakthrough testing and calculations of seal capacity, e.g. from mercury porosimetry. Importantly, a further insight gleaned from the experiments was that the pressure-induced opening of micro-fractures is an important transport mechanism for supercritical CO_2.

However, it is important to highlight that though the shale samples were preserved, drying cracks were still observed in the material (revealed by a high-resolution X-ray CR scanner). Therefore, the sample preservation method may have contributed to the observed micro-fractures. Sample preservation is discussed in more detail in section 7.2.5.

If the creation of micro-fractures observed in the experiments is representative of the in-situ behaviour of shales, it is apparent that the critical pressure for the containment of CO_2 will, therefore, be a complex parameter involving both micro-fracturing and capillary displacement. In the earlier example of stacked aquitards, increasing the pore pressure of the geological system through CO_2 injection may manifest differently in individual strata (i.e. flow in porous media may govern migration in one strata, whilst fractured media may govern flow in another). Both these mechanisms need to be considered when evaluating and modelling the seal integrity for large-scale CO_2 storage (Skurtveit et al., 2012). Note that whilst recent research (Hannon Jr & Esposito, 2015) has sought to provide a guide as to what has constrained the pressure limits for a GCS project (e.g., fault slip or creation of tensile fractures); these approaches are limited to high-level screening studies. A more detailed seal characterisation should be performed in the later site selection/characterisation stages.

Note that general considerations of the impact of increased pressure on seals in a basin (e.g. regional tectonics, dewatering) are discussed later in the report, as well as some of the key considerations for both characterising and modelling seal integrity for GCS.

4.2.1 Capillary Pressure

The relationship between the capillary pressure and the radius of the pipe (or pore space) is derived from the Young-Laplace equation and may be written as:

$$P_c = \frac{2\sigma Cos\theta}{r_c}$$

Where P_c is the capillary pressure, r_c is the radius of the capillary pipe, σ the interfacial tension, and θ the contact angle.

4.2.2 Wettability

The wettability of seals and reservoir rocks to CO_2, and in particular the wettability of geologic minerals in the presence of CO_2 and formation brines, is a poorly understood physicochemical factor that highly influences the trapping processes (especially structural and residual trapping) (Iglauer et al., 2015).

Experimental methods of directly measuring contact angles have several limitations or potential pitfalls that impact the calculated wettability, including surface preparation, ensuring the appropriate balance of forces (which is related to the droplet size and velocity), contamination, as well as appropriately equilibrating the CO_2 brine system. The literature review resulted in a large variation in wettability (7-92°) for CO_2/quartz/water(or brine) systems, Other important conclusions were that $scCO_2$ behaves significantly differently than gaseous CO_2 in terms of wettability, no CO_2 systems is completely water-wet at reservoir conditions (as is often assumed), and that there is a lack of wettability information for important minerals that are not publicly available, including dolomite, anhydrite, siderite, and halite (Iglauer et al., 2015).

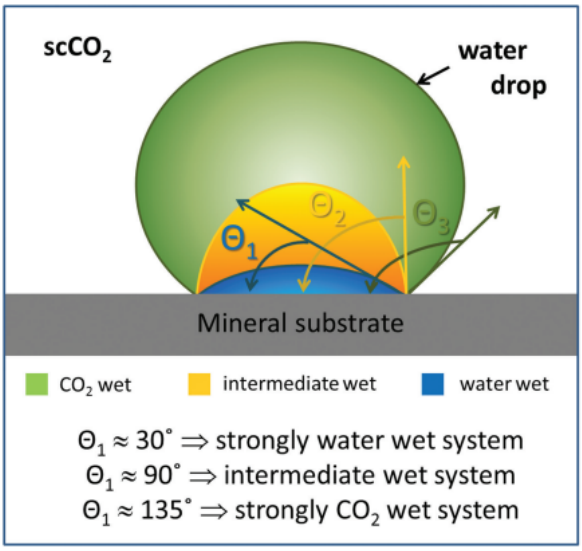

Figure 9: Wettability definitions referenced to CO_2-wet, intermediate and water-wet (Iglauer et al., 2015)

4.2.3 Surface Tension

Surface tension between CO_2 and brine is another key input in determining seal capacity. (Liu et al., 2016) summarised the results of various experimental results in this field of research, as well as conducting further studies using the axisymmetric drop shape analysis (ADSA) method (Figure 10). A general plateau of the interfacial tension (IFT) can be observed once pressures exceed approximately 2000 psi.

In general, the presence of salinity can affect the IFT of reservoir fluids to a large extent (Figure 11). As salinity increases, the solubility of CO_2 in brine decreases, leading to changes in the brine density and IFT.

Though it has also been recognised that the addition of salts into the aqueous phase can significantly increase the IFT of gas/brine systems, it has been demonstrated that brine type only has a limited influence on the

CO_2 -brine IFT and hence brines with relatively simple ionic composition (i.e. limited o Na+ cations) may be used to estimate IFT (Mutailipu et al., 2019)

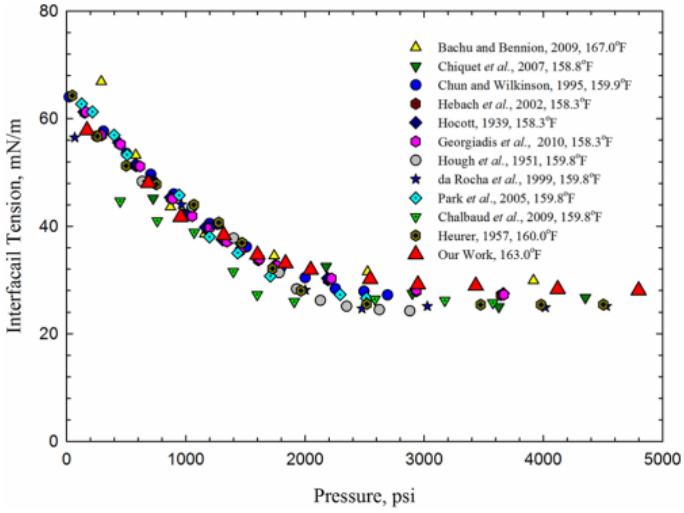

Figure 10: Comparison of CO_2 /H_2O IFTs measured in various studies. Temperature range (158.3 – 167.0 F/ 70 – 75°C) (Liu et al., 2016)

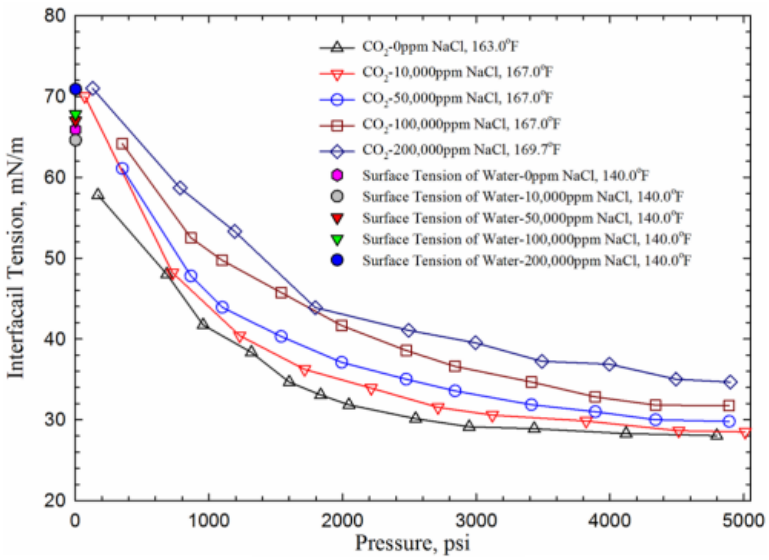

Figure 11: IFT between CO_2 and brine for a range of salinities and temperatures (Liu et al., 2016)

4.2.4 Regional Understanding of Seal Capacity

As outlined earlier in this section, seal potential is a collective term that encompasses seal capacity, seal integrity and seal character. For seal capacity, there are several aspects that it is worthwhile highlighting in more detail.

First, seal capacity calculations should not be performed in isolation from a regional understanding of pressure. Hydrodynamical considerations are important when estimating the seal capacity of both top and fault seals, including the importance of understanding whether there is excess pressure above or below the seal when estimating seal capacity (Underschultz, 2007).

Second, uncertainty in upscaling laboratory tests underlines the importance of using analogous of sites where naturally occurring accumulations of CO_2 has occurred and either been retained or shown evidence of

leakage. This is the topic of a previous IEAGHG study (Natural and Industrial Analogues for Geological Storage of Carbon Dioxide, 2009), where various natural occurrences of CO_2 that have been retained within a variety of structural or stratigraphic trapping mechanisms are outlined in the USA and Turkey. Similarly, sites with natural leakage of CO_2 (e.g. Montmiral, France; Florina Basin, Greece) also provide valuable learnings on the possible causes for containment; in many cases, the most frequently hypothesised migration pathways are through faults and fracture networks (Natural and Industrial Analogues for Geological Storage of Carbon Dioxide, 2009).

4.2.5 Impact of Heterogeneity on Seals

The heterogeneity of both top and fault seals makes calculating seal capacity challenging.

The impact of these heterogeneities is largely derived from clay mineralogy and mineral surface properties, which are critical factors in determining the sealing capacity of clays in CO_2 storage reservoirs (Hou et al., 2022). As the clay content of shales ranges from 25%-70% (see Section 4.1), their sealing capacity is highly variable. The presence of non-clay grains within shales disrupts the alignment of phyllosilicates, creating passages through the shales (Sneider et al., 1997). The clay platelets give way to open spaces near grains such as quartz or pyrite. If these disturbances occur frequently, they will likely be connected, leading to leakage through interconnected spaces.

Leakage through shales occurs at both micro and macro scales. At the micro-scale, non-clay grains and minerals disrupt the alignment of clay minerals, reducing the triangular spaces. These spaces create conduits through which fluid can flow, diminishing the shale's sealing capacity. The impact of these fluid flow conduits, known as 'bridging,' can be studied using electron microscopes and MICP sampling.

At the macro scale, across large areas and several meters of thickness, shales may not have a uniform mineral composition. Consequently, shales can have regions of increased heterogeneity in the ratio of clay minerals to other minerals and grains, impacting the local seal capacity of the shale unit. The connectivity of these less locally sealing regions can cause a leakage bridge. The distribution of this connectivity can be addressed with geostatistical modelling of seal composition and risked accordingly. Geostatistical models are underpinned by seismic and core data.

These leakage bridges can manifest as local seepage pipes (Cartwright et al., 2007) or, on a larger scale, as gas chimneys (Nourollah et al., 2010). Gas chimneys (depicted in the right-side image of Figure 11) can also result from mechanical failure (e.g., tensile fracturing).

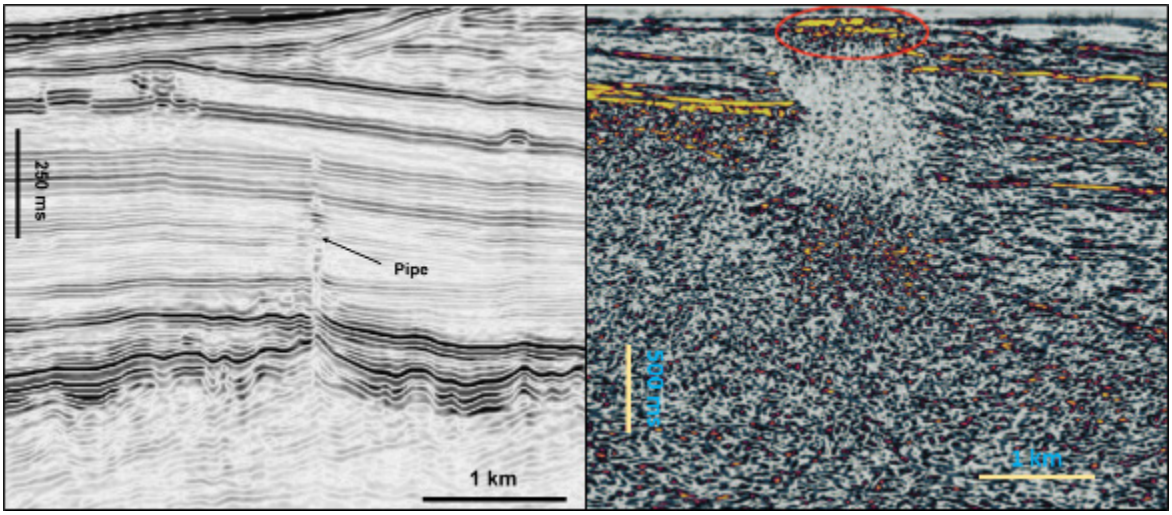

Figure 12: The leakage through a top seal in a localised effect (left) and on a broader breach as demonstrated by a gas chimney (right) can be observed on seismic data (Nourollah et al., 2010)

For shale seals, the spaces between shale platelets function as capillary pipes that can be envisaged as low aspect ratio pores that are connected across the platelets. When clay minerals in a shale sample are perfectly aligned parallel to the bedding and compacted on top of each other, they form a very effective seal that is unlikely to allow any significant amount of fluid to pass through (Figure 12a). The anisotropy (direction-dependent physical properties) of such shales has been extensively studied (Hornby et al., 1994) (Horne, 2013; Sayers, 1994). A particular manner of a leaking seal can be visualised as an aligned set of platelets with capillary pipes passing through this "domain" (Figure 12b). These capillary pipes can be considered connected, low-aspect-ratio pore spaces. The ability of a seal to resist fluid pressure depends on the radii of the capillaries (blue pipes in Figure 94b) as well as their abundance within the sample.

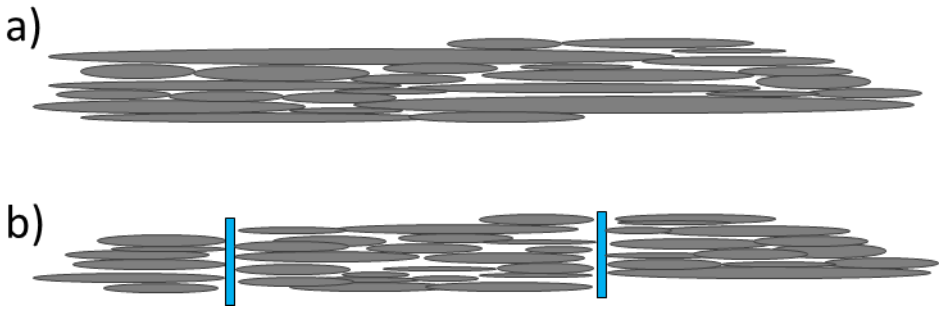

Figure 13: Schematic representation of a shale with all clay particles perfectly aligned along the bedding, which forms a very good seal (top) and a leaking seal (bottom). Leakage pipes or capillary pipes are represented in blue low aspect ratio connected pores across the bedding.

Any detectable breach in the seal occurs when the inter-platelet pore spaces exceed tens of nanometres. In comparison, the inter-platelet pore spaces, with typical intra-clay spacing range from 1-5 nanometres. When a seismic wavefront encounters the "clay and pore" medium, it generates stress (according to the effective medium theory proposed by (Berryman, 1995; Berryman, 1992; Jakobsen et al., 2000; Nishizawa & Yoshino, 2001) at the boundaries of vertical capillary pipes (or those that are perpendicular to the horizontal coordinate system that is fixed parallel to the bedding). This change is more pronounced in the horizontal direction because of the introduction of excess horizontal compliance, which is not present in the vertical direction. Therefore, the seismic sees a shale unit with a lower sealing capacity as less anisotropic, and in contrast, a more competent seal is sensed as more anisotropic.

A group of clay sheets that share the same orientation and are stacked together act as basic bricks to construct the overall elastic properties of shale. These regions are referred to as domains (Aylmore & Quirk, 1960). Disturbance to the alignment of clay platelets (or domains) is caused by a variety of sources such as silt and pore inclusions, low-aspect-ratio pores or capillary pipes (e.g. pyrite framboids and carbonate intraclasts). Further, shale can play host to burrowing agents that form the bioturbation of originally depositional features, i.e., (near) parallel beddings. A heavily bioturbated shale unit, depending on the type of infill created through bioturbation can be a better or worse seal compared to the undisturbed one. The presence of pore space in the shales essentially means a higher disturbance compared to the perfect alignment case of the domains.

It is uncommon to find shale formations with a neatly arranged, vertical porous structure that runs perpendicular to the bedding. The capillary pipes rarely occur in the form of undisturbed, vertical pipes. Additionally, in the real world, shale platelets are not uniformly aligned in the direction of the bedding. (Katahara, 1996) noted a significant discrepancy between the mode velocities of clay minerals and shales. The calculated mode velocities in clay materials were up to twice as large as the velocities measured in shales by (Castagna et al., 1985; Han et al., 1986; Tosaya, 1982). This difference can be attributed to the disorder of clay platelets in shales (Sayers, 2005). As a result, disorderly packing of the clay minerals lowers their (seismic) anisotropy and is also associated with a lower sealing capacity. For example, better alignment of sediments in a certain direction (i.e., in shale, this is lateral versus vertical) depicts itself as having higher

anisotropy on seismic. Therefore, well-aligned clay mineral platelets within shale are generally associated with better sealing capacity (i.e. fewer silts, disturbance of platelets, etc).

4.3 Seal Character

Seal character: areal and geometric extent, thickness, and internal heterogeneity of the seal.

Seal character is defined by its areal extent, thickness, as well as lateral and vertical heterogeneity. These characteristics are influenced and controlled by various environmental factors during the deposition of the sealing unit. The thickness and areal extent are largely controlled by the size of the sedimentary basin into which the unit was deposited and the tectonic and hydrodynamic forces acting on the basin (i.e. uplift and erosion, transgression, and regression). Heterogeneities within the seal relate to the provenance of sediments being deposited in the basin at the time of deposition, as well as diagenetic processes acting on the sealing formation after deposition.

Each aspect of the seal character is crucial in ensuring the integrity of a GCS project. However, the thickness of the seal stands out as particularly significant. For instance, in scenarios where no faults or fractures exist or have been induced or reactivated by GCS activities, any seepage through the seal would occur at significantly reduced rates (as discussed in section 4.2). Moreover, a thicker seal not only acts as a barrier against tectonic stress but also provides an additional safeguard against thermal effects. Additionally, considering that faults may be below seismic resolution, a thicker seal diminishes the likelihood of sub-seismic resolution faults penetrating through the entire seal sequence.

According to the *U.S. Geological Survey (USGS) National Assessment of Geologic Carbon Storage Resources*, a storage formation must be overlain by a low permeability, regionally extensive, robust sealing formation of approximately 30 meters thickness for shales and 6 meters thickness for evaporites (Merrill, 2013). It is worth noting that this range of thickness appears somewhat conservative when compared to the ranges found in published studies on natural and modelled CO_2 storage (Merrill, 2013).

To understand seal characteristics, detailed geological studies, including core analysis, well logs, seismic mapping, and calibration to other geophysical datasets, are essential. Environmental factors such as non-deposition or erosion can lead to the development of failed top or lateral seal geometries, particularly when considering saline aquifer storage complexes. Figure 14 illustrates a structure where both units A and C need to be competent seals for Reservoir B to be a viable CO_2 storage option. Appropriate seal characteristics must be present for a storage reservoir to successfully contain and permanently store CO_2. This includes a laterally continuous top seal (unit A, Figure 14), vertical continuity and thickness to prevent leakage via migration and overall integrity of the containment zone.

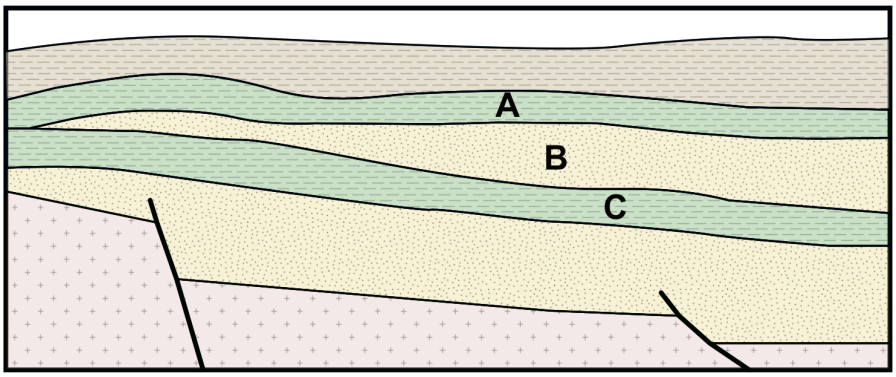

Figure 14: Schematic of a potential CO_2 storage site. Reservoir B is vertically sealed by rock unit A and laterally sealed by rock unit C, both of which are critical for overall containment.

4.4 Seal Integrity

Seal integrity is the propensity of the caprock to fail in a brittle sense or a measure of the ductile behaviour of the caprock (Kaldi, 2011).

This section provides a short primer on geomechanics to provide context to the later sections of the report Readers are encouraged to consult existing literature (Kaldi, 2011; Zoback, 2010) for further details on geomechanics.

Rock Failure

There are three types of rock failure: compression, tension, and shear. A recent review of the geomechanical challenges associated with (GCS) identified the geomechanical mechanisms that may result in CO_2 migration out of a storage complex (Song et al., 2023). Excluding the risk of CO_2 leakage associated with well integrity, which is not addressed in this review, the primary mechanisms identified were:

1. Tensile failure: induce a tensile fracture through the caprock and the risk of subsequent buoyancy-driven CO_2 leakage into shallower horizons (including potable water sources)
2. Shear failure: at the caprock/storage unit interface.
3. Shear failure: fault reactivation.
4. Rock deformation: transferred to surface uplift that may impact facilities, perception etc.

The type of rock failure that forms the highest perceived risk in GCS is shear failure, which may manifest as i) shear failure of the intact caprock or ii) fault reactivation.

A common method used in industry to evaluate the possibility of rock failure by shear is the Mohr-Colomb approach (Labuz & Zang, 2012), which considers only the minimum and maximum principal stresses. It is a simplified model of rock behaviour. The Mohr-Coulomb criterion provides a framework that allows for both simplified analysis with arbitrary failure planes and a more detailed analysis that considers specific geological features such as weak faults (Rutqvist et al., 2008).

In standard applications of the Mohr-Coulomb criterion, the assumption is often made that failure could occur on any plane with arbitrary orientation, and the analysis involves two principal stresses to construct Mohr circles. However, when dealing with weak faults, the analysis becomes more complex because the orientation of the fault is known.

In such cases, a more accurate assessment of fault stability requires considering all three principal stresses, including the intermediate principal stress. This consideration leads to the need for three Mohr circles instead of the usual two. The intermediate principal stress becomes crucial in determining the effective normal and shear stress acting on the weak plane, especially when the fault orientation is not aligned with the maximum or minimum principal stress directions.

A disadvantage of the Mohr-Coulomb theory is that it ignores the effect of the intermediate principal stress, although it has an important influence on the behaviour of materials (Comanici & Barsanescu, 2018). Linear poroelastic isotropic models, such as Mohr-Coulomb, fail to capture the heterogeneous and anisotropic nature of sedimentary rocks (Akono et al., 2019). Alternative theories and criteria exist for shear failure assessment (e.g., Yu, von Mises) that require a larger number of geomechanical tests. By accounting for the intermediate principal stress, these criteria acknowledge the influence of stress states that deviate from simple uniaxial or triaxial conditions. This consideration is particularly relevant in situations where the stress distribution is more complex.

In-Situ Stress

Determining the in-situ stress is critical for seal integrity. Stress conditions can exhibit significant variability both temporally and spatially as determined by different processes that may operate locally or regionally (Grande, 2022). The present-day in-situ stress state is a combination of mechanisms that have occurred over millions of years and therefore, understanding the processes that have contributed to the current stress state is valuable. A seal that has been deeply buried and subsequently uplifted will have the potential for natural fractures to form as the formation is exhumed.

As an example of the complexity of the present-day in-situ stress state, a recent study investigated various structures in the North Sea (Horda Platform, Endurance Structure, Aramis Structure, Lisa/Nini Structures)(Grande, 2022). Eight stress generating mechanisms were identified to have contributed (in various degrees) to the current day stress state of the Horda Platform. These mechanisms are:

1. Ridge push/compression
2. Continental margins
3. Sediment loading rates
4. Deglaciation
5. Differential loading
6. Uplift
7. Diagenesis and thermal compaction
8. Thermal anomalies

The minimum horizontal stress (S_{hmin}) is one of the principal subsurface stresses, typically orthogonal to the maximum horizontal stress. Understanding this stress is crucial for several aspects of operation planning and management, including wellbore stability, reservoir and caprock integrity and fault stability. S_{hmin} can be estimated from formation injection tests such as leak-off testing (LOT), extended leak-off testing (ELOT) and diagnostic fracture injection testing (DFIT). While all these tests differ slightly, they rely on the same principle of pressuring the wellbore to formation breakdown and observing the fracture closure pressure to determine S_{hmin}. Formation integrity testing (FIT) is another type of injection test typically used when drilling to ensure the ability to drill ahead safely with designed pressures. It involves pressuring the wellbore to the designed pressure with no intention of breaking down the formation. In the absence of other injection data, FITs can provide a lower bound for estimating S_{hmin} (Raaen et al., 2022).

During an ELOT (Figure 15) mud is pumped into the open-hole interval just below the casing shoe, resulting in an increasing pressure that is proportional to the volume of mud pumped into the hole. A deviation from a linear increase (at "leak-off pressure") indicates that the formation is losing integrity. In an ELOT, the formation is pushed past the leak-off point until the formation breaks down via fracture propagation. The decay of the fracture pressure after pumping has ceased allows the fracture closure pressure to be determined, which is a measure of minimum horizontal stress. Mini-fracs can be performed on wireline and follow similar principles to ELOTs. However, inflatable packers make it possible to pressurise small intervals (~ 1 m) until a tensile fracture develops.

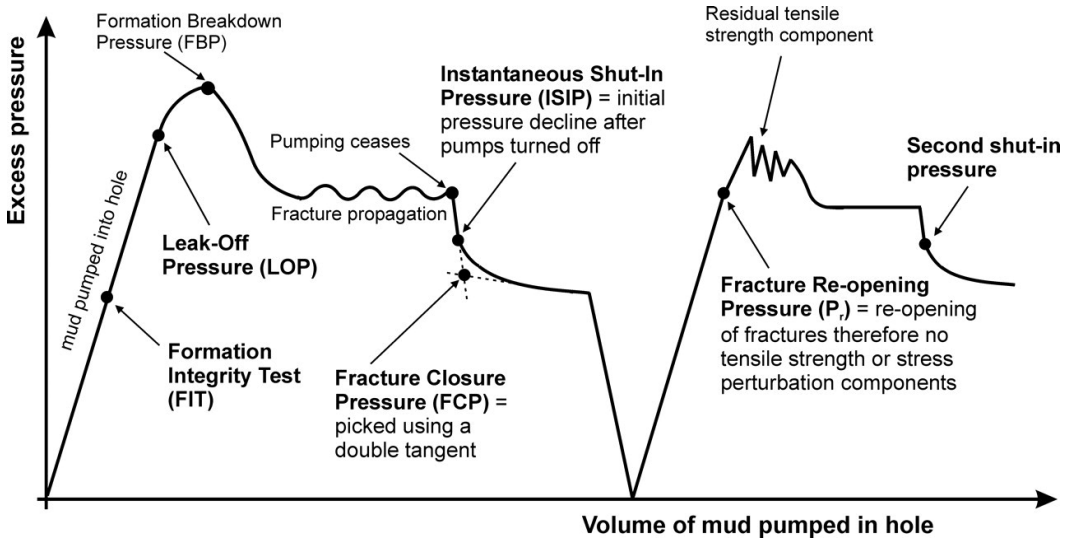

Figure 15: An illustration of the data obtained from extended leak-off testing (White et al., 2002)

In addition, ELOTs allow the tensile and maximum horizontal stresses to be calculated. Tensile stress can be estimated from the fracture breakdown pressure and fracture propagation pressure. This can then be combined with pore pressure obtained from formation testing tools to estimate the maximum horizontal stress. These are essential inputs when modelling fault stability and the geomechanical response of a storage complex.

A recent study detailed the characterisation of the in-situ stresses on the Horda platform related to the Northern Lights project and provides an example of the types of data that may be gathered as part of site characterisation (Thompson, Andrews, Wu, et al., 2022). Equinor has also recently published a study that quantifies the relationship of in-situ stress versus depth and pore pressure with a focus primarily on the Norwegian Continental Shelf (Thompson, Andrews, Reitan, et al., 2022).

In addition to analysing ELOTs and mini-fracs from the region of interest, drilling-induced fractures (DIFs) were identified on image logs. The authors propose that the DIFs in the Eos well were caused by transient pressure, temperature and chemical effects indicating that the Drake caprock shales are sensitive to these effects (Thompson, Andrews, Wu, et al., 2022)

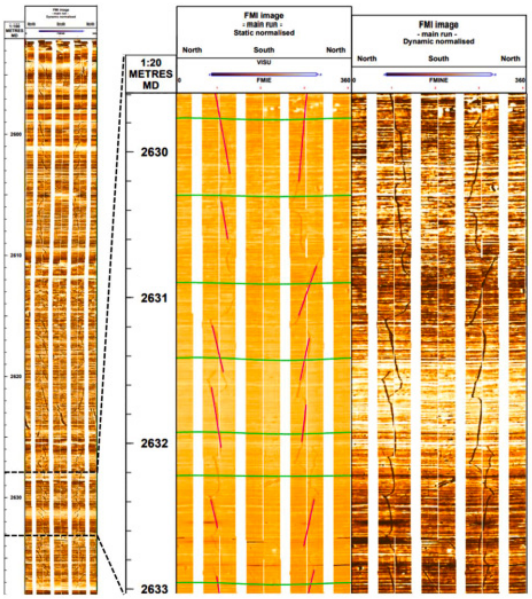

Figure 16: Drilling-induced fractures identified on an image log from the NO 31/5-7 (Eos) well (Thompson, Andrews, Wu, et al., 2022)

Depleted Hydrocarbon CO_2 Storage

Reservoir-caprock systems do not behave in a perfectly elastic manner as changes in pore pressure result in the redistribution of the natural stress state of the system. For depleted hydrocarbon CO_2 storage, pressure changes during the depletion phase can impart some permanent changes to the reservoir such as pore collapse or compression of the rock matrix due to changes in pore pressure and effective stress (Oldenburg, 2006) or fault reactivation (Kivi et al., 2022). This may be due to the simple increase in effective stress that is felt in the reservoir; alternatively, it may be a result of more complex effects in which fundamental far-field stresses are locally modified during depletion and subsequent repressurisation .

Either way, mechanical changes that occur during the depletion phase of an oil or gas field imply that the reservoir-caprock system will likely not return to its initial state when pressurised with large volumes of CO_2. In the case that permanent damage, fault reactivation or pore space collapse (or all of the above) has occurred during the depletion phase, it is easy to understand why the system would not behave elastically. Critical rock properties have changed, new faults or fractures have been created, and the prevailing directions of stresses may have been altered, which means that the CO_2 storage complex is different than before production was started. Even in the case where no obvious damage has been imparted to the field during production, the field is unlikely to return to its original state due to the complex poroelastic responses of the reservoir and caprock.

Any contraction of the reservoir that results from poro-elastic deformation also relieves the in-situ lateral stress, which causes the minimum horizontal stress to decrease by some degree. The reduction in the minimum horizontal stress during reservoir compaction due to poroelastic deformation is attributed to the predominant compaction occurring in the vertical direction (uniaxial strain). As lateral movement is confined the strain is accommodated through a reduction in lateral stress. When the reservoir is pressurised, the same phenomenon occurs but in the opposite sense, with the minimum horizontal stress increasing.

There are also corresponding stress changes in the overlying caprock to preserve an average regional stress tensor because of the imparted stress changes at the reservoir level. If the minimum horizontal stress decreases in the reservoir, then an increase is expected in the cap rock, and vice versa. This example of stress transfer within a reservoir-caprock system is shown in Figure 17, with corresponding effects on brittle

deformation processes in the caprock. Stress evolution in the reservoir caprock system starts to get very complex as depletion and re-injection occurs, especially if some plastic deformation or reservoir compaction has occurred, which fundamentally changes the rock's mechanical properties.

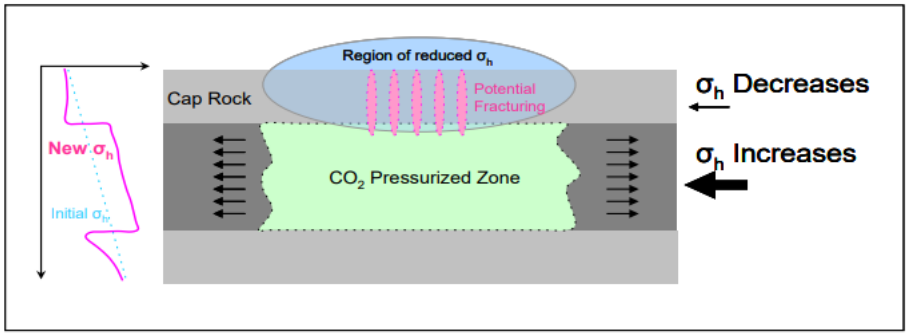

Figure 17: Schematic showing the opening of the tensile fractures in the case of CO_2 injection. The pre-existing (closed) fractures (top) may open as well as new fractures to form (bottom) (Marsden, 2007)

A recent review of caprock integrity in depleted hydrocarbon reservoirs highlighted that mechanical rock properties for caprocks are less readily available than the highly characterised flow units (Paluszny et al., 2020). A summary of the caprock properties from a selection of pilot GCS sites globally is provided in Table 5It highlights the measured rock mechanical data (Young's modulus (E), Poisson's ratio, and Unconfined Compressive Strength (UCS)) that are publicly available at the pilot sites.

In the absence of direct measurements, mechanical rock properties can be inferred through various methods using seismic data and petrophysical well logs. Seismic velocity analysis, involving the study of compressional and shear wave velocities, can provide estimates of parameters such as Young's modulus and Poisson's ratio. Petrophysical well logs, including density, sonic, and shear sonic logs, offer valuable data for estimating elastic constants and mechanical properties. If available, laboratory measurements from core samples can be used to calibrate empirical relationships between mechanical properties and petrophysical logs.

Table 5: Caprock integrity data for GCS in depleted hydrocarbon reservoir projects (Paluszny et al., 2020)

Project/ Region	Storage Site	Age	Primary Seal	Thickness (m)	Porosity (%)	Permeability (m^2)	E (GPa	Poisson (:)	UCS (MPa)
Snøhvit	Snøhvit Field	Mid Jurassic	Nordmela Fm.	60–105, 62–200	13	1–23×10^{-15}	-	-	-
Heletz	Heletz-Kokhav	Lower Cretaceous	Rewaha shale	23–54	6-10	1×10^{-18}	0.3-8	0.4	-
K12-B	Leman Gas Field	Late Carboniferous-Permian	Upper Permian Zechstein anhydrite, halite evaporites	550	-	-	-	-	-
Schwarze Pumpe	Ketzin	Upper Triassic	Claystone	165	-	-	-	-	-
Lacq	Rousse Gas Field	Jurassic	Flysch Sequence (clay and marl)	> 2000	-	-	-	-	-
In Salah	Krechba Gas Field	Carboniferous	Carboniferous Visean mudstone	900–950	1	1 × 10^{-14}	-	-	-

Otway International Test Centre	Naylor Field	Late Cretaceous (91–89.5 Ma	Belfast Mudstone (89–82 Ma)	280	<15	$<1\times10^{-15}$	8-16	0.3	9970–14,830
ROAD	P18-4 depleted reservoir	Triassic	Solingen, Rot, Muschelkalk and Keuper Fm., Upper Germanic Trias Grp	200	-	-	26	0.3	-
Peterhead	Goldeneye Field	Cretaceous	Carrack Fm.	40–100	6	1×10^{-20}	20	0.15	-
Barendrecht	Barendrecht	Triassic	Claystone	90	-	-	-	-	-
Hunterston	East Irish Sea Hamilton	Triassic	Sandy mudstones and halite, Mercia Mudstone Grp. Leyland Fm.	< 594	20-40	-	-	-	-
Edmonton, Alberta	QUEST	Cambrian	Middle Cambrian shale (Deadwood Formation)	50	-	-	-	-	-

Practical Seal Integrity

Seal integrity is a function of many factors such as lithology, rock fabric, regional stresses and orientation and stress change due to depletion or repressurisation. The concept of a *relative integrity factor* for assessing the integrity of seals based on their ductility and compressibility has been presented previously (Kaldi, 2011). Ductility/compressibility are inversely related to the sonic velocity/strength of a lithology. Figure 18 illustrates this relationship for the relative change in properties of various lithologies. This approach was developed to be applied when assessing CO_2 closure storage (section 3).

An underlying premise is that as the carbonate content of the siliciclastic composition of the caprock increases, the integrity factor decreases, and the propensity to develop structural permeability increases (Figure 18).

- **Excellent:** Halite, Sulphate, Organic Shale
- **Good:** Silicate shale, Calcareous shale
- **Marginal:** Argillaceous / Dolomite, Limestone
- **Poor:** Chert, Sandstone, Siltstone

Whilst anhydrite can be an excellent seal, a high fraction of brittle dolomite in anhydrite intra-beds can impact the seal integrity, allowing greater potential for along-fault leakage.

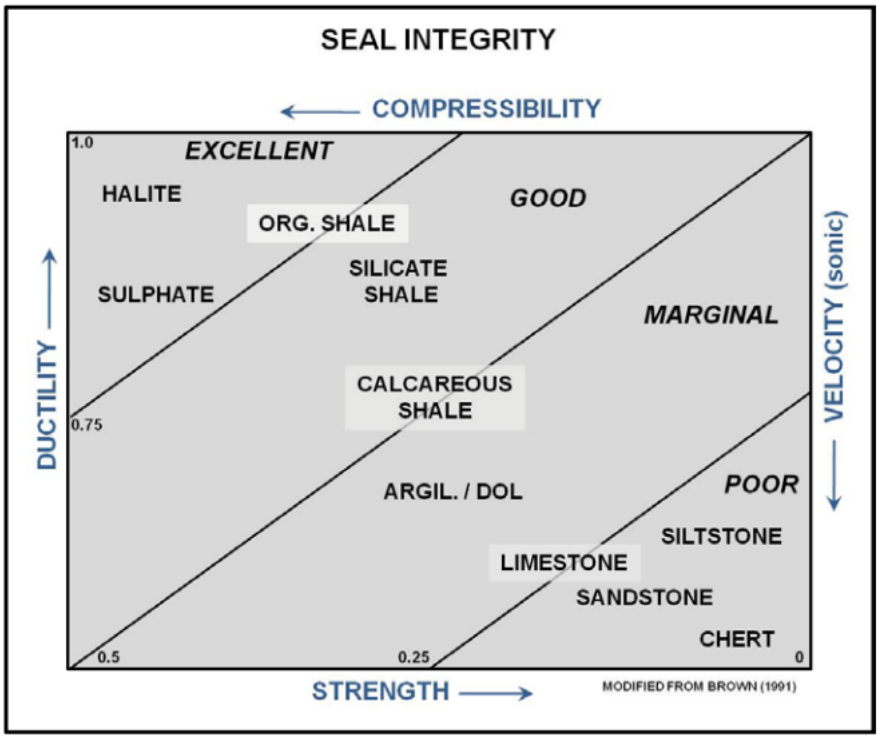

Figure 18: Seal Integrity Factor for different seal types (Kaldi, 2011). A relative integrity factor can be assigned from 1 in the upper left to 0 in the lower right.

The concept of developing an index that reflects the brittleness of different caprocks as an approach to a practical assessment of seal integrity has been discussed previously (Kaldi, 2011). In this work, the authors provide an overview of determining the Brittleness Index (BRI) by applying a method in which the unconfined compressive strength (UCS) of the sealing lithology is calculated using an empirical correlation based on p-wave velocity and represented as a ratio to the UCS of a normally consolidated rock at the same depth (Ingram & Urai, 1999). A BRI > 4 can be considered as brittle. The BRI can be combined with an assessment of the available data for the caprock, which may range from plentiful (core, FMI, etc.) to a complete absence of data and geological concepts.

Table 6: Brittleness Index Ranges and Qualitative Definitions (Kaldi, 2011)

Qualitative Definition	Range
Very Good	1 < BRI < 2
Good	2 < BRI < 4
Bad	4 < BRI < 6
Very Bad	6 < BRI < 8

4.5 Basin-Scale Processes

The following section provides several thematic examples of the large-scale impact of pressure on seals. This is an important topic. There is currently a dearth/shortage of research in this field of research, and it will have significant implications for both the assessment of seal integrity and the large-scale global implementation of GCS.

Several mechanisms can drive pore pressure increases, including:

- Disequilibrium compaction
- Hydrocarbon generation
- Tectonic loading
- Fluid migration
- Overpressured shales
- Salt diapirism

The key relationship with geomechanics is pore pressure stress coupling. This varies depending on the basin, and the stress path is not completely reversible. For example, if you deplete a reservoir and inject again, it is unlikely to follow the same stress path.

Gippsland Basin, South-Eastern Australia: Facies-Related Changes in Top Seal Integrity

The Gippsland Basin is situated in southeastern Australia, approximately 200 km east of Melbourne, Victoria. The basin, which has onshore and offshore elements, is a world-class hydrocarbon province, containing several giant oil and gas fields (Figure 19). Reservoirs are principally the Latrobe Group siliciclastics, of Late Cretaceous to Eocene age, sealed by the Oligocene Lakes Entrance Formation, which is dominated by thick, smectitic claystones in more basinal settings. Lakes Entrance Formation smectites are very high-quality seals, but seal integrity decreases rapidly towards the margins of the basin, where thinner, more carbonate-rich facies dominate (Figure 19).

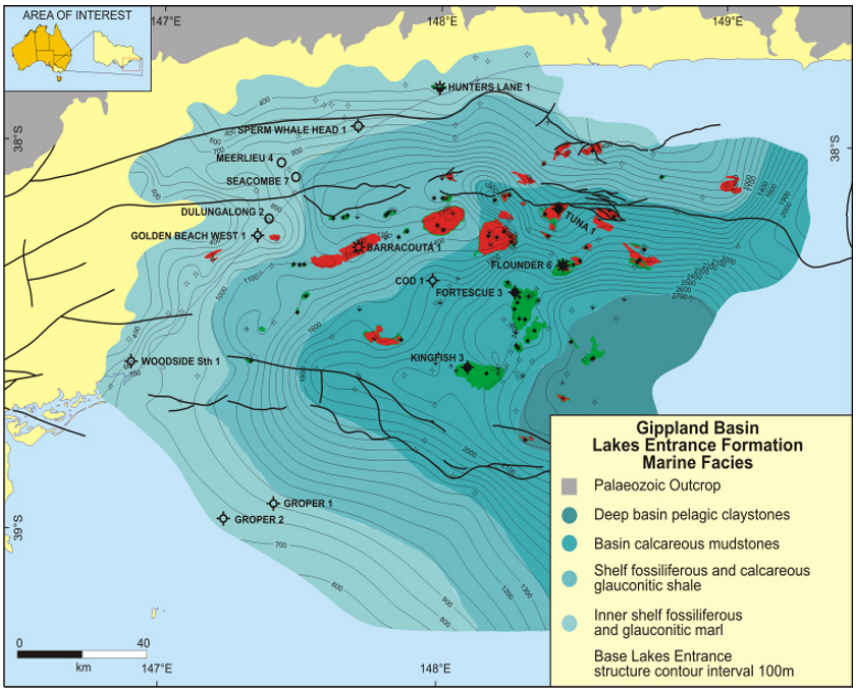

Figure 19. Basal sedimentary facies identified within the Lakes Entrance Formation marine sequence. Modified after (O'Brien et al., 2008)

The basin's fluid flow architecture is dominated by two highly connected fill-spill chains (Figure 20)(O'Brien et al., 2008)(O'Brien et al., 2013) at the base of the regional seal (top reservoir), where over 85% of the hydrocarbon inventory has been discovered. Strong hydraulic connectivity exists between the onshore and offshore reservoir elements, with strong recharge flowing broadly from west to east. Petroleum production from giant oil and gas fields offshore, combined with very high water cuts within the oil fields over the last 25 years, has resulted in the substantial pressure and physical draw-down of the Latrobe Group aquifer.

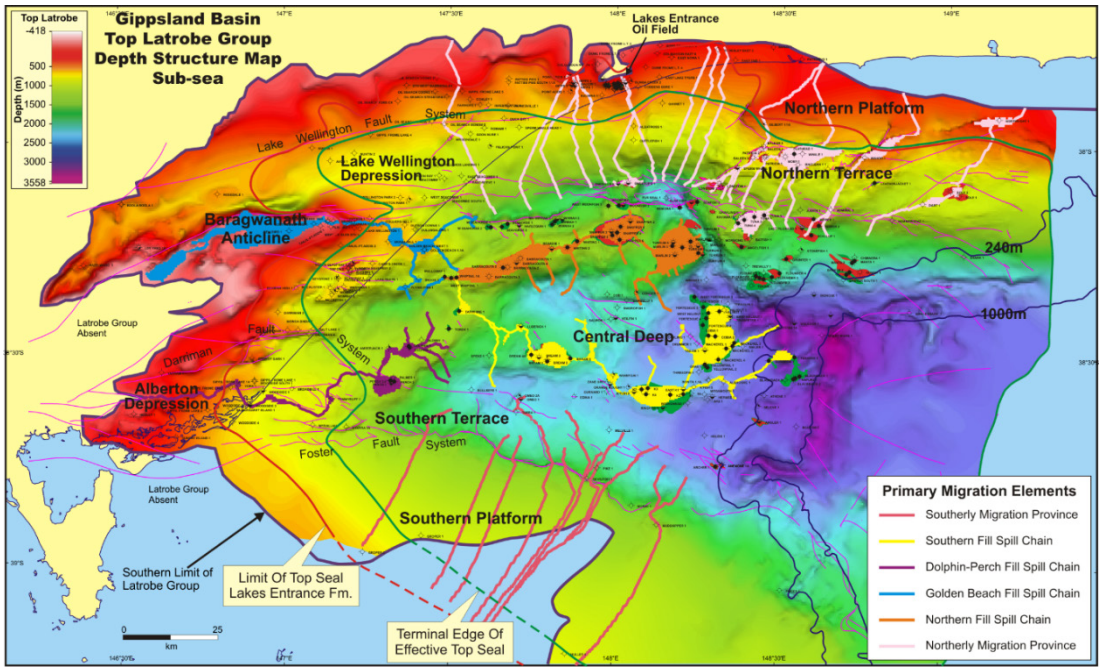

Figure 20. Top Latrobe depth map, Gippsland Basin, showing migration vectors sourced from a northernly and southernly migration province. Injection within the Contral Deep will migrate into Top Latrobe traps and fill spill between trans due to highly focussed migration pathways. Modified after (O'Brien et al., 2008)

The Gippsland Basin, in general, and the depleted Latrobe Group siliciclastics, in particular, have long been recognised as representing Australia's premier potential carbon storage sinks, with a combination of world-class reservoirs and top seals (O'Brien et al., 2008; O'Brien et al., 2013). Two GCS projects are currently being actively considered for the basin: the nearshore CarbonNet Project and, in the mid-basin, ExxonMobil's SEA CCS Project. These multi-million tonne per annum (Mtpa), multi-decadal projects represent welcome investments but in combination, and especially if complemented over time by other, as-yet-unannounced injection projects, also represent potential long-term challenges regarding the management of the storage resources (and the pressure space or headroom) within the basin.

Unpublished data (O'Brien, unpublished studies; Dr Jim Underschultz, personal communication) suggest that the reinflation of the depleted Latrobe Group siliciclastic system could be partially to significantly achieved by 10-20 Mtpa of CO_2 injection over 30+ years. Such a reinflation could potentially place additional stress upon the regional top seal. Work on the top seal integrity by (O'Brien et al., 2008; O'Brien et al., 2013) has shown that the Lakes Entrance Formation top seals around the edges of the basin are thinner, much more carbonate-rich and can support much smaller CO_2 columns (Figure 19; Figure 21a, b and c respectively) than the more deeply buried, smectitic seals that dominate the more central parts of the basin. In addition, the smectite-dominated seals are inherently more plastic and would respond in a more ductile manner than the relatively brittle, carbonate-rich seals around the basin's edge.

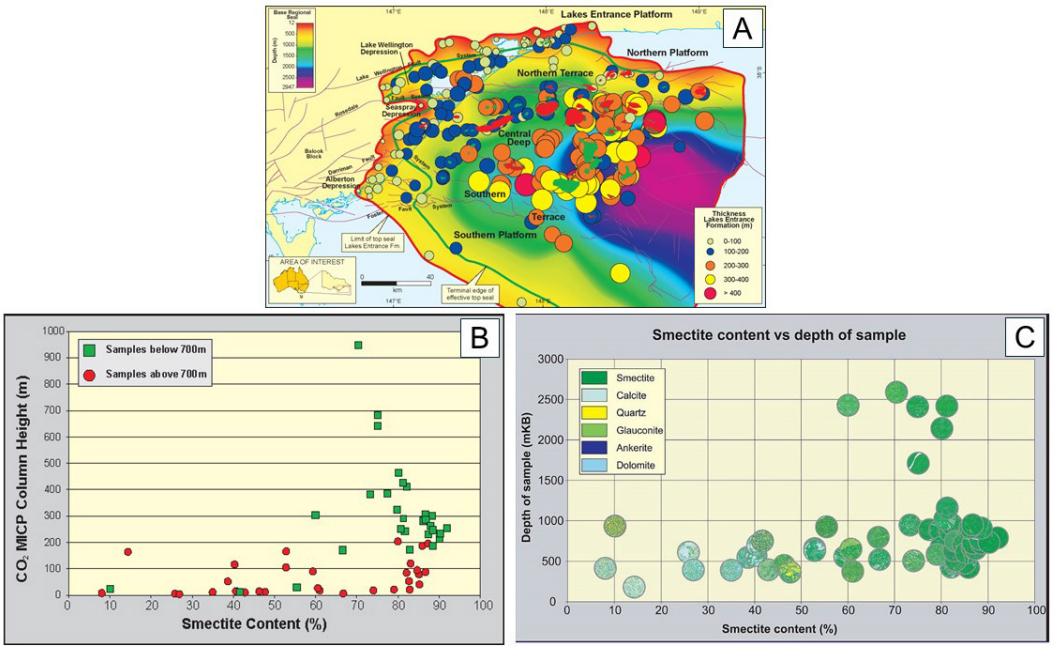

Figure 21. Mineral and seal quality of the Lakes Entrance Formation. A) Thickness map of the Lakes Entrance Formation B) CO_2 MICP column height vs smectite content of the Lakes Entrance Formation C) Smectite content vs depth of sample in the Lakes Entrance Formation

The above contention is supported by observations on the distributions of gas chimneys and other direct hydrocarbon indicators within the Gippsland Basin (O'Brien et al., 2013), which can, at a minimum, be used as proxies for seal quality, at least in areas where an active petroleum system is present. Leakage and seepage indicators in the Gippsland Basin are almost exclusively present in areas where the top seal is thin and carbonate-rich. Furthermore, automated mineral mapping has revealed that these carbonate-rich seals often contain micro-scale fractures and voids, in contrast to the very dense nature of the smectitic claystones (O'Brien et al., 2013).

Other surrogates for seal integrity have been identified in the Gippsland Basin. For example, Fluid Inclusion Stratigraphy (FIS) data is consistent with the indicators provided by seepage indicators. In well data from around the basin's edge, the FIS data reveal the presence of thermogenic hydrocarbons above the regional seal, whereas deeper in the basin, where the seal is of high integrity, no such anomalies are found (O'Brien et al., 2013). This observation suggests that approaches such as FIS might be a useful tool in assessing seal integrity, either above depleted fields in mature basins or especially in less well-constrained saline aquifer settings.

These observations, taken together, indicate that a regional assessment of seal quality and integrity can be used as part of a first-order management tool for not only initially predicting the locations of lower-risk carbon storage sites and then assessing the likelihood of seal failure in mature storage settings when the basin is well into the pressure reinflation phase. This, of course, applies primarily to storage systems situated at the base of the regional seal. It can also be used to assess the probability of the presence of a robust secondary containment system through a basin's storage lifecycle for storage systems relying upon deeper (sub-regional seal) sealing systems or baffles.

Vulcan Sub-basin, Bonaparte Basin, Timor Sea: Fault Seal Failure

The Vulcan Sub-basin within the Bonaparte Basin, Timor Sea is an area of significant Pliocene fault reactivation, which resulted in the partial to complete breaching of numerous charged traps within the region (Figure 22) (O'Brien et al., 1996; O'Brien & Woods, 1995). This tectonism was related to the flexural extension associated with the formation of the Timor Trough, located immediately to the northwest of the Vulcan Sub-

basin. The fault reactivation, which resulted in Neogene faults with 50-300 m of displacement, produced distinct seismic anomalies called hydrocarbon-related diagenetic zones (HRDZs) (O'Brien & Woods, 1995) above the leaking reservoirs. Mapping of these HRDZs (Figure 23) has allowed the leaky fault segments to be mapped accurately throughout the Vulcan Sub-basin.

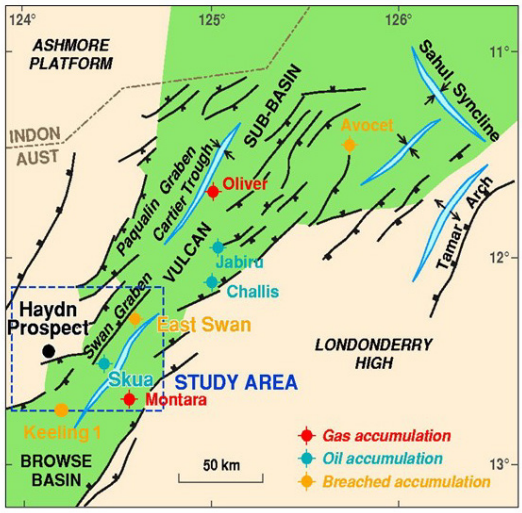

Figure 22. Location Map of the Vulcan Sub-basin showing key hydrocarbon accumulations. Modified after O'Brien & Woods, 1995.

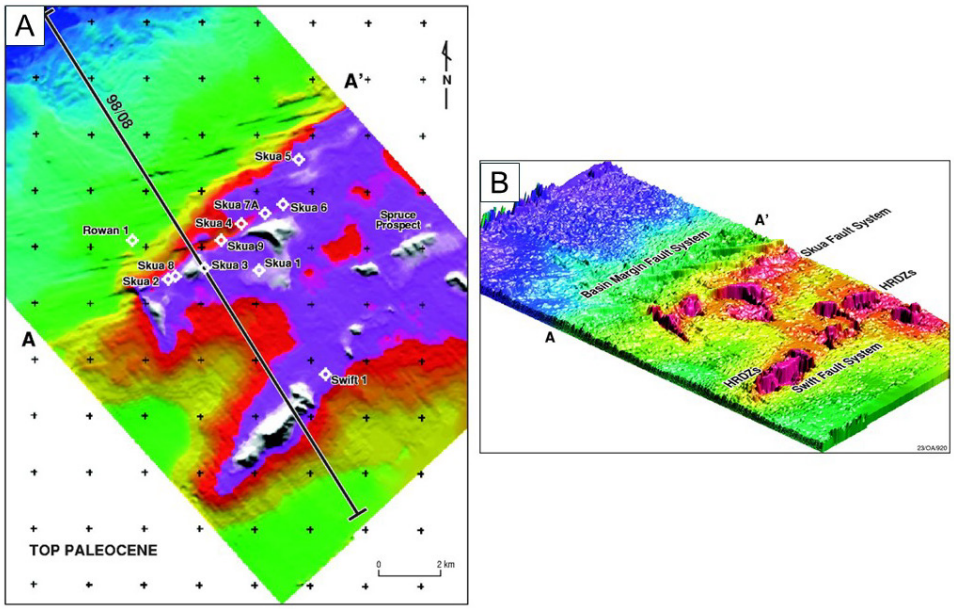

Figure 23. Top Palaeocene TWT images. Zones of leakage are revealed as top Palaeocene highs and are caused by leakage-related carbonate-cementation in the overlying Eocene section A) plan view B) oblique view. Modified after O'Brien & Woods, 1995.

Integration of the mapped HRDZs with detailed fluid inclusion-based charge history mapping of the underlying reservoirs and water column geochemical "sniffer" and other remote sensing data (O'Brien et al., 1996; O'Brien et al., 1998; O'Brien & Woods, 1995; O'Brien et al., 2002) has provided several key insights:

- Some of the traps in the Vulcan Sub-basin were completely breached during the Pliocene; the HRDZs above such traps are generally large, implying a substantial leaky fault segment (3,000-5,000 m long HRDZs) was present.
- Many of the traps in the region were partially breached and are still leaking hydrocarbons. HRDZs above such traps are generally small (<1,000 m long)
- Some traps, such as the Keeling gas accumulation, originally contained an oil leg 34 m thick; this leg was completely breached in the Pliocene; subsequently, the trap was refilled to spill point with gas (and the gas is not leaking).
- Traps that did not leak at all during the Pliocene (no HRDZs are present), such as the Oliver gas field (O'Brien et al., 1996) originally contained a thick oil leg which was subsequently displaced almost completely by later gas.

The observations from the Vulcan Sub-basin may have significant relevance to the concept of "sealing" in depleted reservoirs in particular.

Firstly, it is often stated that a given trap can hold injected CO_2 (i.e., it is a suitable storage location) because "*it has trapped hydrocarbons*". This is not necessarily the case, although it *could be* the case. Many of the commercial hydrocarbon accumulations within the Vulcan Sub-basin are still leaking at the present day via natural seepage. They would be, in the authors' opinion, *unsuitable for GCS because of sub-optimal containment*. The presence of a hydrocarbon column itself is not a guarantee of its suitability as a storage site. In the absence of clear seismic indicators (such as HRDZs) it may well be difficult to quantify the risks associated with trap breach in an area equivalent to the Vulcan Sub-basin. As such, the determination of the detailed charge history from fluid inclusion analysis represents a key derisking approach for previously charged but now depleted reservoirs; the authors strongly recommend this approach be adopted.

Secondly, traps such as Keeling were completely breached (i.e., lost their oil column) but then, with the relaxation of the Pliocene extensional stresses, resealed and resealed well enough to hold a gas column. Again, assessing the charge history for such traps provides the key observations. It may be that the assessment that previously breached traps such as Keeling would represent a significant containment risk.

Finally, unlike the Keeling Field, the Oliver gas field has always enjoyed high fault seal integrity and would represent a storage opportunity with low containment risk. However, in the absence of seismic indicators of fault seal failure (HRDZs) in a region, discriminating between a Keeling-type and an Oliver-type storage opportunity would be challenging.

In conclusion, areas such as the Vulcan Sub-basin provide insights into the complex interplays between potentially multiple charge histories and fault seal reactivation and fault seal integrity. In this region, the currently active gas generation and migration system could easily lead to erroneous interpretations of a given trap's GCS seal potential. Consequently, even where traps have traps have contained commercial volumes of hydrocarbons, a genuine multi-disciplinary approach to the assessment of seal potential should be adopted.

Multi-Project Interactions

The current greenhouse gas storage legislation in Australia and in many other jurisdictions (as discussed in section 11.3), does not recognise or consider what future multiple GCS developments within basins might look like and how these developments might operate or interact. If multiple, large GCS projects are active within a basin, such as within the Gippsland Basin, or on the northeastern flank of the offshore Bonaparte Basin in north-western Australia, for example, the interactions or potential interactions between individual storage projects will rapidly become significant, especially for million tonne scale storage within connected aquifer systems.

Issues such as increasing formation pressures resulting from injection, leading to rapid pressure inflation or reinflation, will need to be managed and perhaps managed actively (for example, section 6.2), as such processes could decrease the future storage potential for the entire basin system. Consequently, consideration of the likely "future states" for GCS in offshore Australia and elsewhere should be considered in the near- to medium-term. Such conceptual thinking, combined with future action, will help to mitigate what could become significant barriers to an expanding GCS network within these regions.

4.6 Summary

This section of the report introduced the various seal lithologies. While shale is the most common seal lithology for CO_2 storage, many other lithologies can serve as effective seals. These include less common lithologies such as chalks, coals, and evaporites and the potential to utilise composite seals for future GCS projects.

Later in the section, the concept of seal potential, which comprises seal capacity, seal geometry and seal integrity, was introduced. Seal capacity refers to the extent to which a column of CO_2 can be prevented from percolating through the entire thickness of the seal, which is primarily controlled by the permeability of the sealing lithologies; seal geometry is the areal extent of the seal (lateral continuity) and thickness; and seal integrity is the propensity of the caprock to fail in a brittle sense or its ductile behaviour. In reality, however, there is a mutual interdependency between capacity, geometry and integrity that is site-specific; therefore, these aspects cannot be analysed in isolation.

Seal capacity estimates should never be made in isolation from a regional understanding. Therefore, hydrodynamic considerations and using both CO_2 and oil/gas analogues are critical.

As mentioned, the existing definition of seal capacity relates to the capillary threshold pressure. However, it should not be assumed that once the capillary threshold pressure is exceeded, there is a substantial loss of containment from the storage formation. Invasion percolation (drainage) through low-permeability, porous media (i.e., a homogenous unfractured seal) progresses extremely slowly. An example of the quanta of leakage rates, if percolation across the seal occurs, is provided.

This section also provides an overview of seal integrity. This includes topics such as in-situ stress and rock failure mechanisms and a summary of the mechanical data derived from the GCS site using direct or indirect methods. Seal integrity, including the key risks and requirements for characterisation and monitoring, will be discussed in more detail later in this report.

Finally, several thematic examples of basin-scale processes are presented. These processes can have significant implications for assessing seal integrity and the large-scale global implementation of GCS. Therefore, given the current dearth of research in this field, future studies must aim to close this knowledge gap.

5. Long-Term Impact of CO_2 on Seal Formations

In addition to understanding the immediate to short-term effectiveness of a seal in preventing the upward migration of CO_2 from a storage reservoir, it is important to assess the long-term containment capability of the seal. Stakeholder concern over long-term seal integrity, despite significant leakage being highly unlikely, poses a barrier to the widespread implementation of CO_2 geological storage as an effective climate mitigation technology (Alcalde et al., 2018). Given the geological uncertainties and complex dynamic processes within a CO_2 storage site spanning thousands of years, accurately predicting the exact impact that CO_2 will induce on the seals of storage systems over these timescales is challenging. A capability to understand the processes that may lead to long-term risk is important, even when accurate prediction is unlikely given limitations in current modelling capabilities, to enable the reduction of risk to as low as reasonably practicable and to design appropriate monitoring plans.

CO_2 containment failure, in the unlikely case that it occurs, would take place over the short term around the injection phase of the project when seals are subjected to high levels of pressure, temperature, and geomechanical changes caused by the introduction of large volumes of pressurised CO_2 into the injection zone (Benson, 2007). Hydraulic fracturing, fault reactivation due to reservoir overpressure, and capillary breakthrough are the highest potential mechanisms for seal leakage, all of which occur in the short-term.

Over time, the pressure within the storage system decreases, particularly for an open saline aquifer, as it reaches equilibrium with the surrounding sedimentary system, and CO_2 dissolves into water. (Benson, 2007) illustrated that, due to pressure recovery, trapping processes and an increasing understanding of the storage system with operation, the risk of environmental impact associated with CO_2 storage is highest at the end of injection, and long-term risk is low (Figure 24).

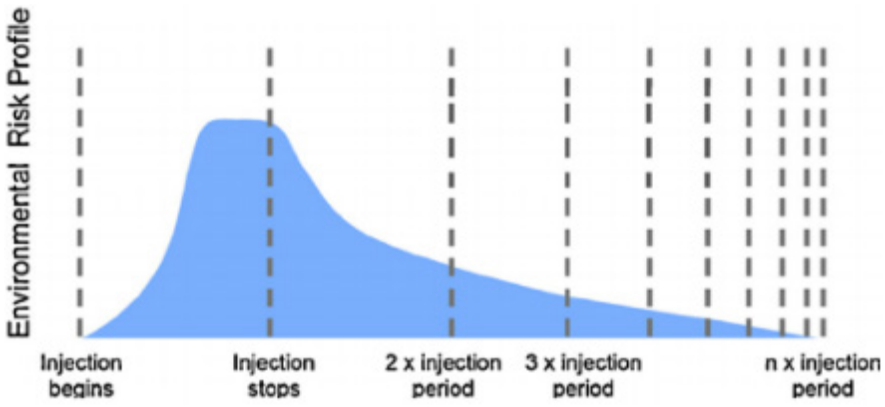

Figure 24: Risk profile for CO_2 storage (Benson, 2007)

Buoyancy-induced pressure and diffusion processes from injected CO_2 can bring about complex chemical and mechanical processes that should be considered for understanding long-term CO_2 containment. A top seal's capacity and integrity can alter from various CO_2 processes including:

- Dry and wet CO_2 induced fluid-rock interactions at the reservoir-seal interface or fracture-seal interface.
- Wet CO_2 diffusion into top seal's water, leading to changes in fluid chemistry and consequently fluid-rock interactions (Watson, 2012).

- Less investigated processes including CO_2 intercalation in clays (Myshakin et al., 2013) changes in electrical interaction between clay particles due to water acidification and displacement by CO_2 and caprock dehydration and capillary-driven volumetric contraction (Espinoza & Santamarina, 2012).

These processes can feasibly lead to an extremely slow migration of CO_2 through the top seal, although they are strongly controlled by the specific geological and in situ conditions at each individual storage site. Further, the migration through the top seal, particularly in such a slow diffuse manner, does not equate to leakage to the atmosphere or necessarily have any impact on other resources such as potable water, hydrocarbons, coal, or other minerals.

5.1 Geochemical Changes to a Top Seal

Geochemical reactions in sealing mechanisms are an important consideration for long-term containment of injected CO_2 and geomechanical integrity of the top and fault seals, although in most cases, the ability to seal geochemical reactions with CO_2 is severely hampered by seal permeability, and therefore, the importance of this process in site characterisation has reduced. If CO_2 can enter a previously near-equilibrium water-rock seal by diffusive processes, chemical conditions will be modified, and geochemical alteration will occur.

The impact of top seal chemical changes on rock strength can vary depending on the specific chemical reactions occurring and the characteristics of the rock. Due to the nature of a competent top seal, a barrier to fluid migration, it is fair to state that CO_2-related alteration is restricted by the fact that CO_2 entry into a seal rock is limited to the very slow processes of CO_2 diffusion or progressive chemical alteration at the reservoir-seal interface. Exceptions to this are when there are open fractures, poorer than expected capillary breakthrough, or other pathways into a seal.

CO_2 migration by diffusion relates to molecular transport of the CO_2 through the water-saturated seal's pore system. Diffusion is thought not to present a leakage process of significance in most cases (Busch et al., 2008). CO_2 diffusion studies are rare: diffusion investigations through caprocks from natural gas reservoirs concluded that, while diffusion is an ongoing process at the reservoir/caprock boundary, significant losses of reservoir gas occur in geological time scales of tens of millions of years (Krooss et al., 1996). Encouragingly, since CO_2 is reactive when diffusion occurs, the seal presents further storage potential, either dissolved in formation water or by geochemical processes. In most CO_2 storage cases, the rate of diffusion into the seal will simply be the determining factor for CO_2 mineral trapping reactions (Busch et al., 2010).

Mixing of CO_2 and reservoir formation water causes dissolution of the CO_2 and formation of carbonic acid and carbonate aqueous species (Xu et al., 2004). Note, that formation water is also able to be refreshed in certain cases due to density-driven convection cells, which can potentially further enhance dissolution (Ennis-King & Paterson, 2007). CO_2 dissolution is controlled by the temperature, pressure and composition of the formation water. In a non-buffered system, the initial dissolution results in acidic water.

In a reservoir system containing reactive minerals, the decrease in pH caused by CO_2 dissolution is buffered by reactions involving these mineral phases and hydrogen ions (H^+). Susceptible minerals are commonly Fe/Mg-rich clays, Ca/Mg-rich carbonates, Fe/Mg/Ca-rich ferromagnesian minerals and Ca-rich feldspars (Watson, 2012), although many more specific mineral phases may also exist. A breakdown of the likely order of susceptible mineral reactions is given in Figure 25. These reactions can result in the dissolution and precipitation of minerals depending on the availability of cations and evolving chemical conditions. These changes can modify the porosity, permeability, and rock strength. In all cases, the dissolution and precipitation reactions are a function of the thermodynamic factors, and the rates of the reactions are a function of the chemical kinetic parameters for the minerals involved (Xu et al., 2004).

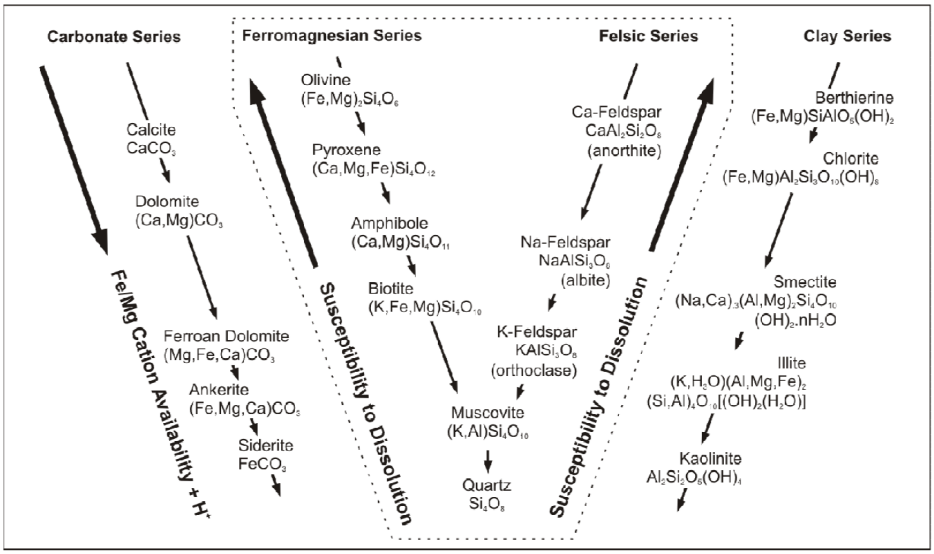

Figure 25: Preferential order of minerals susceptible to CO_2-related buffering and dissolution reactions. This order has been modified (after Watson 2012) from the Goldich (1938) series.

As with reservoirs, certain clays, carbonates, and other minerals, if present, are susceptible minerals to dissolution, so understanding the mineralogy of the seal is important. In reservoir rock, dissolution of minerals due to reactions with CO_2 can occur in as little as a few days, where CO_2 and acidified formation waters continually feed the reaction (Worden, 2023). Conceivably, in seals where minerals have a higher surface area, this reaction could be even faster. However, in seals, the reaction speed is strongly dependent on the flow of the CO_2 and acidified formation waters, which is severely hampered by the very low permeability. Furthermore, this hampered ability to refresh the formation water within the seal can result in re-precipitation of new mineral phases. Further still, the pH buffering capabilities of most seal lithologies can quickly overcome the capacity of the fluids to continue the dissolution process.

Therefore, the resulting reaction of acidic CO_2-rich fluids on the seal is likely to be slow and of limited penetration (depending on seal rock properties) and can be advantageous or disadvantageous to containment. A primary dissolution process may increase the seal's permeability, leading to the potential movement of CO_2 through the seal. Yet, in other cases, a re-precipitation process will decrease the permeability of the seal and contribute to the seal's capacity and integrity.

For example, studies of chlorite-rich reservoirs show the reaction of iron-rich chlorite (chamosite) in the presence of CO_2-enriched acidic waters does not result in net dissolution but rather the alteration to kaolinite and quartz. Further, the iron yielded from this reaction is then precipitated as siderite, mineralogically trapping the CO_2 (Watson, 2012).

In addition to changes in mineralogy resulting from dissolution and precipitation reactions, the impact on geomechanics must be considered. Alteration of cement may affect the overall cohesion of the rock. Weakening or strengthening of the cementing materials can influence the rock's strength. Further chemical changes can also cause the top seal to undergo swelling or shrinkage. Some minerals may expand or contract upon hydration or dehydration (at the reservoir-seal interface), which can induce stress within the rock and potentially impact its integrity.

Montmorillonite, a primary clay mineral in many top seals (along with other clay minerals such as illite, kaolinite, and chlorite), is a particularly important mineral to understand. Montmorillonite is a type of smectitic clay mineral known for its expandable layered structure. The interlayer spaces between these layers can accommodate various guest molecules, including water and CO_2. Montmorillonite changes can strongly influence the geomechanical properties of a top seal due to its plasticity, permeability, and ability to swell

through water absorption or shrink through CO_2 intercalation (Myshakin et al., 2013). Understanding the CO_2 intercalation process into montmorillonite is relevant as it may impact the performance of the seal.

At a fundamental level, there is a reasonable understanding of the reactions involving acidic CO_2-rich fluids in seals based on generic studies in reservoir rock. However, there is still limited knowledge about the geochemical reaction kinetics and how they relate to changes in flow properties and even less is known regarding the changes to geomechanical properties specific to top seals. A study by (Rohmer et al., 2016) investigated the changes in geomechanical properties due to chemical changes to reservoir and seal rock. Generally, this study found that the short-term impact on the intact seal rock was limited and that further work, based on CO_2 natural analogues, is required to improve the understanding of long-term geomechanical impacts, ideally combined with dynamic modelling. (Rohmer et al., 2016) also found that chemical-mechanical changes associated with fault were low, although it was noted that data for carbonate-filled fault gouge was absent.

Improving our understanding of top seal behaviour can be achieved through laboratory studies, modelling, and analysis of natural analogues. To conduct these studies, obtaining samples is essential for investigating the chemical and geomechanical properties. This emphasis on acquiring high-quality core samples from top seals marks a significant departure from the traditional priorities of petroleum exploration and production projects, which typically focused on demonstrating the effectiveness of top seals based on the presence of trapped hydrocarbons (Worden, 2023).

5.2 Role of Faults and Fractures

Geological deformation can form fractures, faults, and fault arrays across a storage system due to a range of natural processes (including tectonic plate movement, folding, gravitational sliding, volcanic intrusions, crustal unloading and salt movement) and anthropogenic activities (including fluid extraction or injection, thermal change).

For some potential CO_2 storage systems, the resulting deformation can provide fluid conduits, sufficient displacement for juxtaposition of reservoir against non-seal, or lineaments of geomechanical weakness relative to the intact top seal. By developing an understanding of the locations, geometries, displacements and properties of faults and fractures in the target storage reservoir and caprock, and how will these faults and fractures impact (either positively or negatively) the flow of CO_2 during and after injection, decisions can be made for whether a storage system containing faults and fractures is suitable for CO_2 storage (Kaldi et al., 2013).

The storage system, at least in most cases, experiences the maximum change in pressure, temperature, and geomechanical conditions during the storage operational phase (Benson, 2007) the risk of seal leakage through faults and fractures is most acute during the injection phase. However, there are some long-term geochemical processes that can occur, particularly if CO_2 can flow along or through a fracture or fault plane, which may result in CO_2 loss or changes in geomechanical properties of the seal system.

The geomechanical properties of a caprock seal are controlled by the interplay between the regional stress regime, pre-existing faults and fractures; these can be enhanced by pressure and temperature changes associated with the stored CO_2. Understanding the changed stress state and geomechanical properties of the caprock due to the CO2 storage operation and then potential changes in material properties (e.g., cement types, shale gouge/clay smear) as a result of interaction with CO_2 is important for the long-term evaluation of seal integrity.

5.3 Geochemical and Geomechanical Modelling of Seals

Free-phase CO_2 intrusion into seals, assuming no mechanical failure of the caprock, is unlikely due to their high capillarity. In the cases where this could occur, the process would be very slow. As such, top seals are commonly treated using no-flow conditions in simulation models. However, some efforts have been to model the long-term impact of CO_2 on seals. This modelling considers the likely degree of change caused by chemical reactions and the resulting modifications caused by seal geomechanics. It represents a complex challenge, as the models need to represent the processes of CO_2 flow into the seal, the evolving chemical changes in the CO_2-brine-rock reaction, and the changes in geomechanical properties as the top seal or fault seal materials evolve.

Some simplified geochemical modelling, commonly supported with laboratory work, of CO_2 transport process and the CO_2–brine–rock reaction into top seals has occurred, mostly for shale top seals (Fatah et al., 2022; Gaus et al., 2008; Liu et al., 2012). These studies have concluded the following regarding CO_2–brine–rock reaction modelling and relevance for CO_2 storage:

- CO_2-brine-rock reaction modelling is hampered by limited knowledge of thermodynamics and reaction kinetics in seal lithologies, making it difficult to attribute adequate timescales for reaction and trapping processes. There are insufficient details to provide a complete basis for geochemical modelling (Liu et al., 2012). This is further complicated by the complexity of considering geomechanical effects (Gaus et al., 2008). More laboratory and modelling-based studies are recommended to progressively build the knowledge base for CO_2-brine-rock reaction modelling in seals.

- When CO_2 invasion can occur, top seals will be generally reactive due to the heightened presence of reactive minerals and higher surface areas. There is much variance in the rates of reaction, with authors varying their modelled reaction duration from 10s to 1000s of years for initial dissolution reactions. While models show an initial vertical migration of CO_2 into the caprock, the vertical migration process slows down rapidly, and vertical transport distance of CO_2 is almost unchanged over periods of 100 to 1000 years.

- Modelling commonly indicated that feldspar, calcite, and clay minerals dissolved in CO_2-saturated brine due to the formation of carbonic acid, while quartz, secondary clays and carbonates can precipitate, at a high level, as indicated in the process in Figure 25. The CO_2–brine–rock reaction during CO_2 intrusion into the caprock can change porosity and permeability, initially by dissolution reactions, then precipitation. Many researchers suggest that in the long term, the sealing capacity of top seals is enhanced due to geochemical processes (Gherardi et al., 2007; Yang et al., 2020).

Other laboratory testing of note has been performed on samples from carbonate-bearing sandstone samples, specifically the Captain Sandstone from the depleted gas condensate Goldeneye Field in the UK North Sea, which is being considered for GCS (Hangx et al., 2013). In this study, the primary objective was to assess the effect of carbonate cement dissolution on mechanical and ultrasonic properties and its impact on failure strength. It was concluded that the continuous flushing of the material with CO_2-saturated brine and the removal of calcite did not affect material strength or elastic properties. However, other candidate fields at shallower depths may have a composition with less cementation (i.e. quartz). These fields will have generally been subjected to less diagenesis than the Captain Sandstone and should still be assessed site-by-site (Hangx et al., 2013).

5.4 Analogues for Understanding Long-Term Seal Capacity and Integrity

As CO_2-water-rock interactions typically unfold over extended time periods and considering that geological storage of CO_2 involves long-term storage, studying the effects of CO_2-reservoir interaction in natural occurrences of CO_2 within geological reservoirs, provides valuable insights analogous to potential storage sites, as does studying hydrocarbon accumulations to some extent. Many natural CO_2 and CO_2-rich hydrocarbon accumulations have been identified and studied to improve the understanding of CO_2 storage. These include the NACENT project in Europe (Pearce, 2005), the NACS project in the USA (Stevens & Tye, 2005) and a natural analogues study in Australia (Watson, 2012). These and other studies provided rich information on the CO_2 storage processes within the reservoir, yet limited data and samples from the seal rock itself. However, the existence of known analogous accumulations where CO_2 has breached the seal and CO2-induced diagenesis has taken place is extremely scarce. Compounding this challenge, seal sampling has seldom been conducted in sporadic instances of CO_2 infiltration, and the available data is typically limited to drilling cuttings alone. This limitation restricts the application of various petrological techniques, further complicating the analysis.

(Watson, 2012) conducted a study to assess the impact of CO_2 alteration in fractured seal rock within the Pine Lodge Gas Field, Otway Basin, Australia, which has a historical presence of CO_2. This field provided a unique opportunity to observe the interaction between CO_2 and the fractured Belfast Mudstone top seal. The study demonstrated a significant connection between CO_2-induced precipitation of siderite cement, occurring when CO_2 diffused approximately 1-2 cm into intact rock from fractures, and the enhancement of seal capacity (Figure 26 and Figure 27). Further CO_2 infiltration into the seal rock (>2 cm) is now impeded due to this enhanced seal capacity. This top seal enhancement relied on specific chemical conditions during CO_2 interaction, particularly the presence of Fe^{2+} cations for siderite formation.

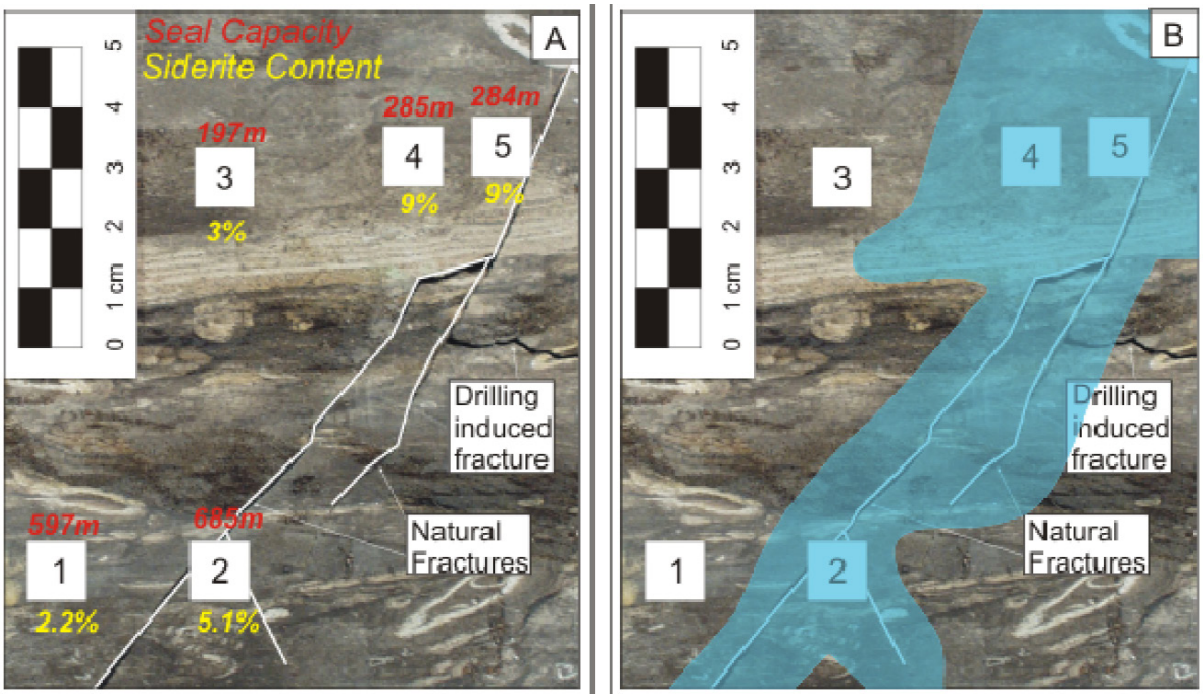

Figure 26: (a) Pine Lodge core of the Belfast Mudstone, indicating fractures and numbered sample points. (b) representation of CO_2 infiltration, determined by late-stage siderite cement precipitation. MICP results showed significantly higher capacity for samples 2, 4 & 5.

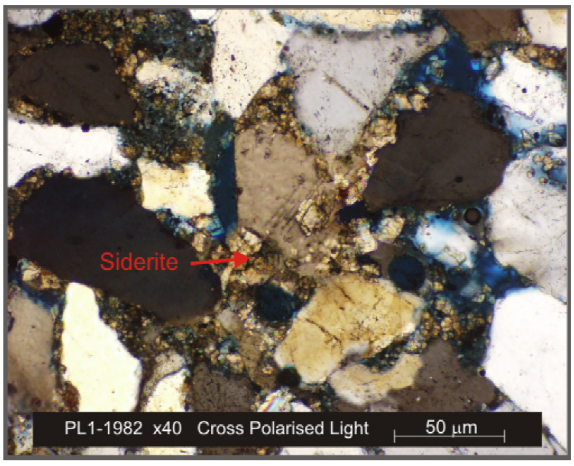

Figure 27: Thin section image illustrating the late-stage precipitation of siderite into pore throats of a siltstone facies of the Belfast Mudstone.

This study also examined unfractured top seal and intraformational baffles associated with CO_2-rich reservoirs. No evidence was found for chemical alteration of the top seals, yet intraformational baffles did show signs of CO_2 alteration. The intraformational seal alteration resulted in kaolinite clay precipitation, demonstrating that CO_2-induced reactions can occur if CO_2 infiltrates seals.

A further study examined the impact of CO_2 on seal rock using the Huangqiao CO_2-oil reservoir in the northern Jiangsu Basin, eastern China, as a natural CO_2 storage analogue (Liu et al., 2023). Despite substantial alterations caused by CO_2-rich fluid in the sandstone reservoirs, the CO_2 storage capacity over millions of years remains intact. CO_2-rich fluid migration into the seal resulted in the precipitation of calcite cement in pre-existing fractures of the mudstone. This process effectively self-sealed the fractures and enhanced the sealing capacity of CO_2 storage. Numerical simulations of artificial CO_2 injection further support these findings, demonstrating that the injection of CO_2 into the depleted oil reservoir of Jurong can be carried out safely and effectively. The presence of calcite cement in the fractures prevents rapid CO_2 leakage, indicating that the combination of sandstone reservoirs and mudstone caprocks in depleted petroleum reservoirs is suitable for long-term and secure carbon capture and storage in geological formations.

Green River, Utah, USA is an excellent analogue for CO_2 storage and fault migration, in this case from a natural CO_2 reservoir, where some CO_2 (dissolved or gaseous) migrates along two fault zones to the surface. This site has examined both the CO_2 storage system and CO_2 leakage processes along faults, with a large dataset providing a strong basis for developing characterisation and modelling methodologies for the appraisal of the storage system's containment and seal leakage processes. (Busch et al., 2014) examined core from the higher permeability reservoir and low permeability sections of the storage system, both exposed and not exposed to the reservoir CO_2. Key changes in the geochemical, mineralogical, petrophysical and geomechanical parameters between core exposed to CO_2 were determined to quantify the effect of long-term CO_2/brine/rock interactions.

The Green River system investigations progressed in more detail, with the 'mineral reaction front' for the CO_2 reservoir-caprock system examined. (Kampman et al., 2016) determined that the reaction front is limited by the CO_2 mineral dissolution and precipitation reactions, reducing the expected penetration into the caprock by an order of magnitude. This result aligns well with the limited self-healing behaviour in caprocks exposed to CO_2 observed in the Pine Lodge field, Otway Basin, Australia.

Importantly, the Green River system was also an analogue for CO_2 leakage, where CO_2 currently migrates along two fault zones to the surface (Snippe et al., 2022). Data from this along-fault leakage analogue has enabled a methodology developed to predict leakage locations and rates to be successfully tested and refined. This result, based on one example, provides good evidence that the capability to characterise fault

zones to predict the risk of leakage does exist. This methodology can now be strengthened by incorporating other analogue and test site data to improve predictive accuracy.

5.5 Summary

In addition to understanding the immediate to short-term effectiveness of a seal in preventing the upward migration of CO_2 from a storage reservoir, it is important to assess the long-term containment capability of the seal. Stakeholder concern over long-term seal integrity, despite significant leakage being highly unlikely, poses a barrier to the widespread implementation of CO_2 geological storage as an effective climate mitigation technology (Alcalde et al., 2018). Accurately predicting the exact impact that CO_2 will induce on the seals of storage systems over these timescales is challenging. However, understanding the underlying processes can inform plans to reduce containment of risk to as low as reasonably practicable and to design appropriate monitoring plans.

Buoyancy-induced pressure and diffusion processes from injected CO_2 can bring about complex chemical and mechanical processes that should be considered for understanding long-term CO_2 containment. These processes can feasibly lead to slow migration of CO_2 through the top seal. However, they are strongly controlled by the specific geological and in situ conditions at each individual storage site.

Geochemical reactions in sealing mechanisms are an important consideration for the long-term containment of injected CO_2 and the geomechanical integrity of the top and fault seals. However, in most cases, the ability to seal geochemical reactions with CO_2 is severely hampered by seal permeability, reducing the importance of this process in site characterisation. Since CO_2 is reactive, when diffusion occurs through the water-saturated pore system of a seal, the seal presents further storage potential, either dissolved in formation water or by geochemical processes.

In a reservoir system containing reactive minerals, the decrease in pH caused by CO_2 dissolution is buffered by reactions. Understanding the mineralogy of the seal is important as certain clays, carbonates, and other minerals, if present, are susceptible minerals to dissolution. However, the low permeability of the seal and pH buffering reduces the rate of reactions.

Seals can be geomechanically altered through swelling, shrinking or dehydration, which can induce stress within the rock and potentially impact its integrity. There is still limited knowledge about the geochemical reaction kinetics and how they relate to changes in flow properties and even less is known regarding the changes to geomechanical properties specific to top seals.

From a modelling perspective, some simplified geochemical modelling, commonly supported with laboratory work, of CO_2 transport process and the CO_2–brine–rock reaction into top seals has occurred, mostly for shale top seals. There is limited knowledge of thermodynamics and reaction kinetics in seal lithologies and much variance in the reaction rates. Many researchers suggest that in the long term, the sealing capacity of top seals is enhanced due to geochemical processes (Yang et al., 2020); (Gherardi et al., 2007).

Many natural CO_2 and CO_2-rich hydrocarbon accumulations have been identified and studied to improve the understanding of CO_2 storage. These and other studies provided rich information on the CO_2 storage processes within the reservoir, yet limited data and samples from the seal rock itself.

Therefore, laboratory studies, modelling, and analysis of natural analogues, with an emphasis on acquiring high-quality core samples, can improve our understanding of top seal behaviour.

6. Risk Assessment for CO_2 Containment

Assessment of risk is essential across the lifecycle of a CO_2 storage project. Many of the potential pathways for CO_2 loss of containment are related to vertical migration through the seal, and so seal evaluation can be a crucial element to the risk profile for a CO_2 storage site. Risk mechanisms for CO_2 containment and their relevance to seal integrity are discussed in section 2.

Unlike uncertainty, where the probabilities of an event occurring and associated outcomes are unknown, "risk" refers to the likelihood of an event occurring that will have one or multiple consequences, where the impact is significant enough to influence the project's objectives, outcomes, stakeholders, or overall success. The impact of a consequence is assessed against a set of metrics specific to the project and meaningful to the operating company. A risk assessment is a systematic process of identification, analysis and evaluation of all potential risks that could impact the project. Best practice is to perform a risk assessment as early in the project lifecycle as is practicable, which enables an appropriate risk management strategy (i.e., risk avoidance, risk reduction, risk transfer or risk acceptance) to be developed.

Uncertainty management is intricately linked with managing risks and can be a precursor to effective risk management. Measures can be taken across the project lifecycle to reduce uncertainty so risk can be better characterised. For example, in provinces or basins that are being evaluated for GCS but have no previous geological data, appropriate uncertainty assessment may result in the identification of an uncertainty reduction strategy that highlights the value of acquiring seal(s) data during an appraisal campaign (e.g. conventional or sidewall core for further characterisation including geomechanical, geochemical and other laboratory testing, as well as other opportunities including performing leak off testing etc). This data can lead to a more robust seal evaluation, resulting in a more robust risk assessment. Uncertainty management is further discussed in the IOGP Report 670 – 'Risk and Uncertainty Assessments for Geologic Storage of CO_2'(*Risk and Uncertainty Assessments for Geologic Storage of CO_2 - Report 670*, 2023).

Another benefit of conducting a risk assessment early in the project lifecycle is that it enables the development of monitoring strategies directly linked to the identified risks. Further details on monitoring technologies for seal integrity are discussed in section 10.

It is important to highlight that risk is not static but can change or evolve across the project lifecycle. A risk of CO_2 loss of containment depends on two elements: the failure threshold of the risk receptor (i.e. any entity that is vulnerable to adverse effects due to the event occurring) and the conditions that the risk receptor is exposed to, such as the geological and operational scenarios. It is common that, at the start of operations, a suite of credible geological scenarios is carried, and these scenarios can reduce over time as more data is collected. Figure 24 illustrates how a risk profile can change across the injection period, assuming the operational scenario remains fixed. If the operational scenario changes (i.e. rate is increased or a neighbouring project that is in pressure communication with the storage unit commences), changes in the conditions experienced by the risk receptor can influence the risk profile. Consequently, risk should be re-evaluated at key milestones or stage gates during the appraisal and development phases of the GCS project. A risk assessment pertaining to the geological storage of CO_2 is required in all jurisdictions covered in this report (section 11), albeit at different points during in the appraisal/development lifecycle.

The Monitoring & Verification (M&V) Plan should be regularly reviewed during the injection and post-injection phases of the project, noting whether any deviations from the plan have been detected. If so, appropriate corrective measures should be implemented, and/or contingency monitoring may be conducted to help characterise and track the deviation. Conversely, as risk reduces, so too can the level of monitoring effort; for example, if the increased pore pressure on the seal has dissipated in the post-injection phase or the behaviour of the storage complex is better understood.

6.1 Risk Assessment Methods

Multiple risk framing and assessment approaches have been published in literature, and these approaches can be broadly categorised as qualitative or quantitative. The key difference between a qualitative and quantitative risk assessment is the approach to the process. A qualitative risk assessment tends to be subjective and focuses on the identification, analysis, and evaluation of risks without assigning specific numerical values to them. This relies on qualitative judgements and subjective analysis to assess the relative likelihood and potential consequences of different risks. Conversely, a quantitative risk assessment is more objective and focuses on analysing risks by assigning specific numerical values to various risk factors. This can include calculating the probability of occurrence and potential financial impact. Formulating a quantitative method that relies solely on probabilistic and financial evaluation without some form of qualitative influence is often challenging, especially in high-uncertainty situations with very few benchmarks from other GCS projects. As a result, semi-quantitative methods can also be employed, where probabilistic evaluation is applied to risks that are qualitatively identified and analysed.

Integrated multi-disciplinary analysis ("IMDA") is common to both qualitative and quantitative methods, and expertise from a variety of fields must be integrated to analyse complex systems such as GCS storage sites. Many risks are multidimensional and multifaceted, and so they must be analysed by considering multiple disciplines simultaneously. IMDA also enables a more comprehensive risk identification process by considering a wide range of potential threats, vulnerabilities, and consequences. IMDA enables a systematic approach to risk analysis by considering the interactions and interdependencies among different factors.

Qualitative and semi-quantitative methods are suitable for site screening and in the earlier stages of the project lifecycle, i.e. before injection. Such methods provide fit-for-purpose screening of potential risks that can assist in site selection and development of monitoring strategies before injection. Semi-quantitative methods, which are underpinned by inputs generated from expert judgment, are appropriate to support injection permitting and ongoing management of risk during operations. Before injection, a quantitative method that considers the probabilistic failure of each risk mechanism can be applied and then re-evaluated on an ongoing basis as more data is collected during injection. Qualitative and quantitative methods are discussed below, with examples.

It is important to note that, to date, there is no universally mandated approach to conducting risk assessments for GCS projects.

6.1.1 Qualitative Assessment Methods

Qualitative risk assessment is the process of rating or scoring risk based on the perception of the severity of the risk and the likelihood of consequences. It relies on qualitative judgments and subjective analysis. This approach is often used when limited data is available or when it's difficult to assign precise values to risk factors.

The key characteristics and steps involved in a qualitative risk assessment are described in both the ISO Risk Management Guidelines (International Standard Organisation, 2018) and the IOGP Report 670 – 'Risk and Uncertainty Assessments for Geologic Storage of CO_2'(*Risk and Uncertainty Assessments for Geologic Storage of CO_2 - Report 670*, 2023), and are summarised in Table 7 and Figure 28.

Before conducting the risk assessment, it is important to establish scope, context, and criteria so that the overall risk management process is customised to meet project objectives. When establishing the scope, a definition should be given to the decisions that need to be made by assessing risk, outcomes expected and appropriate tools and techniques to employ. The context refers to the environment that the organisation and project operate in and can include both internal (i.e. current process management guidelines) and external (industry regulations) factors. The risk criteria refer to the likelihood and consequences of each risk that will

be defined and measured (i.e. the metrics and categories in a risk matrix or risk bow-tie) and the failure threshold that will be applied to identify risks of tangible impact that requires treatment.

Following the risk assessment process, options for addressing and managing risks are selected and implemented as part of a 'risk treatment' process. These are commonly in the form of data acquisition tools and monitoring techniques that are highlighted in an M&V Plan.

Processes such as communication & consultation, monitoring & review and recording & reporting should be implemented throughout the risk management process. Communication about risk is important to ensure information is well understood to facilitate decision-making and avoid oversight. Consultation can be both internal and external and involves bringing together various expertise to facilitate decision-making. Monitoring and review can include collecting and analysing new data to facilitate ongoing review of the robustness of the M&V plan and ensure that all risks are relevant. The risk management process and its outcomes should be continuously recorded and reported internally and to the relevant external stakeholders.

Table 7: Qualitative Risk Assessment Framework (International Standard Organisation, 2018)

Step #	Title	Description
1	**Risk Identification**	Identify and describe all potential risks that could impact the project. *Common methods: workshop or premortem assessment to brainstorm and list all relevant risks.*
2	**Risk Analysis**	Analyse the identified risks qualitatively by considering factors such as their potential impact, likelihood of occurrence, magnitude of consequences and effectiveness of existing controls. *Common methods: Risk Matrix, Risk Bow-Tie, Layers of Protection Analysis ("LOPA").*
3	**Risk Evaluation**	Evaluate the risks by comparing the results from the risk analysis with the established risk criteria to determine whether the risk and its magnitude are acceptable and where additional action is required. If required, additional action can involve risk treatment options (e.g. implementation of new controls) or further risk analysis to better understand the risk.

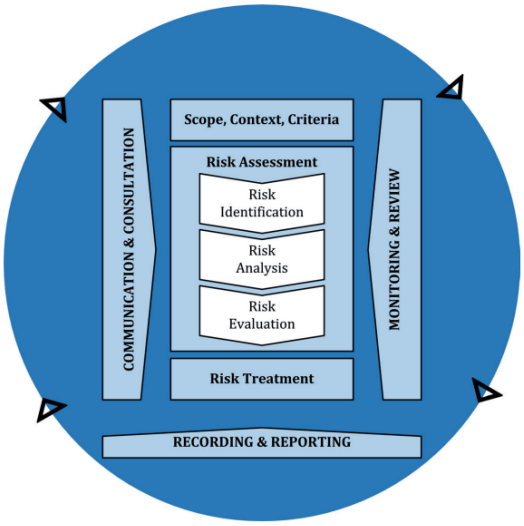

Figure 28: Risk Management Process(International Standard Organisation, 2018)

Risk Matrix

Ref. ISO 31000	Consequence				
Likelihood	Insignificant	Minor	Moderate	Major	Catastrophic
Almost Certain	Moderate	High	Extreme	Extreme	Extreme
Likely	Moderate	High	High	Extreme	Extreme
Possible	Low	Moderate	High	Extreme	Extreme
Unlikely	Low	Low	Moderate	High	Extreme
Rare	Low	Low	Moderate	Moderate	High

Figure 29: Typical Risk Matrix(International Standard Organisation, 2018)

A Risk Matrix is a visual tool used to analyse and evaluate the identified risks based on their perceived likelihood of occurrence and potential consequences. Under this method, risk analysis can be described as a combination of the likelihood of occurrence and the associated consequences. The descriptions and details of each category will be specific to the project and the organisation implementing the risk assessment. A "risk factor" can be determined as "likelihood multiplied by consequence", which can be easily read from the matrix. An example of a typical Risk Matrix is provided in Figure 29.

Risk Bow-Tie

A Risk Bow-Tie is another visual tool used to analyse and communicate the causes, consequences and controls of a specific risk. The term "Bow-Tie" is derived from the shape of the diagram. A Risk Bow-Tie typically consists of six main components: hazard, top event, threat, consequence, preventative barrier, and mitigation barrier. Bow-Ties may also be integrated with a semi-quantitative analysis technique such as Layers of Protection Analysis ("LOPA"), where the Risk Bow-Tie is used as an input to identify, quantify and

determine if a consequence can be acceptably managed. An example of a typical Risk Bow-Tie is provided in Figure 30, with definitions of the components provided in Table 8.

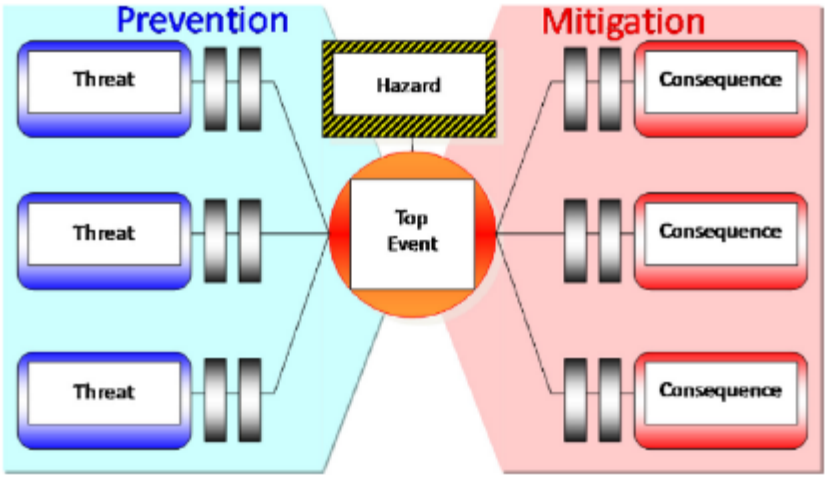

Figure 30: Typical Risk Bow-Tie with Barriers or Safeguards

Table 8: Definitions of the Key Components in a Risk Bow-Tie

Component Name	Component Description
Hazard	An operation, activity, or material with the potential to cause harm.
Top Event	The undesirable outcome or incident occurs if the hazard is not adequately controlled.
Threat	Possible cause or initiating event that can trigger the top event.
Consequence	The result from the top event.
Preventative Barrier	A barrier that can prevent the top event from occurring. Placed between the “threat” and the “top event”.
Mitigation Barrier	A barrier that can either stop the consequence from occurring or reduce the magnitude of the consequence. Placed between the “consequence” and the “top event”.

Qualitative risk analysis methods specific to GCS projects are leveraged from Oil & Gas industry best practices. As a result, the two most common methods for qualitative risk analysis in GCS are Risk Matrix and Risk Bow-Tie. The Risk Matrix method was adopted by Shell for the Peterhead CCS project (Shell UK Ltd, 2016), and applied to the Shenhua CCS Project Environmental Assessment in China (Li et al., 2017). The Risk Bow-Tie method was adopted for the Northern Lights Project at the Aurora Storage Site (Zweigel, 2021), and has been documented as a risk assessment framework applicable to GCS under the SECURe Project (Risktec Solutions, 2021). Shell is acknowledged as the first major energy company to integrate the bowtie methodology into best practices for the oil and gas industry, and the method is widely applicable to GCS.

Shell developed both the bowtie and matrix methods to assess the risk of loss of containment above the ultimate seal for the Quest CCS Project (Groot, 2011). An example of such a risk bowtie is provided in Figure 31, although it is not identical to the one developed by Shell. Many of the threats and prevention mechanisms outlined in Figure 23 align with the risk mechanisms in Table 2. This example is a useful demonstration of how effective a risk bowtie can be as a visual communication tool and to compare qualitative and quantitative aspects. The prevention mechanisms can be categorised as either passive or active safeguards. A passive safeguard refers to a safety mechanism that operates automatically or without need for human intervention, such as geological scenario and reservoir fluid behaviours. An active safeguard requires human input or

control to function and thus covers interventions and M&V protocol. A key limitation of this and other risk bowties is that it is often difficult to rank the risks/threats and thus identify those that require the most attention. This is often where quantitative methods can be impactful.

It is important to note that the act of monitoring itself is not a preventative or mitigation barrier, as suggested in Figure 31. Instead, monitoring is tied to a timely response that acts as a barrier or a safeguard.

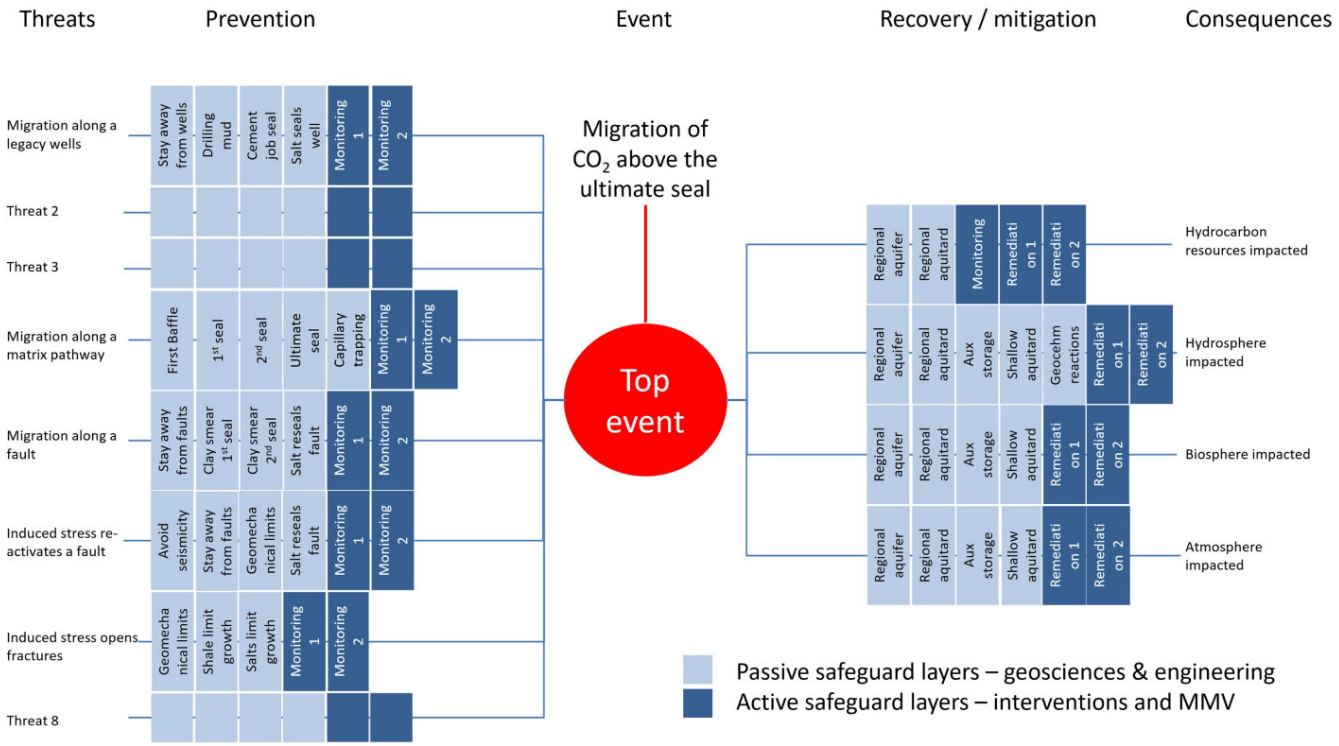

Figure 31: Example of a Risk Bowtie Considering Event of CO_2 Loss of Containment Above the Ultimate Seal (Hunt, 2024)

6.1.2 Semi-Quantitative Assessment Methods

Various semi-quantitative risk assessment methods exist that have been applied for large-scale and pilot-scale CO_2 storage projects, including the Evidence Supported Logic approach (Tucker et al., 2013), Bayesian networks (Wang et al., 2021), The Certification Framework (Oldenburg et al., 2011), National Risk Assessment Partnership (US Department of Energy) (Vasylkivska et al., 2021) and Quantitative Risk Through Time (QRTT, described in (Dodds et al., 2011)). Additionally, a quantitative method risk assessment method for subsurface stress, rock mechanical failure and seismicity has been developed as part of the Stress History and Reservoir Pressure ("SHARP") Project, a transnational consortium of research institutions and commercial companies (Pearson & Kupoluyi, 2022). Fully quantitative risk assessment, as understood from engineering disciplines, is not possible in geological systems. Even in modelling studies, expert judgment defines the input distributions for geologically derived parameters, such as the variogram parameters that may underpin geological depositional modelling.

One example of a semi-quantitative risk framing and assessment approach is the RISQUE method (The Risk Identification and Strategy using Quantitative Evaluation), developed by (Bowden, 2011). This technique has been previously applied to many CO_2 storage projects, including multiple sites in Australia (Bowden & Rigg, 2004; Watson, 2014) including the In Salah CO_2 Storage Project (Dodds et al., 2011) and the Weyburn–Midale Project (Bowden et al., 2013).

Whilst it is typically challenging to quantitatively assess risk at such an early stage in a project's development process, the RISQUE method encourages necessary multi-discipline considerations in subsurface risk, rather than siloed subject analysis, to provide a more balanced identification and assessment of risk and uncertainty. The resulting risk analysis prioritises and appropriately focuses attention on risk management and monitoring requirements relative to the risks of the highest importance.

The quantification aspect of this assessment requires that an acceptable leakage limit for the CO_2 storage project is established (for example, 1% of the injected mass over 1000 years, which is in line with retention masses suggested by the IPCC (Metz et al., 2005). This leakage is defined as out of the storage complex but not necessarily to the surface or anywhere of impact. This 'leakage out of the storage system' can also be referred to as 'out of zone migration'. Examples of calculated leakage rates from natural CO_2 accumulations in Australia, North America and Europe have previously been reported in literature (Kaldi, 2011).

The process of quantification of containment risks is to define each risk on the following basis systematically:

- Likelihood of leakage occurrence (0 – 1 represented on a log scale).
- Impact in terms of leakage rate (tonnes CO_2 per year).
- Duration of leakage (time that the event would be active).

This approach frames risk as the chance and magnitude of a potential loss of containment from the defined storage system's geological boundaries. It assesses the consequence of a loss of CO_2 only as the magnitude of loss from the storage system relative to the acceptable leakage mass limit of 1% of the injected mass.

The inputs for this risk assessment include a simple description of the potential event, the likelihood of an event occurring (Table 9), rate of CO_2 loss and duration based on expert judgement. Table 9 provides an example of the risk likelihood metrics that can be applied, noting that the probabilities associated with likelihood can be project-specific and thus subjective. A qualitative probabilistic framework links to a quantitative meaning of the likelihood input, hence recognising the RISQUE method as "semi-quantitative".

All risk assessment inputs can be subjected to a probabilistic analysis using the RISQUE tool's in-built Monte Carlo method. An example output from this assessment is provided in Figure 32. The vertical axis plots the risk quotient, the likelihood of occurrence multiplied by the consequence. Different confidence levels ("CL") can be selected as the model outputs for each risk. In Figure 32The three levels are pessimistic (95% CL), planning (80% CL), and optimistic (50% CL). The risk quotient can be normalised against the acceptable project containment risk or "target risk quotient" (red dashed line). This makes it easy to identify if any containment risks (plotted along the horizontal axis) have the potential to be at an unacceptable level.

Table 9: Semi-quantitative basis table that may be used by the subject matter experts to assign a consistent quantification to expert judgement within an order of magnitude range (Bowden, 2011).

Quantitative Description	Likelihood	Basis
A. Certain	1 (or 99.9%)	Certain, or as near to as makes no difference
B. Almost Certain	0.2-0.9	One or more incidents of a similar nature has occurred here
C. Highly Probable	0.1 (10%)	A previous incident of a similar nature has occurred here
D. Possible	0.01	Could have occurred already without intervention
E. Unlikely	0.001	Recorded recently elsewhere
F. Very Unlikely	1×10^{-4}	Has happened elsewhere
G. Highly Improbable	1×10^{-5}	Published information but in a slightly different context
H. Almost Impossible	1×10^{-6}	No published information of similar case

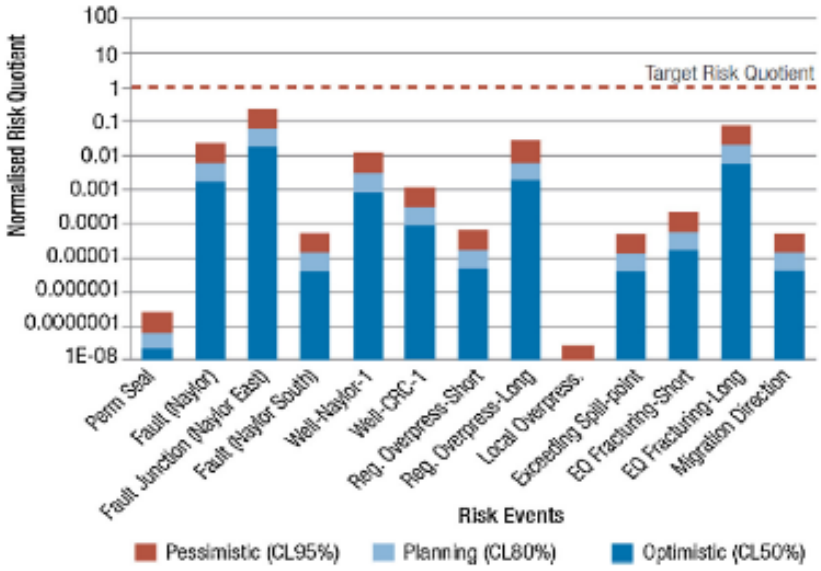

Figure 32: Quantitative risk assessment output for the Otway Stage 1 experiment (Watson, 2014)

An example of a quantitative risk assessment tool is the National Risk Assessment Partnership (NRAP) Open-Source Integrated Assessment Model (NRAP-Open-IAM). The NRAP is a research initiative funded by the United States Department of Energy, National Energy Technology Laboratory, and is focused on assessing and mitigating risks associated with GCS. The NRAP-Open-IAM is a computational modelling tool designed to assess the potential impacts and risks associated with a GCS project. The NRAP-Open-IAM tool is particularly useful for performing risk assessments associated with geological containment. The tool is written in the Python 3 programming language and is available as an open-source tool to be customisable by its users (Vasylkivska et al., 2021).

The NRAP-Open-IAM model framework consists of four major component model types connected to each other. These are described in Table 10 and summarised in Figure 33.

Table 10: Summary of NRAP-Open-IAM Component Model Types (Vasylkivska et al., 2021), of which many components require expert judgement

Component Type	Description
Stratigraphy	The geological model is defined by stratigraphic parameters that describe the strata, depth/thickness, overlying seal, and aquifer layers. All subsequent component models are dependent upon and linked to the parameters set in the stratigraphy component.
Reservoir	The generated arrays represent changing pressure and fluid saturation at the top of the reservoir (reservoir-cap rock interface) over the spatial domain.
Leakage Pathways	The upward migration pathways (either geological or wellbore-related) are a function of path length and effective permeability.
Receptors	Either atmospheric or overlying aquifer intervals (e.g., potable groundwater aquifers) that receive the leaked substance flow rates. The leakage pathways component acts as an input to calculate the magnitude of leakage into the receptors of concern. The aquifer receptor component calculates the volume of groundwater impacted over time due to leakage. The atmospheric receptor component calculates the CO_2 dispersion in the atmosphere due to leakage.

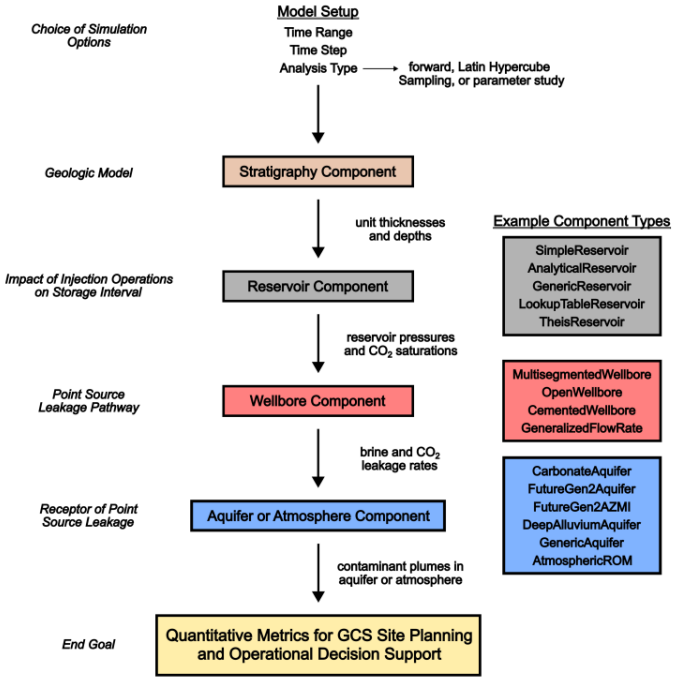

Figure 33: Standard System Model Design (Vasylkivska et al., 2021)

The "end goal" of the NRAP-Open-IAM tool is to provide quantitative metrics for GCS projects. These metrics are determined from computational simulations using three analysis types: Forward, Latin Hypercube Sampling (LHS), and Parameter Study. A Forward analysis is deterministic, and each parameter is fixed at a specified value. LHS simulations are stochastic, and the parameters are varied between minimum and maximum values according to their distribution. The Parameter Study uses different parameter values in each realisation, and the user specifies the number of parameter values to use for each stochastic parameter. The number of realisations is an output of the Parameter Study, which increases exponentially with the number of stochastic parameters the user selects.

An overview of the Risk Assessment process using NRAP-Open-IAM is provided in Figure 34. The software is designed for computational efficiency, which is enabled via reduced-order approximations, lookup tables, or analytical/semi-analytical models. This approach allows for a robust representation of the risk environment with a much lower computational demand than traditional reservoir modelling software. It is important to note that NRAP-Open-IAM is not designed to replace traditional reservoir simulation methods for GCS site characterisation. Instead, it is designed specifically to enable deterministic and stochastic quantification of potential risks.

The NRAP-Open-IAM tool has been applied to the Quest Carbon Capture and Storage Facility owned by the Athabasca Oil Sand Project (AOSP) to complement the Bow-Tie risk assessment conducted for the site and demonstrate the integration of qualitative and quantitative risk assessment methods for GCS projects (Brown, 2022).

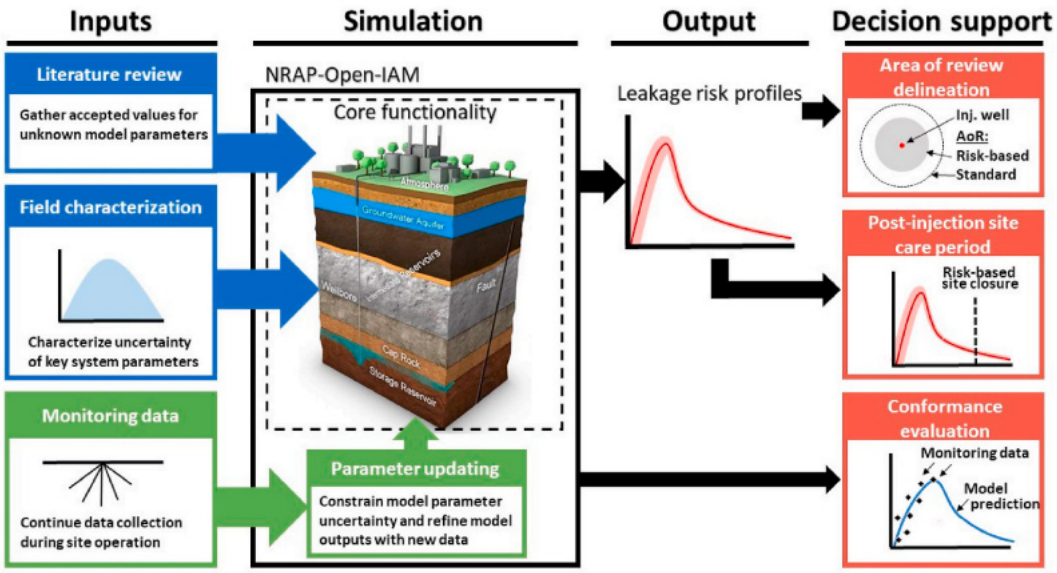

Figure 34: Overview of Risk Assessment Using NRAP-Open-IAM (Vasylkivska et al, 2021). Many inputs require expert judgement.

6.2 Risk Mitigation

Standard risk management approaches identify risks and undertake uncertainty reduction activities to characterise the perceived impact and likelihood risks effectively. Subsequently, risk mitigation strategies can be devised and applied. This section focuses on risk mitigation through active and passive pressure management. However, there are many ways in which seal integrity risks can be mitigated, such as selecting storage plays that minimise buoyancy pressure or the use of secondary seals.

Many jurisdictions and resource management frameworks stipulate that a GCS project should not have an adverse impact on other resources. Therefore, the impact of both pressure and displaced fluids must be considered in addition to the containment and conformance of the injected CO_2. Hence, pressure and fluid management through the extraction or diversion of fluids from the storage unit may help to reduce storage integrity risks. For example, in some scenarios, APM may be a useful method for controlling brine flow within an area of review. In confined aquifers, removing water from a storage unit helps prevent a large pressure build-up that may result in a seal integrity-related issue (e.g., fault re-activation) and increase the reservoir's storage capacity.

Various studies have evaluated strategies for managing CO_2 storage reservoirs by producing brine to reduce the pressure buildup due to CO_2 injection (Buscheck et al., 2017). Voidage is created by removing brine from the storage unit, which, when managed appropriately, will limit the build-up in pore pressure and help manage several risks, including risks associated with seal integrity. Further, average field pressures are kept lower if brine extraction is implemented effectively, which will reduce the drive for any brine to seep through legacy wells. In addition, extraction of brine from the lower sections of a storage formation can help to counteract the effect of buoyancy, lessening the volume of CO_2 in contact with the seal and enhancing other (non-structural) trapping mechanisms (Buscheck et al., 2012). Other proposed benefits of pressure management include the concept of geo-steering a CO_2 plume to reduce the likelihood of a CO_2 plume interacting with a geological risk or limiting the project footprint for permitting or monitoring purposes (Hamling, 2022).

A recent study identified several possible economic benefits of implementing brine extraction at various prospective GCS sites in the UK North Sea (Gammer, 2018). Though the benefits varied across the sites studied, the modelled storage capacity of Tay (an open aquifer) tripled and a 33% cost reduction was also estimated at another potential site (the Forth site, another open aquifer). Through a portfolio approach, savings in infrastructure can be realised by expanding the capacity of lower-cost CO_2 stores and deferring the deployment of more expensive stores (Gammer, 2018).

The extraction of brine may be a valuable resource in some instances depending on factors including the total dissolved solids in the brine or the presence of valuable minerals (GCCSI, 2016). However, in other cases, the brine could be hot and highly saline and, therefore, require treatment before disposal, resulting in higher capital and operating expenditure.

Two of the different pressure management approaches discussed in literature are termed active pressure management (APM) and passive pressure management (PPM) (Goudarzi et al., 2017). An APM system for pressure management involves extracting brine to the surface. In contrast, a PPM system utilises wells in which a shallower formation is open to flow as a method of pressure relief (Figure 35).

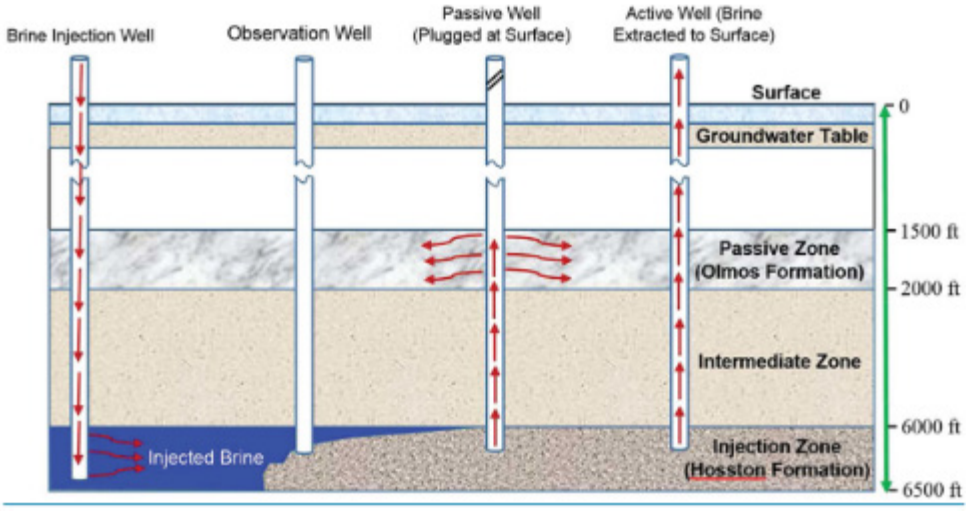

Figure 35: Illustration of different extraction scenarios (APMS and PPMS) in Hosston Formation of Devine Test Site (Goudarzi et al., 2017).

In APM, the produced brine can be treated and disposed of in the marine environment or a dedicated brine storage reservoir. An alternative form of APM, which is termed enhanced water recovery (EWR), utilises the produced brine for economic benefit (e.g., CO_2 capture plant, desalination, valuable minerals) (GCCSI, 2016). Therefore, there can be increased capital expenditure (through the drilling of dedicated brine production wells) and increased facility design requirements (e.g., water handling) that may be economically prohibitive. In contrast to water handling associated with oil developments, where the produced water is treated on the surface before disposal, lower CAPEX opportunities are being considered for APM in GCS. The lack of a saleable product means that it may be possible to simplify the disposal of the produced water without flowing the brine back to a surface facility. However, this would require an environmental impact assessment for the direct disposal of brine into the marine environment and the advancement of current technologies to explore if brine could be released at depth using subsea infrastructure (Gammer, 2018).

Various authors have discussed different strategies for implementing pressure relief, including brine production prior to the commencement of CO_2 injection, which provides information on reservoir connectivity, simultaneous CO_2 injection and brine production (via different development wells), or the phased introduction of pressure management wells based on early-project surveillance data. A key risk to pressure management is that the CO_2 injection and brine production wells are not in pressure communication.

To date, Gorgon CCS is the only commercial-scale GCS project that has deployed APM. In this project, four pressure management wells partially offset the increasing pressure due to CO_2 injection within the Dupuy Formation, extracting the brackish water and, after treatment, reinjecting it via the water injection wells into the overlaying Barrow Group saline formation (Flacourt and Malouet Formations), which is geologically isolated from the surface environment (Chevron, 2018) (Figure 36). A pressure management strategy that creates a dependency between two geological systems must effectively characterise the geological uncertainties of the project's CO_2 storage and water disposal aspects.

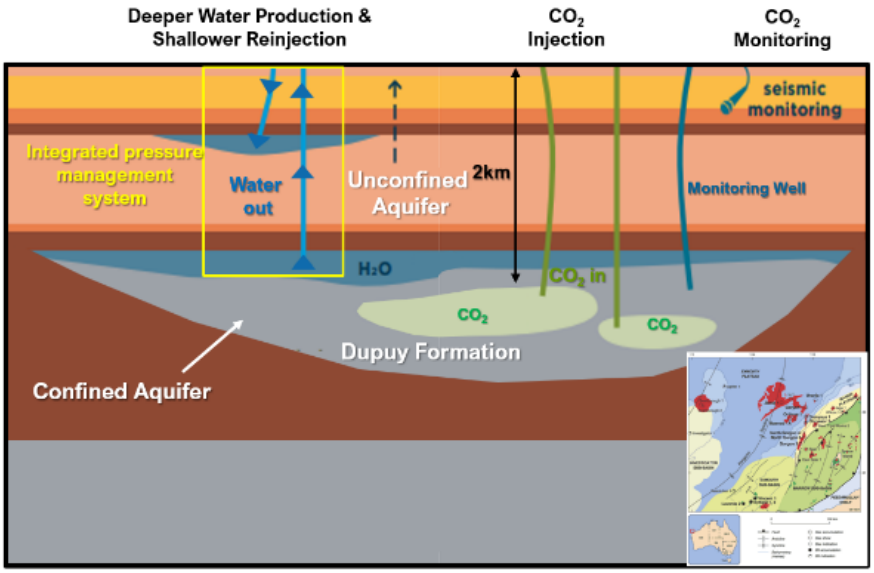

Figure 36: Pressure management (APM) at Gorgon CCS (image modified after the Gorgon Carbon Capture and Storage Fact Sheet)

The Brine Extraction and Storage Test (BEST) program has initiated several field projects to address reservoir pressure management. For example, the second phase of the Plant Smith field demonstration will validate both active and less technically mature passive management approaches.

A recent example of brine extract testing was undertaken in North Dakota (USA) as part of the US DoE-sponsored BEST program (Hamling, 2022). In this study, field measurements (pressure and rate) were acquired from three wells (saltwater disposal and extraction wells) over a two-year testing period. Data was then used to history match a model of the Inyan Kara Formation and forecast several hypothetical CO_2 injection cases, and subsequently evaluating development scenarios including pattern type, pattern spacing and extraction rates. The study also illustrated an example of geo-steering the CO_2 plume further to the southwest using brine extraction, though the difference in plume migration with and without water extraction was relatively minor (Figure 37).

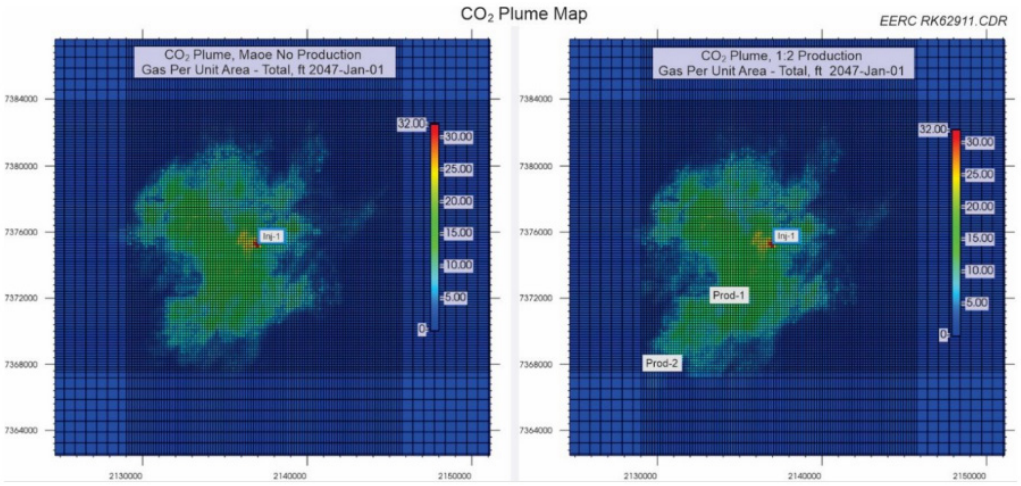

Figure 37: CO_2 plume migration without water extraction (left) and with water extraction (1:2 ratio of injection to production) (Hamling, 2022)

An alternative approach to the voidage balance scenario discussed above is impact-drive pressure management (IDPM) (Birkholzer et al., 2012)Rather than pursuing a 1:1 brine production: CO2 injection volume approach, this strategy targets localised brine extraction to help manage pressure near key risks to containment (e.g., a critically stressed fault).

6.3 Summary

Assessment of risk is essential across the lifecycle of a CO_2 storage project. Many potential pathways for CO_2 loss of containment are related to vertical migration (e.g. faults and fractures) through the seal. Therefore, seal evaluation can be a crucial element in the risk profile for a CO_2 storage site.

Risk assessment requires appropriate uncertainty management and should be undertaken early in a GCS project lifecycle to develop appropriate risk management strategies. Risk is not static but evolves through the project lifecycle. Hence, the site-specific GCS M&V Plan should be regularly reviewed during the injection and post-injection phases of the project, noting whether any deviations from the plan have been detected. Potential seal integrity monitoring technologies are discussed in a later section of this report.

Qualitative and quantitative risk assessment techniques exist, and both methods have been applied to GSC projects. Qualitative techniques rely on qualitative judgments and subjective analysis (e.g. risk matrix or risk bow-ties). Quantitative (or semi-quantitative) risk assessment techniques are generally more challenging early in a project's development process. However, they encourage integrated multi-disciplinary analysis ("IMDA"), critical for effective risk analysis of complex systems such as GCS storage sites. Several applications of qualitative and quantitative risk assessment techniques have been discussed.

As per the original project specification, a dedicated discussion on risk mitigation via active and passive pressure management has been included in this report section. An APM system for pressure management involves extracting brine to the surface. In contrast, a PPM system utilises wells with a shallower formation open to flow as a pressure relief method. Various research has cited the benefits of pressure management in limiting the build-up of pore pressure and, therefore, help in managing several risks, including risks associated with seal integrity. Regardless of the approach, a pressure management strategy that creates a dependency between two geological systems must effectively characterise the geological uncertainties of the project's CO_2 storage and water disposal aspects to be effective.

7. Methods to Characterise and Evaluate Seal Integrity

Irrespective of whether a qualitative or semi-quantitative method is adopted, an output from the risk assessment described in section 6 is the subsequent decisions (or series of activities) taken to reduce the uncertainty associated with the risk and increase confidence in the risk characterisation. When characterising and evaluating seal integrity for GSC, several factors need to be considered, including the seal's areal extent and local quality, as well as stress fields and local fractures. Understanding the lithology of the seal(s) and surrounding formations is also essential.

Understanding the regional stress field is also crucial as it provides insights into the primary stress directions in the subsurface. This information helps predict how faults and fractures may behave under stress, which is critical for seal integrity assessment. Characterisation will typically seek to determine the applicable stress regime in the area of the GCS project, which influences how fractures and faults may propagate and impact seal integrity. Regional stress understanding can also analyse fault seal capacity and assess whether faults will act as barriers or conduits to fluid flow, including CO_2 migration. Regional stress information. Forming a view of the regional stress regime helps characterise the fracture network within the seal and surrounding formations, indicating whether fractures are likely to open or close due to GCS injection operations. Incorporating regional stress data with rock properties (i.e. Young's modulus, Poisson ratio) enables geomechanical models to be developed that help predict how the storage unit(s), seal(s) and surrounding formations will deform due to CO_2 injection and increased pore pressure. Geomechanical modelling is discussed in more detail in section 9.

The extent and quality of the seal may require characterising faults through seismic imaging. Fault analysis helps assess how faults impact seal integrity. 3D seismic surveys offer detailed subsurface images, aiding in identifying geological structures, faults, and stratigraphy. While seismic imaging may not resolve all faults, semblance analysis enhances fault detection and mapping, though limitations in resolution persist. This analysis helps identify fault zones that could affect seal integrity. Amplitude Versus Offset (AVO) analysis examines rock layers' seismic response to differentiate lithologies and fluid content, offering insights into caprock sealing capacity. Seismic attributes, like coherence, amplitude, and frequency, extracted from 3D seismic data help characterise the subsurface and identify potential sealing mechanisms. The application of several of these techniques is discussed in section 10.

In this section, focus is placed on log acquisition and laboratory testing for the purposes of characterising and evaluating seal integrity, including:

- Targeted log acquisition or well testing (e.g., petrophysical logs, image logs).
- Laboratory testing of samples (e.g., tri-axial testing, imaging studies).

7.1 Log Data Acquisition

7.1.1 Detailed Stress Field Characterisation

As part of characterising a potential GCS site, it is necessary to analyse the geological features, sedimentary structures, and rock properties near the wellbore. This can help identify bedding planes, fractures, faults, and other geological features that may affect the productivity and integrity of the reservoir. This information is crucial for developing a local view of the stress regime and contributing to a regional understanding.

Several tools and techniques can be employed to determine stress orientations, each with advantages and limitations. All these techniques evaluate local stresses. Some commonly used methods and their pros and cons are as follows:

- **Borehole breakout analysis** directly measures stress orientations near the borehole wall. The depth of investigation is limited, and the interpretation may be subjective. Expertise is required to differentiate natural fractures from borehole-induced features. Moreover, breakouts may not always form in predictable orientations, especially in complex geological settings and can be influenced by drilling parameters such as mud weight, drilling speed, and borehole size.

- **Caliper logs** are widely available and routinely acquired during well logging operations, directly measuring borehole diameter. Changes in borehole diameter can reflect stress-induced breakouts and drilling-induced tensile fractures, providing indirect information about stress orientations. Unfortunately, this technique is limited to indirect indications of stress orientations based on borehole deformation features. It presents limitations compared to other methods, such as FMI logging, which produces high-resolution images of the borehole wall by directly visualising stress-induced features (e.g. breakouts and drilling-induced tensile fractures).

Borehole formation micro-resistivity imaging has been utilised in the oil and gas industry since the 1980s. Micro-resistivity image logs (e.g., formation micro-resistivity imaging, FMI) are a data-gathering method for evaluating fractures, the directions of principal stress and formation dip. In addition to resistivity-based image tools, acoustic and density image logs can also be used.

The depth of investigation of these techniques is limited to the borehole itself, and information about stress orientations beyond the borehole wall is not obtained directly. Other specialised logging tools, such as dipole sonic, can directly measure acoustic anisotropy, which can be correlated with stress orientation.

Research at multiple large-scale GCS projects has described the benefits of formation micro resistivity imaging, including In-Salah and the Frio project (Bond et al., 2013; Müller et al., 2007). A wealth of research exists on detecting and identifying fractures, facies, and dips using different algorithms (edge detection algorithms, convolutional neural networks, etc.).

A recent example of the role that FMI can play in GCS caprock/seal assessment in the UK, where FMI images were used to not only provide sedimentary, textural, and structural detail but also to provide an improved understanding of the distribution of insoluble material both through the entire bedded halite section and within mudstone interbeds showing interconnected halite-filled fractures, providing an understanding of potential migration pathways through the caprock (Evans et al., 2012).

Seismicity data sets can also provide valuable insights into stress and strain distribution at a regional scale. Analysing stress regimes using seismicity data involves studying seismic events' distribution, orientation, and characteristics to infer the stress field within a region. An analysis of the focal mechanism solution is needed to provide information about fault plane orientations and slip direction during earthquakes, determining the faulting type (e.g., normal, reverse, strike-slip). After fitting the observed faulting data, a stress inversion can provide insights into the stress regime (i.e. orientations and magnitudes of the principal stresses).

Seismicity data typically represents relatively small-magnitude earthquakes, which may not fully capture the behaviour of larger and potentially more significant events. Therefore, extrapolating stress information from small-magnitude earthquakes to larger-scale tectonic processes should be done with caution. Moreover, the quality and resolution of seismicity data depend on factors such as monitoring network density and event detection thresholds. Low-quality data or inadequate spatial resolution can limit the accuracy and reliability of stress analyses.

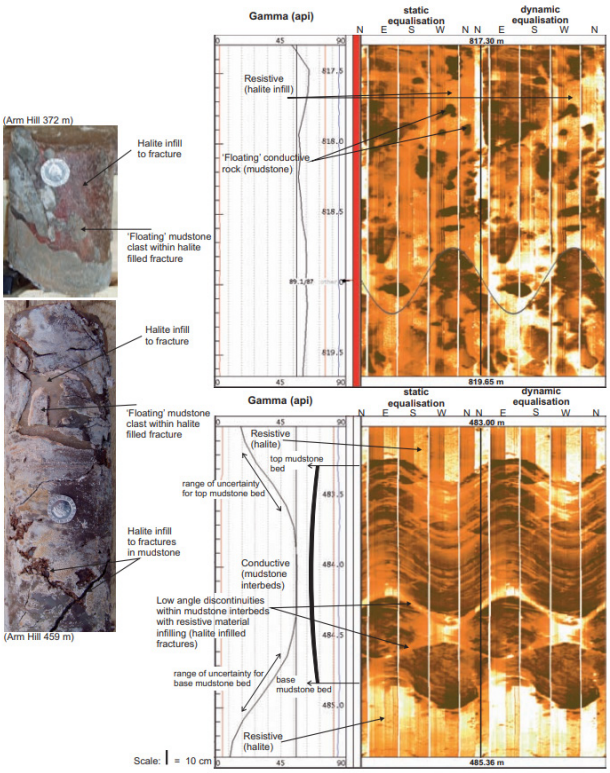

Figure 38: FMI images illustrating examples of halite-infilled fractures in the interbedded mudstone (from Evans et al, 2012)

7.2 Laboratory Testing

7.2.1 Scratch Testing

Petrophysical logs, including sonic and density logs, are vital for deriving rock elastic and strength properties (the application of these properties is discussed in more detail in section 9).

An example of the more recent development of techniques for the characterisation of top and fault seals is the ability to derive fault rock strength from logs using scratch testing performed on the core to trace grooves (~1cm wide) at constant depth into the core (Tenthorey et al., 2019). This enables specific mechanical properties to be characterised (e.g., unconfined compressive stress (UCS), friction angle) at a relatively affordable cost as an alternative to tri-axial testing. Other benefits of scratch testing include that it is non-destructive and can be performed at high spatial resolution. The results indicated that log data can be combined to create a proxy that can be used to predict UCS, which can then be used to predict lithologies in an offset well and for fault reactivation pressure estimations.

7.2.2 Imaging Studies

Non-destructive digital core analysis techniques (X-ray micro-computed tomography (µCT) and Scanning Electron Microscope (SEM) are helpful to characterise prospective CO_2 seals at multiple scales. These techniques can provide high-resolution images of porosity and fractures and essential information on seal reactivity with CO_2 and water (Golab et al., 2012).

The dimensions of samples required for µCT can vary from a few millimetres to several centimetres. The choice depends on the resolution desired in the analysis and, above all, on the acquisition timing. Thin sections are needed for SEM. Typically, geological thin sections have dimensions of approximately 2.54 cm (1 inch) in diameter and 0.03-0.05 cm (30-50 micrometres) in thickness.

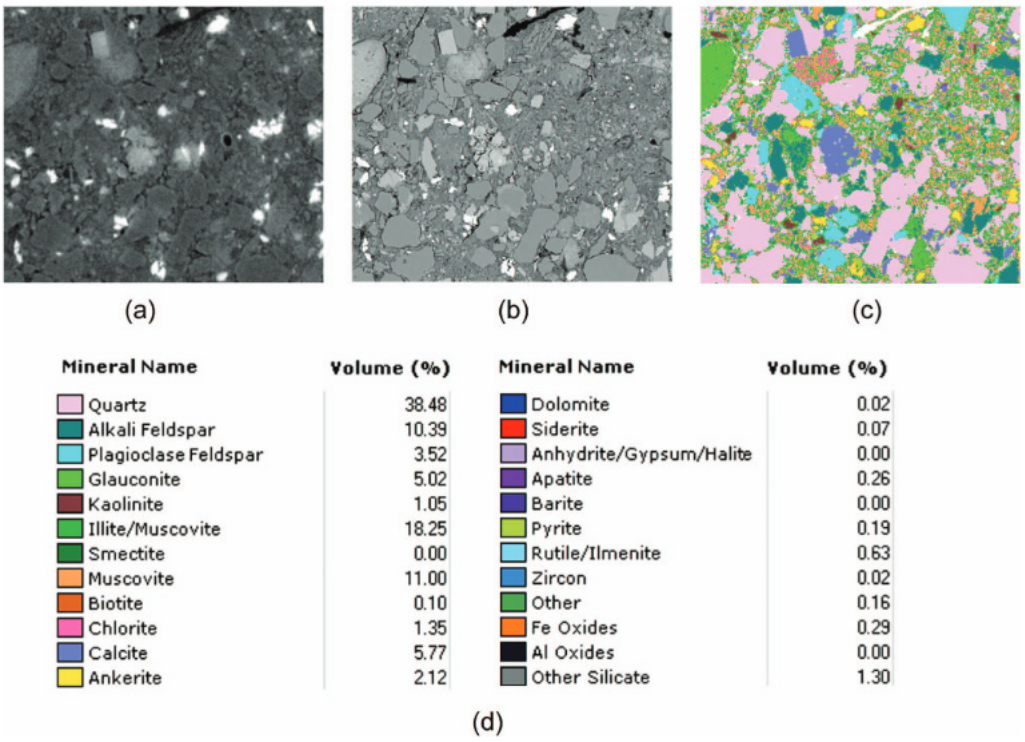

Figure 39: Horizontal plane through a core of potential seal rock 1: (a) micro-CT, (b) matching SEM, and (c) SEM mineral phase map (Golab et al., 2012)

Figure 40: µCT image of connected porosity and fractures in a bituminous coal sample (Golab et al., 2012)

Imaging studies can be undertaken on various sample sizes, including cuttings, thin sections (e.g. 1" x 2"), sidewall cores or core plugs from conventional cores. Selecting sidewall cores over standard cores offers several advantages and disadvantages. Advantages of choosing sidewall cores include:

- **Reduced drilling time:** sidewall coring is typically faster than conventional coring methods, as it allows for core recovery while drilling without the need to stop and pull out the entire drill string.

- **Minimized formation damage:** since sidewall coring can be performed while drilling, it minimises the time the wellbore is open and exposed to drilling fluids, reducing the risk of formation damage.

- **Increased sampling resolution:** sidewall cores provide high-resolution sampling of the formation due to their ability to target specific intervals of interest. This allows for detailed analysis of reservoir and caprock properties and fluid characteristics.

- Anticipating the measurements of rock properties (e.g., petrophysical, mineralogical, and geomechanical parameters) already on material from the exploratory wells also enables a better and more effective design of operations in subsequent wells and, consequently, the reduction of drilling/completion costs.

Disadvantages of sidewall cores include:

- **Bias:** Sidewall coring may introduce sampling bias, as the selection of intervals for coring is based on well logs or other data, which may not accurately represent the true lithology or reservoir properties.

- **Difficulty in handling and processing:** Sidewall cores are smaller and may be more fragile than standard cores, making them more challenging to handle and process in the laboratory. Specialised equipment and techniques may be required for sample preparation and analysis.

- Although service companies are moving towards developing tools to identify the orientation of sidewall cores, this information is currently lacking. This poses a challenge since the standard for conducting geomechanical tests recommends testing along the vertical direction. This must be deduced using other techniques (e.g., visual inspection and analysis of bedding planes if present, comparison between lab CT scan and image log), which are not necessarily accurate. Even considering the ability to identify the vertical direction, subsampling of the sidewall cores is necessary to obtain non-standard-sized plugs for geomechanical testing. This requires custom-built equipment and procedures to scale the obtained results.

Advantages of selecting cuttings include:

- Drilling is relatively inexpensive compared to coring operations, as it does not require specialised equipment or additional rig time.

- Cuttings provide immediate information about lithology and drilling conditions encountered while drilling, facilitating quick decision-making and adjustments to drilling parameters.

Disadvantages of selecting cuttings include:

- Depth uncertainty: cuttings may not accurately represent the formation at specific depths due to mixing and contamination during transport to the surface.

- Loss of core properties: cuttings may not preserve specific core properties, such as porosity, permeability, and rock strength, which are crucial for reservoir characterisation. Even if the structure remained unchanged, the lack of a cylindrical shape would prevent the application of the most common measurement techniques for petrophysical and geomechanical properties. Moreover, cuttings may not capture features such as hydrocarbon shows and fractures, which are essential for reservoir evaluation.

Geoscientists and reservoir engineers can effectively differentiate coring-induced fractures from natural fractures through a combination of approaches:

- First, the integration with geological context should be considered. Geological mapping, seismic interpretation, and well-log analysis can provide valuable insights into the distribution and orientation of natural fractures within the reservoir, aiding in differentiating from coring-induced fractures. Subsequently, many other assessments can be made based on:

- Fracture analysis: analyses of the fractures observed in core samples, considering characteristics such as orientation, spacing, roughness, and infill material. Coring-induced fractures often display distinct features, such as consistent orientation perpendicular to the core axis, along laminations, or smooth surfaces resulting from the coring process. In contrast, fractures formed under reservoir conditions may exhibit varying orientations and roughness, reflecting natural stress conditions and fluid interactions.

- Core Imaging Techniques: advanced imaging methods like SEM or CT scanning are used to examine fractures in detail. These techniques provide high-resolution images that can reveal the nature and origin of fractures, distinguishing coring-induced fractures from natural ones.

- Fracture Density Analysis: quantifying the density of fractures within core samples for comparison with known distributions in reservoirs of similar lithology and stress conditions. Coring-induced fractures often show higher densities near the core external margin, while natural fractures may have a more random distribution throughout the core.

7.2.3 Pore Scale Imaging and Upscaling Methods

Upscaling data from millimetre scale contact angle to field-scale flow simulation appropriately representing pore scale physics is challenging. A growing field of research is that of digital core analysis (pore-scale imaging and modelling), which is a method of both representing and predicting the multiphase flow dynamics and the geometry of the rock (Bakke & Øren, 1997; Keehm et al., 2004). A typical workflow for this approach is illustrated in Figure 41.

Pore-scale (i.e. micron length scale) imaging techniques range from X-ray-based imaging (e.g. µCT as discussed in the previous section, as well as synchrotron techniques) as well as focused ion beam (FIB) techniques. FIB essentially provides three-dimensional imaging equivalent to 2D SEM (resolutions of 10s nm can be achieved) but is destructive (Blunt et al., 2013).

Various modelling methods can be applied to reconstruct the pore space statistically using these pore-scale images as a fundamental input. These methods include direct modelling approaches (e.g. lattice Boltzmann method (Chen & Doolen, 1998), modelling techniques based on solving the Navier-Stokes equation), which are computationally inefficient and, hence, at least historically, have been primarily limited to single-phase flow. Alternative ‘network modelling’ techniques that leverage the similarities between flow in porous media and random resistor networks also exist (Fatt, 1956).

However, it remains a challenge to upscale the results of micro-scale experiments to generate field-scale representations of the range of possible subsurface outcomes. Further, any upscaling method that can be integrated with predictive capabilities must be able to do so with a computational efficiency appropriate to inform GCS-based business decisions.

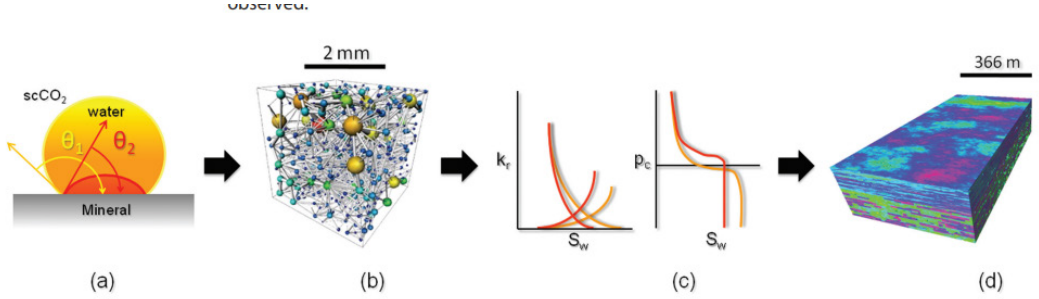

Figure 41: Digital core analysis up-scaling workflow from millimetre scale contact angle measurements to full-field simulation (Blunt et al., 2013)

7.2.4 Estimation of Brittleness Index

The Ingrahm and Urai method, introduced in section 4.4, is only one method by which the brittleness of caprocks can be evaluated. In recent work, the various methods for calculating the brittleness index were reviewed (Figure 42), encompassing mineral-based, log-based, and elastic-based methods. The wealth of data generated from the growth of the unconventional oil and gas industry in the United States has provided a large dataset by which these various methods could be evaluated (Mews et al., 2019). A universal correlation cannot be derived from the brittleness index, noting an overall trend that high quartz or carbonate content yields high brittleness values (Mews et al., 2019).

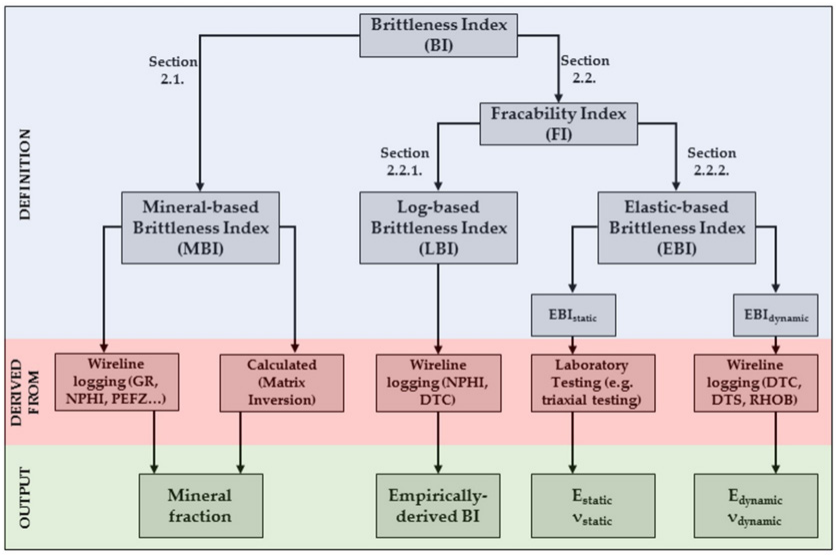

Figure 42: Various methods for calculating Brittleness Index (Mews et al., 2019)

Another example of applying all three general approaches (mineral-based, log-based and elastic-based) to calculate a brittleness index was performed on Indonesian shale, concluding that elastic properties-based and mineralogical methods produced a consistent Brittleness Index (Nababan et al., 2022).

More recently, a top-seal assessment (Thompson, Andrews, Wu, et al., 2022) was conducted as part of the Northern Lights project in offshore Norway, utilising a significant existing dataset (including 50 exploration wells and multiple 2D/3D seismic surveys) (Rahman, Fawad, Jahren, et al., 2022)The primary seal for this development is the Early-Jurassic Drake and Burton Formation shales. Two different elastic-based brittleness index methods (Fawad & Mondol, 2021; Grieser & Bray, 2007) were utilised as part of this effort. The former method is based on shear wave (Vp) and compressible velocity (Vs) inputs, while the latter also uses acoustic impedance and deep resistivity.

Fundamentally, all these methods are only an indicator of lithology (where a high brittleness index indicates a quartz-rich lithology and a low brittleness index indicates clay-rich) and do not link directly to the efficiency of fracturing or failure behaviour. Young's modulus and Poisson's ratio are elastic and have little to do with rock failure. The commonly used brittleness calculations (e.g. elastic and mineralogy-based) may only highlight relative differences for specific rock properties between different zones. These results might not be representative of actual rock behaviour during failure.

To achieve a more accurate prediction of the rock's propensity to fracture, methodologies for evaluating the fracability index exist (Jin et al., 2015). Fracability evaluation is based on the following parameters:

- Brittleness is related to rock stiffness and can be estimated using correlations with mineralogy or elastic moduli, either dynamic or static.

- Toughness represents the resistance of rock to fracture propagation. It can be estimated via lab measurement or by correlation with other rock parameters (e.g. tensile strength, elastic moduli, compressional wave velocities). The higher the fracture toughness, the higher the breakdown pressure

- The strain energy release rate is the energy dissipation per unit surface during the creation of a new fracture. When the value of the strain energy reaches the critical value, fracture propagates. Under certain commonly adopted assumptions, the critical value can be related to toughness and elastic moduli.

For an even more comprehensive assessment, the fracability index model should then be integrated with information regarding the in-situ stress state and the existence of natural fractures.

The brittleness index derived from well data can potentially be used to calibrate or invert seismic data and create estimates of brittleness more regionally. This approach integrates information from well logs and core samples with seismic attributes to infer properties such as brittleness across a broader area. A detailed well-scale evaluation requires the following inputs:

- Rock strength and stiffness mechanical properties and mineralogy from core data to properly calibrate logs and create correlations.

- Bulk density of the formation from density logs. High-density intervals are often associated with more brittle formations.

- Compressional and shear wave velocities of the formation from sonic logs can be used to estimate rock mechanical properties such as Young’s modulus and Poisson’s ratio. These properties are essential for assessing brittleness.

- Identification of organic-rich shale intervals, which are typically more brittle. Gamma-ray logs can be used as a proxy for lithology.

- Information related to the in-situ state of stress from the calliper and image logs.

By leveraging seismic data, it is possible to extend the assessment of brittleness to areas with sparse well coverage. However, it should be noted that if the availability of log and core data is limited, establishing a robust calibration with seismic data may be complicated. This can introduce too large of an uncertainty in the regional brittleness estimates.

7.2.5 Core Preservation

Preservation and sealing of cores are crucial steps in geomechanical analysis to maintain the integrity and representative nature of the core samples. This is particularly true when clay minerals are present in

significant percentages in the core's mineralogy. More specifically, clay minerals consist of alternating sheets of silica and alumina called T-O-T layers, held together by positive interlayers containing exchangeable ions and water molecules, effectively becoming part of the material's structure. This is especially true in the presence of minerals such as chlorite and smectite, which have a high cation exchange capacity (CEC). The objective, therefore, is to prevent any swelling phenomena or chemical reactions caused by contact with brines that are not chemically balanced with the formation brine. Specific key areas of focus include:

- **Preparation:** cores should be carefully handled during extraction to minimise disturbance and maintain their original structure. Once extracted, they must be cleaned to remove any drilling fluids or contaminants that may affect subsequent analysis.

- **Sealing:** cores should be sealed after cleaning to prevent moisture loss or gain, which can alter their mechanical properties. This is typically done using plastic wrap or paraffin wax (or other materials such as silicone sealants or epoxy resin coating). The sealing process should be conducted promptly to minimise exposure to atmospheric conditions. Finally, the core should be maintained in a humidity-controlled environment.

- **Sampling:** sampling for geomechanical testing will inevitably induce some disturbance in the core. Due to their pore-bridging morphology, certain clay minerals like illite can be easily damaged during core handling and sampling. Suppose manual sampling is not possible due to the stiffness and hardness of the material. In that case, coring procedures using appropriate equipment should consider using fluids such as air, oil (in cases where it is a non-wetting fluid), or brines that chemically replicate the formation brine.

- **Testing:** It is essential to use brines that chemically replicate the formation brine for conducting tests, employing adequate preliminary procedures to verify the complete saturation of the material (i.e., B-Skempton).

Table 11: Tri-Axial Testing Laboratory Testing (EOS Well, Northern Lights Project) (Barnhoorn, 2022)

Test Type	Drainage	Parameters
Isotropically consolidated triaxial	Drained	Loading/unloading loop for elastic moduli, elastic moduli during main loading phase, stress at failure
Isotropically consolidated undrained (CIU) triaxial	Undrained (+drained cycling from in-situ stress)	Loading/unloading loop for elastic moduli, elastic moduli during main loading phase, stress at failure. Horizontal and vertical direction (anisotropy)
Hydrostatic	Drained	Bulk modulus during the main loading phase, during unloading/reload from in-situ
Uniaxial strain test (UST)	Drained	Grain stiffness, bulk compressibility, constrained modulus, stress ratio
CO_2 flood and “weakening”	Drained	Bulk modulus with supercritical CO_2 saturation and time, geophysical response vs saturation (velocity, resistivity)
CIU + temperature	Undrained	Shear modulus, stresses at failure at the relevant temperature
Thermal effects	Drained	Thermal expansion coefficient, horizontal response to cooling
Thermal expansion/integrity test	Undrained – drained (depending on test duration)	Thermal expansion coefficient (undrained), horizontal response to cooling

Extended triaxial tests have also been performed at the Otway, encompassing a comprehensive exploration of the storage interval’s poroelastic and strength properties (Tenthorey et al., 2018). These tests were instrumental in characterising post-failure frictional properties and assessing the rate-dependent behaviour of the rocks. The experiments, conducted at varying confining pressures, provided critical insights into the rate dependence of sliding resistance, a key factor in determining whether fault movement would be seismic or aseismic. The results of these tests were especially valuable, as they shed light on the behaviour of rocks in the post-failure stage, an aspect with significant implications for fault movement and the potential for induced seismicity.

These recent studies underscore its significance in overcoming testing limitations, understanding stress path effects, and enhancing our knowledge of fault stability in GCS operations.

7.3 Summary

There are many methods to characterise and evaluate seal integrity, including targeted log acquisition or well testing (e.g., petrophysical logs, image logs, extended leak-off testing, diagnostic fracture injection testing, micro-frac) as well as laboratory testing (e.g., tri-axial testing, imaging studies).

In this section, detailed stress field characterisation using image logs for GCS projects was discussed, including examples of when FMI has been applied to not only provide sedimentary, textural, and structural detail but also to provide an improved understanding of the distribution of insoluble material within a seal providing an understanding of potential migration pathways through the caprock. FMI or other image log tools can be combined with other logging tools or more regional data (e.g. seismic) to help characterise the stress field and stress-induced features.

Further, imaging studies (μCT and SEM) are helpful in characterising prospective CO_2 seals at multiple scales. Imaging studies can be undertaken on various sample sizes (e.g., cuttings or sidewall cores). This section discusses the advantages and disadvantages of each approach, and core imaging studies can help identify coring-induced fractures from natural fractures.

Pore-scale imaging is an emerging field of research in which various imaging techniques (e.g. μCT) can be combined with computational approaches to create a numerical representation of the pore space that can then be upscaled to form pore physics inputs (e.g., capillary pressure and relative permeability curves) for flow simulation. The appropriate method of upscaling these techniques remains a challenge given the high computational requirements for some methods, though this remains an interesting field of research that warrants more attention.

Methods for evaluating the brittleness of caprocks were discussed in this section. Three general approaches exist (mineral-based, log-based, and elastic-based) for calculating a brittleness index. One recent top seal study for the Northern Lights project concluded that no single approach to establishing a brittleness index can be applied across all basins. The best practice is to consider all data sources. The limitations of the various brittleness index methods were described, mainly in terms of how these methods indicate lithology rather than rock failure. A more accurate prediction of the rock's propensity to fracture can be achieved by undertaking a fracability evaluation.

Preservation and sealing of cores are crucial steps in geomechanical analysis to maintain the integrity and representative nature of the core samples. This is particularly true when clay minerals are present in significant percentages in the core's mineralogy. Specific focus areas in core preservation have been outlined, including preparation, sealing, sampling, and testing.

Finally, triaxial testing was discussed briefly. Triaxial testing determines critical mechanical properties of reservoirs and seals by subjecting samples to controlled stress conditions to understand how these rocks behave under the pressures and stress pathways experienced during CO_2 injection and storage. An example of a testing program of mechanical experiments for the EOS well (Northern Lights Project) has been provided, which helps demonstrate the range of geomechanical testing that should be considered for a GCS project.

8. Modelling of Faults and Fractures for CO_2 Flow

As identified in section 2, several possible risk mechanisms may result in a loss of CO_2 in GCS from a storage complex. While the initial GCS projects avoided faults and fractured systems, as GCS transitions to “at-scale” to achieve national and global emissions reduction targets, it is inevitable that sites with faults and fracture systems will be assessed for storage potential. Simply excluding these sites increases the cost to society of decarbonisation. Therefore, it is important to understand the broad context of what defines a “good fault” for GCS and which faults or fault systems should be avoided.

The presence or creation of faults and fractures may provide a geological conduit for the migration of injected CO_2. Leakage or loss of containment from a storage complex may occur through a lithological top seal or due to either across or up-fault flow. In some cases, this could lead to the injected gas being liberated into shallower formations or, in a worst-case scenario, the surface or water column. The increase of pressure and the consequent modification of the stress field during the injection phase may also enhance those properties (mainly, the permeability), the fault acting as a flow conduit along the fault plane. In addition, leakage can occur in a lateral sense through a ‘fault seal’ due to cross-fault flow.

When undertaking subsurface characterisation or subsequent modelling for GCS assessment, the dynamic characterisation of the faults is critical to predicting CO_2 migration. While modelling properties of flow across fault is common practice in reservoir simulation, the study of possible flow along/up the fault is an active area of research for GCS, and it has had many publications over the past decade.

For several reasons, obtaining a complete understanding of fault properties and behaviour can be challenging. Importantly, it is not possible to generalise fault behaviour as each fault has its unique origin and characteristics. Additionally, collecting data from subsurface faults, particularly those in saline formations being assessed for prospective geological storage of CO_2, can be difficult where there are little to no well penetrations through faults in some formations. In addition, faults may exhibit localised differences in properties, such as permeability, which can significantly affect the flow behaviour and result in unexpected impacts.

This section presents several studies identified from a literature review that focus on analysing the properties of the flow along faults. These studies evaluate the impact of these properties on potential CO_2 leakage in saline formations using numerical simulations. The simulations also consider the interaction with possible shallower permeable formations.

Additionally, the literature describes new methodologies for the numerical modelling of subsurface dynamics. These methods allow for shorter simulation times and efficient modelling of CO_2 injection in saline formations. This is especially important because these scenarios typically require geo-models with high cell counts and significant simulation times, including post-injection behaviour modelling for assessing CO_2 plume stability and pressure field impacts, particularly after the injection has ceased.

Finally, research is presented on how the interaction between faults and injected fluids can lead to fault reactivation and increase the risk of CO_2 containment.

8.1.1 Modelling Faults as Flow Conduits

Several parameters that determine their structure influence subsurface faults' characteristics. These structures can be quite complex, with multiple components present. In the petroleum industry, a simplified model is commonly used (Figure 43), which identifies the fault core area where the primary throw surfaces are found and the surrounding damage area, characterised by fractures caused by the faulting process (Nicol et al., 2017).

In the core of a fault (Figure 43a), low permeability clay-rich rock is commonly found due to smearing that occurred during the formation of the fault. This acts as a barrier to fluid flow across the fault and, in extreme cases, can even seal off horizontal fluid movement. In contrast, the damage zone comprises sets of fractures, usually sub-parallel to the main fault plane. These fractures may allow fluid to flow vertically depending on factors like their extension, aperture, and density. If these fractures extend through the sealing layer of the overlying caprock, they could compromise its ability to contain fluids.

Figure 43b provides a conceptual diagram of a complex fault zone. It considers a scenario where multiple fault planes are present while the damage zone consists of heterogeneous bodies that include sub-faults. This is a common occurrence at the outcrop scale and accurately reflects the spatial variability associated with faults. In this more complex setting, a detailed study of the outcrop area of the faults is needed to understand best the origination mechanisms, which, in the end, can support the representation of the flow behaviour inside the fault (Childs et al., 2012).

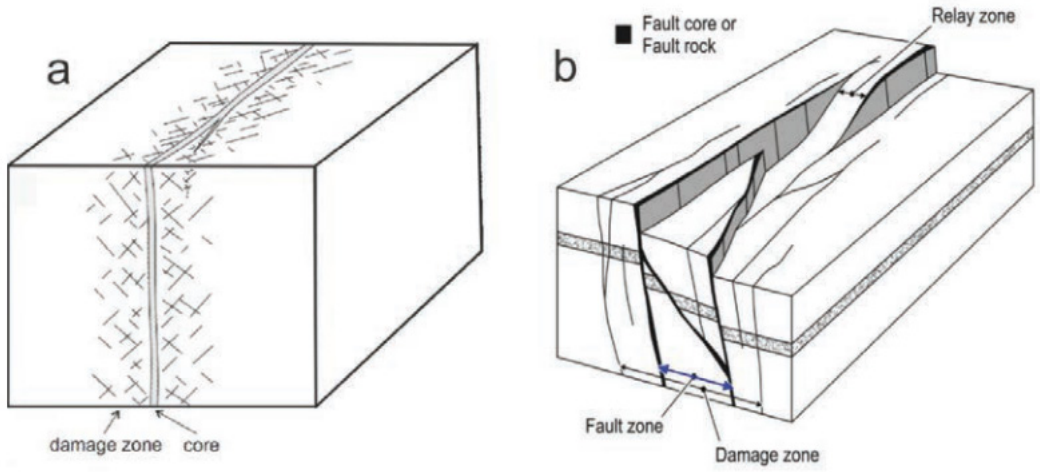

Figure 43: Exemplification of the structure of a fault (Nicol et al., 2017). (a) The fault is represented through the core-damage zone model. (b) A more complex model, typically representing a fault in the outcrop area. Original image (Childs et al., 2009)

Due to the flow characteristics of the fault and its particular areas, the simplified core-damage zone model gives rise to a dual barrier-conduit system (Nicol et al., 2017). Therefore, the flow behaviour at the fault can be defined by assigning flow properties, particularly permeability, to the fault rock, which in turn includes the entire fault zone (core and damage areas).

Local areas with specific properties caused by tectonic deformation can be detected and discretised inside the complex fault envelope. These areas are called “fault facies” and are characterised by their morphology, extension and location with respect to the main fault core and their lithology (Braathen et al., 2009). Their presence and distribution in the fault area determine the fault properties even from a fluid dynamic behaviour perspective.

Using fault facies can be the basis of a detailed representation of the fault in a geo-cellular model. However, the representation of a fault in a dynamic numerical model tends to scale up the local properties of the fault, adopting an approach that generally aligns with Figure 43a and, in some scenarios, may even adopt a more simplified description of the fault.

Various models available for assessing permeability across faults are presented in the literature, most of which rely on clay content within the fault core. The Shale Gouge Ratio (SGR) is a well-known analytical method for evaluating clay content along the fault displacement plane (Yielding et al., 1997). Calculating SGR,

which ultimately determines the amount of shale present in the fault at different depths as a function of the depth, is illustrated in Figure 44.

Using this parameter, the horizontal permeability (across fault) is calculated through the correlation found in the equation (Manzocchi et al., 1999):

$$\log k_h = -4\,SGR - \frac{1}{4}\log D \cdot (1 - SGR)^5.$$

Here, k_h represents the horizontal permeability (in mD), and D is the displacement of the fault (in m), measured along the fault plane.

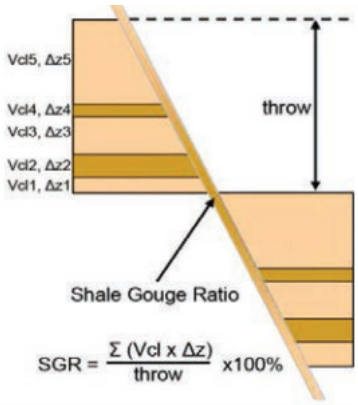

Figure 44: Shale Gouge Ratio (SGR) model for the calculation of shale content along the fault throw (Nicol et al., 2017). Original image from (Yielding et al., 2010)

Typical values for across-fault permeability result in the 10^{-3} – 10 mD range. Vertical permeability is then calculated, usually assuming anisotropy for the fault rock. Although there is significant uncertainty regarding the anisotropy ratio, it is commonly observed that the vertical permeability in faults may exceed the horizontal permeability by some order of magnitude, ranging from 1 to 1000 mD (Nicol et al., 2017).

The SGR model underpins the geo-cellular modelling study of the Vette fault (Horda platform, North Sea, Norway) (Bjørnarå et al., 2021)In the geocellular model, the fault's geometrical and hydraulic structure is approximated by an arrangement of rectangular geocells with variable length and width. The isotropic hydraulic property of each geocell is populated stochastically from a reference value based on the fault's shale gouge ratio (SGR).

The concept of the geo-cellular model for the representation of fault properties was validated through the probabilistic evaluation of the flow across and along the fault itself. The stochastic population of the fault zone in terms of SGR was combined with different vertical discretisations of the underlying grid (Figure 45). Increasing the variability of fault properties results in a more consistent resolution of the fault zone. As a result, it was observed that the along-fault flow is relatively stable with respect to the different discretisations, while the across-fault flow decreases with increasing granularity.

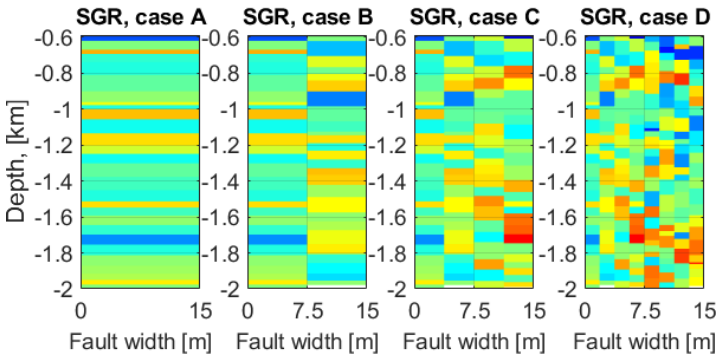

Figure 45: Four cases (1, 2, 4 or 8 vertical layers) of fault discretisation in the horizontal direction (Bjørnarå et al., 2021). The SGR values are assigned stochastically to each cell and here represented with a colour scale from cold blue (SGR=0%) to hot red (SGR=100%).

(Bense & Person, 2006) proposes a more refined method for the calculation of the hydraulic properties of the faults. The main parameters used as inputs are fault width and permeability, the calculation of which is based on the variation of the clay content of the sediments that move along the fault zone. In this respect, this approach is based on the previously described SGR model, but it provides the flexibility to incorporate strongly contrasting lithologies on both sides of the faulting plane. The fault permeability is independently calculated for the hanging wall and the footwall, starting from the effective porosity (determined by the effective stress and, in turn, by the burial pressure) and the clay content. The total fault permeability is then obtained from the contributions of the two sides; the horizontal permeability (across the fault) is calculated as the harmonic average, and the vertical permeability (along the fault) is the arithmetic average. The fault widths, calculated for the two sides as a function of the depth and dependent on the fault displacement and the clay content of each involved formation, are used in the weighted averaging calculation.

Using the harmonic average to calculate the across-fault permeability enhances the effect of the low-permeability layers contributing to the hydraulic properties of the fault so that the transversal barrier effect is assured. On the other hand, the arithmetic average used for calculating the along-fault permeability favours the contribution of high-permeability layers, allowing the fault to work as a vertical conduit among different layers. This results in a strong anisotropy in the fault, resulting in vertical permeability of up to seven orders of magnitude higher when very low-permeability rocks are juxtaposed with very high-permeability material.

This method was used in a sensitivity analysis of the hydraulic behaviour of the Vette Fault (Bjørnarå et al., 2023) as an extension of the previous study discussed earlier. In the latest work, the permeability across and along the fault was evaluated based on different combinations of the original permeability for the host rocks at the sides of the fault. The combinations of these parameters resulted in the creation of 1250 2D dynamic models. Among other parameters, different values for the fault width were considered in the sensitivity analysis, including several cases in which the fault was not characterised but considered only as a discontinuity in the subsurface lithology (i.e. assigning a null width). The simulations were run in a simplified scenario where leakage potential under steady-state conditions was assessed when the CO_2 was injected in the most permeable layer (the reservoir) at constant pressure.

A primary qualitative result from this study was that including a fault with an anisotropic permeability significantly alters the flow rate. The main effect is that an along-fault pathway is introduced into the flow model, allowing vertical communication and bypassing upward and downward sealing units. Compared to this fault model, the geo-cellular model presented in (Bjørnarå et al., 2021) did not provide an effective seal and behaved more similarly to the no-fault models considered in the recent work.

Due to the limitations in the dynamic modelling approach (e.g., steady-state conditions with single-phase flow of resident brine), the results need to be refined to evaluate the potential of CO_2 leakage in more realistic scenarios. This includes, for example, specific operating conditions (e.g. injection periods) or the thermodynamic behaviour of the injected and reservoir fluids.

Therefore, it is critical to accurately determine relative permeability curves for both CO_2 (gaseous and dense phase) and water and the capillary pressure curve to describe the behaviour of such flow along a fault. An example of this can be found in Figure 46, where residual saturation for water and gas is calculated using analytical models found in the literature (Prasun, 2021).

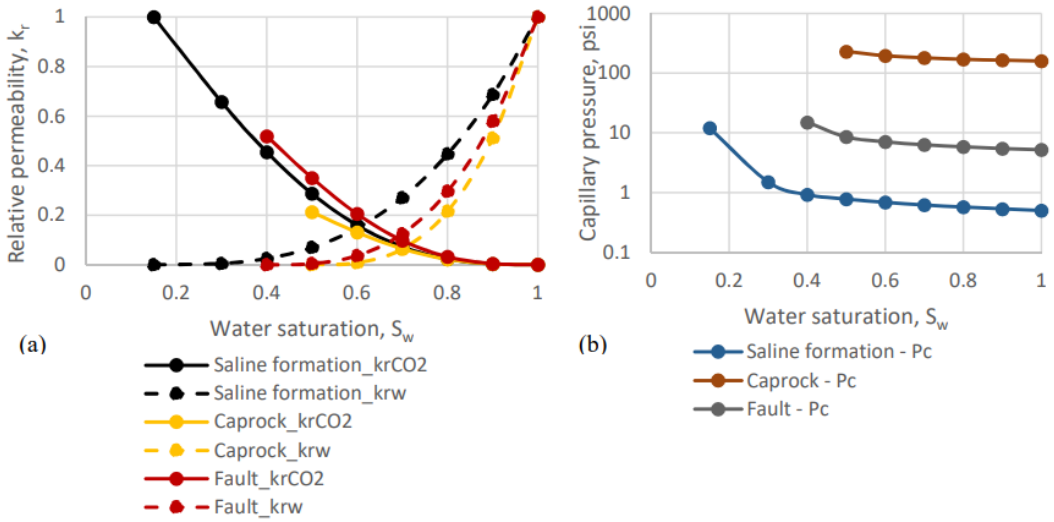

Figure 46: Relative permeability curves (a) and capillary pressure curves (b) used in numerical modelling for the formations involved in CO_2 injection and possible leakage, including saline formation (host rock), shale caprock, fault rock (Prasun, 2021).

It is then necessary to include faults in the numerical model to simulate fluid flow accurately and evaluate potential CO_2 leakage from the storage unit. Any modelling results must be constrained by observations. For example, the Vette fault has constrained the Troll Gas Field and therefore vertical migration must have been limited (Bretan et al., 2011). The traditional method of representing faults using a transmissibility multiplier at the edge of cells is insufficient as it cannot account for vertical flow. Instead, using traditional structured gridding techniques, a fault must be modelled in a set of cells with specific flow properties (such as absolute horizontal and vertical permeability and relative permeability, and calculated as per the method described previously. The model grid must be refined appropriately, particularly in the horizontal direction perpendicular to the fault plane, to represent the geometry of the fault properly (Figure 47). Consequently, adjusting the simulation timesteps is essential to ensure numerical stability during dynamic simulations.

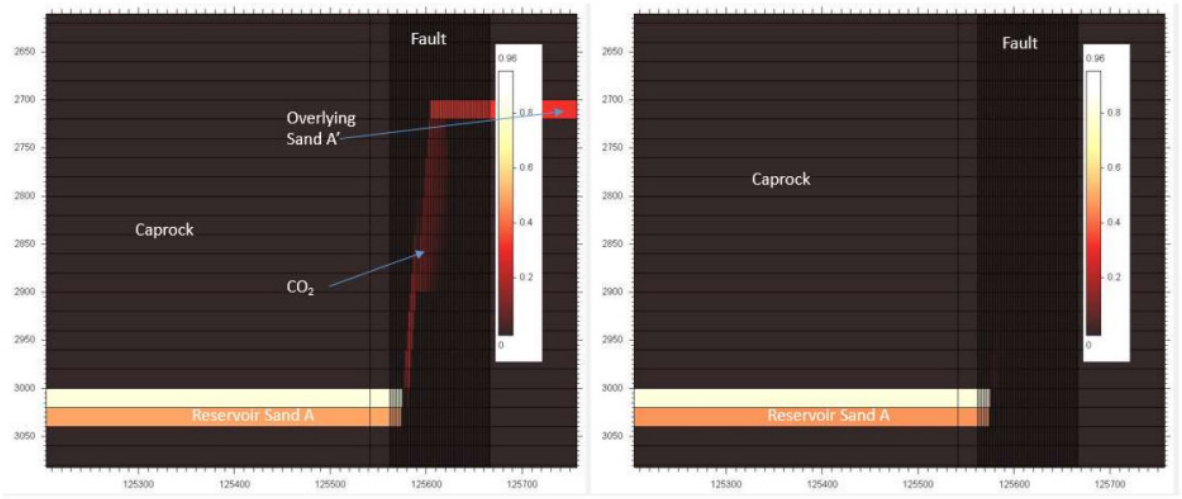

Figure 47: Vertical section of the numerical model used for the simulation of CO_2 injection and leakage (Prasun, 2021). The refinement of the numerical grid is evident in the vicinity of a fault. (Left) The reservoir sand A is in communication with shallower layers (only A' is visible in the picture). (Right) The shallower layers are not present.

8.1.2 Worked Examples of Simplified Fault Modelling

The objective of modelling fault flow behaviour is described in section 8.1.1 is evaluating the effects of the possible leakage from a target formation due to CO_2 injection under the fundamental assumption that a fault enables hydraulic communication between the injection formation and shallower layers (Prasun, 2021; Tao et al., 2013). An example of the subsurface architecture considered for a numerical study is presented in Figure 48.

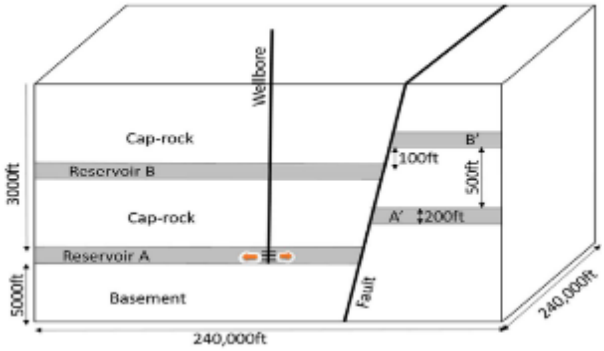

Figure 48: Notional synthetic model for the simulation of injection and leakage of CO_2 (Prasun, 2021) The fluid is injected in sand A. The fault in the model puts formation A in possible communication with shallower layers: A', B, B'.

In the study, the fault's permeability is calculated using the SGR model. The effect of the fault throw (compared to the fixed thickness of A and A') on the permeability is evaluated. Figure 49 illustrates the permeability across faults resulting from the application of the SGR model and vertical distribution for different values of fault throw and input parameters.

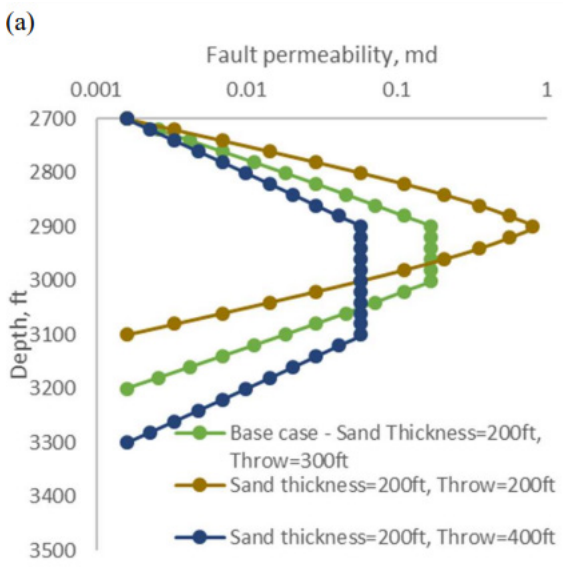

Figure 49: The fault across-permeability for different vertical throws using the SGR model (Prasun, 2021) . The top depth of the plot (2700 ft) corresponds to the top of Formation A' (see Figure 48).

The geomechanical effects on the along-fault permeability, critical for the CO_2 flow in the vertical direction, were evaluated in the work presented in the paper. It was calculated that the volumetric strain of the rock, due to the pressure build-up during the injection phase, leads to a relative enhancement of the permeability by approximately 15%, which is considered negligible, particularly for low permeabilities. For this reason, this kind of phenomena were not included in the simulations.

The vertical permeability of the fault rock was modelled as constant and uniform. Whereas a value of 0.05 mD was considered reliable, the simulations' results were presented with a vertical permeability of 0.5 mD. This value can be regarded as an extreme case, obtained with no to little shale-to-shale juxtaposition on both sides of the fault, and hence magnifies the effects of the flow of CO_2 along the fault.

A sensitivity analysis was conducted to quantify the impact of several reservoir, fault, and injection scenarios (i.e., total CO_2 injected in formation A for 30 years) (Prasun, 2021). The study also evaluated the plume evolution over 170 years after injection had ceased.

One of the main qualitative conclusions of this study was that there is effective vertical communication between formation A and shallower layers, and CO_2 has the potential to migrate. It is observed from the modelling that the CO_2 plume ceases to propagate up the fault beyond the immediate shallower zone A' (see Figure 47a). Flow from formation A' toward even shallower layers is strongly attenuated because of the strong transmissibility contrast between layer A' itself and the fault. The flow of CO_2 into A' is then favoured to the migration upwards toward other permeable layers, resulting in a thief zone for the migrating fluid.

Similar behaviour was observed in numerical analysis conducted on 3D models from the Mahogany field, Trinidad (Tao et al., 2013). In this work, the permeability across the fault was on the order of micro-to-millidarcy with an average of 50 microD. To assess the quantitative impact on the flow, a vertical anisotropy ratio varying in the range 1 – 10 was considered for calculating permeability along the fault.

An additional scenario was investigated where the overlying formations were not present to observe the potential leakage directly to the surface attributable to a fault. It was concluded that little to no migration is established, and only a small quantity of CO_2 can leave the injection layer (Figure 47b). This result led to the conclusion that the possibility of CO_2 leakage through a fault is the result of the entire system considered, which includes the designated CO_2 storage unit, the fault itself, and the shallower permeable formations (particularly the immediate shallower one) which the migrating gas may encounter.

Figure 50 shows the results of the sensitivity assessment. It is evident that the fault throw (compared to the thickness of the storage unit) has the most significant impact; fault distance from the wellbore, fault thickness and reservoir transmissibility can result in more than 0.1% of the CO_2 migrating to sand A'.

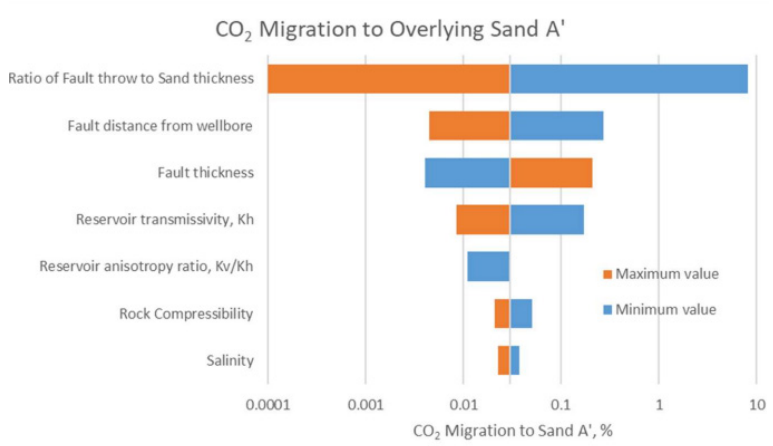

Figure 50: Tornado plot showing the results of the sensitivity analysis performed. The sensitivity of the CO_2 migration to fault parameters, sand or operating parameters is reported (Prasun, 2021).

An alternative numerical approach represents the fault as a quasi-1D model CO_2 communication with a CO_2 storage layer at the bottom and to other permeable layers at shallower depths (Chang et al., 2008).

In this simplified model, the flow equation concerning the migration of CO_2 along the fault includes a source/sink term, which is calculated as the product of a leak-off coefficient times a potential factor:

$$q(z,t) = q_{leak}(z,t)\,[\Delta p(z,t) + G(z,t)].$$

In the equation, Δp represents the deviation of the pressure at a certain depth and time with respect to hydrostatic pressure: $\Delta p(z,t) = p(z,t) - p_z(z)$, being z the vertical depth, t the time and p_z the hydrostatic pressure; G is the gravitational term: $G(z,t) = \rho(z,t) \cdot g \cdot z \cdot CO2$, where ρ is the fluid (CO_2) density, g is the gravitational acceleration, and γ is the inclination angle of a possible permeable formation with respect to the horizontal (this allows the CO_2 to migrate correctly towards the upward vertical direction in case of inclination).

A key aspect of this model is the definition of the leak-off coefficient q_{leak} which is calculated as follows:

$$q_{leak}(z,t) = \frac{\rho \cdot k_r \cdot k_{layer}}{\mu \cdot L}.$$

This coefficient shows dependence on the properties of the fluid (density ρ, viscosity μ), properties of the rock (absolute permeability k_{layer}), flow properties (relative permeability k_r), and the length L, representing a characteristic distance from the fault at which the pressure disturbance in the permeable layer can be considered irrelevant. The dependence on the permeability of possible leakage formations assures that the coefficient (and therefore the CO_2 leakage) can be regarded as null on the entire length of the fault but where the permeable formations are located.

The mathematical model confirms that the CO_2 storage formation (which in this scenario is considered an infinite reservoir of leaking CO_2), the fault and the shallower permeable layer should be viewed as a whole system. Figure 51 illustrates the CO_2 migration from a storage formation (not shown) into shallower formations.

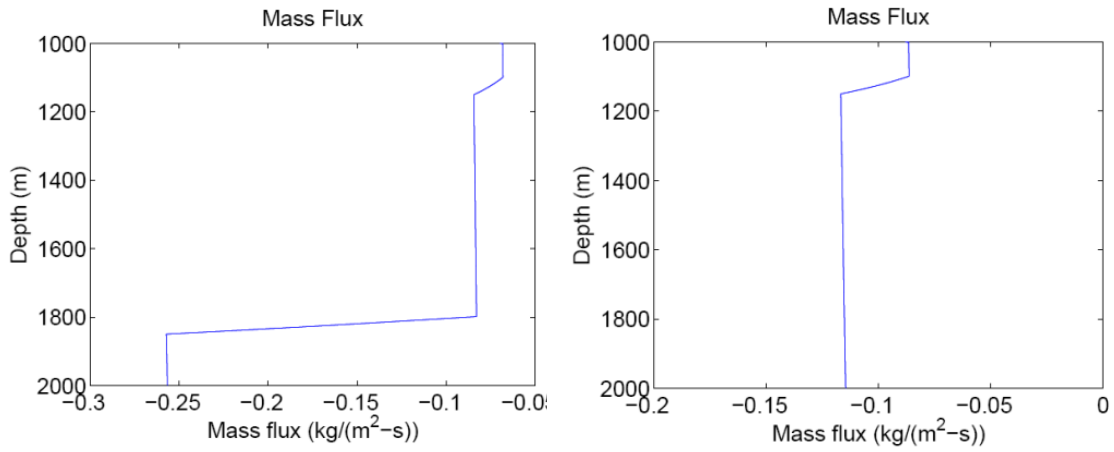

Figure 51: CO_2 mass transfer (in kg/(m²/sec)) obtained in two simulation cases from a quasi-1D simulation model (Chang et al., 2008). The storage formation is not pictured. The negative sign indicates that the mass transfer acts from the fault to the formation. (a) Two permeable layers are encountered along the fault at about 1800 m and 1100 m of depth. The deeper layer (closer to the leaking formation) is responsible for most leakage. (b) If only one permeable layer is present (the shallower one), the leakage occurs at a different rate; however, it is less efficient with respect to the global leakage of case (a).

8.1.3 Increased Definition Fault Modelling

The approach presented in Section 8.1.1 may result in an oversimplification of the fault architecture and its flow properties for cases where the fracture network at the sides of the fault core is extended in the host rock and can impact flow. In such cases, the explicit description of the fault zones should be considered.

The examples presented here aim to describe the system of fractures induced by a fault in carbonate formations. Indeed, in the case of carbonates, the fracture network has a more significant impact than in softer lithologies, for example, because of the stiffness of the host rock, which allows the fractures to maintain a relevant aperture and, therefore, contribute to the potential vertical flow.

A critical challenge is to define vertical permeability for fault modelling. If the vertical permeability is not known, the simulations (and the insights that are subsequently derived from modelling) will depend on an unconstrained choice of the vertical permeability.

An essential study in the evaluation of leakage of injected CO_2 along faults was performed in the DETECT project (Dean, 2020). The project resulted in the development of a comprehensive methodology (Figure 52) for assessing the risk of CO_2 leakage and determining the most appropriate mitigation measure. This work was primarily based on data from the Green River site (Utah, USA). This site is well characterised by previous hydrocarbon exploration activities, where natural seepage of CO_2 is observed.

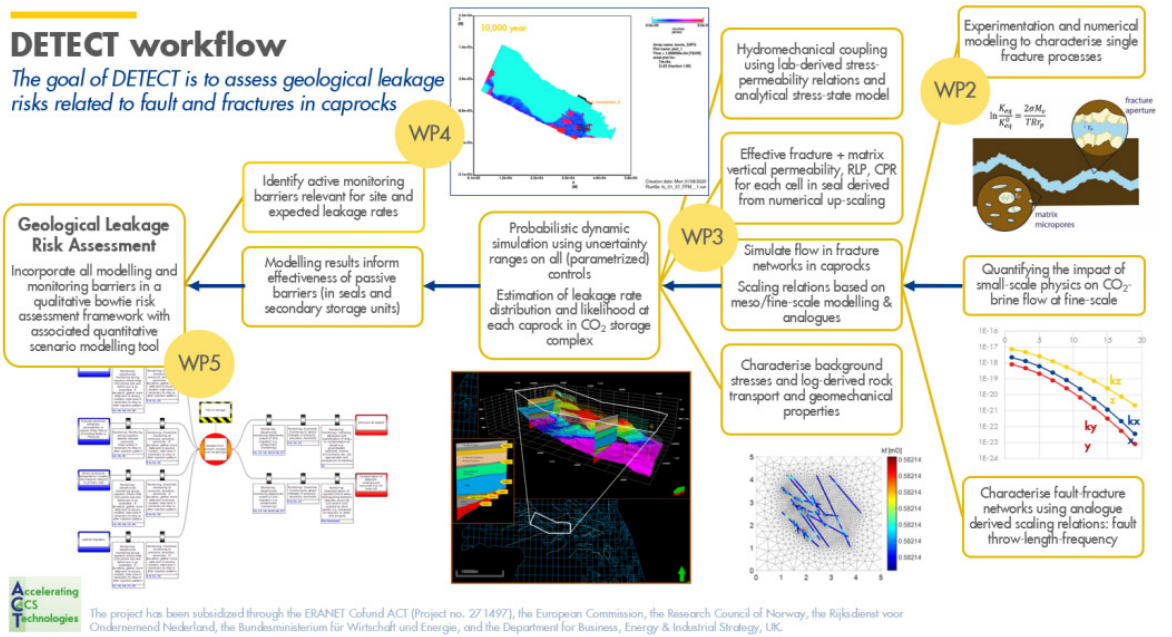

Figure 52: The DETECT workflow for assessment of CO_2 leakage risk and selection of monitoring and remediation actions (Dean, 2020).

The DETECT project aims to study the leakage of CO_2 caused by flow through existing fault fracture networks. The goal is to model the flow behaviour as a function of mechanical parameters, such as pressure increases due to injection. Additionally, the comprehensive study investigated the chemical impact on the caprock of the CO_2 and the formation brine. The results were then used to create a risk assessment tool (a bowtie model, as discussed in section 6.1.1) that provides guidelines for monitoring and selecting the optimal containment mitigation actions.

The Green River site is characterised by reservoir units ranging from aeolian, fluvial and marginal marine sandstones, as well as marine siltstones and lacustrine shales (Dockrill & Shipton, 2010). The Pennsylvanian and Permian formations consist of marine carbonates and shales that are potential sources for the natural accumulations of CO_2 (Heath et al., 2009; Snippe et al., 2022). One of the activity streams of the DETECT project (WP3) was characterising the fault-fracture system present in the subsurface using the extensive available data.

The architecture of the subsurface is impacted by the presence of two main faults: the Little Grand Wash Fault (LGWF) and the Salt Wash Graben fault. These faults allow hydraulic communication between formations and the surface, resulting in the natural seepage of CO_2. Leakage rates at the surface were measured and used as match parameters for the evaluation of the subsurface model, with the primary focus on the LGWF (Snippe et al., 2022).

Two main faults impact the subsurface's architecture: the Little Grand Wash Fault (LGWF) and the Salt Wash Graben fault. These faults allow hydraulic communication between formations and the surface, resulting in the natural seepage of CO_2. Leakage rates at the surface were measured and used as match parameters to evaluate the subsurface model, primarily focusing on the LGWF (Snippe et al., 2022).

The methodology for subsurface characterisation focuses on the study at three scales: single-fracture scale, fracture network scale (mesoscale) and field scale. In the single-fracture scale phase of the study, the available data were utilised to develop an empirical model correlating the permeability of the single fracture to the stress field of the host rock (Figure 53). The permeability is also related to the stiffness of the host rock through Young's modulus. This permeability trend is then upscaled through the fracture-network study. The

mesoscale study concluded that fracture conductivity plays a role when considering horizontal flow. In the context of CO_2 leakage, where vertical flow is prominent, a simplified relationship can be obtained, considering that only fractures passing through the caprock contribute to the flow. Consequently, the effective vertical permeability can be approximated as the product of single-fracture permeability, fracture aperture and linear density of passing-through fractures. This simplified model was then imported into the numerical model for field simulations.

Fracture flow properties, including relative permeability and capillary pressure curves, were also evaluated at a single-fracture scale. Fine-scale numerical simulations with explicit fracture roughness representation were set up for this purpose. Stochastic simulations were then performed by considering nine classes of fracture roughness. In conclusion, for each class, a set of capillary number-dependent relative permeability and capillary pressure curves were obtained (Figure 53), thus keeping the pressure-dependent balance between viscous and capillary forces into account. Curves based on fracture roughness, fracture aperture and fluid pressure gradient were incorporated into the meso- and field-scale models.

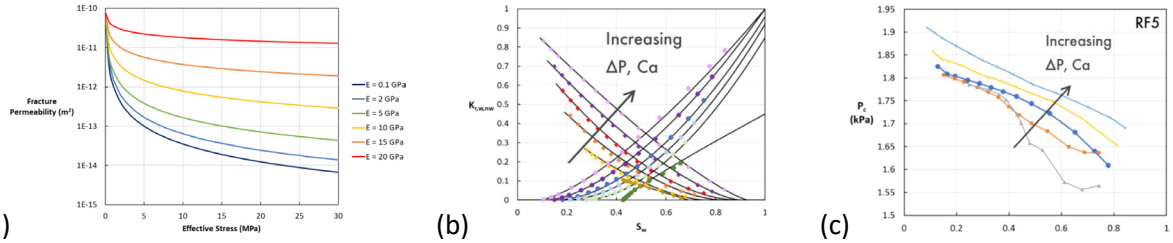

(a) (b) (c)

Figure 53: Results of the single-fracture scale study fracture permeability trend (a) as a function of effective stress field (for several Young's moduli) (a); for a single fracture class, an example of sets of relative permeability curves (b) and capillary pressure curves (c) for several capillary numbers, Ca. (Dean, 2020)

As a conclusion of the study, the results of the 3D numerical simulations are presented. A sensitivity assessment indicated that using a relatively coarse grid was representative of the results obtained from more detailed models despite the narrow fracture apertures. A grid with a lateral resolution up to the fault damage zone's width and a vertical thickness of two to three layers per formation was finally implemented in the model around the fault. In particular, the upscaled permeability calculated through the simplified relation was included. At the same time, an upscaling of porosity was performed to ensure that the correct CO_2 storage capacity was assigned to the damage zone, even considering the CO_2 diffusion in water.

The migration of gaseous CO_2 from the initially mineralised formations is observed with the formation of secondary gas caps on shallower layers. It is evident from Figure 54 that gaseous CO_2 is found in the original Whit Rim formations (basalmost layer in the Figure) and other layers. Moreover, since the model also accounts for the phase behaviours of the CO_2-brine mixture, even CO_2 dissolved in the aqueous phase is observed to migrate to shallower layers. Due to other simplifications in the model (e.g., geochemical reactions are neglected), which was outside of the study scope, the quantitative match of the surface seepage rates of CO_2 is not entirely achieved. However, the observed (field) trend is qualitatively represented by the study outcome.

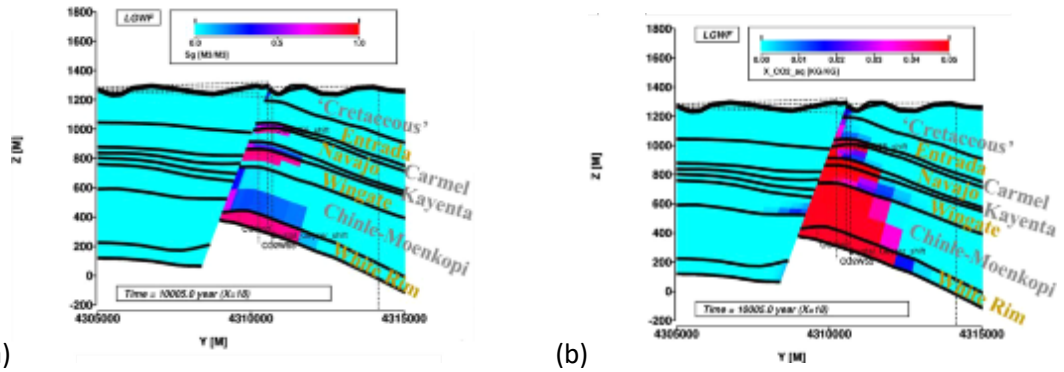

Figure 54: The 3D simulations at the field scale of the Green River site show the migration of gaseous (a) and dissolved (b) CO_2 from deeper to shallower layers (Snippe et al., 2022).

A fault's core and damage zones were also characterised by a shallow, outcropping fault in the Maiella site (Italy) (Romano et al., 2020). This study directly measured fracture properties (density, aperture, orientation, etc.) at the surface. The permeability of the fracture set was determined by constructing a discrete fracture network using commercial and open-source simulators, which were then imported into a 3D model (Figure 55).

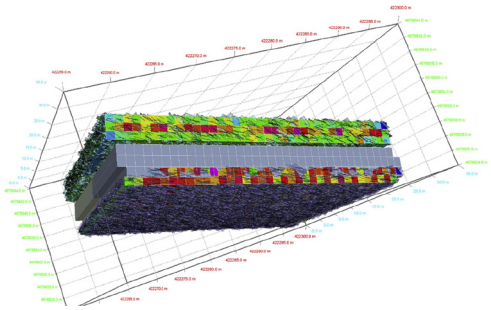

Figure 55: The Discrete Fracture Network model representing the damage zone around the fault core (in grey (Romano et al., 2020).

The flow properties are then upscaled for the damage zone at each side of the fault, using upscaling methods and correlations from literature (mainly following (Hyman et al., 2015)) alongside statistical analysis of stochastic simulations based on the distribution of fracture properties. The resulting distribution of properties is shown in Figure 56. Since the fracture distribution is different on the fault's two sides, two different permeability values are assigned for the hanging wall and the footwall.

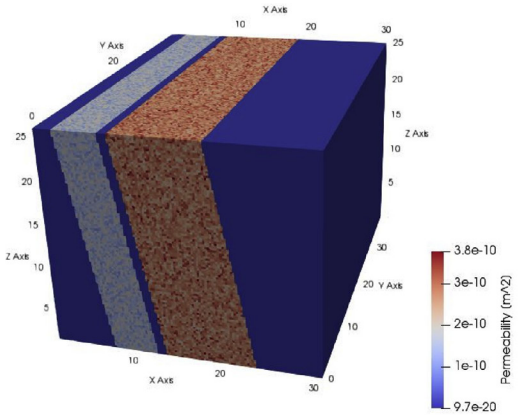

Figure 56: The permeability distribution resulting from the analysis. The low permeability at the host rock and the fault core is evident. The damage zones are characterised by higher permeability but with different values for the hanging wall and the footwall (Romano et al., 2020)

The results of the fault characterisation were then used in (Romano, 2022) for dynamic flow simulations of CO_2 injection and migration in the fault zone. In this study, CO_2 injection in the fault damage area (in particular, the footwall) was considered due to the extremely low flow properties of the original host rock. A sensitivity analysis examining the location of the injection well and the injection rate was performed, even implementing phase equilibrium between injected CO_2 and resident brine.

The simulations showed that the injected CO_2 primarily flows up the fault along the permeable fault footwall (Figure 57a). In the case of injection close to the fault core, part of the CO_2 passes across the core, invading the hanging wall because of overpressure (Figure 57b). This is an interesting result, showing that overpressure can cause a change in the stress field along the fault, potentially giving rise to related risks (see section 8.1.5).

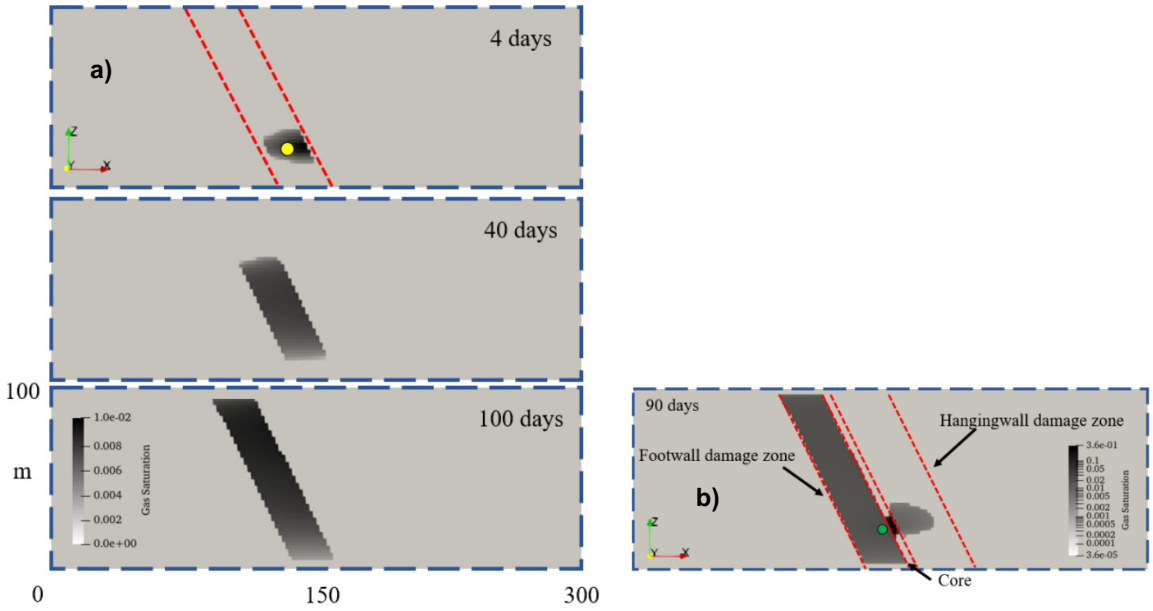

Figure 57: Results of dynamic simulations in (Romano et al. 2022) for two different locations of CO_2 injector well. a) Injection in the footwall, relatively far from the fault core. b) Injection close to the fault core. The breakthrough of CO_2 in the hanging wall is observed due to overpressure.

8.1.4 Advanced Numerical Modelling

Accurate simulation of CO_2 injection in saline formations involves modelling several phenomena related to multiphase (brine-CO_2) flow, phase behaviour, and geochemical reactions with the host rock, caprock minerals, and, if present, fault rock.

Moreover, models with large cell counts are required due to the large areal extent and appropriate gridding requirements. In many instances, particularly if saline aquifer storage systems are being evaluated, the model scale can be an order of magnitude larger than standard petroleum industry models. A common approach to avoid numerical divergence is to use grid refinement in the areas where high impact or abrupt behaviour is expected to occur (e.g., high mass exchanges around the injection wellbore) and where the geometry of the subsurface is more refined, like in fault zones.

Recent advanced gridding techniques propose using unstructured grids, in which the geometry of the cells is not fixed, to characterise best these attributes (Littmann & Littmann, 2012). This gridding technique can ensure communication between numerical cells belonging to different layers (as is required in case of a fault)

and, therefore, overcome the inherent limitations present in structured grids like corner point grids that are typically limited by the geometry of the layering. In unstructured gridding, even the most geometrically complex structures can be appropriately represented in a numerical grid (Figure 58).

These grids can benefit from novel methodologies for constructing geological models. For example, the so-called "surface-based" geological modelling allows the distribution of static properties on geometrical bodies controlled by grid-free curves and surfaces (Jacquemyn et al., 2019). These models can capture the geological details of complex subsurface systems, like the structure of a complex fault, that traditional discretisation techniques cannot capture or need to approximate. The more accurate representation of the architecture of subsurface features will subsequently lead to a more realistic range of forecasts of CO_2 migration in the storage formation and complex.

Fewer numerical constraints for grid construction result in increased computational efficiency, which in turn allows the construction of multiple realisations of the property distribution. Recent studies employ artificial neural networks to create such distributions, considering the uncertainty due to the limited number of control points (i.e., the data from the wells) (Titus et al., 2022).

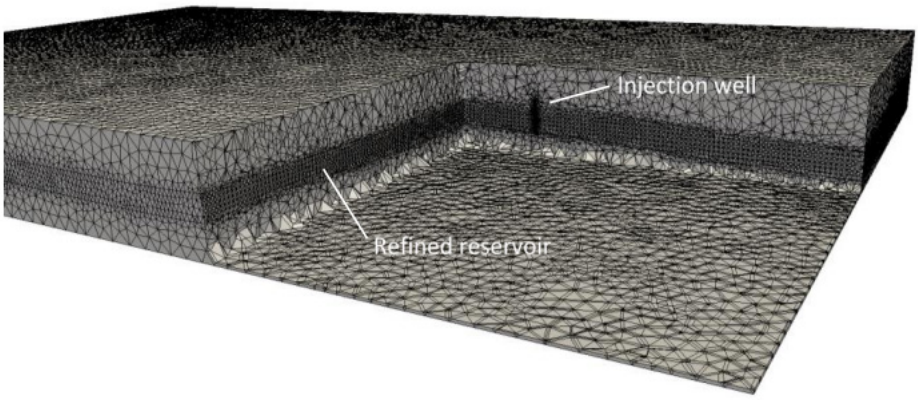

Figure 58: Use of an unstructured grid for the simulation of CO_2 injection in the subsurface (Shao et al., 2018). The refinement of the grid at the permeable formation and around the injection well is evident.

Timestep discretisation also plays a vital role in the efficiency of the dynamic simulations. The computational time required for simulating the injection of CO_2 in subsurface formations and the post-injection period (usually tens to hundreds of years) to assess the natural evolution of the CO_2 plume can be significant (often weeks to months).

This is primarily due to the discretisation of the timesteps during the simulation. The maximum timestep must fulfil the Courant-Fredrich-Levy (CFL) condition: $\Delta t \leq \frac{V_p}{F_{out}}$, being V_p the pore volume of a given grid block and F_{out} the total outflow to ensure numerical convergence of the simulation. This constraint ensures that the fluid flow leaving a single block in a single timestep is not larger than the block's pore volume, so the fluid volume internally to the cell cannot be negative. Otherwise, numerical convergence will not be achieved.

The CFL condition is the basis of synchronous time-driven simulations. A novel approach for timestep management using Discrete Event Simulations (DES) is proposed in the literature (Shao et al., 2018). This technique is based on a self-adaptive algorithm for solving flux-conservative equations. The discrete events, crucial for the simulation management, are related to the saturation of CO_2 in the grid blocks, and the rate of CO_2 saturation in each grid block at each timestep determines the scheduling of subsequent local events. These events, linked to a defined timestep, are then added to a dynamically updated list every time the flow and mass conservation equations with the neighbouring cells are solved for a grid block.

Due to the targeted locality of the simulation events, the mathematical model for fluid flow is solved only in the grid blocks and at the timesteps in the dynamic list. This means that, at each time step, the computational effort for solving the fundamental equations of the numerical model is limited to that part of the grid where non-negligible changes in CO_2 saturation are occurring. Fundamentally, in asynchronous simulations, the time advancement is unequal for every grid block and varies based on local discretisation.

Moreover, the locality of the discrete events at each timestep allows the parallelisation of numerical calculations, significantly reducing the total simulation time.

Figure 59 shows the application of the principle of asynchronous simulations to a case of CO_2 injection in a saline formation (Shao et al., 2018). On the left, the plume evolution is reported five years after the beginning of the simulation (end of the injection phase) and after a further five years of plume evolution. On the right of the figure, the cumulative number of events for each grid block is reported: it is evident that most of the entire grid was not involved in the simulation, resulting in a significant reduction in computational time.

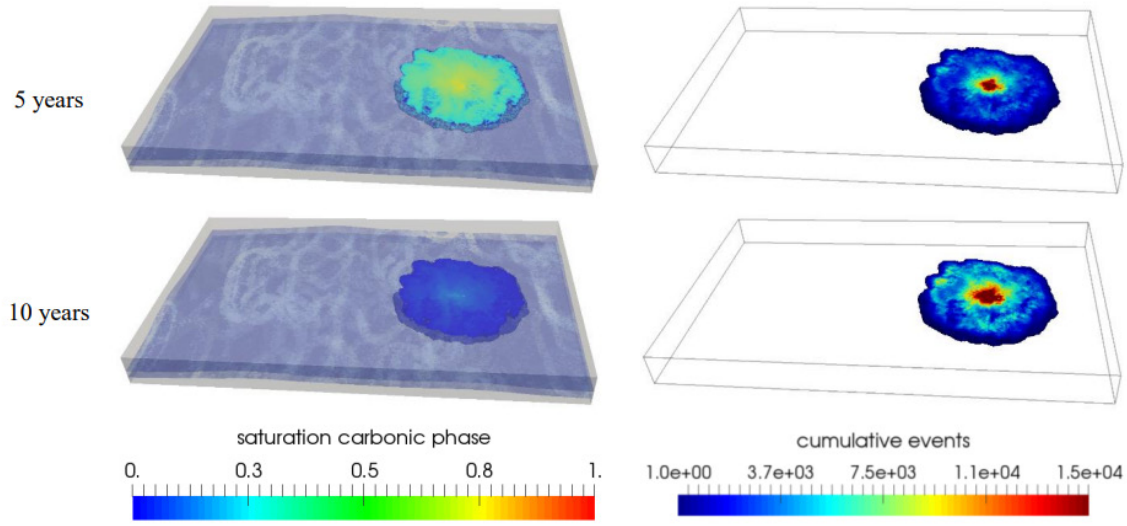

Figure 59: Results of asynchronous simulation of CO_2 injection in the subsurface (Shao et al., 2018). Left: Evolution of the CO_2 plume after five years (end on injection) and ten years of simulation. Right: The number of events simulated for each grid block. It Is evident that most of the model was not involved in the simulation, resulting in significant time saving.

The use of asynchronous time management in the case of an unstructured grid described here was also applied in the case of faulted formation (Matthai, 2020; Shao & Matthai, 2020). In Figure 60, the unstructured gridding (with clear refinements at the faults) and the plume evolution at different simulation times are illustrated. Due to the leakage through faults, the secondary invasion of shallower formations by injected CO_2 is observed.

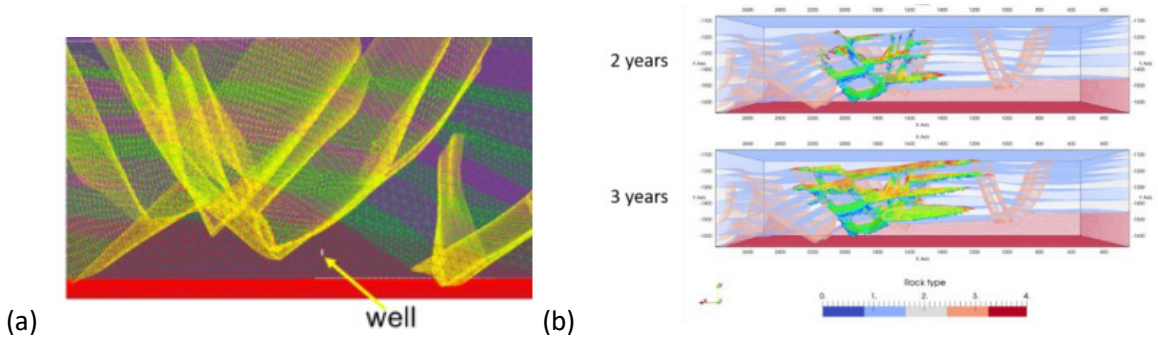

Figure 60: Application of asynchronous simulation to CO_2 injection in a faulted formation. (a) The unstructured grid; (b) The CO_2 plume evolution, showing secondary invasion of shallower formations (Matthai, 2020)

8.1.5 Fault Reactivation

CO_2 injection for GCS leads to an increase in pressure in the storage complex and a consequent decrease of the effective stress acting on the faults, which, if poorly managed, can lead to rupture of the fault rock and fault reactivation that may result in seismic events. For example, when the pressure changes due to fluid injection, it affects deep sedimentary units or faults coupled to a critically stressed basement (Luu et al., 2022). At present, it is recognised that seismic events induced by CO_2 injection to date have been low in magnitude and are rarely felt at the surface (Vilarrasa & Carrera, 2015; Vilarrasa et al., 2017). However, the risk of fault reactivation should always be considered as part of a GCS risk assessment (refer to section 6).

The modification of the geomechanical properties of the rock results in changes to the fault zone flow properties. Due to the uniqueness of each fault-rock system, it is difficult to formalise an analytical model that can describe the general response of faults due to CO_2 injection. Numerous publications describe the phenomena in specific geological contexts: the injection of CO_2 in extended aquifers bounded by a fault (Vilarrasa et al., 2017); the reversibility of fault activation in mudstones (with a possible definition of opening hysteresis) (Ohno & Ishii, 2022); the activation of faults that are undetected by seismic analysis of the formation (Blanco-Martín et al., 2022).

Significant differences in fault reactivation depend on the lithology of the rock hosting the fault itself. In-situ experiments of controlled CO_2 injection close to faults are described by (Guglielmi et al., 2021). The behaviour of shale faults, which represent caprock faults, is observed in Mount Terri (Switzerland) and Tournemire (France) underground laboratories. In contrast, carbonate faults are observed in the LSBB site (France). In the experiments, data pertaining to the flow behaviour of the formation-fault system was collected. Moreover, the modification of the main fault structural parameters (opening, possible slip of fault planes) was observed using dedicated bottom hole sensors.

In all the cases, seismic activation of the faults was observed, but with different timing and trends (Figure 61). The carbonate fault experiment demonstrated a gradual increase in flow rate (and permeability) with pressure, as well as the slip and the opening of the fault in time. In contrast, the shale fault demonstrated a steep increase in flow rate at a threshold pressure, which can be identified as the Fault Opening Pressure (FOP). At the FOP, the shale fault primarily shows a sudden slip and opening of the planes, corresponding to a sharp increase in permeability. The very low initial permeability of the shale fault and the low rigidity of the rock surrounding the fault create the conditions for a mixed tensile opening and shearing rupture mode. A relatively limited variation of permeability is observed for the carbonate fault, corresponding to a slip of the order of millimetres. Conversely, a slip of fractions of millimetres causes an increase in permeability of several orders of magnitude in a shale fault.

These focused mesoscale experiments provide useful information to illustrate conceptual models of fault reactivation for large-scale CO_2 storage projects in which an increased pressure originates at the injection

point and spreads in time until encountering a fault intersecting both the injection formation and the overlying caprock.

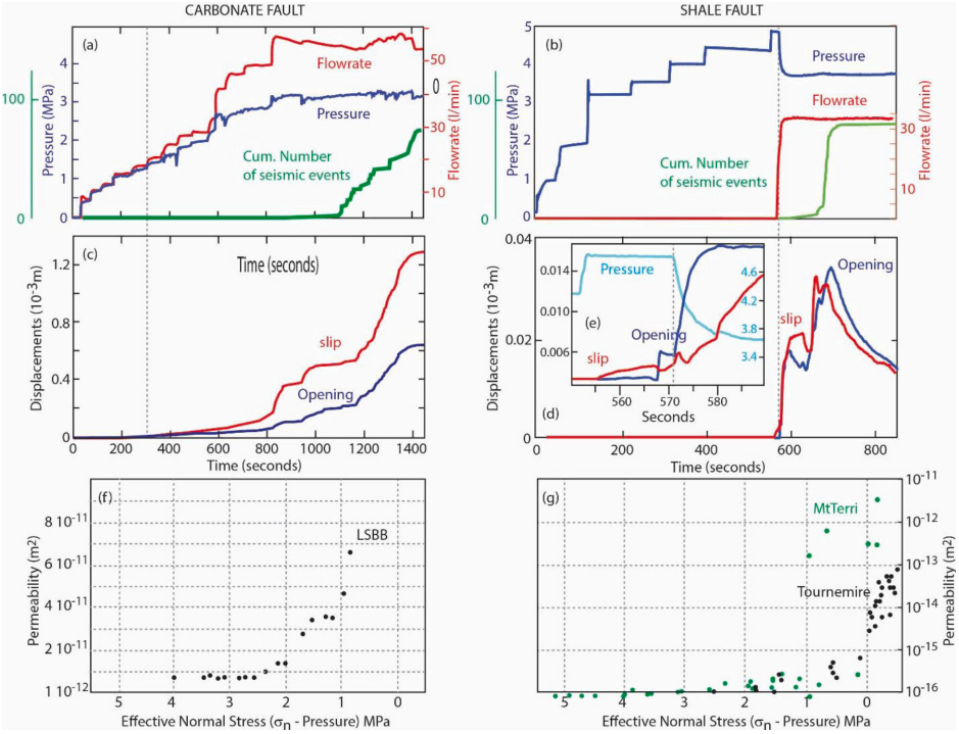

Figure 61: Comparison of the hydromechanical response of an initial permeable formation fault (left column, LSBB experiment) and an impermeable caprock fault (right column, Mount Terri experiment). (a) and (b) Fault leakage response to pressure increase. (c) and (d) Fault slip and opening (detail in (e)). (f) and (g) Fault permeability variation (different scales) (Guglielmi et al., 2021)

The two different behaviours observed in mesoscale experiments are analogous to large-scale CO_2 storage formations. A distributed pressure disturbance on the fault inside the permeable formation can cause the opening slip of the main planes with seismic events. In the low permeability caprock, the flow is mainly constrained along the fault itself; the opening is aseismic (and thus difficult to detect) until the pressure threshold is met and more significant seismic events are observed.

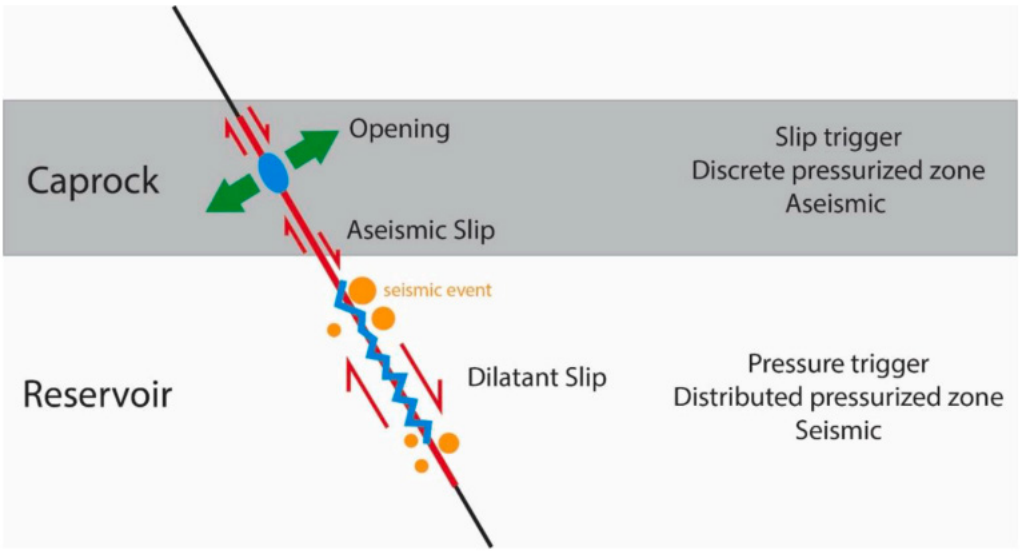

Figure 62: Combination of fault activation mechanisms in a conceptual reservoir-caprock system (Guglielmi et al., 2021)

Research is ongoing about the possible hydromechanical scenarios that describe post-activation fault behaviour in a formation-caprock system. Large-scale field experimental data, as well as multi-physics numerical simulations, will be crucial in increasing our understanding of the behaviour of these systems, as shown in recent studies where coupled fluid flow (TOUGH3) and finite-differences geomechanical (FLAC3D V7) simulators are coupled in a comprehensive tool (TOUGH-FLAC) for the representation of geomechanical effects on the faults (Luu et al., 2022).

Simplified models of fluid-geomechanical numerical modelling are tested and calibrated on real cases. (Choi et al., 2023) verified the validity of the “uniaxial strain condition” when evaluating the stability of faults in target formations for GCS projects (Figure 65). The authors concluded that the simplified model only applies when faulting occurs within an assumed homogeneous reservoir with a homogeneous pore pressure build-up on each side of the fault. In this case, negligible lateral displacement occurs due to lateral confinement. However, the uniaxial strain hypothesis leads to underestimating the change of horizontal stress, particularly in bounding faults subjected to a significant change in pore pressure gradient and rock properties across the fault. In these cases, the simplified stress path assumption can lead to overestimating the fault stability by up to 60% and a misrepresentation of the conditions required to critically stress the faults.

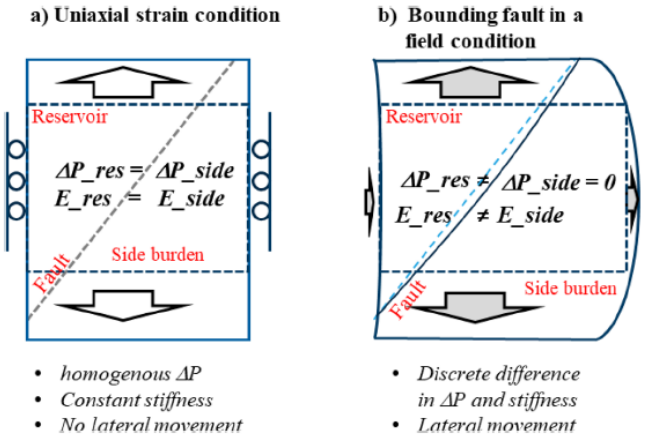

Figure 63: A simplified uniaxial strain condition model (left), valid for reservoir faults (for which the "side" is included in the reservoir), and the mechanical conditions for bounding faults (right). In the pictures, ΔP is the pressure variation due to the injection, while E is the measure of host rock stiffness (Young's modulus) (Choi et al., 2023)

8.1.6 Controlled Release of CO_2 Experiments

A recent IEAGHG workshop focused on faults and their significance for large-scale CO_2 storage (IEAGHG, 2020)Several conclusions were drawn from this workshop, including the observation that although numerous proposed methods for modelling CO_2 migration through faults exist, little experimental data underpins or supports one method over another. However, several planned experiments may provide a rich dataset to support the development of fault modelling methodologies for CO_2 storage applications.

A recent example of a controlled release of CO_2 experiment was performed in the south-west of Western Australia. This experiment injected approximately 40 tonnes of CO_2 at a depth of ~ 350 m. The plume migration was monitored using pressure and temperature gauges, DTS, borehole seismic, electric resistivity imaging, downhole logging, and assurance (e.g., soil monitoring)(Michael et al., 2020).

A controlled CO_2 release experiment will be undertaken at the Otway International Test Site in Victoria, Australia, in 2024. The experiment intends to inject approximately 10 tonnes of (gaseous) CO_2 into the Port Campbell Limestone near the Brumbys fault at a depth of approximately 80 m. The Brumbys fault has been described as a slip-strike fault following an extensive appraisal program. The migration of the CO_2 will be tracked using a combination of remote sensing techniques (e.g., reverse vertical seismic profiling), distributed fibre optics (distributed strain sensing (DSS), distributed temperature sensing (DTS)) and other monitoring technologies (Tenthorey, 2022).

Various authors have also reported that other controlled release experiments are currently less mature in planning. Other examples of CO_2 leakage experiments include the planned experiments at the Sotacarbo Fault Lab, which is now in the preliminary site characterisation phase with the intent to inject CO_2 into the fractured carbonate of the Sulcan Basin in Sardinia, Italy (Zappone et al., 2021) as well as the Mont Terri experiment (Switzerland) (National Energy Technology Laboratory, 2023).

Note, however, that all previous or imminent controlled release experiments were or are planned to be performed at relatively shallow depths. Therefore, whilst providing valuable data for testing various monitoring technologies and predictive modelling methodologies, there remains uncertainty in transforming insights into deeper, prospective CO_2 stores that will support large-scale CO_2 storage roll-out. One benefit of these experiments is that they are useful in helping to understand and improve CO_2 monitoring approaches for leakage into potable aquifers or into the atmosphere(Michael et al., 2020). Ultimately, however, large-scale GCS projects will almost exclusively inject CO_2 in dense phase at greater depths, and therefore, the conditions (interfacial tension, densities, thermal effects) will differ significantly.

8.1.7 Summary

In recent years, the body of literature focusing on the description and numerical reproduction of fault seal and fault flow properties has grown. This research has primarily focused on assessing the risk of CO_2 leakage from geological formations and quantifying the leakage rates.

Most of the research in this field considers it appropriate to adopt the conceptual model of a fault as a barrier for across flow and conduit for along flow, arising from the simplified core-damage zone architecture Figure 43(a). This is mainly valid for faults in subsurface formations unaffected by structural complexity (e.g., multiple fault planes).

Two main numerical modelling approaches have been presented in this section. The first approach (Section 8.1.1) represents the fault as a quasi-vertical channel in the model grid that has been refined to account for the size and orientation of the fault. The second (section 8.1.3) explicitly describes the two main zones of the fault: the core zone, characterised by low permeability and barrier/baffling to flow, and the fractured damage zone, which typically has a higher vertical permeability that provides a conduit for vertical flow of CO_2.

If the fault is present within an extensive aquifer system and the size of the fault exceeds the width of the fault-fracture system, then modelling the fault as a vertical conduit may be appropriate. Conversely, if the storage formation is characterised as a closed aquifer system of finite extent, an explicit core-damage zone description may be required.

Ultimately, the mineralogy of the host rock plays an important role in the architecture of the fault and, therefore, in the selection of the preferred model. Relatively soft formations like sandstones or shales typically result in less extensive fracture zones with lower fracture density (possibly even facilitated by the so-called “self-healing” phenomenon of the fractures). For these cases, the vertical conduit model can be representative.

In contrast, carbonate formations are characterised by high stiffness and, during faulting processes, can give rise to an extensive fracture network with vertical permeabilities of more than a Darcy. In this case, the core-damage zone model technique presented in section 8.1.4 would be the preferred approach.

Focused data acquisition may reduce uncertainty in the flow properties of the fault if faults are identified as a critical risk to CO_2 containment. The discretisation of the volumes (Figure 56) in the damage zones also allows the effect of the faults/fractures to be appropriately evaluated as the linear density (and the consequent permeability) usually decreases with the distance from the core. Further, identifying analogues is an important activity to assess whether similar fault systems can hold hydrocarbons or, for example, whether there are indications of migration up faults in seismic sections.

In addition to the characterisation of the fault in the storage formation and extension into the seal, a site characterisation should also consider any shallower formations to which the CO_2 may migrate as the storage formation, fault and shallower formations (outside of the storage complex) may establish a comprehensive flow system (section 8.1.2). The magnitude of the leakage may be strongly impacted by the presence of one or more thief zones at shallower intervals (as seen in the Green River, USA examples).

From a numerical point of view, simulations for the two fault modelling techniques most prevalent in literature were performed in the presented works with a traditional approach to discretisation and gridding. A structured grid with refinement in the fault zone (Figure 47) accounts for fault size, geometry, and possible local heterogeneities. On the other hand, an effective upscaling of flow properties in the fault zone allows the representation of the fractured damage zone with a relatively coarse grid (Figure 54).

Nevertheless, recent numerical techniques using unstructured grids to model subsurface formations can effectively simulate fault scenarios. These advanced solutions can be implemented to appropriately characterise the geometry, particularly formation discontinuities like wells or faults. Moreover, unstructured

gridding can help resolve issues when the communication between grid blocks is unrelated to geological layering, such as faults.

The novel aspects of unstructured gridding have computational implications, mainly when large grids are employed for extended durations (tens to hundreds of years), as is often the case in GCS forecasts. For this reason, the efficient asynchronous simulation solution (section 8.1.4) can be extremely valuable.

The pace of simulation-driven workflows is decoupled from the much slower acquisition of representative experimental/GCS site test data to inform or condition CO_2 fault flow modelling. In this section, several CO_2 controlled release experiments have been discussed which, though they are valuable for testing various monitoring technologies at shallow depths, a plethora of “scale-up” challenges remain when attempting to transfer the learnings to commercial-scale GCS projects that will be at deeper depths and in structural and geological settings that are site-specific.

9. Large-scale Geomechanical Modelling

In certain jurisdictions, a detailed analysis of the storage formation's geological features, including the effective sealing mechanism associated with the formation, is required. This necessitates obtaining information during a GCS appraisal program that may not have been acquired traditionally for petroleum appraisal.

For example, in Australian Federal waters, GCS appraisal programs must consider acquiring data demonstrating that the *"confining zones of the storage formation constitute an effective and sound sealing mechanism"*. This may involve quantification of the range of porosity and permeability of the seal; the reactivity of rock types with the proposed GHG storage substance in both the reservoir and seal rocks; and the local stress regime, fracture gradients, fault stability and the geomechanical response of the storage formation to injection. Hence, conventional coring programs will likely be more extensive, and expanded logging (e.g. FMI), or in-situ testing (e.g. ELOT) programs may be required.

Extensive appraisal programs, particularly in offshore settings, result in higher costs before final investment decisions for a GCS development have been made. Therefore, within this context, both GCS project proponents and regulators need to work together to define the appropriate geomechanical model at each stage of the GCS project lifecycle.

Reservoir simulation is becoming more widespread as computational performance improves (e.g., CPU and GPU capabilities), resulting in a trend of increasingly more complex reservoir (or total "storage system") models. Whilst not all problems require the practising subsurface geoscientist or engineer to utilise numerical simulation, there are undoubtedly problems that require the interaction between fluid flow and heat transfer (i.e., conventional reservoir simulation) with induced stresses within the reservoir, caprock, over-, under-, and side burden (i.e., geomechanical modelling).

This section of the report will address (i) the fundamental inputs for geomechanical modelling as well as standard workflows; (ii) the concept of reservoir-geomechanical coupling and examples of different methods; (iii) provide examples of publicly available large-scale reservoir-geomechanical simulation studies. In addition, a review of geochemical modelling for GCS.

9.1.1 Geomechanical Modelling for GCS

In GCS, the role of geomechanics is analogous in many ways to the role of geomechanics in oil and gas production, with several key differences. These fundamental differences include:

- In petroleum projects, the containment mechanism for the hydrocarbons is mainly irrelevant and, in some cases, can be unknown throughout the project's life. GCS, in contrast, must demonstrate the nature of the trapping and sealing mechanisms, as well as demonstrating long-term seal integrity.
- In GCS, assessing a larger area of interest (AOI) is often required. This is because a CO_2 plume increases in size (areally) with time until the point of stabilisation and the pressure envelope extends far beyond the edges of the plume. Many jurisdictions stipulate that a CO_2 storage project must not harm the natural environment (especially groundwater and other resources, both discovered and undiscovered), which drives the modelling AOI requirements so that the CO_2 plume, pressure footprint, and injected and displaced fluids can be evaluated.

In CO_2 storage, there are several scenarios in which there is a benefit in integrating/coupling reservoir simulation with geomechanical modelling. Coupling is required only when there is a feedback loop (i.e. CO_2 injection resulting in the creation of fractures that subsequently impact reservoir/seal properties and injectivity). Examples for GCS include:

- Predicting irreversible deformations of the storage complex, including caprock fracturing and fault reactivation.
- Predicting changes in reservoir properties (e.g., porosity and permeability) that impact injectivity and CO_2 plume migration.
- Predicting fracture directions.
- Predicting surface/seabed deformation.

9.1.2 Fundamental Inputs for Geomechanical Modelling

Irrespective of the method of coupling reservoir simulation with geomechanical modelling, which is discussed in section 9.1.4, a coupled reservoir-geomechanical model will only provide reliable results if both the reservoir model(s) and the geomechanical model(s) are appropriately designed and capture an appropriate range of outcomes.

Whilst it is tempting to adopt the "full-field" approach and create models with high vertical resolution and large vertical and lateral extent, model framing should identify the model's purpose (Ringrose & Bentley, 2016). Near wellbore assessment of the impact of thermal effects on fault reactivation would likely be a fine-scale assessment with initial sensitivities of both the geomechanical and thermal effects of the vertical extent of the model. In contrast, geomechanical investigations of the basin-scale response can be underpinned by more coarse and areally extensive. They may not require coupling to reservoir simulation, especially in the early phases of a GCS project assessment.

A standard geomechanics workflow starts by building a 1D mechanical earth model (MEM) based on well data (Zain-Ul-Abedin & Henk, 2020). 1D MEMs intend to generate a model that estimates the direction and magnitude of the local/regional stresses and can be compared to other data to validate the model (e.g., breakouts identified using the calliper log or FMI data). The typical inputs for a 1D MEM include rock elastic and strength properties (e.g., Young's modulus, Poisson's ratio, UCS and friction angle), in-situ stresses (e.g., from density log, dedicated stress determination tests (e.g., ELOT) understanding of the regional stress regime) and pore pressure (e.g., from a formation pressure tester).

The 1D MEM then seeds the inputs for a 3D geomechanical model, which requires the rock elastic and strength properties to be distributed geospatially away from well control, a grid to be defined (which is typically, but not always, larger than the reservoir modelling grid) and the appropriate boundary conditions (tectonic stresses and pore pressure) to be set. A typical example of a 3D geomechanical workflow is illustrated in Figure 64. The specific outputs from a geomechanical simulation include displacement, stress maps, and rock failure plots (e.g., Mohr-Coulomb or Barton-Bandis).

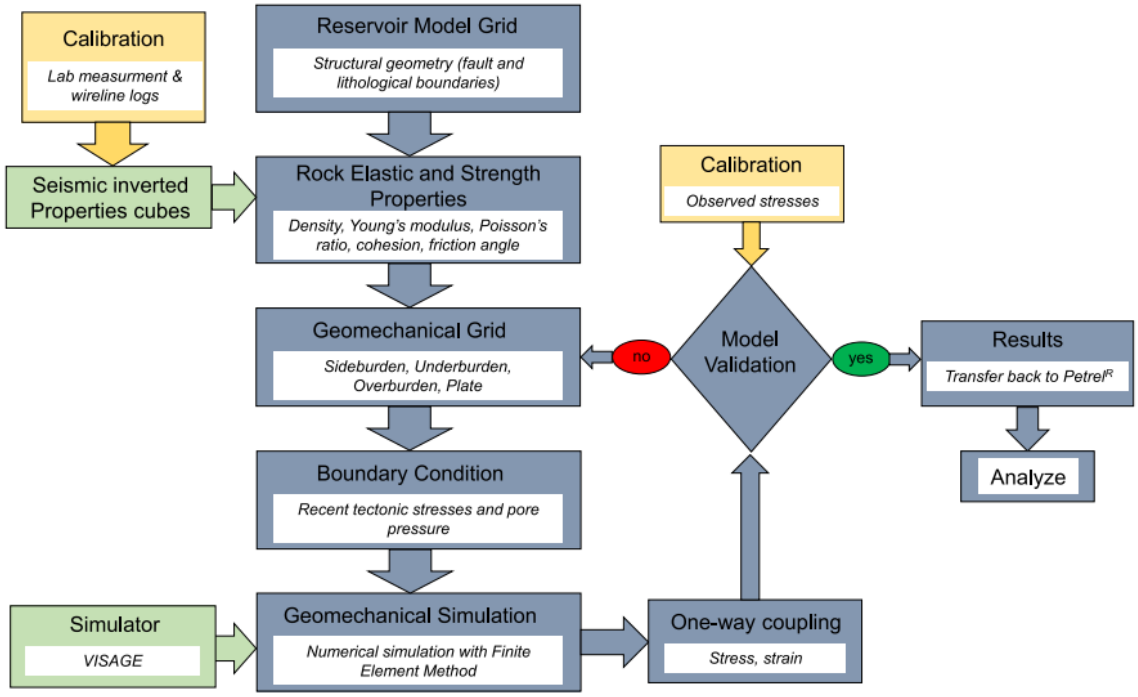

Figure 64: An example of one-way coupling (Rahman, Fawad, Choi, et al., 2022)

9.1.3 Methods to Derive the Rock Elastic and Strength Properties for a Geomechanical Simulation

As described in section 9.1.1, 3D geomechanical simulation requires a method for geospatially distributing rock elastic and mechanical strength properties away from well control, typically involving probabilistic algorithms (possibly linked to seismic attributes).

One of the critical decisions when building a 3D model for geological CO_2 storage is selecting the vertical extent of the modelling domain. For example, whether the seal or seal and overburden (or even underburden (Chang, 2022)) should be included to evaluate injection-induced mechanical risks for containment. Further, the modelling approach should consider whether the seal and overburden (if modelled) can be modelled simplistically or whether it is essential to capture the overburden anisotropy.

Recent studies focused on seismic data-derived 3D field-scale geomechanical modelling of potential CO_2 storage sites in Smeaheia, offshore Norway, highlighting the importance of capturing the anisotropy of the overburden (Rahman, Fawad, Choi, et al., 2022). In this study, the geomechanical properties used as inputs for the geomechanical modelling were derived from seismic data, enabling the capture of spatial variabilities of seal and overburden rock properties. One key finding from this modelling study was that the maximum estimation of the vertical rock deformation was two times greater in the simplified (isotropic) overburden rock property model compared to the spatially variable (anisotropic) overburden rock property model. An implication of this is incorrectly modelled risks related to rock deformation at a CO_2 storage site may result in the storage site operator imposing a reduced maximum pore pressure threshold and, therefore, under-utilise the storage resource (Rahman, Fawad, Choi, et al., 2022).

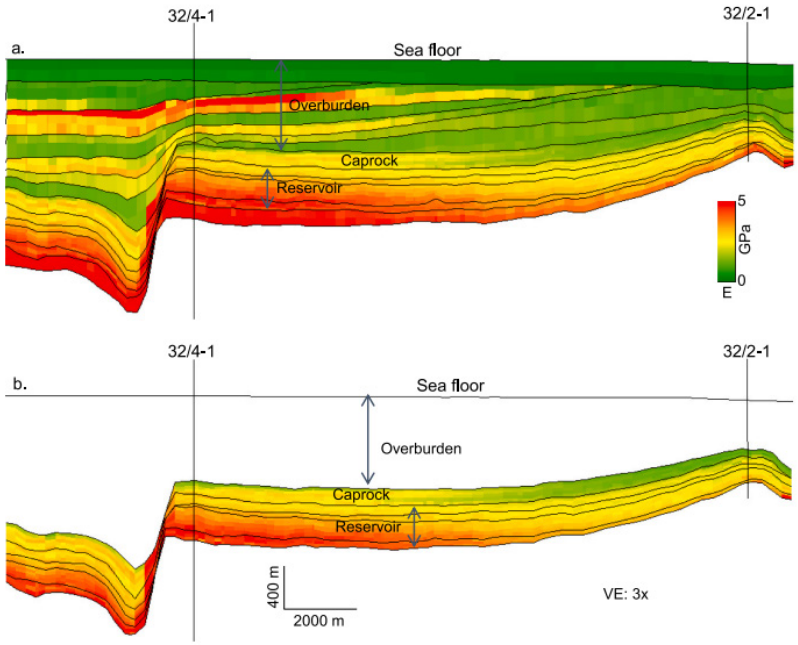

Figure 65: Young's modulus including (top) and excluding (bottom) the overburden (Rahman, Fawad, Choi, et al., 2022)

Various modelling approaches have been applied to assess the surface deformation recorded during the In-Salah project. One study used a 2D finite element (FE) model (Abaqus) to demonstrate that linear-elastic deformation could only predict approximately half of the uplift at In-Salah and that it was necessary to include fault/fracture zones for both the storage unit and sections of the overburden to match the observed data (Gemmer et al., 2012).

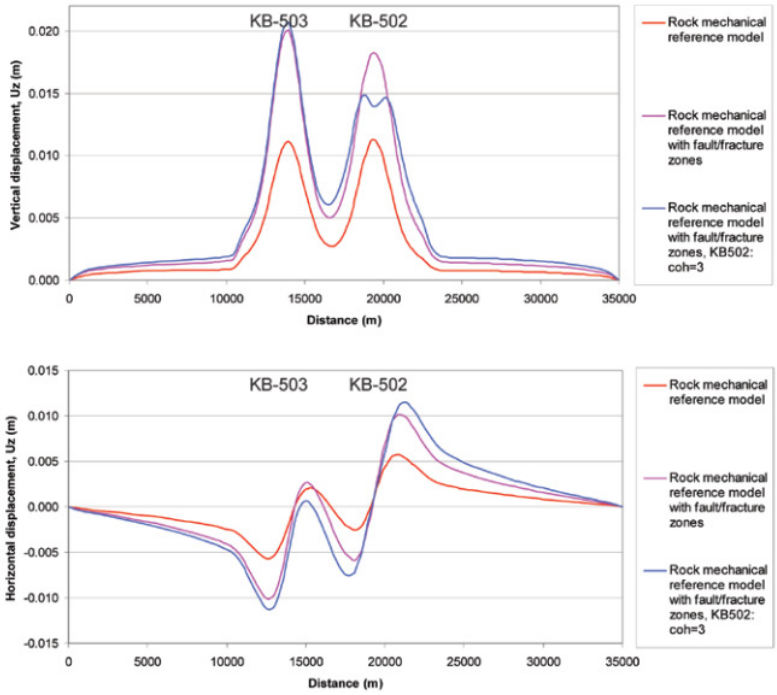

Figure 66: Modelled vertical (top) and horizontal (lower) surface displacements from multiple FE models of In-Salah injection (Gemmer et al., 2012)

Another detailed sensitivity analysis was undertaken using InSAR data from the In-Salah project during the CO_2 injection phase (Rohmer et al., 2017). The study used TOUGH2 (as the flow simulator) and a specialist geomechanical code. The Young's modulus and Poisson's ratio of the overburden, caprock, reservoir and basement (i.e., eight variables) formed part of the sensitivity analysis, in addition to two parameters that defined the initial stress state. The study demonstrated that the main effects over the whole region of interest were associated with Young's modulus of the reservoir section, with the second most crucial parameter corresponding to Young's modulus of the caprock but with limited influence (Rohmer et al., 2017).

The various monitoring technologies for evaluating seal integrity or monitoring surface deformation to help constrain models (e.g., Interferometric Synthetic Aperture Radar (InSAR)) are discussed in section 10.

9.1.4 Coupling Methods

The selection of an appropriate coupling method between the reservoir and geomechanical simulators can be critical for the large-scale reservoir-geomechanical simulations for GCS. In classical dynamic reservoir simulators, the geomechanics is approximated via changes in the pore volume due to rock compressibility. These changes can be selected as constant or based on a pressure-dependent parameter, the only geomechanical parameter in a conventional reservoir simulator (Gao & Gray, 2022).

A plethora of different reservoir-geomechanical simulation options exist for assessing geomechanical-related risks for the geological storage of CO_2, including software providers that enable reservoir and geomechanics coupling within a single application (e.g., CMG-GEM, TNavigator, GEOS), coupling between different software packages from the same developer (e.g., SLB Eclipse and Visage; TOUGH and FLAC), or options when users create their coupling algorithms between simulators. Recent literature (e.g., Table-1 (Song et al., 2023)) summarises the capabilities and applications of the more prevalent coupled simulators for modelling geological CO_2 storage.

These changes can impact modelling properties such as permeability and fault transmissibility. Hence, in specific scenarios (e.g., when the geomechanical deformation can cause significant changes in permeability and porosity), there is a requirement for coupling between the thermo-hydrodynamic model (traditional reservoir simulation model) and a geomechanical solver. Two coupling methods are the most reported in the literature: sequential and fully coupled. Sequential coupling (Figure 67) solves for the hydraulic and geomechanical variables independently and in sequence (Tillner et al., 2014). Pressure and saturation (and in some cases temperature) are first solved in the reservoir fluid simulator in the first timestep before being passed to the geomechanical solver to calculate mechanical impact before these changes are passed back to the reservoir simulator in terms of property changes (permeability, porosity). A fully coupled approach requires all the governing equations for hydraulic-mechanical (or thermal-hydraulic-mechanical) to be solved simultaneously, which can be computationally expensive (Evgenii Kanin, 2023).

An example of the feedback loop for GCS is the development of a coupling algorithm to enable an academic simulator (MUFITS) to be coupled to a commercial geomechanical simulator (FLAC3D) to study the impact of CO_2 injection into a saline formation in the vicinity of a tectonic fault (Evgenii Kanin, 2023). The coupling algorithm uses a relationship between the strain (calculated via the mechanical model) and porosity (Chin relationship), as well as the modified permeability relationship (power law), to update the hydrodynamic model. An example of reservoir modelling/geomechanical coupling for a CO_2 application for a carbonate reservoir in Malaysia, illustrating the link between the volumetric strain output from the geomechanical simulator (in this instance, SLB's Visage) and the reservoir simulator (SLB's Eclipse) via a permeability modifier (Masoudi et al., 2011). The study aimed to evaluate the cap rock integrity of the depleted carbonate M4 gas field with CO2 injection to increase the initial reservoir pressure. The authors reported that the reservoir and cap-rock remained elastic despite the degradation of material elastic and strength properties with increased CO_2 saturation and increased permeability of up to 70% locally due to injection (Masoudi et al., 2011).

Various authors report concerns with using sequential coupling instead of a fully coupled approach. Sequential coupling performs poorly in tightly coupled processes since transient interaction between variables may not be computed accurately (Bastías Espejo et al., 2021). Further, because the time scale of pressure and thermal diffusion vary by many orders of magnitude for geological media, a sequential/staggered implementation of pressure, saturation and thermal processes is usually warranted. However, the pressure and stress equations are strongly coupled, and inaccuracies may occur if full couplings are not fully accounted for (Prevost, 2013).

An example of possible inaccuracies of sequential coupling in CO_2 storage is from In-Salah, where the modelled maximum tensile stresses in the caprock after 12 years were more than an order of magnitude higher (0.085 vs. 1.06 MPa) using two-way coupling than using a one-way approach (Prevost, 2013).

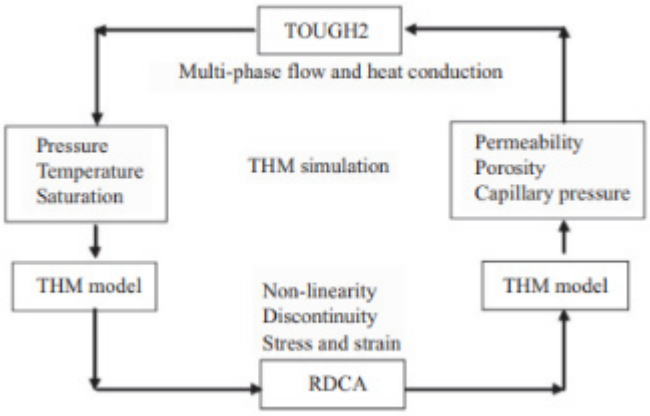

Figure 67: Schematic of a sequential coupling scheme for thermo-hydraulic-mechanical (THM) simulation (Pan et al., 2016)

9.1.5 Tensile and Shear Failure

The likelihood of tensile and shear failure was studied as part of the CO_2-enhanced oil recovery (EOR) phase of the Weyburn (Canada) project. A one-way coupled reservoir-geomechanical model was defined to the likelihood of tensile and shear failure in the sealing layer due to poroelastic effects from the CO_2 injection and was not intended to predict seismicity (Khazaei & Chalaturnyk, 2017) directly. The modelling was performed using CMG-GEM (isothermal reservoir simulation) and FLAC3D (a geomechanical model with a more significant extent than the GEM model both laterally and vertically to capture the over, under and side burden).

To assess the likelihood of tensile failure of the seal, it was assumed that failure would occur if the pore pressure of the top reservoir unit (M1) reached a critical value equal to the minimum principal stress of the zone above it. For the shear failure assessment, a Mohr-coulomb approach was adopted. It was particularly conservative because it assumed a weak plane could exist anywhere with arbitrary orientation and applied zero cohesion.

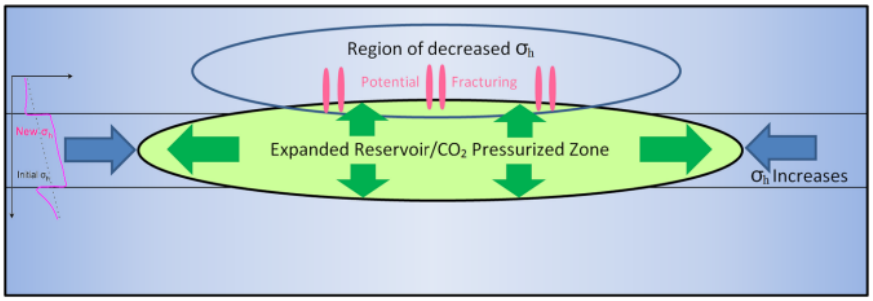

Figure 68: Schematic of stress transfer in a caprock-reservoir an idealised system (not fractured)

The results demonstrated a period in which the pore pressure could have resulted in both shear (most likely) or tensile failure of the lower section of the (anhydrite).

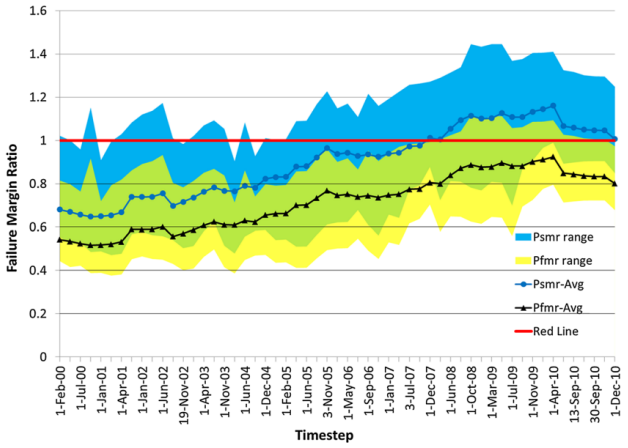

Figure 69: Modelled failure margin ratio through time during the CO_2 -EOR phase of the Weyburn project. Psmr = pressure margin ratio for shear; Pfmr = pressure margin ratio for fracturing (Khazaei & Chalaturnyk, 2017)

An alternative modelling approach is constructing a discrete element model to study micro-seismic events. An example of this discontinuum modelling approach was adopted by (Khazaei et al., 2016), who used Particle Flow Code 3D to enable the damage mechanism to be directly modelled under conditions analogous to the Weyburn project. The study indicated that the recorded events in the caprock were more likely to have originated due to slip along weak planes, while crack-induced events are too small to be recorded by geophones.

9.1.6 Optimisation of Storage Performance

An existing gap in GCS modelling is integrating the balance between storage optimisation and geomechanical risk (Zheng et al., 2021).

A methodology for optimising well placement/configuration is presented in Figure 70. This work outlined three objective functions as part of the well placement optimisation approach (multi-objective optimisation, 'EMO'). The objective functions were to maximise the mass of CO_2 stored, minimise the vertical displacement (uplift) and minimise the plastic strain to avoid irreversible deformation (Zheng et al., 2021). Although the analysis was only performed on a single reservoir/geo-model, the study is insightful as it visually represents the range of different geomechanical-related outcomes for the stipulated mass of CO_2 injected, enabling an informed discussion on risk management with various stakeholders.

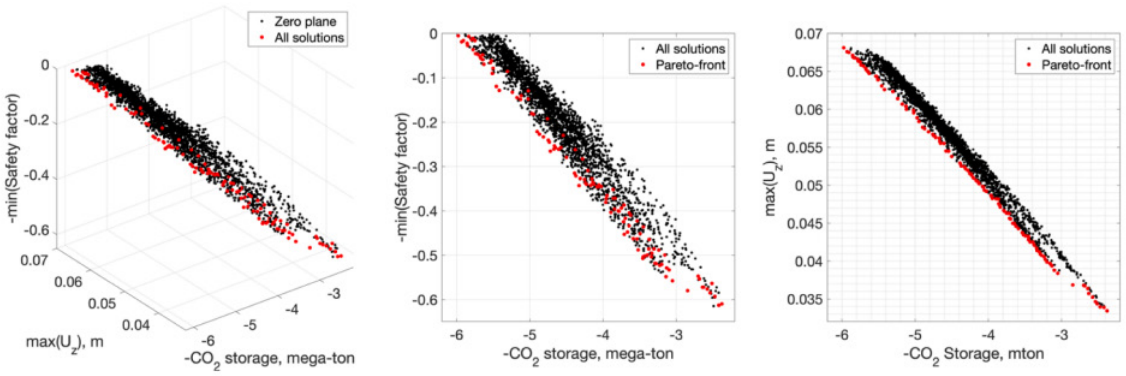

Figure 70: 3D and 2D views of multi-objective optimisation for all three well CO_2 injection scenarios. Vertical axis represents safety margin from the plastic strain criterion (Zheng et al., 2021)

9.1.7 Thermal Modelling

Aside from thermal effects in the wellbore (which are not within the scope of this study), injecting CO_2 that is (relatively) cooler than reservoir temperature can adversely impact the integrity of GCS seals; cooling of the host rock results in contraction and the reduction of stresses within the lower temperature region, and subsequent redistribution of stresses outside of this region; tensile failure may occur, or the fault reactivation potential of nearby faults may increase. The impact of thermal effects on GCS is discussed in detail in a recent literature review (Vilarrasa & Rutqvist, 2017)

The temperature of the CO_2 at the sand face will generally be lower than the reservoir temperature unless a conscious decision was made during the development phase to pre-heat the injection stream and select construction/well-completion materials with specific insulating properties. In the subsurface, properties such as injection rate and reservoir quality, as well as the thermal conductivity and heat capacity of both the reservoir and seal, are also crucial in quantifying the magnitude and spatial extent of the cooling front. Therefore, thermal modelling should be strongly considered.

Including the top seal in a thermal modelling study is essential to accurately capture the heat transfer between the top of the reservoir and the overlying top seal and quantify the extent to which the top seal could potentially experience a temperature drop during cold CO_2 injection. For example, it has been reported that a 20°C decrease in the reservoir temperature near the wellbore can lead to a 30% reduction in the fracture strength of a rock (Loizzo et al., 2009). The seal is typically much more prone to failure due to its higher Young's modulus and, therefore, its tendency to fracture due to a temperature contrast (Sagu & Pao, 2013). Thermally-induced fracturing of the caprock may be of more significant concern in depleted hydrocarbon fields, where crestally located former producing wells near the seal are reutilised for CO_2 injection as opposed to injection towards the base of the reservoir formation in saline formations (i.e., to maximise residual trapping and dissolution processes).

Irreversible deformation may occur if the thermal expansion coefficient of the seal is larger than the thermal expansion coefficient of the storage unit. In one modelling study, CO_2 was injected into a saline formation at a temperature that was 35°C cooler than the formation temperature (Vilarrasa & Laloui, 2016). The difference in thermally induced stresses between the caprock and the reservoir (which in this instance were caused by selecting a thermal expansion coefficient for the seal three times larger than the storage unit) generated shear stress at the reservoir-seal interface, reducing the minimum effective stress. Consequently, shear slips can induce micro-seismicity as the rock yields. However, in the study, the deformation was limited to a few metres into the seal and, hence, will have minimal impact on the caprock sealing capacity. Though the minimum effective stress was reduced through the cooling effect, it remained in the positive regime and therefore, tensile fractures would not be formed (Vilarrasa & Laloui, 2016).

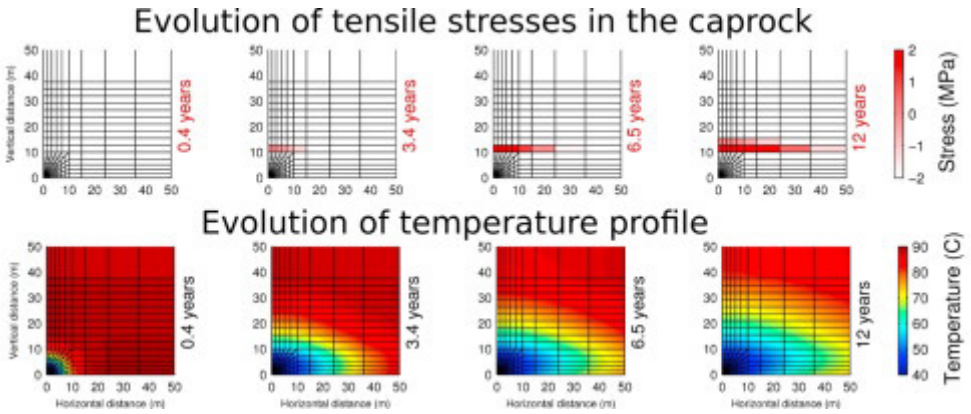

Figure 71: Changing effective horizontal stresses (left) and temperatures (right) around an injection well. Temperature of injected CO_2 is 40 °C and initial reservoir temperature in 90 °C (Gor et al., 2013)

Simplified modelling choices (e.g. omitting the seal or overburden from thermal modelling) can also result in material differences in the estimation of the thermal front advancement (Andersen & Nilsen, 2018).

Fully-coupled hydraulic-thermal-mechanical modelling for the In Salah project indicated that when the injected CO_2 at the sand face was approximately half of the reservoir temperature (40-50 ^{O}C vs 90 ^{O}C), stresses in the caprock near the injection well became tensile in less than ten years. Increased pressure in the reservoir may result in the fractures propagating, which were analytically calculated to extend approximately 50 m (Gor & Prévost, 2013).

However, fault reactivation may be of more significant concern for CO_2 storage. Though there is currently limited field data that can assist in calibrating the thermal effects associated with CO_2 injection for large-scale GCS projects, low-temperature CO_2 injection may create a temperature front in the order of hundreds of metres. Note, however, that thermal fronts advance slowly. Therefore, an assessment of the locations of faults relative to the CO_2 injector locations and the different juxtaposition scenarios in the event of fault reactivation must be considered in the early stages of planning. The redistribution of stresses may also impact the stability of faults at further distances from the CO_2 injection wells (Jeanne et al., 2014).

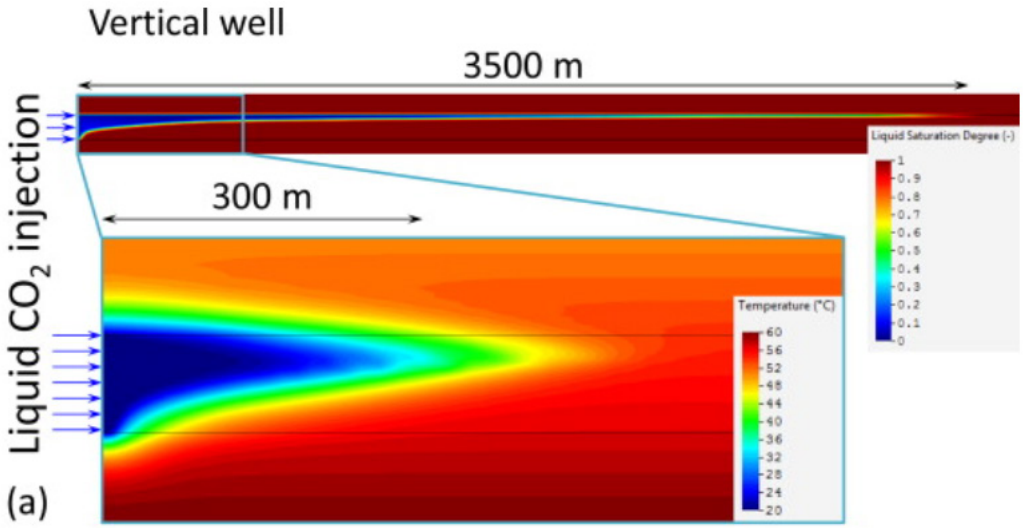

Figure 72: CO_2 plume and temperature distribution after 30 years of injecting 1 Mt/yr of CO_2 at 20 °C through a vertical well (Vilarrasa et al., 2014)

In GCS, a simplistic “first-pass” approach could be to calculate the changes in thermal stresses away from the wellbore by using a 2D Mohr’s circle analysis to see how the stress envelope shifts relative to the intact rock and faults (which have lower cohesion) at a maximum temperature contract before undertaking a dedicated thermal modelling or coupled thermal-geomechanical modelling study. The 2D approach is a conservative approach that allows the impact of thermal stresses on faults to be evaluated on the assumption that the faults are in the optimal orientation to be reactivated. This approach can be applied to regions of the storage unit and storage complex away from wellbores and utilise the properties from 1D MEMs.

Specific completion design or field development options may be considered to mitigate the thermal impacts of CO_2 injection on the seal or the risk of reactivating faults. These include the depth of CO_2 injection relative to the position of the seal, lowering injection rate or preferentially injecting CO_2 into wells at a greater distance from faulted or fractured regions.

9.1.8 Coupled Geochemical-Mechanical Modelling

A geochemical modelling effort is generally recommended when it is recognised that there is potential for CO_2 to flow in a fault. However, it is neglected when the risk of fault flow is low. Geochemical reactions of the fluid mixture (CO_2 and formation brine) with fault rock can impair the CO_2 vertical flow in case of mineral precipitation or enhance it in case of mineral dissolution. Thus, some scenarios should consider this interaction for a complete and integrated evaluation of leakage risk assessment. In addition, geomechanical aspects such as alteration to the friction angle, cohesion, or poroelastic constants caused by brine–CO_2 interaction are usually not considered.

Most of the literature in the public domain focuses on coupling dynamic flow simulation with geomechanics or dynamic flow simulation with geochemistry. A summary of some examples for both experimental and numerical modelling of geomechanical/geochemical interactions from 2016 and prior is provided in Table 12 (Raza et al., 2016).

Table 12: Summary of studies carried out on the geochemical effects of injection on geomechanical parameters. Adapted from (Raza et al., 2016)

Approach	Rock/medium	Experiment time	Effect	Conclusion	Reference
Experimental	Sandstone/aquifer and Oil	6 days	Yes	No significant impact on mechanical properties	(Hangx et al., 2010)
Experimental	Sandstone/aquifer	Several months	Minor	A slight increase in porosity	(Zemke et al., 2010)
Experimental	Sandstone/aquifer	63 days	Minor	Dissolution of calcium-rich plagioclase, K-feldspar and anhydrite, and stabilisation or precipitation of albite, together with slight changes in petrophysical properties	(Fischer et al., 2011)
Experimental	Sandstones	-	Minor	Minor effect on geomechanical properties of sandstone after CO_2 flood	(Evans et al., 2014)
Experimental	Sandstones	2-4 weeks	Yes	The exposure to pure $scCO_2$ in the autoclave system induces reduced strength	(Marbler et al., 2013)

				parameters, modified elastic deformation behaviour and changes in the effective porosity in comparison to untreated sandstone.	
Experimental	Sandstones	6 days	No	Calcite-dissolution-induced weakening may have a significant impact on non-quartz cemented sandstone	(Hangx et al., 2013)
Numerical modelling	Sandstone/aquifer	> 50 years	Yes	Mechanical stability of the storage medium is affected by geochemical reactions	
Numerical modelling	Sandstone/aquifer	25 years – injection 1000 years - monitoring	Minor	Geochemical processes do not have a significant influence on porosity and geomechanical properties of reservoirs	(Kempka et al., 2014)
Experimental/ Pore network modelling	Sandstone/aquifer	2 months	Yes	Modification in the pore system after two months of injection	(Varre et al., 2015)
Experimental	Sandstone/depleted oil reservoir	Short-term (hours to days)	Minor	Minor effect on the petrophysical and geomechanical properties of sandstone	(Campos et al., 2015)
Experimental/ Numerical modelling	Sandstone/-	6 days	Yes	The predominant dissolution of anhydrite causes an increase in concentrations of calcium and sulphate at an early stage of injection. The permeability of sample increases due to the dissolution of cement	(Hangx et al., 2015)
Experimental	Sandstones/-	Some weeks	Yes	Changes in deformability and compressive strength of rocks due to compositional changes	(Erickson et al., 2015)

To understand the impact of geochemistry on the integrity of the sealing unit(s), it is important to start with a simple system model before building complexity (as required). This may, for example, require the construction of a 1D geochemical model (e.g. PHREEQC) to do an initial mineralogy check and then undertake more detailed studies if necessary.

The complexity of the interaction between the chemical, mechanical, hydraulic, and thermal aspects is illustrated in Figure 73. Extending and coupling the number of simulated processes can result in significant computational costs, particularly in the fully coupled scenario (per the concepts described in section 9.1.4). An alternative to a fully coupled approach is to sequentially couple by first simultaneously solving for THM and then solving the chemical processes (solute transport and chemical reactions).

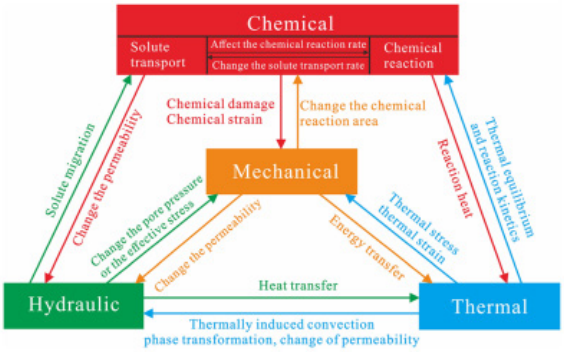

Figure 73: Thermal–hydraulic–mechanical–chemical coupled processes and their numerical simulation: a comprehensive review (Zhang et al., 2023)

There are limited recent examples (Alsayah & Rigby, 2023; Yong et al., 2019) of hydraulic–mechanical–chemical (HMC) or thermal-hydraulic–mechanical–chemical (THMC) modelling for GCS.

A coupled geochemical-transport-geomechanical model to address caprock integrity during long-term CO_2 storage was reported by (Veer et al., 2015), who developed a coupled HMC model to study the impact of injecting CO_2 in a simplified representation of the mineralogy of the Opalinus Clay Formation (Switzerland) (Figure 74). The Opalinus Clay shales are represented by calcite (26 vol.%), quartz (30 vol.%), muscovite (27 vol.%), and chamosite (17 vol.%). The injection stream of CO_2 included a ~1% SO_2 impurity.

In this study, the maximum increase in porosity observed was approximately 15% (i.e. from 30% porosity to 34.5% porosity), which occurred at a distance of 5 m from the interface of the reservoir/caprock; changes occurred after 500 years. The modelled pressure changes were small ($\Delta P \geq -2$ MPa), and the mechanical stability of the caprock system was not impacted. The authors concluded that coupled modelling is preferred in cases with a greater tendency for significant porosity increases and risk of fault slip, e.g., for larger flow velocities, more (impure) CO_2 streams, higher pressure gradients and higher injection pressures.

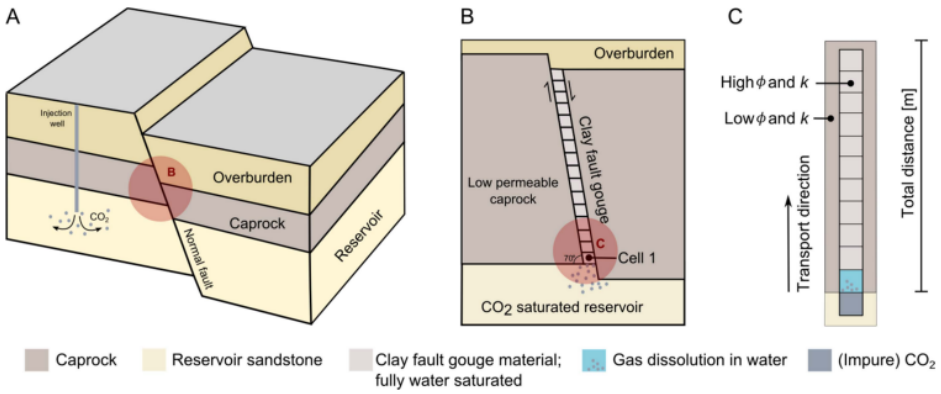

Figure 74: Schematic overview of a normal fault through a caprock, which acts as a sealing horizon for CO_2 storage above a sandstone reservoir (A). Detail of the normal fault in contact with a CO_2 saturated reservoir (B), and the translation of boundary conditions for numerical simulation of couple hydraulic-mechanical-chemical process (C) (Veer et al., 2015)

Geochemical, petrophysical heterogeneity, capillary sealing and diffusion processes must be included to ensure that numerical simulations accurately represent seal integrity (Alsayah & Rigby, 2023). This study constructed a field-scale HMC model based on information from the Sleipner field, focusing on the impact of shale interlayers with a sandstone reservoir, including hypothetical fracture zones within the shale interlayers. The chemical processes did not significantly affect the porosity of the Nordland Shale over 10,000 years.

However, thin (0.3 m) shale inter-layers had a higher efficiency for CO_2 containment than the thicker (3 m) inter-layers. The CO_2 leakage observed is the diffusion of CO_2 dissolved in the aqueous phase. No free-phase CO_2 is observed in the simulations above the shale inter-layer. Several geomechanical and geochemical factors enhance the dissolution of the CO_2 invading the shale interlayer, and these factors are more effective in thicker layers (3 m) than in thinner layers (0.3 m).

For even thicker shale layers, like the caprocks (a threshold order of magnitude of the thickness is not specified), the injected CO_2 is expected to invade only partially at the bottom of the layer itself without reaching the above formation.

Re-activation of natural fractures, capillary breakthrough pressure and diffusion were key processes that resulted in the modelled CO_2 migration out of the storage complex for the thicker inter-layer scenarios. The interaction of the various methods is complex, and clear research gaps exist (Alsayah & Rigby, 2023).

9.1.9 Summary

In this section, the fundamentals for the creation of a geomechanical model have been outlined, ranging from a simplistic 1D mechanical earth model approach to more expansive and computationally intensive coupled 3D modelling that captures the hydraulic, mechanical, thermal, and chemical behaviour of the storage complex and overburden. Successful modelling efforts require that the model purpose is established first, and from that starting point, an appropriate modelling approach can then be developed.

To this end, examples of modelling for GCS have been presented that cover key themes, including recent literature examples that convey aspects including the vertical extent of the modelling domain, the considerations of coupling hydraulic and mechanical models, tensile and shear failure of a GCS seal based on both continuum and discrete fracture network methodologies; and an example of a CO_2 injection well placement methodology that simultaneously assess both injected volumes and geomechanical failure.

Finally, a limited number of HMC modelling case studies in the public domain pertain to assessing cap rock integrity. A recent literature review of geo-mechanical-chemical impacts comprehensively describes the complexity of this topic. It highlights several research gaps (e.g., reaction models that appropriately account for mineral formation via precipitation and permeability-porosity relationships for different mineralogical compositions for GCS) (Akono et al., 2019). Further work in the modelling domain should focus on developing guiding principles for when the interaction of geochemical and geomechanical effects needs to be considered for GCS, which would benefit both technical professionals and regulators.

10. Monitoring Technologies

The following section provides an overview of the developments in seal integrity monitoring technologies.

Several established in-well monitoring technologies, such as downhole pressure and temperature gauges, have decades of research and development across multiple industries (particularly the oil and gas industry). These technologies can be both permanent (providing continuous "online" streams of data) or temporary, and, in the case of pressure gauges, they can directly measure changes in pore pressure, which is incredibly valuable for seal integrity monitoring.

Importantly, no "silver bullet" exists for seal integrity monitoring; historical monitoring, measurement, and verification (MMV) plans have deployed multiple complementary technologies. Over the past decade, there has been a steady progression from complex multi-modal "research" MMV deployments to more focused MMV deployments based on a smaller number of commercially proven and informative technologies.

Regulators and project proponents should avoid assuming that because a technology was used in one project, it should be used in another. This is especially true as the site context changes significantly, e.g., between onshore and offshore or deep versus shallow water. Further, high-cost monitoring technologies, such as the drilling and completion of a dedicated monitoring well or the acquisition of repeat 3D seismic surveys, may not necessarily result in improved monitoring results; the portfolio of available technologies should be evaluated on a site-by-site basis based through assessments that encompass the appropriate risks (e.g., safety, environmental, compliance, public perception).

A recent review (IEAGHG, 2020) described the different monitoring technologies for CO_2 containment and outlined the accuracy/resolution of each technology, the technology readiness level, and typical unit costs (refer to Appendix B). A monitoring selection tool, which contains forty monitoring technologies covering all stages from site characterisation through to post-injection, has also been developed by IEAGHG (IEAGHG/British Geological Survey, 2019).

It is essential to understand the dimensionality of the monitoring solutions. In this context, distinguishing between point, well bore or wide-angle datasets should be considered. Wellbore data, such as saturation logs at GCS observation wells, provide high vertical resolution (~30 centimetres) but with a limited depth of investigation, restricting their effectiveness in providing insights into events tens of metres away. Conversely, surface seismic data provides greater coverage at a more limited vertical resolution. An optimal monitoring solution should utilise the range of technologies to offer fit-for-purpose coverage over the required scale.

This section acknowledges the valuable previous work undertaken by the IEAGHG/BGS to avoid duplication of effort. It seeks to provide additional insight on the technologies directly applicable for monitoring seal integrity and recent insights on value of information (VOI) assessments for CO_2 monitoring technologies. Note that wellbore integrity monitoring technologies are explicitly excluded from this report.

10.1.1 Above Zone Pressure Monitoring

Aside from the value of monitoring the pore pressure in the storage unit using permanent downhole gauges, an increasingly deployed method of evaluating seal integrity is monitoring the zone(s) above the defined storage unit (above zone monitoring intervals, AZMIs) for changes in pressure. Monitoring pressure in a zone above the seal is a method to assess retention in the injection zone (Hovorka et al., 2011). The optimal well placement for above zone monitoring is site-specific. It depends on several factors, including what has been identified as the key risks to containment, the geology of the overburden, whether existing wells could be utilised, and whether a new, dedicated monitoring well is necessary. In some scenarios, DAS/noise logging may provide similar or better results.

Several challenges with the interpretation of pressure fluctuations, including identifying “real” responses that can be linked to CO_2 migration into the monitor zone or other factors (e.g., barometric effects, tidal effects, gauge drift, regional-scale groundwater variations, pressure diffusion) (Ennis-King et al., 2017). Examples of AZMI in CCUS projects include Cranfield, Ketzin and the CO2CRC Otway International Test Centre. Recent work investigated more advanced techniques for characterising CO_2 leakage using AZMIs (Gundersen et al., 2021). Based on simulated pressure data, the study proposed a methodology for applying convolutional neural networks to detect, localise and quantify leakage, with future aspirations to test the method on field data.

10.1.2 Fibre Optic Monitoring

Engineering advancements in fibre optics (FO), which have a broad range of applications in the telecommunication industry, have found ever-increasing applications in seismic acoustic, thermal and strain measurements. For data acquisition, a laser beam is sent down the length of the fibre (Figure 75), and the backscattered light is sampled at high frequencies using an interrogator. The energy of these back-scattered light is analysed to identify the nature and location of the anomaly.

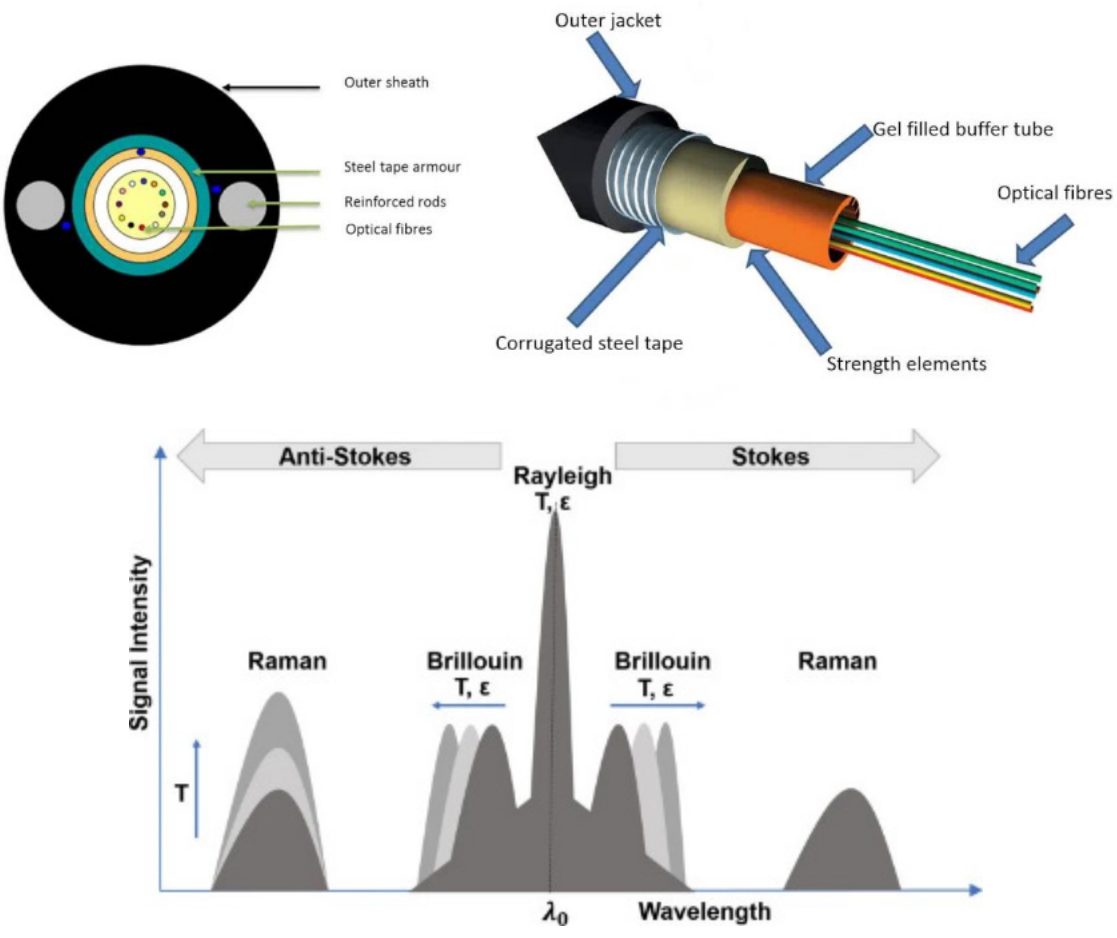

Figure 75: Top: An image of optical fibre and housing (Silixa). Bottom: Spectrum of backscattered light from DFOS (Ekechukwu & Sharma, 2021). Different backscatter wavelengths with specific amplitudes correspond to various external changes (temperature, strain) for measurement.

More recent developments in in-well technologies include engineered fibre optics, which are now a proven in-well monitoring solution. Fibre optics' performance has been tested extensively through pilot and large-

scale CO_2 storage projects. Fibre optics cables can be installed behind the casing or on the production tubing and have been demonstrated to perform most effectively when cemented behind the well casing (Correa, 2019).

Scattering occurs when the medium through which the incident wave travels is not perfectly uniform. This means that the refractive index of the medium varies in different regions (Hartog, 2017). Three types are considered (Figure 75), and in all three cases, the variations in the refractive index occur on a much smaller scale than the wavelength of the incident light. One type of scattering is called Rayleigh scattering, which is characterised by small-scale fluctuations in the refractive index frozen in the material, such as glass. In Rayleigh scattering, the elastic process does not involve the movement of these small-scale fluctuations. This type of scattering measurement forms the oldest Distributed Sensing technology, DAS (Distributed Acoustic Sensing).

DTS is another fibre-optic technology deployed on large-scale CO_2 storage projects. Data is high-resolution, distributed, and continuous. DTS utilises the Raman effect to measure temperature (Figure 75). An optical laser pulse sent through the fibre results in some scattered light reflecting to the transmitting end, where the information is analysed. The intensity of the Raman scattering is a measure of the temperature along the fibre. The Raman anti-Stokes signal changes its amplitude significantly with changing temperature; the Raman-Stokes signal is relatively stable.

Data acquisition through fibre optics is distributed, which means that information can be obtained along the length of the fibre (rather than point source data), providing a rich dataset for surveillance of both the storage formation and shallower intervals. Clearly, including fibre behind the casing means that the impact of the fibre deployment on cement quality must be considered. High-quality cement bond logging tools should be considered to provide an image of any impedance (as an indicator of cement contamination, sub-optimal curing or channelling) behind the casing.

One of the key advantages of fibre optics deployment and data collection is its longevity. Fibre cables can last several decades depending on their construction specifications and the host environment (e.g., reservoir conditions) (Shiach et al., 2007). The fibre cable can be deployed in different modes: behind the casing (in newly drilled wells), on production tubing (for the existing wells) or hung inside the well, similar to a logging tool. The data quality of each deployment mode varies under the circumstances (Bóna et al., 2017; Pevzner et al., 2021) but is comparable to the acceptable signal/noise recorded by geophones.

Using fibre optics cables as long-term downhole sensing tools brings a clear financial advantage versus deploying geophones (Wilson et al., 2020). Vertical seismic profiling (VSP) operations require mobilisation/demobilisation of the tools and the temporary pause of production/injection operations for the well. This requirement can be equivalent to several million dollars for each round of data collection, while fibre optics offers the option for continuous data collection.

Data obtained from fibre optics comes in a variety of forms, which are collectively termed distributed fibre optic sensing (DFOS), and include distributed acoustic sensing (DAS), distributed temperature sensing (DTS), distributed strain sensing (DSS) and distributed pressure sensing (DPS). Several major worldwide GCS projects utilise DFOS technology (Sun et al., 2021)The Quest project in Canada is using a combination of DAS/DTS for leakage detection and well integrity evaluation. Various other international CCUS or CCUS pilot projects are also using DAS/DTS to track CO_2 plume migration.

Distributed Acoustic Sensing

The measurements resulting from DAS are generally considered equivalent to those of conventional geophones. There are fundamental differences in what geophones and DAS measure; however, the changes in the strain rate sensed through Rayleigh scattering can be converted and compared to geophone measurements (Bóna et al., 2017). The deployment of fibre optics (DAS) has been tried on surface and near-

surface, and it has been most successful in downhole (VSP) systems (White et al., 2022). Figure 75 illustrates that the amplitude of the Rayleigh backscattered light is larger and easier to measure.

Distributed Temperature Sensing

DTS is a valuable monitoring technology to assist in calibrating thermal effects primarily when injecting CO_2 that is (relatively) cooler than reservoir temperature as temperature contrast may theoretically adversely impact seal integrity; cooling of the host rock results in contraction and the reduction of stresses within the lower temperature region, and subsequent redistribution of stresses outside of this region; tensile failure may occur, or the fault reactivation potential of nearby faults may be increased (refer section 9.1.7.).

Examples of DTS deployment for CO_2 projects include the Aquistore Site (Saskatchewan, Canada), the Otway International Test Centre (Stage 1 and Stage 2B experiments) and the Quest CCS project (Shell Canada Ltd, 2017). (Rangriz Shokri et al., 2019) Outlines a methodology for calibrating the results from DTS (starting from the construction of geological model through to non-isothermal CO_2 injection modelling) and highlights the importance of non-isothermal effects for more accurate modelling of cold CO_2 injection. Analysis of the DTS data as part of the Otway Stage 1 experiments concluded that the temperature contrast (~20°C between the sand-face injection temperature and reservoir temperature, Figure 76) only propagates a few tens of metres into the reservoir (LaForce et al., 2013). The injection rates, however, were much lower than a commercial project would likely require.

Due to the lack of operational examples of large-scale CO_2 injection into pressure-depleted oil and gas reservoirs, which could result in issues such as hydrate formation causing blockages, corrosion, erosion, slugging and thermal effects, there is a clear opportunity for a field demonstration that could help in validating the results of different models of phase behaviour used in commercial multiphase flow simulation and the impact of this behaviour in a CO_2 injection network. However, depletion must be significantly below the critical point for CO_2 to cause large amounts of Joule-Thomson cooling. Hence, the thermal impact is likely to be very different depending on their abandonment pressure and the strength of the attached aquifer.

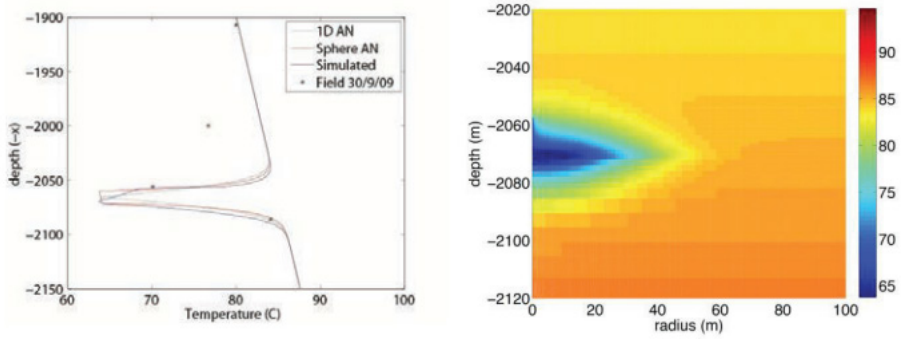

Figure 76: Variation of injection-related temperature change from CO_2 injection and accompanying modelling results from the CO2CRC Stage 1 experiment (LaForce et al., 2013)

Distributed Strain Sensing

DSS is a relatively new technique in fibre optics sensing that utilises the backscattered light at the Brillouin and Rayleigh wavelengths (Figure 75), unlike DAS, which uses only the Rayleigh wavelength backscattering.

Newer instruments can measure the changes in the Brillouin domain, which is more sensitive to stress changes. A high-quality cementing operation is essential when assessing distributed strain sensing (DSS) data, as the fibre needs to be offset from the casing and coupled effectively to the formation via the cement in the annulus. Therefore, if coupled to the rock, DSS measurements provide valuable data from the variation of the stress field in the surrounding environment of the fibre cable, which may be caused, for example, by changes related to CO_2 injection and plume movement.

DSS is currently the least mature DFOS technology, specifically because it has yet to be tested on a large-scale GCS project. It has been deployed at research/pilot sites in Canada, Korea, and Japan, where it has been used to evaluate CO_2 leakage, induced micro-seismicity and geomechanical responses. DSS has also recently been deployed at the Otway International Test Centre in two shallow bores (and is planned to be installed in a third, deeper well) to test further its applicability in the detection of geomechanical strain, which can be used to infer the direction of CO_2 plume migration and the stress imparted on the storage formation. To date, DSS technology has been used to detect strain in the order of 10's of metres away from the well in which it is deployed (Zhang et al., 2020).

The real-time observations from DSS can be integrated with surface-deformation monitoring technologies (e.g., InSAR or tiltmeters, refer to 10.1.5) to constrain geomechanical studies in both the areal and vertical extent (Zhang et al., 2021). The increased understanding of the geomechanical response of the storage complex and overburden to CO_2 injection enables risks related to seal integrity to be actively managed to prevent the mechanical failure of the seal.

10.1.3 Seismic Monitoring

The geophysical monitoring of the subsurface has been a core part of exploration and development programs in many industries, including energy, construction, and the environment. Among many geophysical methods, seismic-related monitoring has proved to be an effective mechanism to detect migration. All seismic methods require a combined source and receiver system to function. When the seismic source is provided synthetically (i.e., human-made devices such as vibrators), the phrase "Active Seismic" is used. On the other hand, if seismic monitoring relies more on listening for events and the source is provided by natural sources such as ocean waves and earthquakes or the changes in the subsurface, "passive seismic" is being deployed.

Each method has its pros and cons regarding the cost of utilisation and the accuracy of its results. In general, passive seismic methods are relatively newer (and in development) and rely more heavily on technological advances in detecting the slightest signals. A detailed discussion of the costs for active and passive seismic methods is beyond the scope of this report as they are site-specific. However, the following list introduces some insight into the potential application of each seismic monitoring method in GCS.

Active seismic monitoring

Conventional seismic monitoring technologies that require an active seismic source are mature technologies for the CO_2 storage and oil and gas industries. Active seismic monitoring is a powerful technique that can be applied for conformance and assurance monitoring in GCS. It was successfully deployed in small-scale research projects such as the OITC and large-scale commercial projects. Usually, in land time-lapse surveys, the seismic survey is designed to have a very high trace density to ensure time-lapse data quality. This increases the cost of the survey and usually results in high-quality data covering a minimal area. While this is an appropriate approach if a detailed image of the plume is required, an alternative approach is to develop monitoring solutions by exploring sparse and relatively inexpensive monitoring systems.

Active seismic source methods vary in the observation methodology and techniques. An overview of geophysical methodologies for CCS purposes is discussed (Davis et al., 2019). All such techniques attempt to model, detect and monitor the changes in the rock-fluid system due to CO_2. The in-situ model states the current condition of the reservoir/seal system. From the initial point, replacement fluid modelling can predict a gas-filled reservoir (natural migration of gas to reservoir), subsequent depletion (industrial production) and re-inflation by CO_2 (sequestration). The rock physics models (Bjorlykke & Avseth, 2010; Davis et al., 2019; Mavko et al., 2020) predict that the following changes in the system may be detected/measured through geophysical time-lapse methods:

- Changes in pore fluid type, saturations (e.g., CO_2 injection)
- Changes in pore fluid pressure or confining stress

- Changes in temperature due to advective heat/ fluid flow and diffusion
- Geomechanical deformation or fracturing
- Geochemical reactions

Time-lapse (4D) seismic imaging has been applied in several studies to monitor the integrity of seals over time (Anyosa et al., 2021; Arts et al., 2004). A time-lapse signal can be caused by any of the changes mentioned above in the reservoir or the overburdened rock. Such signals can be observations of changes in the seismic amplitude, phase, frequency content or travel time.

Commercial CCS projects such as Snøhvit and Sleipner have seen success in implementing spectral decomposition, time shift analysis, and amplitude difference methods to monitor the injected CO_2 plume.

Elevated pore pressure leads to a reduction in effective stress within the formation, resulting in a decline in P-wave velocity (White, Williams, & Chadwick, 2018). If substantial enough, this reduction can produce a discernible signal in the seismic differential data. The injection of fluid into reservoirs with constrained interconnected pore volumes has been demonstrated to produce seismic amplitude responses attributable to changes in both pressure and saturation (Angelov et al., 2004; Landrø, 2001).

Spectral decomposition has proven to be useful in imaging of complex stratigraphical sequences (Chen et al., 2008; McArdle & Ackers, 2012; Partyka et al., 1999) and detection/characterisation of thin CO_2 layers at sites such as Snøhvit (White et al., 2015), Ketzin (Huang* et al., 2015) and Sleipner (Williams & Chadwick, 2012).

Adjusting the input data could affect the scale of saturation and pressure, and it's reasonable to consider some level of uncertainty in this adjustment. Detection of anti-correlated inversion results would suggest potential issues related to inversion crosstalk (Grude et al., 2013). Despite attempts to scale and deduct the inverted pressure and fluid, a persistent pressure impact remains. When utilising closely related (seismic) offset data (such as near and mid offset), there is evident leakage between the pressure and saturation 3D cubes, underscoring the importance of maintaining substantial separation between the offset datasets. This separation is crucial for treating the input as distinct measurements, thus enhancing the stability of offset inversion. Ensuring separation between the offset cubes is critical for stabilising the inversion process and effectively distinguishing between the impacts of saturation and pressure on the seismic data.

Research has indicated that minor variations in reservoir parameters, such as porosity, can result in significant uncertainties in the predicted pressure and saturation levels, as noted by (Trani et al., 2011) and (Shahraeeni, 2012). A comparison of time-shift values derived from cross-correlation and those obtained through pressure and saturation inversion is depicted in Figure 77,. The input involves a somewhat fragmented fluid distribution following Brie e = 3. The time-shift data exhibit a strong correlation spatially and in magnitude. This alignment suggests that saturation and/or pressure alterations likely occurred in the deepest layer. Relying on RMS values rather than peak values for accuracy, a satisfactory quantitative alignment is achieved. This observation implies a fluid distribution lying between perfectly uniform and extensively patchy configurations.

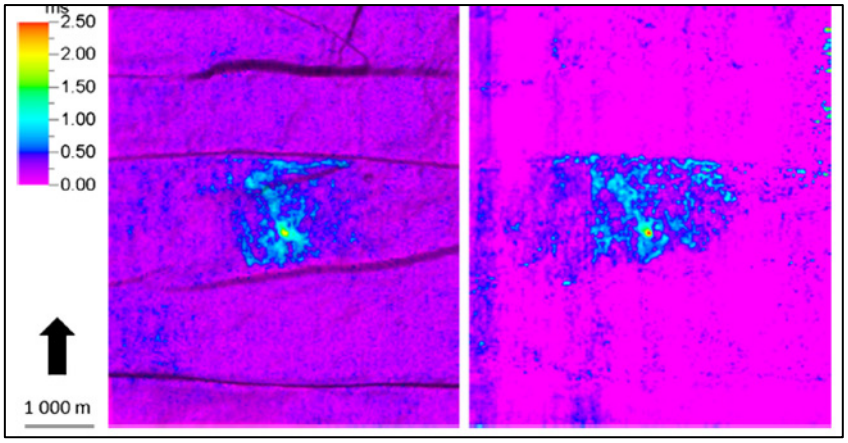

Figure 77. Estimated time shift at Snøhvit from the inverted saturation and pressure (left) and cross-correlation (right). Modified after (Grude et al., 2013).

The spectral analysis of the seismic monitoring data at Snøhvit suggests minimal energy content in the highest frequency segments, resulting in a practical inability to achieve the desired layer thickness resolution. This is because the tuning thickness correlates with a peak frequency of 35 Hz, indicating a wide spectrum with a steep decline at higher frequencies for the reflections depicting the Jurassic sequence. Findings from the 2012 dataset indicate a prevalence of lower frequencies in the vicinity of the injection point (Figure 78).

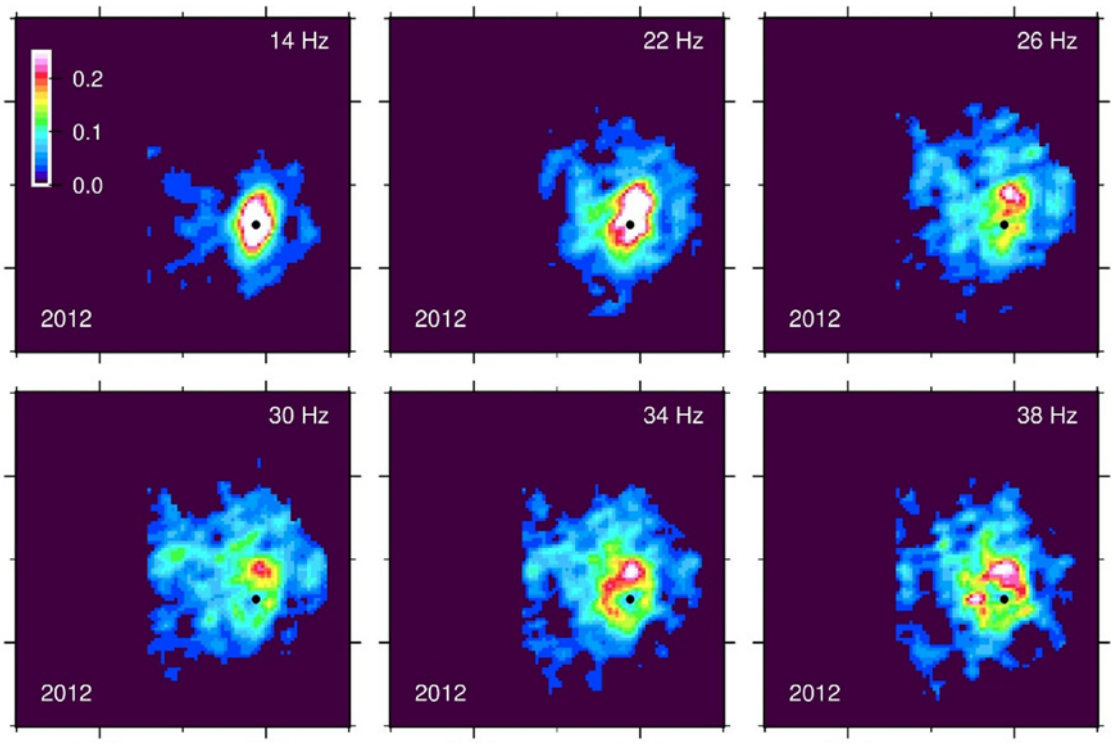

Figure 78. Normalised discrete frequency reflection amplitudes of the CO_2 layer in the Stø Formation from the 2012 seismic difference data (White, Williams, & Chadwick, 2018).

A similar assessment was conducted on Sleipner (White, Williams, Chadwick, et al., 2018) to identify tuning frequencies throughout the layers and extrapolate temporal thickness for the plume and reservoir. The temporal thickness data range from negligible values at the layer boundaries to approximately 16 ms in the central regions of the layer, showing a strong correlation with the topography of the base seal. Compared to alternate methodologies like amplitude analysis, temporal shifts, and direct temporal spacing measurements, spectral techniques offer a dependable means of determining temporal thickness well below the tuning

threshold. When combined effectively with other techniques, spectral decomposition allows for a reliable estimation of temporal thickness ranging from close to zero to significantly beyond the tuning thickness, resulting in clear layer resolution.

To better understand the controlling flow processes in the Sleipner plume, it is important to learn as much as possible about layer geometry, and seismic data play a key role here. A generalised approach to determining layer geometry directly from seismic data depends on establishing the two-way travel-time thickness of the layer (here termed the temporal thickness).

Seismic data plays an important role in gaining deeper insights into the governing flow mechanisms within the Sleipner plume, which in turn requires comprehensive knowledge of the layer geometry is crucial.

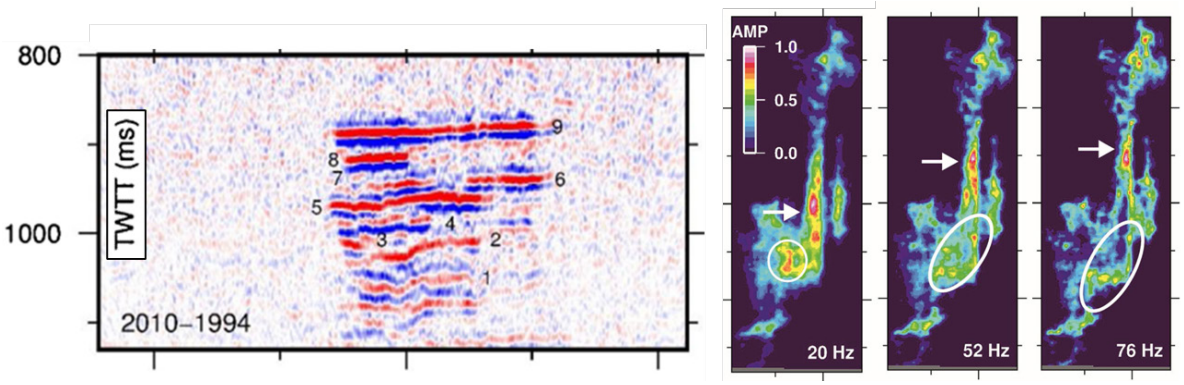

Figure 79. Time Lapse difference data (left) shows the layered nature of the reservoir/CO_2 plume and the spectral decomposition of the seismic amplitude data (right). The arrows and circles are to highlight the peak tuning features. Image modified after (White, Williams, Chadwick, et al., 2018).

Discrete frequency reflection amplitude cubes, sampled every 2 Hz, were generated by the SPWVD (Smoothed Pseudo Wigner-Ville Distribution) (White et al., 2015) using time-lapse processed data acquired in 2008 and time-lapse and optimal image-processed data acquired in 2010. This approach enabled the determination of the temporal thicknesses of the layers with precision matching the highest practical frequency in the seismic wavelet, surpassing the tuning thickness.

Geomechanically induced time shifts were observed in the overburden of fields produced from sandstone reservoirs close to hydrostatic pressure (Rickett et al., 2007; Røste & Ke, 2017). Undrained areas were identified based on the overburden time shifts (in 4D seismic), which were, in turn, caused by pressure changes and geomechanical response. Direct-wave travel times and amplitude variations were utilised in CO2CRC's Otway project to monitor the formation stiffness and density (Pevzner et al., 2022). In their methodology, Fibre Optics DAS data was utilised for time-lapse monitoring of a small CO_2 plume (15 kilotonnes) injected into a saline aquifer. When the transmission loss is small, the induced axial strain amplitude, ϵ, is shown to be related to the P-wave velocity (Pevzner et al., 2020):

$$\epsilon_0 = \left(\rho V_P^3\right)^{-1/2}$$

Further, temporal changes of the formation velocity will change the direct-wave travel times below the formation. Such changes are shown to be (Pevzner et al., 2022):

$$\Delta t = \frac{h}{(V_P + \Delta V_P)} - \frac{h}{V_P} \cong -\frac{h\Delta V_P}{V_P^2}.$$

Where h is the formation thickness, and V_p is the P-wave velocity.

To verify compliance in extensive GCS projects, an alternative method was suggested by (Pevzner et al., 2024), which involves employing head waves instead of reflected waves. This methodology may also be applicable to identify substantial leakage. Assuming there is a notable increase in P-wave velocity beneath

the reservoir housing the CO_2 plume, a distant source can produce refracted waves (head waves or diving waves), which will traverse the plume on their return to the surface, encountering travel time delays due to the velocity reduction induced by the injected CO_2.

The concept of seismic monitoring recognises the great strengths of conventional seismic and its utility in monitoring CO_2 injection. There is always a desire to reduce cost and invasiveness, increase sensitivity and reliability, and make results available to decision-makers in close to real-time.

Some of these concepts were demonstrated during CO2CRC's Stage 3 "risk-based monitoring", which had the following components:

1- Permanent, automated monitoring with offset VSP, using a sparse array of permanent surface sources and optical fibres (DAS) cemented externally to the casing of the monitoring wells.

2- 4D conventional surface seismic and 4D VSP (Mateeva et al., 2017). This provided "ground truth" for comparison with the experimental monitoring methods.

3- Permanent monitoring of micro-seismic activity caused by the pressure perturbations associated with the CO_2 plume.

The combination of downhole DAS and permanent surface sources, which was achieved in CO2CRC's Stage 3 experiments, represented a technical advance that had previously been postulated in literature to have clear benefits (Dou et al., 2016). These include reduced cost and increased reliability (compared to conventional receivers), improved sensitivity, and the possibility of near-continuous automated monitoring. The permanent automated VSP, therefore, is conventional VSP only in name as it involves changes in receiver and source and automation of processing technology. The permanent seismic monitoring concept can apply the following aspects:

1- Permanently deployed downhole receivers external to the casing, with the consequent benefits of cost, longevity, sensitivity, and high data density.

2- Permanent sources, known as SOVs (surface orbital vibrators) (Daley & Cox, 2001; Dou et al., 2016).

3- Automated (unmanned) data acquisition and data processing, using full-wave inversion, to deliver high-fidelity information to decision-makers without the current lengthy delays associated with VSP data (Isaenkov et al., 2021).

The DAS-SOV VSP was used to detect the presence of the plume in the well by tracking the temporal variations of travel times and amplitudes of direct P-waves (Popik et al., 2021; Popik et al., 2020). This method detected an abrupt increase in travel times below the injection interval on the second injection day (after 300 tonnes of CO_2). It allowed an accurate estimation of the plume thickness. Analysis of the results (Tertyshnikov et al., 2020) showed that this approach is sensitive to changes in velocity and density in very thin layers within the entire length of a DAS cable (often the whole length of a deep well), both in the reservoir and in the overburden.

A recent study focused on the Smeaheia aquifer (offshore Norway), establishing a methodology for calculating the value of information to support a seismic monitoring program focused on determining whether CO_2 leakage may occur via a specific fault (Anyosa et al., 2021). The detailed workflow outlines the geophysical, reservoir simulation, rock physics and seismic modelling aspects that describe the various plausible states of nature, the statistical methods (e.g., random forest, convolutional neural networks) applied and the value of information assessment. The authors concluded that the optimal monitoring time, which is site-specific and focused on an explicit risk mechanism, is about ten years after injection starts.

Another example of applying seismic to evaluate cap rock integrity is at the Weyburn CO_2 storage site (Canada). AVOA (amplitude variation with offset and azimuth) techniques to assess cracks and fractures by

mapping horizontal transverse isotropy (HTI) (Duxbury et al., 2012). Anomalies in the HTI could be correlated with the salt dissolution structures of the evaporites that form part of the reservoir cap rock. Any changes to the integrity of the top seal will result in changes in the local stress field and the generation of systematic cracks and fractures. Under targeted and suitable seismic monitoring, these potential seal integrity failures can be detected (Li et al., 2014; Mbia et al., 2014), and pre-emptive/reactive measures can be taken to address the risks.

Seismic anisotropy can be used as a proxy to predict the sealing capacity of shales. More anisotropic shale sequences contribute to higher sealing capacity, while less anisotropic sequences are likelier to have a lower sealing threshold (Nourollah et al., 2015). Conventional 2D and 3D seismic data can be utilised in this method to evaluate the sealing potential away from calibration points (well data or MICP analyses). This method was applied near a known gas chimney in the Gippsland basin (Nourollah & Urosevic, 2019). The theoretical background of this method is mentioned in section 4.2.5.

This approach can provide field-scale seal evaluation and baseline surveys for monitoring the top seal in CO_2 storage projects. Any baseline seismic survey will act as the appraisal tool and risk assessment. Subsequent seismic data will monitor any changes in the seal characteristics/dynamics and can assist with the above-zone monitoring of the CO_2 plume.

Variations of the seismic anisotropy can also reveal the status of the top seal. Prior production from existing hydrocarbon reservoirs would have changed the state of stress. Future carpet/localised seismic data (e.g. 3D, 2D, VSP) can measure and verify the top seal capacity variations (leakage, weak spots, etc) over time.

A seal monitoring strategy may comprise a baseline and subsequent targeted monitor surveys. A baseline can be produced from the conventional seismic data over the field. This baseline provides detailed information on the variation in sealing capacity and areas of weakness. Subsequent comprehensive or spot seismic surveys (surface or VSP) can be designed to recalculate the top seal attributes. The difference between monitor surveys and the baseline is monitored for any changes.

Passive seismic for monitoring micro-seismicity

Typical disadvantages of surface time-lapse seismic acquisition, such as the high cost, invasiveness, and the requirement for land access, give credit to methods that require no active seismic source, i.e. passive seismic. Recent improvements in DAS technology have had a significant impact on the application of seismic monitoring. Relatively cheap and highly durable fibre optic cables are easy to deploy and can acquire good-quality seismic data (dos Santos Maia Correa, 2018). Hence, permanently deployed optical fibre cables as receiver arrays in borehole reservoir surveillance can significantly reduce the cost and invasiveness of monitoring.

Reducing the active seismic source effort could further reduce cost and the level of invasiveness of seismic monitoring operations. Therefore, the seismic energy associated with ambient noise and non-primary body waves excited by the controlled seismic source, including multiples and converted waves, can be used to monitor.

Typically, the objective of this monitoring technology is to passively acquire micro-seismic data to establish how CO_2 injection operations alter the stress state of the storage complex and overburden, primarily how it impacts pre-existing fractures or results in the creation of new fractures. Two general mechanisms for micro-seismic events: crack-induced emissions within intact rocks and slip-induced emissions along weak planes (Khazaei & Chalaturnyk, 2017).

Acoustic waves can be detected without any control over the source parameters and location, and the parameters may be estimated using seismic interferometry techniques. However, this technique requires sufficient Signal-to-Noise Ratio (SNR), which is often hard to achieve in a reservoir monitoring application that utilises geophone arrays deployed on the surface only (in contrast to earthquake seismology). Borehole-recorded seismic data are advantageous since they enjoy their lack of surface wave contamination.

Micro-seismic monitoring is a relatively mature monitoring technology deployed at several pilot and large-scale CO_2 storage/CCUS projects, including Weyburn, QUEST, In-Salah, Mountaineer and China (Meng et al., 2023). Micro-seismic can be deployed to monitor at surface, near-surface, above or within the primary storage reservoir. The conventional approach is to monitor by deploying (tri-axial) geophones.

A DAS cable functions as a series of closely interspaced seismic detectors capable of assessing the linear strain of the fibre. The measured strain intensities captured by the DAS cable are influenced by the properties of the geological formation surrounding the well; softer materials result in greater strain readings. Therefore, it is feasible to deduce the characteristics of these formations by examining the relative shifts in the amplitude of seismic waves travelling through the well (Pevzner et al., 2020). A significant benefit of this method for analysing and monitoring subsurface characteristics is that it does not necessitate an active seismic source. Instead, it can employ passive sources like natural seismic events like earthquakes. CO_2 plumes in the saline aquifer were detected using Rayleigh waves generated by the ocean (Pevzner et al., 2023). Time-lapse analysis of the wave amplitudes was used to indicate temporal changes in the stiffness of layers caused by changes in saturation or pressure.

The amplitude variation of microseisms displays specific changes with depth across different frequencies and source regions in the ocean (Glubokovskikh et al., 2023). Surface waves reverse polarity at the depth where porous weathered carbonates transition to consolidated stiff clastic rocks, resulting in a notable shift in the depth trend of the seismic properties. Analysis of the observed amplitude variation with depth indicates (Figure 80) that higher-order Rayleigh modes' contribution is significant even for classic double-frequency microseisms (~150 mHz).

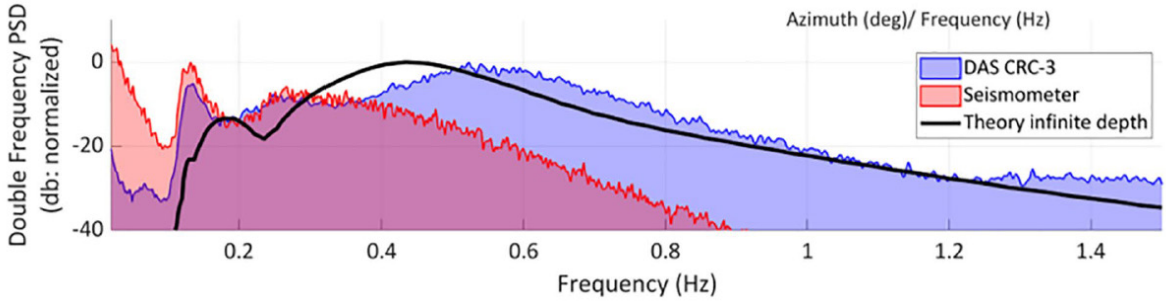

Figure 80: The maximal PSD (Power Spectral Density) for the seismometer is at 0.15 Hz, at 0.55 Hz for DAS, 0.45 Hz for the predicted PSD time series. DAS corresponds to 300 m depth in CRC-3 (Otway Site), seismometer corresponds to S1.AUHPC seismometer and the ocean wave spectra are retrieved from the WBAST1 buoy.

Using the concept of the seismogenic index, the Otway injection site's seismotectonic potential has been subject to a rigorous study (Glubokovskikh et al., 2023). Estimates of the focal mechanism for events with M_w>-1.5 were made despite the limitations in the angular coverage of the wells. The DAS array proved sensitive to detect and locate induced events with ~M_w -2, which occurred nearly 1500 m deep (Figure 81).

Detailed geomechanical data is typically scarce for CO_2 storage locations. Hence, it becomes critical to investigate both the magnitude and patterns of the micro-seismic reactions, as it was conducted at the Otway site. Identifying the probable spots and times of the most significant injection-induced quakes would allow a more precise evaluation of the risk of earthquakes for large-scale injections within the same seismotectonic context.

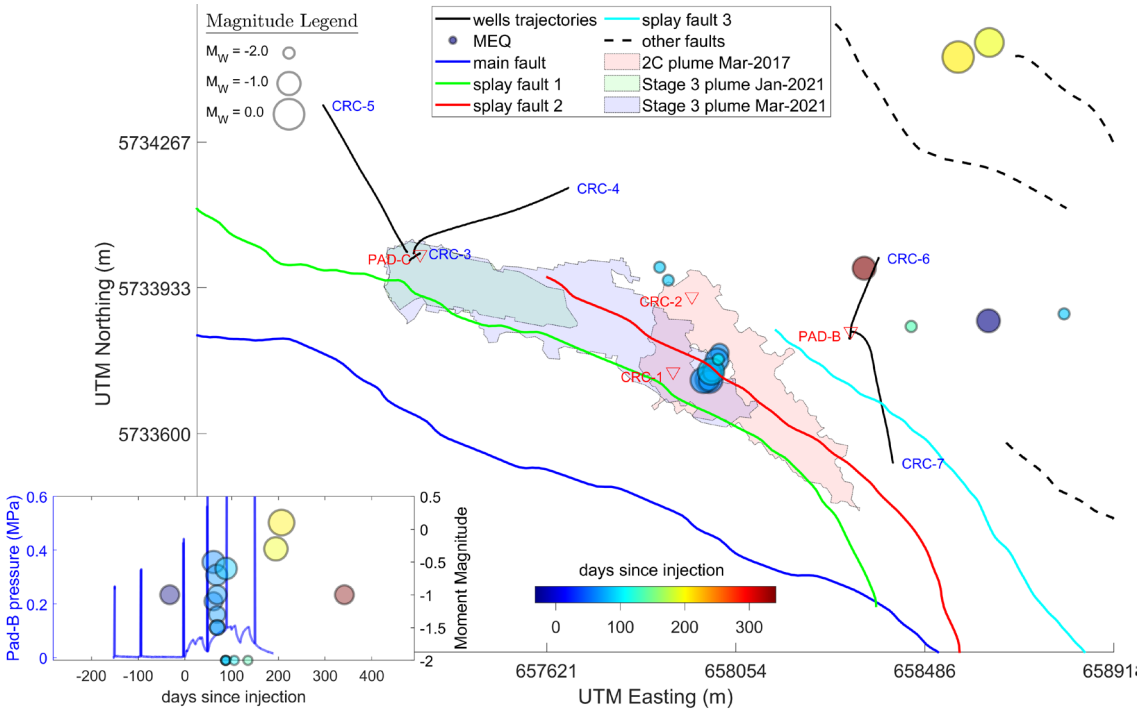

Figure 81. The catalogue of detectable micro-seismic events that could be attributed to the CO_2 injection at the CO2CRC Otway site (Glubokovskikh et al., 2023)

There is a consensus in the literature that an array of micro-seismic stations located in shallow boreholes is preferable to a monitoring design deploying a single, downhole geophone due to the limitations that the latter provides concerning areal coverage and directionality. However, a single borehole array has (to date) been the most prevalent observation system design (Chen & Huang, 2020).

Multiple authors highlight the importance of acquiring pre-injection baselines to distinguish between micro-seismic events induced by CO_2 storage versus naturally occurring seismic events. Historically, several large-scale CO_2 storage projects (In-Salah, Mountaineer) did not collect baseline micro-seismic but later acquired this data during the operations phase. Whilst micro-seismic data is valuable, an induced micro-seismic event does not necessitate concern per se, and any should be linked back to the appropriately identified risks.

The QUEST project was one example in which a pre-injection micro-seismicity baseline was acquired using an eight-level, three-component geophone array installed in a monitoring well (Shell Canada Ltd, 2017) No ambient micro-seismic events were detected within the monitoring range of the array during this baseline. Six years of micro-seismic monitoring observations resulted in the detection of 486 locatable, low-level events within the QUEST micro-seismic area of review (Harvey et al., 2021). The location of all these events was within the Precambrian basement (i.e. deeper than the CO_2 injection was occurring) - statistical analysis and geomechanical modelling studies of the reservoir and basement are being conducted to understand further the mechanism that generates these events. Importantly, the authors concluded that there was no risk of leakage associated with the micro-seismic events (Harvey et al., 2021).

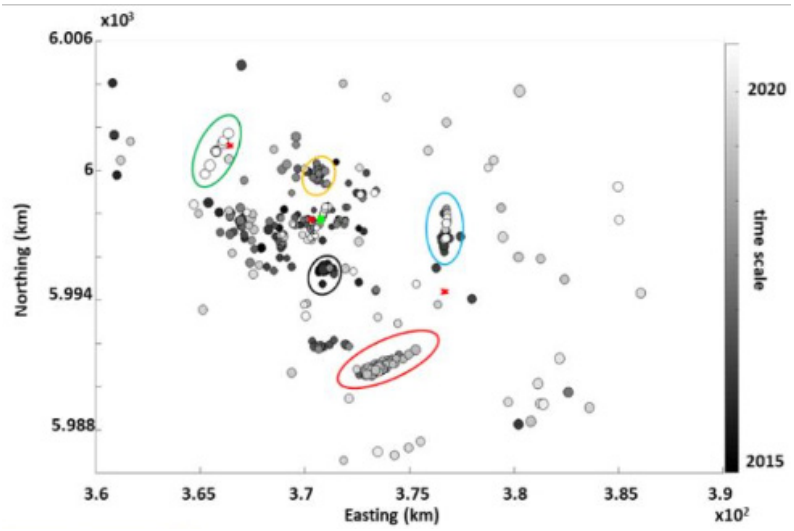

Figure 82: A map of the first 400 event locations at the QUEST project. The size of location dots is proportional to the magnitude, while the colour is a function of the time they occurred. The green dot indicates the deep monitoring well, while the three red stars indicate the injection wells. The cluster highlighted in red was recorded as a burst of seismic activity in 2017. A maximum event magnitude of 0.8 was recorded (Harvey et al., 2021).

In contrast to the conventional micro-seismic approach (geophones), there has recently been research to assess the feasibility of fracture imaging using DAS-recorded micro-seismic events DAS (Becker et al., 2017; Jin & Roy, 2017). Hydraulic fracturing analysis from unconventional production operations demonstrated that fractures could be imaged using DAS-based micro-seismic monitoring through fibre cemented behind casing in two wells (Stanek et al., 2022). Whilst the technology has challenges in spatially locating the source of micro-seismic events when deployed in a single well, there are several solutions (multi-well fibre configurations or helical fibres) (Lim Chen Ning & Sava, 2018).

Recent developments in the micro-seismic monitoring domain leverage the growing capabilities in combining geophysical processing techniques with advancements in artificial intelligence (e.g., neural networks). This is best illustrated by the micro-seismic data acquired as part of the Decatur CCS project, where the adaptation of an existing algorithm resulted in the successful relocation of over 4,000 micro-seismic events (Figure 83) (Dando et al., 2021).

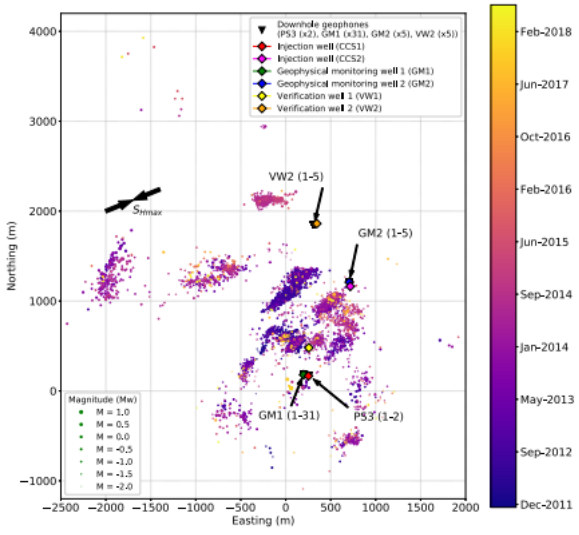

Figure 83: Decatur micro-seismic events (Dando et al., 2021)

Passive seismic for monitoring CO_2 leakage

As highlighted previously (Section 10.1.2), DAS is the most mature of the fibre-optic-based technologies used for monitoring large-scale CO_2 storage projects, providing distributed data across a broader frequency range than other technologies (e.g., conventional geophones). Recent research has emphasised the opportunity to utilise DAS for CO_2 leakage detection and the more familiar method of employing DAS for plume migration monitoring (Sidenko et al., 2022)The authors outlined the possibility of utilising DAS to monitor pressure variations as low as 10-4 psi per second along the entire well, which would allow for the identification of CO_2 migration out of the storage unit(s). Figure 84 illustrates the strong positive correlation between the DAS response and the time derivative of the pressure response from the same observation well.

Passive seismic data was acquired over the Lacq-Rouse area, southeast of France, to monitor a naturally fractured depleted reservoir utilised as a GCS pilot site (Payre et al., 2014). The monitoring plane was designed to observe the seal integrity, separate natural and induced seismicity and assess the risk of the injection-induced seismicity. The experiment proved the system could be an efficient hazard monitoring tool despite the low-level detected seismicity (magnitude -0.6).

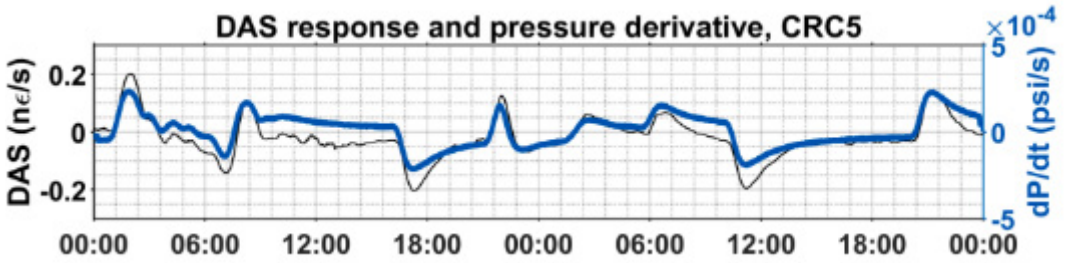

Figure 84: DAS response compared to the time derivative of the pressure response (Sidenko et al., 2022)

10.1.4 Electromagnetic Monitoring

Alternative geophysical monitoring techniques of varying levels of technical maturity have been developed to investigate the integrity of CO_2 seals. Electromagnetic or controlled-source electromagnetic (EM/CSEM) are two such techniques.

Due to the high resistivity of hydrocarbon-bearing formations, CSEM has historically been deployed by the oil and gas industry as a method for indicating the presence of hydrocarbons in the subsurface. Simplistically, a typical deployment involves towing the E/M source by a vessel and deploying the EM receivers on the seabed.

CSEM has been applied at both Sleipner (Park et al., 2011) and at the Ketzen Pilot Site in Germany (Schmidt-Hattenberger et al., 2011). CSEM is most effective in shallow to intermediate depths (up to a few kilometres) and is less effective at greater depths due to signal interpretation. Disadvantages of CSEM include limitations in vertical resolution for thin layers or small-scale structures, complex signal interpretation, and interference caused by other electromagnetic signals.

A recent study used the combination of seismic and EM to investigate the integrity of a CO_2 storage seal, suggesting that the technologies could be combined to detect CO_2 plume migration and potential CO_2 leakage pathways (Fawad & Mondol, 2021). In this example, using an acoustic-impedance resistivity ratio, the Smeaheia aquifer (offshore Norway) was used to evaluate the differences in CO_2 saturation from repeat seismic and CSEM surveys. Two scenarios were considered: one in which 3D seismic and CSEM surveys were acquired every ten years and the second in which only a baseline 3D seismic survey was developed, followed by repeat CSEM surveys. This study concluded that the design of a possible hybrid seismic/EM surveying program needs to consider the vertical resolution limitations of E/M and the attenuation of E/M energy.

Further, CSEM may have future applications for CO_2 leak detection. A recent 2D synthetic study was performed to assess the detection of CO_2 escape and saturation changes within a submarine chimney connected to a CO_2 storage site in a marine environment (Yilo et al., 2024). In the study, the modelling simulates and analyses CO_2 leakage through a feature analogous to some fluid escape features that naturally exist in the North Sea. The study indicated that CSEM would detect leakage when CO_2 saturations exceed 20 per cent, even though seismic velocities will remain almost constant for the same event. Therefore, in this work, the authors state a vision for applying CSEM in combination with seismic monitoring to enable fluid substitution, lithology, and mechanical effects to be distinguished.

10.1.5 Surface Deformation Monitoring

Surface deformation does not directly measure changes in the storage complex seal(s). However, it enables the storage complex plus overburden to be monitored; changes related to seal(s) integrity may be inferred from this data. Various surface deformation monitoring methods, including tiltmeters, InSAR and differential global positional systems (DGPS), have been proposed for GCS (McColpin, 2009). An illustration of the various monitoring technologies is provided in Figure 85.

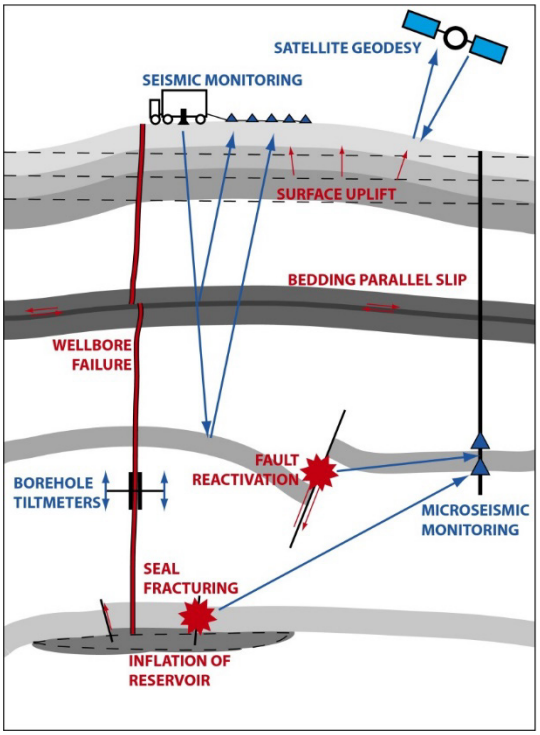

Figure 85: An illustration of various geomechanical deformation-related risks and potential monitoring options (Verdon et al., 2013)

The underlying principle behind this approach is that changes deep in the subsurface strata will cause enough elastic and plastic deformation in the overburden that can be measured at the surface or in the shallower rock layers. Inherently, such measurements require a large enough seal/reservoir deformation to be transferred to the surface. As a result, the overall Poisson ratio of the overlying strata is an important factor that can reveal or mask the subsurface deformation.

InSAR

Interferometric Synthetic Aperture Radar (InSAR) is an onshore monitoring method for identifying, measuring, and monitoring the movements and deformations of the Earth's crust using suitable satellite images. InSAR is beneficial for detecting ground movement during the depletion of onshore basins due to anthropogenic

activities at oil, gas, or CSG reservoirs (Moghaddam et al., 2021) The magnitude of the ground movement (during both depletion and repressurisation) provides information as to whether the field is behaving elastically during pressure cycling..

One of the benefits of InSAR is that data can often be collected retrospectively using historically collected satellite data, which is helpful if data has not been collected from the beginning of the depletion phase or had not been identified as a risk in early framing exercises. The inversion of InSAR deformation maps can detect deformation patterns over time, including in hard-to-access areas.

A recent study analysed the suitability of deploying InSAR at several GCS sites, proposing eight primary influencing factors (vegetation coverage, topography, onshore/offshore, land use, injection rate, storage unit depth and monitoring duration) (T. Zhang et al., 2022). Anomalies observed with InSAR can be associated with seismic velocity variation within the overburden (i.e. overburden time shifts in 4D), highlighting how monitoring technologies can be deployed in a complimentary manner. A multi-method monitoring system combining fibre optics, micro-seismic, InSAR and CO_2-detecting unmanned aerial vehicles (UAV) was also hypothesised as a potential monitoring solution (Figure 86).

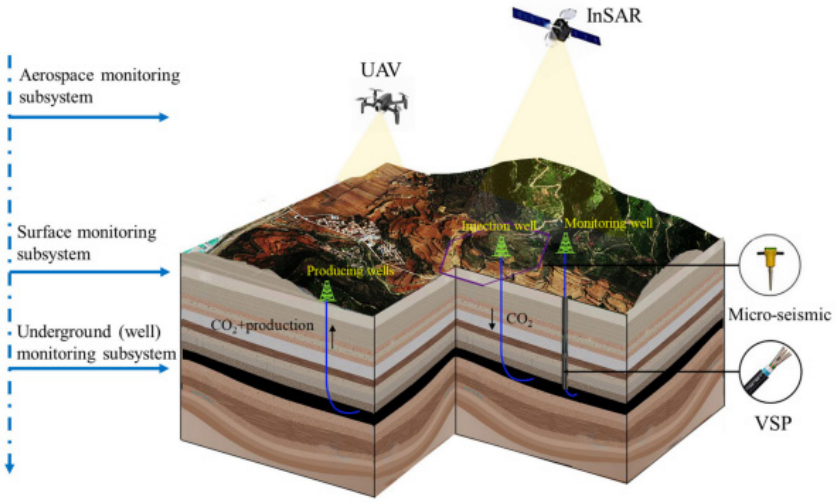

Figure 86: A multi-method monitoring system (T. Zhang et al., 2022)

InSAR has been deployed on several large-scale CCUS projects, including In-Salah (Rucci et al., 2013), the QUEST project, and Gorgon CCS (Verdon et al., 2013) (Haynes et al., 2023). No direct measurements of geomechanical deformation, either geodetic or micro-seismic, have been carried out at Sleipner. Still, with the estimated small pore pressure change, it is unlikely that significant geomechanical deformation will have occurred (Verdon et al., 2013).

In-Salah is an example of CO_2 injection into a formation with relatively low permeability (< 10mD) (Shi et al., 2019). An uplift of up to 14 mm/year occurred around two injector wells immediately after the commencement of CO_2 injection, with an uplift pattern that could be correlated with the location of the injection wells (Bohloli et al., 2018).

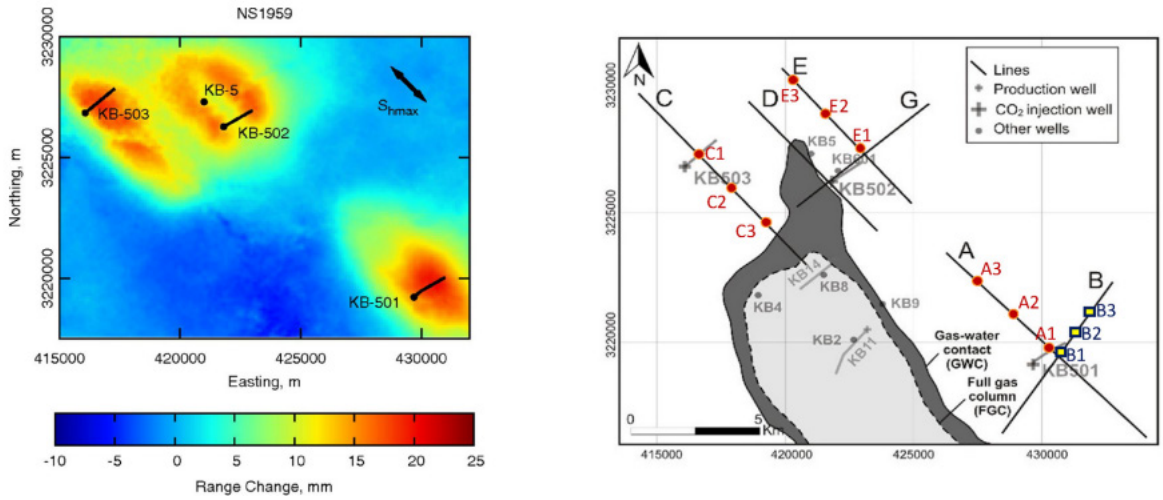

Figure 87: Surface uplift around three injection wells at In-Salah (Bohloli et al., 2018) after (White et al., 2014) (left); and the selected lines for analysis of surface uplift (right)

InSAR is one amongst a suite of technologies that have been utilised for monitoring Gorgon CCS, with inferred vertical surface movement limited to "single-digit" millimetres since CO_2 injection commenced in 2019, providing qualitative support for connectivity and pressure distribution (Haynes et al., 2023). InSAR inversion has been applied to relate surface displacement changes to reservoir changes, enhancing the calibration of the reservoir-geomechanical modelling (Haynes et al., 2023).

Tiltmeters

Tiltmeters have been deployed as a deformation monitoring tool at several CO_2 storage sites, including Aquistore (Canada)(Worth et al., 2014) and in the CO_2-ECBM project in the San Juan Basin (USA) (Koperna et al., 2009).

Tiltmeters' high sensitivity is an advantage compared to other surface deformation methods. It can be deployed as a cost-effective seabed monitoring technology (if it is competent enough to support the tiltmeter without compaction of shallow sediments resulting in tilting). Tiltmeters are typically deployed in surface arrays combined with GPS but can also be deployed in wellbores (Verdon et al., 2013).

The strategy for the tiltmeters placement as part of the Aquistore MMV program was informed by the reservoir modelling study's CO_2 plume migration pathway prediction (Worth et al., 2017). The tiltmeters were buried approximately 30 m below the surface to reduce errors in the deformation interpretation (e.g., due to road/vehicle noise, mining operations, etc.)

A (retrospective) large-scale geomechanical study was undertaken for the In-Salah project to assess the feasibility of using tiltmeters to predict the shape and direction of the CO_2 plume (Salimzadeh et al., 2022). The synthetic tilt meter readings were of sufficient magnitude such that they could be resolved from background noise levels and that reliable readings could be detected before those measured by other deformation monitoring methods (e.g., InSAR) (Salimzadeh et al., 2022).

10.1.6 Value Of Information for Monitoring Technology Selection

Monitoring technology selection is site-specific, and as regulatory requirements also vary across jurisdictions, it is impossible to provide a blueprint/one-size-fits-all outline for the design of monitoring programmes. As standard practice, designing a monitoring programme for seal integrity should include a risk assessment (as discussed in section 6) and the subsequent identification of monitoring technologies that help manage that risk. Importantly, if the technology selection criteria are value-based (as opposed to mandated), then value of information (VOI) analysis should be considered.

VOI is commonly applied in the oil and gas industry to support decision-making, and similar principles can be readily applied to the design of CO_2 storage monitoring programmes. The fundamental principles for developing VOI assessments for monitoring technology selection within the context of CO_2 storage and uncertainty include (Sato, 2011):

- **Relevant:** The information provided through monitoring must potentially change our beliefs about the uncertainty.
- **Material:** The information provided through monitoring must potentially change a decision we would otherwise make. This could manifest as an appraisal-based VOI assessment leading to a high-value GCS development decision or trigger a decision on a contingent activity in the injection or post-injection monitoring phase.
- **Economic:** The cost of information gathering must be less than its value.

The timing of the information gathering (frequency, commencement, and cessation) is critical to the monitoring programme design. Therefore, where appropriate, monitoring programmes should be phased and adaptive.

VOI has been applied to assess the likelihood of CO_2 leakage into a groundwater source planned for irrigation purposes (Trainor-Guitton et al., 2013), with the analysis informing the development of an electrical resistivity monitoring program. Alternatively, active safeguards (i.e. those that require human input or control to function, refer section 6.1.1) may be applied in a risk bow-tie. Monitoring tools can be deployed, and a suitable response logic should be developed to ensure that a response to a possible containment issue can be implemented in a timely manner.

An assessment of seal integrity may require the various interactions of hydro-thermal-mechanical-chemical processes to be modelled (section 7.2.2). Consequently, large volumes of data may be created, and it would be beneficial to utilise techniques specifically designed for extracting actionable insights from complex datasets. A decision and data analytics framework for maximising the value and reliability of CO_2 storage monitoring has been developed (Tadjer et al., 2021). In this study, a focused 4D seismic VOI assessment for the Utsira saline aquifer, machine learning techniques were used to estimate the VOI and determine the optimal time to stop CO_2 injections into the reservoir based on information from seismic surveys.

Another example, in this instance from the geothermal sector, is the comparison of the VOI from deploying single-component DAS to sparsely spaced two-component geophones (Jreij et al., 2020). The primary objective of this study was the statistical comparison of spatial models (fault location in this example) using machine learning methods (convolution neural networks). It was concluded that DAS was a slightly preferable monitoring technology for locating fault positions in 2D for this specific application. However, DAS may only sometimes be preferable to sparse geophones (Jreij et al., 2020). A similar approach for evaluating different monitoring technologies could be adapted for seal integrity monitoring.

10.1.7 Linking Seal Integrity Monitoring and Modelling

Unlike petroleum projects, where it is less common practice to undertake a detailed seal evaluation, GCS projects must demonstrate the nature of the trapping/sealing mechanisms and, consequently, seal integrity. This can result in increased resource and data gathering in the early stages of the GCS appraisal/development lifecycle to ensure that fit-for-phase geomechanical models are developed to support internal decision-making and the relevant regulatory requirements.

As outlined in section 9, the modelling effort can take various forms, ranging from simple 1D MEMs to coupled 3D models that consider hydraulic, mechanical, thermal, and geochemical behaviour as appropriate. However, once CO_2 injection commences, monitoring data is a critical input in conforming or reducing the range of uncertainty associated with the developed suite of models.

Gorgon CCS illustrates how multiple monitoring technologies have been deployed to help characterise the link between CO_2 injection, pressure distribution and geomechanical changes so that risks can be actively managed. Downhole pressure and temperature monitoring, 4D seismic, InSAR surface deformation monitoring, injection profile surveys, VSPs, saturation logging and passive micro-seismic monitoring arrays help to calibrate not only the dynamic modelling but also the geomechanical models (Haynes et al., 2023).

Ultimately, if there has not been a clear event or series of events that indicate that the seal integrity has been breached in a GCS project (which should have been identified through the monitoring programme), conformed models assist in providing confidence that the seal is working and that the site can be closed. One particularly beneficial aspect of this is in jurisdictions where there is an opportunity to utilise performance-based criteria for site closure (rather than pre-defined time-based site closure criteria). This could result in the earlier transfer of the site liability from the operator to the resource owner without reducing the veracity of regulatory processes.

10.1.8 Summary

As stated at the outset of this section, there is no “silver bullet” for seal integrity monitoring, and any monitoring plan should be risk-based, site-specific and adaptive. Regulators and project proponents should avoid assuming that because a technology was used in one project, it should be used in another. If the monitoring technology selection criteria are value-based (as opposed to mandated), then value of information (VOI) analysis is a technique that should be considered.

Aside from well-established in-well monitoring technologies such as downhole pressure and temperature gauges, which are valuable for seal integrity monitoring, various other technologies and applications exist. This section discussed the more recent developments in seal integrity monitoring technologies in detail.

Fibre optics monitoring is one example of this, and has a broad range of applications relevant to seal integrity through either DAS, DTS or DSS interrogation. Fibre optics offers several advantages, including spatially distributed data acquisition and longevity. DAS and DTS have been deployed as part of monitoring programs at large-scale GCS projects, though DSS has only been deployed to date at pilot sites.

This section presented more novel applications of active seismic monitoring (e.g., overburden time shifts in 4D seismic head waves) and passive seismic monitoring (e.g., for CO_2 leakage and micro-seismicity detection), alongside examples of how these approaches have been applied to GCS projects to illustrate these concepts.

Surface deformation monitoring (e.g. tiltmeters and InSAR) does not directly measure changes in the storage complex seal(s). However, it enables the storage complex plus overburden to be monitored, and therefore, changes related to seal(s) integrity may be inferred from this data. Examples of both InSAR and tiltmeter deployment for GCS projects were provided in this section, alongside the opportunity to combine surface deformation monitoring technologies with distributed strain monitoring of the overburden to offer valuable inputs to help calibrate hydraulic-mechanical models for GCS.

11. International Regulatory Frameworks – CO_2 Seals

Regulations for the geological storage of CO_2 have been developed and implemented across several nations over the last decade (Europe, Australia, and in North America). Successful deployment of GCS on a global scale hinges on establishing comprehensive and effective regulatory regimes. Regulatory frameworks addressing GCS worldwide are multifaceted and reflective of the multitude of domains across which GCS intersects. Understanding the diversity of regulatory approaches across different regions is imperative.

There is some variability across jurisdictions regarding the definition of a reservoir seal, and what is required of a seal from a regulatory perspective. Table 13 summarises the definition of a reservoir seal, the regulatory requirements for a seal, and the corresponding jurisdiction.

Table 13: A summary of the regulatory status for reservoir seal definition

	Regulatory Status		Regulatory Clarity Regarding Seal Integrity
Jurisdiction	**Legislation/ Regulations**	**Guidance Documents**	
European Union*			
United States (Onshore)*			
United States (Offshore)			
Australia (Offshore)*			
Canada (Onshore)*			
Brazil (Offshore)			
Malaysia (Country-wide)			
Malaysia (State of Sarawak)			
Indonesia			
Thailand			

* Detailed discussion provided in this report

In-place

Under development/development required

Awaiting framework

Jurisdiction	Comment
European Union*	Legislative and regulatory framework in place specifically for CCS – Directive 2009/31/EC on the Geological Storage of Carbon Dioxide

United States (Onshore)*	Safe Drinking Water Act and UIC Program Class VI Rule
United States (Offshore)	The Infrastructure Investment and Jobs Act/Bipartisan Infrastructure Law introduced, development of rules/regulations underway
Australia (Offshore)*	OPGSS Act 2006 and OPGSS (Greenhouse Gas Injection and Storage) Regulations 2011
Canada (Onshore)*	Directive 065 CO_2 – Resources Applications for Oil and Gas Reservoirs and Directive 051 – Injection and Disposal Wells
Brazil (Offshore)	Bill 1425/2022 proposed a regulatory framework for CCS activities in Brazil, approved by Senate in August 2023, awaiting approval by the House of Representatives (Hernandez, 2023)
Malaysia (Country-wide)	CCS-Specific legislation currently under development
Malaysia (State of Sarawak)	CCS-Specific regulatory framework in place – The Land Code, Land (Carbon Storage) Rules, 2022
Indonesia	CCS-Specific regulatory framework in place – Regulation on the Implementation of CCS (Carbon Capture and Storage) and CCUS (Carbon Capture, Utilization and Storage) in Upstream Oil and Gas Business Activities** (Ashurst, 2023)
Thailand	CCS Specific legislation currently under development

** Currently only available in Indonesian

The following section will examine key legislative frameworks that regulate GCS activities, focusing on policy and regulatory measures related to reservoir seals and the permanency of CO_2 storage. The following frameworks will be examined:

1. European Union: Directive 2009/31/EC on the Geological Storage of Carbon Dioxide (European Parliament, 2009)
2. Australia: Australian Offshore Petroleum and Greenhouse Gas Storage Act 2006 (Australian Government, 2006)
3. United States: Class VI Wells Used for Geological Sequestration of CO_2
4. Canada: CO_2 sequestration schemes

11.1 GCS Legislative Framework – Europe

11.1.1 Background to the Legislation

Directive 2009/31/EC on the geological storage of CO_2 (CCS Directive) was established to provide nations within the EU with a legal framework for the safe and permanent geological storage of CO_2 (European Commission, 2017). The CCS Directive establishes comprehensive criteria for all elements of the CCS project

life cycle, including the selection of sites for CO_2 storage, composition of the CO_2 stream, operation, monitoring obligations, and site closure and post-closure obligations. The CCS Directive was introduced in 2009 and was required to be transposed into national law by June 2011. As of 2017, EU Member States have successfully implemented the CCS Directive (European Commission, 2017).

The overall aim of the CCS Directive is to establish a legal framework for 'the environmentally safe storage of CO_2 to contribute to the fight against climate change' (European Parliament, 2009). The CCS Directive is organised into eight chapters, three of which are relevant to reservoir seals and permanent CO_2 storage:

1. Selection of Sites and Exploration Permits (Chapter 2)
2. Storage Permits (Chapter 3)
3. Operation, Closure and Post-Closure Obligations (Chapter 4)

The requirements to fulfil the obligations outlined in the Directive are provided in Annex I (Criteria for the Characterisation and Assessment of the Potential Storage Complex and Surrounding Area Referred to in Article 4(3)) and Annex II (Criteria for Establishing and Updating the Monitoring Plan Referred to in Article 13(2) and for Post-Closure Monitoring). It is noted in the Directive that these Annexes are intended to be general and should be able to be amended.

To support EU nations in implementing the CCS Directive, the European Commission published four guidance documents in 2011. Guidance Document 1 (CO_2 Storage Life Cycle Risk Management Framework) and Guidance Document 2 (Characterisation of the Storage Complex, CO_2 Stream Composition, Monitoring and Corrective Measures) are most applicable in reservoir seals and permanent CO_2 storage. It is important to note that these guidance documents are not legislation but instead intended to support the coherent implementation of the CCS Directive across EU Nations (European Commission, 2011).

External Consultants have been engaged by the European Commission to collect opinions and feedback for a technical revision of the four 'Guidance Documents' (European Commission, 2024). The aim is to align them with the current global advancements in GCS and address any uncertainties noted during the initial implementation of GCS deployments in the European Economic Area (EEA). The Consultants are expected to provide a final report with recommendations for additional guidance in mid-2024 (European Commission, 2022).

11.1.2 Legislative Framework Related to Reservoir Seals and Permanent Storage – CCS Directive

Several articles within the CCS Directive relate to seal integrity via reference to the 'storage complex'. The 'storage complex' is defined as 'the storage site and surrounding geological domain which can affect overall storage integrity and security; that is, secondary containment (European Parliament, 2009). Table 14 outlines sections within the CCS Directive that refer to topics related to reservoir seals and permanent storage. Annex 1 of the CCS Directive provides specific criteria for characterising and assessing a storage complex, which is carried out in three steps, according to best practices. Each of these steps refers specifically to the caprock.

Table 14: Sections within the CCS Directive relevant to reservoir seals and permanent CO_2 storage

Chapter 2: Selection of Sites and Exploration Permits	
Article 4	Selection of Storage Site
Chapter 3: Storage Permits	
Article 7	Applications for Storage Permits
Article 9	Contents of a Storage Permit
Chapter 4: Operation, Closure and Post-Closure Obligations	
Article 12	CO_2 stream acceptance criteria and procedure
Article 13	Monitoring
Article 15	Inspections
Article 17	Closure and post-closure obligations
Article 18	Transfer of responsibility

Table 15: Factors listed in Annex 1 that relate to Caprock

Step 1: Data collection	
Sufficient data shall be accumulated to construct a volumetric and three-dimensional static (3D)-earth model for the storage site and storage complex, including the caprock and the surrounding area, including the hydraulically connected areas.	
Step 2: Building the three-dimensional static geological earth model	
Using the data collected in Step 1, a three-dimensional static geological earth model, or a set of such models, of the candidate storage complex, including the caprock and the hydraulically connected areas and fluids shall be built using computer reservoir simulators. The static geological earth model(s) shall characterise the complex in terms of:	
(b)	Geomechanical, geochemical and flow properties of the reservoir overburden (caprock, seals, porous and permeable horizons) and surrounding formations;
Step 3: Characterisation of the storage dynamic behaviour, sensitivity characterisation, risk assessment	
The characterisations and assessment shall be based on dynamic modelling, comprising a variety of time-step simulations of CO_2 injection into the storage site using the three-dimensional static geological earth model(s) in the computerised storage complex simulator constructed under Step 2.	
(l)	The risk of fracturing the storage formation(s) and caprock;
(m)	The risk of CO_2 entry into the caprock;

11.2 Implementation of Legislative Framework – CCS Directive Guidance Document 1 and 2

Guidance Document 1 and 2 provide a framework for stakeholders to implement the CCS Directive. Guidance Document 1 outlines the central principles of the GCS life cycle, including project phases, main activities, major regulatory milestones, and risk assessment (European Commission, 2011). Guidance Document 2 develops the concepts from the first Guidance Document into the specific requirements at each phase of the GCS project (refer Figure 88).

Figure 88: GCS Life cycle phases listed in Guidance Document 1

11.2.1 Guidance Document 1 (GD1)

Reservoir seals are a fundamental component of GCS regulations because they are essential in containing and securing injected CO_2, preventing leakage, and ensuring permanent storage of CO_2. Reservoir seals (caprocks) are covered extensively in GD1, across three key topics – CO_2 storage in depleted oil and gas fields, geological leakage pathways and site characterisation and storage capacity assessment.

The importance of risking caprock integrity is highlighted under CO_2 storage in depleted oil and gas fields. The geological accumulation of oil or gas in a depleted field should not be interpreted as a guaranteed containment, particularly when considering caprock integrity related to CO_2. The guidance document emphasises that caprock integrity needs to be addressed in the risk assessment.

Caprocks are an integral part of understanding geological leakage pathways. The guidelines highlight several potential geological leakage pathways from a geological store site due to caprock failure. These potential pathways are summarised in Table 16.

Table 16: Potential geological leakage pathways from geological storage sites via caprock. Modified after Table 4 in GD1 (European Commission, 2011)

Potential leakage pathway/mechanism	Comments
Through the pore system in low permeability caprocks if the capillary entry pressure is exceeded or the CO_2 is in solution.	The fracturing of the caprock induced by injection.
	Relevant to all storage trap types.
If the caprock is locally absent (includes injection features, pipes and erosion).	Largely a function of caprock distribution and thickness, including facies change or erosion. Requires mapping using seismic and well data.
	Relevant to all storage trap types.
Through a degraded caprock because of CO_2/water/rock reactions.	Depends on site-specific geochemistry and potential reactions between caprock, CO_2 and water phases.
	Largely site specific but possible in all trap types.

The fracturing of the caprock induced by injection.	Depends on the fracture gradient in caprock and pressure build-up in the storage reservoir.
	Relevant to all storage trap types.

Site characterisation and storage capacity assessment will likely require acquiring new data. While conducting exploration and appraisal activities, such data collection may include retrieving drill core, logs, and cuttings samples. This is done to effectively characterise both the reservoir and the seal. It is important to evaluate and sample multiple sealing units for suitability. Additionally, site characterisation efforts may involve the utilisation of seismic surveys, which can be instrumental in delineating both the spatial extent of the caprock and the nature of faulting within the region.

11.2.2 Guidance Document 2 (GD2)

Characterisation of the reservoir seal (caprock) and monitoring of seal integrity over a project's life are key elements of GD2. The following summarises the caprock considerations, as noted in GD2, at each GCS project phase.

Phase 1: Assessment

Site Selection

- Structurally trapping saline aquifers can be advantageous sites for CO_2 storage. Depending on the trap geometry, building a tall vertical column of stored CO_2 may be possible, resulting in large buoyancy forces acting on the caprock. This could challenge the capillary and structural integrity of the seal. GD2 notes that this could challenge the capillary and structural integrity of the seal. However, as referenced in sections 3 and 4 of this report, there are many factors that influence the effectiveness of a seal.

Migration-assisted storage (MAS) relies on large migration distance (tens of kilometres) to trap CO_2 physically and chemically before reaching any potential leakage points. When implementing this storage strategy, the large migration distances introduce the potential for unexpected heterogeneities in the caprock, which could result in potential leakage points. This statement in GD2 does not consider the utility of composite seals as outlined in section 2.1.1. of this report, and further discussed by Bump et al. (2023) and Saadatpoor et al. (2010).

Phase 2: Characterisation

CO_2 Stream

- Geochemical investigation of the potential interactions of the CO_2 stream and caprock will be required.

Static Modelling

- Step 2 in Annex 1 of the CCS Directive involves building a static model of the potential storage complex. The inputs to the static model must include the geomechanical, geochemical, and flow properties of the caprock, seals, porous and permeable horizons, and the surrounding formations.

Dynamic Modelling

- Step 3 in Annex 1 of the CCS Directive involves characterising the dynamic behaviour of the storage complex. The dynamic model should provide insight into (among other aspects): the risk of fracturing the storage formation(s) and caprock, and the risk of CO_2 entry into the caprock.

Phase 4: Operations

Monitoring

- The primary method for monitoring the caprock performance listed in GD2 is by monitoring the formation pressure to ensure it does exceed the fracture pressure of the caprock.

Corrective Measures

- Caprock absence or caprock failure are the two primary ways in which seal rocks can contribute to a loss of containment. There are various items listed in GD2 that pertain to caprock-related failure:
    - Limited CO_2 injection rates to reduce pressure build-up and subsequent caprock-related issues (such as capillary failure)
    - Reduce reservoir pressure by extracting CO_2 or water from the storage reservoir complex.
    - Use hydrofracturing to steer the CO_2 in a favourable direction by creating pathways to access new compartments of the storage reservoir away from leakage areas. Expanding the storage container will decrease the overall pressure.
    - Injecting low-permeability materials (foam or grout) to limit leakage pathways. The effectiveness of this approach is uncertain.

11.2.3 Implementation of the CCS Directive in the UK

The UK has established a comprehensive framework to regulate GCS activities by introducing the Storage of Carbon Dioxide (Licensing, etc.) Regulations 2010 (Instruments, 2010). The regulations are designed to implement the CCS Directive by establishing a framework for the licensing and regulating activities related to the storage of CO_2 in geological formations. Key provisions of these regulations include:

- A licence to explore the licensed area for a storage formation.
- A storage permit that includes a plan of how the license holder intends to inject and monitor the CO_2.
- The planned corrective measures should a significant irregularity or a leakage be detected.
- The post-closure obligations at the end of the injection period.

The United Kingdom Government recently announced plans to introduce a new ‘Energy Security Bill’ to Parliament (UK Parliament, 2022). The Bill will create a new piece of energy legislation that contains several measures, including those related to carbon capture and storage (United Kingdom Government, 2022). Part 2 of the draft Bill refers to ‘Carbon Dioxide Capture, Storage Etc and Hydrogen Production’ and pertains to the capture, transport and storage of CO_2, decommissioning of Carbon Storage Installations and Carbon Dioxide Storage Licences (UK Parliament, 2022). The Bill is in the final stages of passage through Parliament (as of October 2023).

11.2.4 Implementation of the CCS Directive in Norway

The CCS Directive was implemented into Norwegian law in 2014 via the Storage Regulations (Directorate, 2015). Additional chapters were also added to the Pollution Regulations and the Petroleum Regulations.

11.3 GCS Legislative Framework – Australia

11.3.1 Background to the Legislation

The Offshore Petroleum and Greenhouse Gas Storage (OPGSS) Act 2006 provides the legal framework for CO_2 storage projects in Australian Commonwealth waters, with associated regulations and guidelines supporting the implementation of the Act.

11.3.2 Legislative Framework Related to Reservoir Seals and Permanent CO_2 Storage – OPGGS Act

GCS projects in Australian Federal jurisdiction are subject to a regulatory framework that outlines the permitting requirements, including environmental, safety, and technical standards. Three of these permits (Figure 89) specifically cover reservoir seals and permanent storage: Greenhouse Gas (GHG) Assessment Permit, Declaration of Identified GHG Storage Formation and GHG Injection Licence. To date, guidelines only exist for the GHG Assessment Permit and Declaration of Storage Formation.

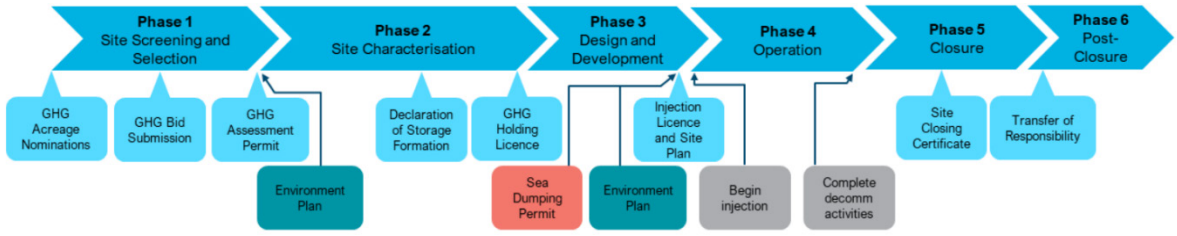

Figure 89: Summary of GCS project life cycle and key regulatory steps under Australian Federal Legislation.

11.3.3 Definitions in the OPGGS Act

Seals are crucial in defining geological formations according to the OPGGS Act. They are considered an integral component of the geological formation, serving as the attribute or mechanism responsible for facilitating the long-term storage of greenhouse gas substances, including CO_2. The presence of an effective seal is among the six *fundamental suitability determinants* used to assess the suitability of a geological formation for eligible greenhouse gas storage.

11.3.4 Implementation of Legislative Framework – Offshore Petroleum and Greenhouse Gas Storage (Greenhouse Gas Injection and Storage) Regulations 2011

The OPGGS GHG Injection and Storage regulations serve the function of regulating activities related to the injection and storage of GHG substances offshore in Australian Commonwealth waters. These regulations establish the legal framework for managing, monitoring and long-term storage of GHG substances. They provide the requirements for obtaining permits, conducting assessments, and ensuring safe and responsible storage of GHG substances in the subsurface.

11.3.5 Greenhouse Gas Assessment Permit

The OPGGS Act requires a GHG Assessment Permit to explore for a potential GHG storage or injection site. GHG Assessment permits are granted via a competitive bidding process. A GHG assessment permit is

granted to the application that presents the most compelling work strategy and program. The work program should effectively enhance understanding of the fundamental suitability determinants of potential GHG storage formations and injection sites. There are six fundamental suitability determinants listed in Table 17.

Table 17: Fundamental Suitability Determinants (Department of Industry, Science and Resources)

Fundamental suitability determinants of the eligible GHG storage formation	
a)	The amount of GHG substance that it is suitable to store
b)	The particular GHG substance that it is suitable to store
c)	The proposed injection point or points
d)	The proposed injection period
e)	Any proposed engineering enhancements
f)	The effective **sealing** feature, attribute, mechanism, or geotechnical characteristics that make it suitable

The work strategy should establish a clear connection between the technical assessment of the release area and the proposed work program throughout the duration of the permit. The aim of the work strategy is to describe how each element of the work program will be used to investigate the fundamental suitability determinants to mature potential storage formations of the area. As the effective sealing feature is one of the six fundamental suitability determinants, describing potential seals in the area will be essential for the GHG Assessment Permit application. Importantly, an eligible GHG storage formation must be capable of permanently storing at least 100,000 tonnes of a GHG substance.

11.3.6 Declaration of Identified GHG Storage Formation

The OPGGS Act states that if a permit holder suspects on reasonable grounds that there may be an eligible Storage Formation location in their Title Area, they must apply for a Declaration of Identified Greenhouse Gas Storage Formation (DoSF). The term Title Area applies to a GHG Assessment Permit, a Petroleum Retention Lease, or a Petroleum Production Licence. NOTE: In the case of the Petroleum Retention Lease/Production Licence, the Storage Formation must be wholly located within the existing Title, and the CO_2 plume cannot migrate beyond the title boundary.

An application for a DoSF must provide sufficient information on all six fundamental suitability determinants (Table 17), including a description of the effective sealing features that make the storage formation suitable for permanent GHG storage. Specifically, the DoSF must provide adequate information to establish that the confining zones within the storage formation serve as a reliable and robust seal. The description of the geology for the storage formation must, at a minimum, include (Department of Industry, 2021):

- A detailed analysis of the stratigraphy, structure, rock types and depositional model of the reservoir and seal rocks
- Identification of any faults in either reservoir or seal rocks
- The porosity and permeability of reservoir and seal rocks
- Reactivity of rock types within the proposed GHG storage substance in both the reservoir and seal rocks.

Additionally, a description of the spatial boundaries of the functional sealing mechanism within the three-dimensional scope of the storage formation must also be included.

11.3.7 GHG Injection Licence

The OPGGS Act allows a permit holder to apply for a GHG injection licence to commence injecting and storing a GHG substance into the Declared GHG Storage Formation. Exploration, injection, and storage must be wholly within the Title Area.

The primary objective of a GHG injection licence application is to ensure that GHG injection and storage is undertaken in a way that ensures safe and secure storage of a GHG substance. The description of how this will be achieved is presented in a Site Plan. There is no specific mention of seals within the Site Plan; however, the Site Plan must explain how the permit holder intends to monitor the containment and long-term storage of the GHG substance in the subsurface.

11.4 GCS Legislative Framework – United States

11.4.1 Background to the Legislation

In the United States, CCS activities are regulated differently based on whether they occur offshore or onshore. Executive Order (EO) 14008, issued by the United States President, called for an all-government initiative to reduce the impacts of climate change (BOEM, 2023). To support the EO, the Infrastructure Investment and Jobs Act (renamed The Bipartisan Infrastructure Law or BIL) was introduced in 2021. The BIL is an extensive Act that includes provisions to allow CO_2 sequestration on the United States Outer Continental Shelf (OCS), and sets out a one-year timeframe to promulgate associated regulations (BOEM, 2023). There are four areas across the OCS that will be considered for CCS – Atlantic, Gulf of Mexico, Pacific and Atlantic. The Bureau of Ocean Energy Management (BOEM) and Bureau of Safety and Environmental Enforcement (BSEE) are currently developing rules/regulations for CO_2 sequestration on the OCS (as of August 2022) (BOEM, 2022).

Onshore, CCS legislation in the United States was introduced in 2021 with the Storing CO_2 and Lowering Emissions (SCALE) Act (US Congress, 2023). The Act seeks to facilitate the expansion of essential CO_2 transportation and storage infrastructure. Its goal is to encourage the deployment of carbon capture, utilisation, and storage (CCUS) technologies alongside initiatives for carbon dioxide removal (International Energy Agency, 2022).

The regulation of CCS projects (construction, operation, permitting and closure of injection wells) onshore in the United States is regulated by the Environmental Protection Agency (EPA). The EPA is authorised by the Safe Drinking Water Act (SDWA) to develop requirements and provisions for the Underground Injection Control (UIC) Program (United States Environmental Protection Agency, 2023a). Under this program, there are six classes of injection wells. Class VI wells are those used for the injection of CO_2 into underground subsurface rock formations for long-term storage or geologic storage (United States Environmental Protection Agency, 2023a)Class VI focuses on protecting underground drinking water sources. In addition to these regulations, several other federal, state, and local requirements govern the implementation of CCS projects.

11.4.2 Legislative Framework Related to Reservoir Seals and Permanent CO_2 Storage – Safe Drinking Water Act and UIC Program

The Safe Drinking Water Act was enacted to safeguard drinking water quality within the United States. This legislation concerns all water sources, whether they are currently used for drinking purposes or have the potential to be used for drinking, whether they originate from surface or subsurface locations (United States

Environmental Protection Agency, 2023b). The SDWA establishes requirements and provisions for the UIC program with the primary aim of protecting public health by preventing injection wells of any kind from contaminating underground sources of drinking water (United States Environmental Protection Agency, 1974).

11.4.3 Implementation of Legislative Framework - Class VI Wells Used for Geological Sequestration of CO_2

Definitions in the Class XI Requirements

In the Class IV guidance documents, the seal or cap rock is called the confining zone. The confining zone refers to a geological formation, group of formations, or part of a formation stratigraphically overlying and underlying the injection zone(s).

The Class VI Rule

The Class VI Rule, established in accordance with the Safe Drinking Water Act, it delineates federal guidelines governing the permitting, siting, construction, operation, monitoring, and site closure of Class VI injection wells. These wells are used for the purpose of injecting CO_2 for geological sequestration. During the course of a Class VI project, regulatory authorities bear the responsibility of ensuring that:

- Class VI wells are constructed in such a way that ensures underground sources of drinking water are protected.
- Class VI wells operate as planned and comply with regulations, as verified by testing and monitoring.
- Post-injection monitoring is conducted until it is demonstrated that there is no risk of deleterious interactions with underground sources of drinking water.

The information required to obtain a Class VI permit is presented in Table 18.

Table 18: UIC Class IV Project Overview

Federal Class VI Rule	Description of Requirements	Corresponding Technical Guidance Document
Class VI permit information	Requirements establish the information that owners or operators must submit to obtain a Class VI permit	
Minimum criteria for siting	Establishes that Class VI wells must be located in areas with a suitable geologic system, including an injection zone that can receive the total anticipated volume of carbon dioxide and confining zone(s) to contain the injected carbon dioxide stream and displaced formation fluids	UIC Program Class VI Well Site Characterisation Guidance

Area of Review (AoR)* and corrective actions	Provisions require the use of computational modelling to delineate the AoR for proposed Class VI wells and the preparation of, and compliance with, an AoR and Corrective Action Plan for delineating the AoR, performing all necessary corrective action, and periodically re-evaluating the AoR and amending the plan if needed	UIC Program Class VI Well Area of Review Evaluation and Corrective Action Guidance
Financial responsibility	Requirements establish that owners or operators must demonstrate and maintain financial responsibility for performing corrective action on improperly abandoned wells in the AoR, injection well plugging, post-injection site care (PISC) and site closure activities, and emergency and remedial response	UIC Program Class VI Financial Responsibility Guidance
Injection well construction	Requirements specify the design and construction of Class VI wells using materials that are compatible with the carbon dioxide stream over the duration of the Class VI project to prevent the endangerment of USDWs	UIC Program Class VI Well Construction Guidance
Pre-Operational Testing	Outline activities, including logs, surveys, and tests of the injection well and formations that must be performed before the injection of carbon dioxide may commence	UIC Program Class VI Well Project Plan Development Guidance
Injection well operating	Requirements provide operational measures for Class VI wells to ensure that the injection of carbon dioxide does not endanger USDWs, along with limitations on injection pressure and requirements for automatic shut-off devices	UIC Program Class VI Well Project Plan Development Guidance
Mechanical integrity	Requirements specify continuous monitoring to demonstrate internal mechanical integrity and annual external mechanical integrity tests	UIC Program Class VI Well Project Plan Development Guidance
Testing and monitoring	Requirements define the elements that must be included in the required Testing and Monitoring Plan submitted with a Class VI permit application and implemented throughout the project to demonstrate the safe operation of the injection well and track the position of the carbon dioxide plume and pressure front	UIC Program Class VI Well Testing and Monitoring Guidance

Reporting	Requirements establish the periodic timeframes and circumstances for the electronic reporting of Class VI well testing, monitoring, and operating results and requirements for keeping records	UIC Program Class VI Well Recordkeeping, Reporting, and Data Management Guidance
Injection well plugging	Requirements specify that a Class VI injection well must be properly plugged to ensure that the well does not become a conduit for fluid movement into USDWs in the future	UIC Program Class VI Well Plugging, Post-Injection Site Care, and Site Closure Guidance
Post-injection site care (PISC) and site closure	Requirements address activities that occur following cessation of injection. The owner or operator must continue to monitor the site for 50 years following the cessation of injection or for an approved alternative timeframe until it can be demonstrated that no additional monitoring is needed to ensure that the project does not pose an endangerment to USDWs, following this, they must plug the injection and monitoring wells and close the site	UIC Program Class VI Well Plugging, Post-Injection Site Care, and Site Closure Guidance
Emergency and remedial response	Requirements specify that owners or operators of Class VI wells must develop and maintain an approved Emergency and Remedial Response Plan that describes the actions to be taken to address events that may cause endangerment to a USDW or other resources	
Class VI injection depth waiver	Requirements provide a process under which Class VI well owners or operators can seek a waiver from the injection depth requirements in order to inject carbon dioxide into non- USDWs that are located above or between USDWs. Including injection depth waiver provisions in a state's regulation is optional	

** The AoR and corrective action provisions outlined in the Class VI Rule aim to guarantee that areas potentially affected by a proposed geologic storage operation are clearly defined, ensuring all necessary corrective actions are taken for wells, and maintaining ongoing updates throughout the injection project. Specific details of these requirements are covered in Geological Sequestration of Carbon Dioxide: Underground Injection Control (UIC) Program Class IV Well Area of Review Evaluation and Corrective Action Guidance (2013)*

There are 5 phases to a Class VI project (Figure 90), comprising a review and evaluation stage before a permit is issued or authorisation is granted. Guidance relating to the Class VI requirements is organised into nine documents. The guidance documents that refer directly to reservoir seals and permanent CO_2 storage is *UIC Program Class VI Well Site Characterisation Guidance*.

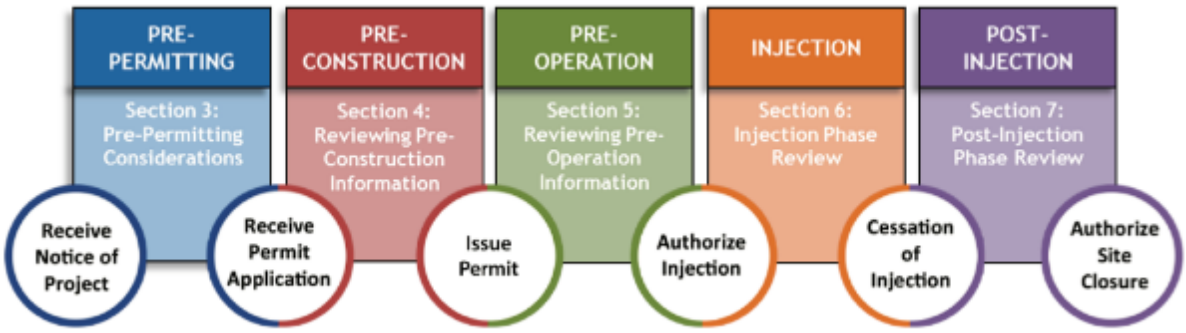

Figure 90: Lifecycle of a Class VI project with key regulatory steps and permits (United States Environmental Protection Agency, 2018)

UIC Program Class IV Well Site Characterisation Guidance

Demonstration of confining zone integrity

According to the guidance document, the confining zone refers to a geological formation, group of formations, or part of a formation stratigraphically overlying and underlying the injection zone(s) that is intended to contain the CO_2. This zone must not allow the migration of CO_2, whether through connected pore pathways across the seal or via faults or fractures within the confining zone. The guidance documents provide specific details of the primary controls of intact seals in a geological sequestration setting:

- *Capillary pressure*: Good seals will have capillary entry pressures between approximately 6 and 40 MPa. It is recommended that project operators verify the capillary entry pressure is greater than the expected pressure from buoyancy-driven accumulation of CO_2.
- *Permeability*: If the permeability of the seal layer is low, it can still make an effective seal even if the capillary entry pressure is exceeded.

In the case of CO_2 injection into depleted oil and gas reservoirs, re-establishing pressure can create issues related to the integrity of the cap rock. The maximum sustainable pore pressure may, therefore, be lower than the original reservoir pressure.

Another important consideration presented in the guidelines is the impact of any potential changes to the mineralogy of the cap rock. The guidelines note that operators should consider the impact of injection activities resulting in precipitation or dissolution of minerals at the interface with the cap rock, which may diminish or improve sealing capabilities.

Lower confining zone

The Class VI requirements also include a discussion of the characterisation of the lower confining zones. The method for evaluation of the lower confining zone is the same as that of the upper confining zone. This method includes estimates of the thickness, permeability, fracture pressure, capillary pressure, and zones of interbedded units of higher permeability.

11.5 GCS Legislative Framework – Canada

11.5.1 Background to the Legislation

In the province of Alberta, Canada, CCS projects are referred to as CO_2 sequestration schemes (Alberta Energy Regulator, 2023b). A CO_2 sequestration scheme involves the permanent storage of CO_2 in an approved storage formation, termed 'dedicated storage' (Alberta Energy Regulator, 2023b). To develop a CCS project, an operator must secure carbon sequestration tenure or agreement from the Government of Alberta.

11.5.2 Legislative Framework Related to Reservoir Seals and Permanent CO_2 Storage

Several acts govern the legal framework for CO_2 storage projects in Alberta. The following overview is provided specifically for reservoir seals and serves as a high-level summary. A comprehensive review of the entire geological storage project is necessary to understand the scope and implications under the relevant legislation fully.

Some of the Acts that provide the legal framework for CO_2 storage projects in Alberta include:

The Mines and Minerals Act – Legislation stipulates that the Crown owns the pore space and, in the context of CO_2 sequestration, bears responsibility for long-term liability (Alberta Energy Regulator, 2023b).

Carbon Sequestration Tenure Regulation – These regulations enable the Alberta Government to grant evaluation permits, agreements, and leases for carbon sequestration within the province of Alberta (Alberta Energy Regulator, 2023b)

The Oil and Gas Conservation Act (OGCA) – Under this Act, the AER is authorised to grant approval for CO_2 projects provided the injection of CO_2 does not interfere with the production or preservation of hydrocarbons, or any pre-existing underground storage of hydrocarbons (Alberta Energy Regulator, 2023b)

Public Lands Act, Surface Rights Act - Surface rights for CO_2 sequestration, CO_2 EOR and other storage projects are administered in a manner consistent with the standard practices for hydrocarbon projects within the province of Alberta. Regulation is carried out in accordance with the Public Lands Act, Surface Rights Act, and the OGCA (Alberta Energy Regulator, 2023b)

11.5.3 Implementation of Legislative Framework - Directive 065: Resources Applications for Oil and Gas Reservoirs

The requirements for CO_2 projects (schemes) across their life cycle are regulated by several directives that set out the requirements or processes that operators must comply with. The directive most applicable to Reservoir Seals and Permanent CO_2 Storage is Directive 065: Resources Application for Oil and Gas Reservoirs (Alberta Energy Regulator, 2023a). Under this directive, there are two types of CO_2 storage projects – CO_2 EOR and Storage or CO_2 sequestration (Figure 91).

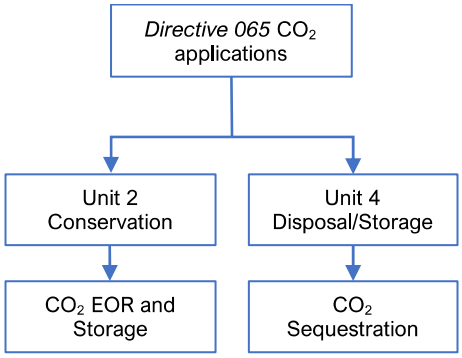

Figure 91: Subsurface requirements for CO_2 schemes (Alberta Energy Regulator, 2023a)

Several other directives are also relevant to CO_2 sequestration:

- *Directive 051* - Injection and Disposal Wells – Well Classifications, Completions, Logging, and Testing Requirements
- *Directive 056* - Energy Development Applications and Schedules
- *Directive 071* - Emergency Preparedness and Response Requirements for the Petroleum Industry
- *Directive 087* - Well Integrity Management

11.5.4 Unit 4 Disposal/Storage

Disposal pertains to the process of injecting fluids into underground formations with objectives distinct from enhanced oil recovery or gas storage (Alberta Energy Regulator, 2023a). According to Directive 051, there are three classes of disposal wells:

- Class IV Wells – used to inject potable water or steam.
- Class III Wells – used to inject hydrocarbons, inert gases, or other gases for EOR or CO_2 sequestration.
- Class II Wells – used to inject or dispose of produced water or brine-equivalent fluids.

Class III wells used for CO_2 sequestration must meet all the requirements of directive 051 before fluid injection begins. Directive 051 does not contain any specific requirements related to reservoir seals and permanent CO_2 storage.

Applications for a CO_2 sequestration scheme (project) under Directive 065 specifically cover reservoir seals and permanent storage under general requirements and containment requirements.

In the general requirements, a description of the 'confinement strata' must be included.

Containment requirements include discussing the geological setting of the proposed disposal zone, base and caprock. Additional requirements for Class III disposal included information on bounding formations, including: (Alberta Energy Regulator, 2023a)

- Continuity and thickness of base and caprock.
- Lithology.
- Integrity of the base and caprock.

- Explanation of containment assurance if fracturing is evident.
- A comment on the stratigraphic, structural or combination reservoir trap type and its containment features.

11.6 International Standards

In jurisdictions where legislative frameworks for geological storage have not been established, ISO standard 27914: *Carbon dioxide capture, transportation and geological storage — Geological storage* may provide a technical framework for geological storage projects. The purpose of ISO 27914 is to establish requirements and recommendations for the geological storage of CO_2 streams, aiming to facilitate safe and long-term containment of carbon dioxide while minimising risks to the environmental, natural resource, and health (International Standard Organisation, 2017) These standards can be applied both onshore and offshore and encompass activities from site screening to site closure. Regulatory permitting and approvals are critical throughout the project lifecycle. However, the ISO standards do not provide a framework for permitting and approvals (International Standard Organisation, 2017). IEAGHG has conducted a comprehensive review of applying ISO standards to geological storage projects (IEAGHG/DNV, 2022)

Seals are primarily addressed in the site characterisation section of the ISO standard document. In this section (5.4.3.1) five requirements are described in order to adequately characterise the primary seal, which are listed in Table 19.

Table 19: Summary of requirements for the detailed characterisation of a primary seal (IEAGHG/British Geological Survey, 2019)

	Primary Seal Characterisation
a.	Determination of the stratigraphy, lithology, thickness, and lateral continuity of the primary seal based on available data
b.	Evaluation of primary seal integrity, including porosity and permeability, and testing where possible, and assessment of seal mineralogy to determine the suitability for containment of the CO_2 stream
c.	Identification of potential leakage pathways, such as fractures, faults and wells, and their potential to transmit fluids, which can require risk management and further monitoring during the operational stages of the project
d.	Estimation of the capillary entry (displacement) pressure for CO_2
e.	Evaluation of the pressure distribution in the porous and permeable unit immediately overlying the primary seal* above the storage unit and below the secondary seal**

**The primary seal (caprock) is defined as the continuous geological unit above a storage unit that effectively restricts the migration of fluids out of the storage unit and leakage out of the storage complex*

***The secondary seal is defined as geological unit that effectively restricts migration of fluids in the sedimentary succession between the primary seal and protected groundwater, protected resources, or the seabed*

11.7 Summary

Robust legislative frameworks for reservoir seals and permanent CO_2 storage are evident in many jurisdictions, spanning regions including the European Union, Australia, the United States, and Canada. Moreover, several nations are currently in the process of developing regulatory frameworks for CCS, with a likely common focus on detailed requirements for seals and CO_2 storage permanence.

Despite the varied and intricate nature of CCS regulations across these jurisdictions, all jurisdictions include a robust legislative framework to govern reservoir seals and permanent CO_2 storage. These standards ensure the effectiveness and security of CCS deployments by highlighting the importance of seal integrity and

storage permanence. Additionally, the legislation acknowledges the necessity for adaptability, encouraging updates to regulatory requirements as technological advancements emerge. Therefore, CCS project proponents must stay up-to-date on the latest legislative and regulatory developments within their jurisdiction to guarantee legislative compliance.

12. Overview and Conclusions

Seals for the Geological Storage of CO_2

The definition of seal potential, which includes the elements of seal capacity, geometry, and integrity, has been outlined. Marine shale, mudstone and evaporites are the most common seal types for either operational GCS projects or GCS projects in the mature planning phases. Data on seals are sparse for CO_2 storage in depleted hydrocarbon reservoirs (as data from the hydrocarbon-bearing unit was generally not the primary objective) or saline formations (which typically represent less appraised formations). Additional data from unconventional reservoir characterisation of shale/mudrocks can be leveraged to reduce gaps in knowledge on how various lithologies respond to changes in pressure and stress.

Further details on seal integrity, which is the primary focus of this report, are provided, building on previous research. Excluding the risk of CO_2 leakage associated with well integrity, which is not addressed in this review, several primary geomechanical-related leakage mechanisms were identified. These include tensile failure through the caprock, shear failure at the caprock/storage unit interface or due to fault reactivation, and rock deformation. In some cases, deformation within the storage complex may translate to surface uplift and may impact facilities or the public perception of GCS.

Alternatives to the more "conventional" seals for the geological sequestration of CO_2, such as composite seals (e.g., Gulf of Mexico), as well as GCS concepts and projects that rely primarily on other trapping mechanisms (i.e., residual or mineral trapping) have also been presented.

The long-term impact of CO_2 on different formations, especially the rate of migration and reactivity of CO_2 with seal formations, is discussed. Given the geological uncertainties and complex dynamic processes within a CO_2 storage site spanning thousands of years, accurately predicting the exact impact (e.g., geochemical alteration) of the interaction of CO_2 with the seals of storage systems in this unlikely event is challenging and unnecessary. However, it is important to develop logic and fact-based arguments constrained by theory and experiments that demonstrate the expectation of containment. This logic should consider how a seal may alter from various CO_2 processes, including fluid-rock interactions at the reservoir-seal interface or fracture-seal interface for dry and wet CO_2, wet CO_2 diffusion into the top seal, and other processes such as CO_2 intercalation in clays.

CO_2-related alteration is restricted because CO_2 entry into a seal rock is limited to the very slow processes of CO_2 diffusion or progressive chemical alteration at the reservoir-seal interface. Chemical reactions can result in the dissolution and precipitation of minerals depending on the availability of cations and evolving chemical conditions. However, in seals, the speed of the reactions is strongly dependent on the flow of the CO_2 and acidified formation waters, which is severely hampered by the very low permeability. The geochemical process can be advantageous (e.g., re-precipitation) and disadvantageous to containment (e.g., dissolution).

Risk Assessment

The various risk mechanisms and assessment methodologies for assessing CO_2 containment are outlined with qualitative (i.e., ISO standard and risk bow-tie) and quantitative risk assessment techniques. Examples of applying qualitative methods for GCS (e.g., the Northern Lights project and Peterhead Goldeneye project) have been identified. For the quantitative techniques, a worked example of the RISQUE method and a detailed overview of the NRAP-Open-IAM tool, which has been applied to the Quest project, have been provided.

Further, the strategy to mitigate seal integrity risk through active or passive pressure management is discussed. Examples of this strategy are presented at the commercial (i.e., Gorgon CCS) and demonstration scale (US DoE-sponsored BEST program) and conceptually in the modelling domain.

Methods to Evaluate Seal Integrity

In addition to risk mitigation through pressure management, increased risk definition and reduction can be achieved through additional data gathering to inform reservoir characterisation, subsequent reservoir modelling, base monitoring plans and any logic associated with contingent monitoring or corrective actions.

First, insights into recent developments in laboratory or log-based analysis techniques are presented. This includes different methods for calculating the brittleness index, imaging techniques, log-based characterisation of top seal and faults, and a recent example of FMI's role in GCS caprock/seal assessment.

Subsequently, the fundamentals of creating and coupling a hydraulic-geomechanical model for GCS are outlined. Thematic examples of large-scale modelling for various aspects are presented, including the impact of extending the model in a vertical sense (to include the storage complex or storage complex and overburden), the effect of different approaches for hydraulic-geomechanical coupling, tensile and shear stress failure modelling using continuum and discontinuum methods (and links to micro-seismicity); CO_2 injection optimisation for managing geomechanical risk; and coupled hydraulic-mechanical-chemical modelling for seal integrity.

CO_2 migration along faults and fractures has been identified in the literature as a risk mechanism. Therefore, the different approaches to modelling CO_2 migration along or near a fault have been discussed. This includes a literature review of the most recent advancements in this domain, including the research performed as part of the DETECT project and advanced gridding and numerical solver techniques. Further, given the lack of real-world data to compare the different fault/fracture modelling techniques, a summary of recent and upcoming control releases of CO_2 experiments is provided.

MMV is a key component in assessing containment for GCS. Therefore, the different available methods for monitoring or inferring seal integrity in large-scale or pilot CO_2 storage systems have been reviewed. Key case studies to support the efficacy and applicability of these technologies have been provided alongside some fundamental principles for assessing the value of different monitoring technologies.

International Regulatory Frameworks – CO_2 Seals

Regulatory frameworks have been developed to ensure the safe and effective deployment of GCS, including regulations for the long-term monitoring and maintenance of CO_2 storage sites.

The regulatory frameworks from four of the most mature jurisdictions for GCS have been summarised, specifically the EU directive (2009/31/EC), the Australian Federal OPGGS Act, the Safe Drinking Water Act and UIC Program for onshore USA, and the various Acts that provide the legal framework for CO_2 storage projects in Alberta. The requirements for storage complex seals have been outlined for each jurisdiction. From a legislative perspective, fully understanding and evaluating the seal is as important as understanding the storage formation. The connection between the seal and the storage formation is critical to all legislation and regulations related to this topic. It is, therefore, essential to pay close and equal attention to the seal and storage formation when applying for permits to ensure they comply with regulatory components.

In conclusion, this comprehensive seal integrity review provides a detailed, updated exploration of the critical aspects of seal potential in the context of GCS projects. The report highlights the importance of seals in ensuring the containment of CO_2 and the challenges in predicting the long-term impact of CO_2 interactions with seal formations, considering geological uncertainties and complex dynamic processes over extended timescales. The guidance provided underscores the need for site-specific evaluations to determine effective seals, providing risk assessment methodologies, strategies for mitigating risks related to seal integrity and methods to evaluate seal integrity, including laboratory techniques, geomechanical modelling, and monitoring technologies. The review concludes by condensing various international regulatory frameworks to ensure the implementation of GCS technologies safely and effectively.

13. Recommendations for Future Studies

The following is a non-exhaustive list of recommendations for future studies on the topic of seal integrity:

1. More laboratory studies are required for various seal types. For example, more studies should assess the sealing properties of multiple minerals, including dolomite, anhydrite, siderite, and halite.
2. Though the permeability of seals is the limiting factor, more knowledge of geochemical reaction kinetics and how they relate to changes in flow properties, as well as the geomechanical properties of seals, still needs to be obtained. An improved understanding of top seal behaviour can be achieved through laboratory studies, modelling, and analysis of natural analogues. To conduct these studies, obtaining high-quality samples of seals is essential for investigating the chemical and geomechanical properties. A set of recommendations/guidelines for preserving the core from potential sealing units would be valuable to ensure that opportunities are noticed.
3. There are numerous proposed methods for modelling CO_2 migration through faults, but more experimental data is needed to underpin or support one method over another. Several CO_2-controlled release experiments have been discussed in this report, noting that "scale-up" challenges remain when attempting to transfer the learnings to commercial-scale GCS projects. A "post-mortem" of what was learned from these experiments should be undertaken when these experiments are completed. This review should also attempt to collate any key insights from other projects that seek to address scale-up challenges for fault leakage (e.g. the DETECT project).
4. Future studies should focus on creating a framework of the "fit-for-purpose" approaches for undertaking hydraulic-mechanical-thermal (HMT) simulations at the various stages of assessment for regional or site-specific GCS. This framework should include the key model framing decisions that need to be made (e.g. vertical and lateral extent, coupling method, etc). Further, a limited number of hydraulic-mechanical-chemical (HMC) modelling case studies in the public domain also pertain to assessing cap rock integrity. Future work should focus on developing guiding principles for when the interaction of geochemical and geomechanical effects needs to be considered for GCS, which would benefit both technical professionals and regulators.
5. The reality should be reinforced that we expect successful containment in GCS by undertaking effective site characterisation. A comparison between the extensive risk assessment frameworks proposed for GCS and those currently required in the oil and gas industry would be valuable. There is a danger that higher standards will be set for "proving" containment in GCS than have been established in the oil and gas industry without due cause.
6. Outside of dedicated research groups and those at the forefront of the industry, most of the discussion for GCS focuses on CO_2 containment under an aquitard. As highlighted in the report, the containment requirements for GCS differ from those for petroleum. In petroleum, a seal is considered effective if it retains large, mobile hydrocarbon accumulations over geological timeframes. This is fundamentally different from the objectives of GCS. Future engagements with the public, regulators and other stakeholders should attempt to shift this mindset, promoting the use of composite seals and other trapping mechanisms so that the size of the opportunity for emissions abatement is communicated effectively.

References

Akono, A.-T., Druhan, J., Dávila Ordoñez, M., Tsotsis, T., Jessen, K., Fuchs, S., Crandall, D., Shi, Z., Dalton, L., Tkach, M., Goodman, A., Frailey, S., & Werth, C. (2019). A review of geochemical–mechanical impacts in geological carbon storage reservoirs. *Greenhouse Gases: Science and Technology*, *9*. https://doi.org/10.1002/ghg.1870

Directive 065: Resources Applications for Oil and Gas Reservoirs, (2023a). https://static.aer.ca/prd/documents/directives/Directive065.pdf

Alberta Energy Regulator. (2023b). *Directives*. https://www.aer.ca/regulating-development/rules-and-directives/directives

Alcalde, J., Flude, S., Wilkinson, M., Johnson, G., Edlmann, K., Bond, C. E., Scott, V., Gilfillan, S. M. V., Ogaya, X., & Haszeldine, R. S. (2018). Estimating geological CO2 storage security to deliver on climate mitigation. *Nature Communications*, *9*(1), 1-13. https://EconPapers.repec.org/RePEc:nat:natcom:v:9:y:2018:i:1:d:10.1038_s41467-018-04423-1

Alsayah, A., & Rigby, S. P. (2023). Coupled multiphase flow, geochemical, and geomechanical modelling of the impact of shale interlayers on CO2 migration. *Geoenergy Science and Engineering*, *229*, 212101. https://doi.org/https://doi.org/10.1016/j.geoen.2023.212101

Andersen, O., & Nilsen, H. M. (2018). Investigating simplified modeling choices for numerical simulation of CO2 storage with thermal effects. *International Journal of Greenhouse Gas Control*, *72*, 49-64.

Angelov, P., Spetzler, J., & Wapenaar, K. (2004). Pore pressure and water saturation variations; Modification of Landrø's AVO approach. In *SEG Technical Program Expanded Abstracts 2004* (pp. 2279-2282). Society of Exploration Geophysicists.

Anyosa, S., Bunting, S., Eidsvik, J., Romdhane, A., & Bergmo, P. (2021). Assessing the value of seismic monitoring of CO2 storage using simulations and statistical analysis. *International Journal of Greenhouse Gas Control*, *105*, 103219. https://doi.org/https://doi.org/10.1016/j.ijggc.2020.103219

Aplin, A. C., & Macquaker, J. H. (2011). Mudstone diversity: Origin and implications for source, seal, and reservoir properties in petroleum systems. *AAPG Bulletin*, *95*(12), 2031-2059.

Aplin, A. C., & Moore, J. K. (2016). Observations of pore systems of natural siliciclastic mudstones.

Arts, R., Eiken, O., Chadwick, A., Zweigel, P., van der Meer, L., & Zinszner, B. (2004). Monitoring of CO2 injected at Sleipner using time-lapse seismic data. *Energy*, *29*(9), 1383-1392. https://doi.org/https://doi.org/10.1016/j.energy.2004.03.072

Offshore Petroleum and Greenhouse Gas Storage Act 2006, (2006).

Aylmore, L. A. G., & Quirk, J. P. (1960). Domain or Turbostratic Structure of Clays. *Nature*, *187*(4742), 1046-1048. https://doi.org/10.1038/1871046a0

Bakke, S., & Øren, P.-E. (1997). 3-D pore-scale modelling of sandstones and flow simulations in the pore networks. *SPE Journal*, *2*(02), 136-149.

Barnhoorn, A. S., B.P; Chandra, D. (2022). *Rheology data overview for study sites*. https://www.sharp-storage-act.eu/publications--results/

Bastías Espejo, J. M., Wilkins, A., Rau, G. C., & Blum, P. (2021). RHEA v1.0: Enabling fully coupled simulations with hydro-geomechanical heterogeneity. *Geosci. Model Dev.*, *14*(10), 6257-6272. https://doi.org/10.5194/gmd-14-6257-2021

Becker, M., Ciervo, C., Cole, M., Coleman, T., & Mondanos, M. (2017). Fracture Hydromechanical Response Measured by Fiber Optic Distributed Acoustic Sensing at milliHertz Frequencies: Fracture Hydromechanics from DAS. *Geophysical Research Letters*, *44*. https://doi.org/10.1002/2017GL073931

Bense, V., & Person, M. (2006). Faults as conduit-barrier systems to fluid flow in siliciclastic sedimentary aquifers. *Water Resources Research*, *42*(5).

Benson, S. (2007). Addressing long-term liability of carbon dioxide capture and geological sequestration. In. World Resource Institute (WRI) Long-term liability Workshop.

Benson, S. P., R.; Reynolds, C.; Krevor, S.;. (2013). RELATIVE PERMEABILITY ANALYSES TO DESCRIBE

MULTI-PHASE FLOW IN CO2 STORAGE RESERVOIRS.

Berryman, J. (1995). Single-scattering approximations for coefficients in Biot equations of poroelasticity. *The Journal of the Acoustical Society of America*, *91*. https://doi.org/10.1121/1.402518

Berryman, J. G. (1992). Single-scattering approximations for coefficients in Biot's equations of poroelasticity. *The Journal of the Acoustical Society of America*, *91*(2), 551-571.

Birkholzer, J. T., Cihan, A., & Zhou, Q. (2012). Impact-driven pressure management via targeted brine extraction Conceptual studies of CO2 storage in saline formations. *7*. https://doi.org/10.1016/j.ijggc.2012.01.001

Journal Name: International Journal of Greenhouse Gas Control; Journal Volume: 7; Related Information: Journal Publication Date: 2012
Bjorlykke, K., & Avseth, P. (2010). Explorational rock physics–the link between geological processes and geophysical observables. *Petroleum Geoscience: From Sedimentary Environments to Rock Physics*, 403-426.
Bjørnarå, T. I., Haines, E. M., & Skurtveit, E. (2021). Upscaled geocellular flow model of potential across-and along-fault leakage using shale gouge ratio. TCCS–11. CO2 Capture, Transport and Storage. Trondheim 22nd–23rd June 2021. Short Papers from the 11th International Trondheim CCS Conference,
Bjørnarå, T. I., Skurtveit, E., Michie, E. A., & Smith, S. A. (2023). Characterising along-and across-fault fluid flow properties for assessing flow rates and overburden fluid migration along faults-A case study from the North Sea. *Petroleum Geoscience*, petgeo2023-2033.
Blanco-Martín, L., Jahangir, E., Rinaldi, A. P., & Rutqvist, J. (2022). Evaluation of possible reactivation of undetected faults during CO2 injection. *International Journal of Greenhouse Gas Control*, *121*, 103794. https://doi.org/https://doi.org/10.1016/j.ijggc.2022.103794
Blunt, M. J., Bijeljic, B., Dong, H., Gharbi, O., Iglauer, S., Mostaghimi, P., Paluszny, A., & Pentland, C. (2013). Pore-scale imaging and modelling. *Advances in Water resources*, *51*, 197-216.
Boehm, N., Van Buchem, F., & Finkbeiner, T. (2023). Characterising regional evaporite seal for hydrocarbon and CO2 storage—Upper Jurassic, Arab-Hith formations, Saudi Arabia. 84th EAGE Annual Conference & Exhibition,
Boggs, S. (2009). *Petrology of sedimentary rocks*. Cambridge university press.
Bohloli, B., Bjørnarå, T. I., Park, J., & Rucci, A. (2018). Can we use surface uplift data for reservoir performance monitoring? A case study from In Salah, Algeria. *International Journal of Greenhouse Gas Control*, *76*, 200-207. https://doi.org/https://doi.org/10.1016/j.ijggc.2018.06.024
Bóna, A., Dean, T., Correa, J., Pevzner, R., Tertyshnikov, K., & Zaanen, L. (2017). *Amplitude and Phase Response of DAS Receivers*. https://doi.org/10.3997/2214-4609.201701200
Bond, C., Wightman, R., & Ringrose, P. (2013). The influence of fracture anisotropy on CO2 flow. *Geophysical Research Letters*, *40*, 1284-1289. https://doi.org/10.1002/grl.50313
Bonto, M., Welch, M., Lüthje, M., Andersen, S., Veshareh, M., Amour, F., Afrough, A., Mokhtari, R., Hajiabadi, M., & Alizadeh, M. (2021). Challenges and enablers for large-scale CO2 storage in chalk formations. *Earth-Science Reviews*, *222*, 103826.
Bowden, A., Pershke, D., & Chalaturnyk, R. (2013). Geosphere risk assessment conducted for the IEAGHG Weyburn-Midale CO2 Monitoring and Storage Project. *International Journal of Greenhouse Gas Control*, *16*, S276–S290. https://doi.org/10.1016/j.ijggc.2013.02.014
Bowden, A. R., Lane, M.R., Martin, J.H. (2011). *Triple Bottom Line Risk Management – Enhancing Profit, Environmental Performance and Community Benefit*. Wiley and Sons, New York.
Bowden, A. R., & Rigg, A. (2004). Assessing risk in CO2 storage projects. *APPEA Journal*, *44*, 677-702. https://doi.org/10.1071/AJ03034
BP. (2022). *Endurance Storage Development Plan (Key Knowledge Document)* (NS051-SS-REP-000-00010). https://www.gov.uk/government/publications/carbon-capture-usage-and-storage-ccus-innovation-nepnzt-key-knowledge-deliverables
Braathen, A., Tveranger, J., Fossen, H., Skar, T., Cardozo, N., Semshaug, S., Bastesen, E., & Sverdrup, E. (2009). Fault facies and its application to sandstone reservoirs. *AAPG Bulletin*, *93*(7), 891-917.
Bretan, P., Yielding, G., Mathiassen, O. M., & Thorsnes, T. (2011). Fault-seal analysis for CO2 storage: An example from the Troll area. *Norwegian Continental Shelf. Pet. Geoscience*, *18*, 33-42.
Brown, C., Lackey, G., Schwartz, B., Dean, M., Dilmore, R., Blanke, H., O'Brien, S., Rowe, C. (2022). Integrating Qualitative and Quantitative Risk Assessment Methods for Carbon Storage: A Case Study for the Quest Carbon Capture and Storage Facility. 16th Greenhouse Gas Control Technologies Conference, Lyon.
Bump, A. P., Bakhshian, S., Ni, H., Hovorka, S. D., Olariu, M. I., Dunlap, D., Hosseini, S. A., & Meckel, T. A. (2023). Composite confining systems: Rethinking geologic seals for permanent CO2 sequestration. *International Journal of Greenhouse Gas Control*, *126*, 103908. https://doi.org/https://doi.org/10.1016/j.ijggc.2023.103908
Busch, A., Alles, S., Gensterblum, Y., Prinz, D., Dewhurst, D. N., Raven, M. D., Stanjek, H., & Krooss, B. M. (2008). Carbon dioxide storage potential of shales. *International Journal of Greenhouse Gas Control*, *2*(3), 297-308.
Busch, A., Amann, A., Bertier, P., Waschbusch, M., & Krooss, B. M. (2010). The significance of caprock sealing integrity for CO2 storage. SPE International Conference on CO2 Capture, Storage, and Utilization,
Busch, A., B. M. Krooss, T. Kempka, M. Waschbusch, T. Fernandez-Steeger, and R. Schluter. (2009). Carbon dioxide storage in abandoned coal mines. In J. C. P. M. Grobe, and R. L. Dodge (Ed.), *Carbon dioxide sequestration in geological media—State of the science* (Vol. AAPG Studies in Geology 59, pp. 643–653). https://doi.org/DOI:10.1306/13171267St593400

Busch, A., Kampman, N., Hangx, S., Snippe, J., Bickle, M., Bertier, P., Chapman, H., Spiers, C., Pijnenburg, R., & Samuelson, J. (2014). The Green River natural analogue as a field laboratory to study the long-term fate of CO2 in the subsurface. *Energy Procedia*, *63*, 2821-2830.
Buscheck, T. A., Bielicki, J. M., White, J. A., Sun, Y., Hao, Y., Bourcier, W. L., Carroll, S. A., & Aines, R. D. (2017). Managing Geologic CO2 Storage with Pre-injection Brine Production in Tandem Reservoirs. *Energy Procedia*, *114*, 4757-4764. https://doi.org/https://doi.org/10.1016/j.egypro.2017.03.1826
Buscheck, T. A., Sun, Y., Chen, M., Hao, Y., Wolery, T. J., Bourcier, W. L., Court, B., Celia, M. A., Julio Friedmann, S., & Aines, R. D. (2012). Active CO2 reservoir management for carbon storage: Analysis of operational strategies to relieve pressure buildup and improve injectivity. *International Journal of Greenhouse Gas Control*, *6*, 230-245. https://doi.org/https://doi.org/10.1016/j.ijggc.2011.11.007
Campos, R., Barrios, I., & Lillo, J. (2015). Experimental CO2 injection: Study of physical changes in sandstone porous media using Hg porosimetry and 3D pore network models. *Energy Reports*, *1*, 71-79.
Carbfix. *Proven*. Retrieved 26 September from https://www.carbfix.com/proven
Castagna, J., Batzle, M., & Eastwood, R. (1985). Relationship between compressional and shear-wave velocities in classic silicate rocks. *Geophysics*, *50*, 571-581. https://doi.org/10.1190/1.1441933
Chang, K. W., Minkoff, S., & Bryant, S. (2008). *Modeling Leakage Through Faults of CO2 Stored in an Aquifer*. https://doi.org/10.2118/115929-MS
Chang, K. W., Yoon, H., & Martinez, M. J. (2022). Potential Seismicity Along Basement Faults Induced by Geological Carbon Sequestration. *Geophysical Research Letters*, *49*(13). https://doi.org/https://doi.org/10.1029/2022GL098721
Chen, G., Matteucci, G., Fahmy, B., & Finn, C. (2008). Spectral-decomposition response to reservoir fluids from a deepwater West Africa reservoir. *Geophysics*, *73*(6), C23-C30.
Chen, S., & Doolen, G. D. (1998). Lattice Boltzmann method for fluid flows. *Annual review of fluid mechanics*, *30*(1), 329-364.
Chen, T., & Huang, L. (2020). Optimal design of microseismic monitoring network: Synthetic study for the Kimberlina CO2 storage demonstration site. *International Journal of Greenhouse Gas Control*, *95*, 102981. https://doi.org/https://doi.org/10.1016/j.ijggc.2020.102981
Chevron. (2018). *Gorgon Project: Carbon Dioxide Injection System Pipeline and Wells Operations Environment Management Plan: Summary*.
Childs, C., Manzocchi, T., Walsh, J. J., Bonson, C. G., Nicol, A., & Schöpfer, M. P. (2009). A geometric model of fault zone and fault rock thickness variations. *Journal of Structural Geology*, *31*(2), 117-127.
Childs, C. J., Manzocchi, T., Walsh, J. J., & Schopfer, M. P. J. (2012). Fault Core/damage Zone; an Unhelpful Description of Fault Zone Structure? https://doi.org/https://doi.org/10.3997/2214-4609.20143012
Choi, J. C., Skurtveit, E., Huynh, K. D., & Grande, L. (2023). Uncertainty of stress path in fault stability assessment during CO2 injection: Comparing smeaheia 3D geomechanics model with analytical approaches. *International Journal of Greenhouse Gas Control*, *125*, 103881.
Comanici, A. M., & Barsanescu, P. D. (2018). Modification of Mohr's criterion in order to consider the effect of the intermediate principal stress. *International Journal of Plasticity*, *108*, 40-54. https://doi.org/https://doi.org/10.1016/j.ijplas.2018.04.010
Comisky, J., Santiago, M., McCollom, B., Buddhala, A., & Newsham, K. (2011). Sample Size Effects on the Application of Mercury Injection Capillary Pressure for Determining the Storage Capacity of Tight Gas and Oil Shales. *CSUG/SPE*, *3*. https://doi.org/10.2118/149432-MS
Cook, P. (2014). *Geologically storing carbon: Learning from the Otway Project experience*. CSIRO publishing.
Correa, J., Pevzner,R., Bona,A., Tertyshnikov, K., Freifeld,B., Robertson,M., Daley,T. (2019). 3D vertical seismic profile acquired with distributed acoustic sensing on tubing installation: A case study from the CO2CRC Otway Project. *Interpretation*, *7*(1). https://doi.org/https://doi.org/10.1190/INT-2018-0086.1
Cosenza, P., Ghoreychi, M., Bazargan-Sabet, B., & De Marsily, G. (1999). In situ rock salt permeability measurement for long term safety assessment of storage. *International Journal of Rock Mechanics and Mining Sciences*, *36*(4), 509-526.
Daley, T. M., & Cox, D. (2001). Orbital vibrator seismic source for simultaneous P-and S-wave crosswell acquisition. *Geophysics*, *66*(5), 1471-1480.
Dando, B. D. E., Goertz-Allmann, B. P., Kühn, D., Langet, N., Dichiarante, A. M., & Oye, V. (2021). Relocating microseismicity from downhole monitoring of the Decatur CCS site using a modified double-difference algorithm. *Geophysical Journal International*, *227*(2), 1094-1122. https://doi.org/10.1093/gji/ggab255
Daniel, R., & Kaldi, J. (2009). Evaluating Seal Capacity of Cap Rocks and Intraformational Barriers for CO2 Containment. *AAPG Stud. Geol.*, *59*, 335-345.
Daniel, R., & Kaldi, J. (2012). *Atlas of Australian and New Zealand Hydrocarbon Seals: Worldwide Analogs for Cap Rocks and Intraformational Barriers in Clastic Depositional Settings, AAPG Studies in Geology 60* (Vol. 60). AAPG.

Dávila, G., Luquot, L., Soler, J. M., & Cama, J. (2016). Interaction between a fractured marl caprock and CO2-rich sulfate solution under supercritical CO2 conditions. *International Journal of Greenhouse Gas Control*, *48*, 105-119.
Davis, T. L., Landrø, M., & Wilson, M. (2019). *Geophysics and geosequestration*. Cambridge University Press.
Dean, M., Snippe, J., Busch, A., Fink, R., Hursyt, S., Lidstone, A., Claes, H., Forbes Inskip, N., Rizzo, R., Phillips, T., Doster, F., Geiger, S., March, R., Kubeyev, A., Kampman, N. and Bisdom, K. (2020). *Final report of the DETECT project.*
Offshore Greenhouse Gas Guideline for Declaration of Identified Greenhouse Gas Storage Formation (2021). https://www.nopta.gov.au/_documents/guidelines/GHG-Guideline-Declaration-of-Storage-Formation.pdf
Regulations relating to exploitation of subsea reservoirs on the continental shelf for storage of CO_2 and relating to transportation of CO_2 on the continental shelf, (2015). https://www.npd.no/en/regulations/regulations/exploitation-of-subsea-reservoirs-on-the-continental-shelf-for-storage-of-and-transportation-of-co/
Dockrill, B., & Shipton, Z. K. (2010). Structural controls on leakage from a natural CO2 geologic storage site: Central Utah, U.S.A. *Journal of Structural Geology*, *32*(11), 1768-1782. https://doi.org/https://doi.org/10.1016/j.jsg.2010.01.007
Dodds, K., Waston, M., & Wright, I. (2011). Evaluation of risk assessment methodologies using the In Salah CO2 storage project as a case history. *Energy Procedia*, *4*, 4162-4169. https://doi.org/https://doi.org/10.1016/j.egypro.2011.02.361
Dolson, J., He, Z., & Horn, B. W. (2018). Advances and perspectives on stratigraphic trap exploration-making the subtle trap obvious. *Search and Discovery*, *60054*.
dos Santos Maia Correa, J. (2018). *Distributed acoustic sensing for seismic imaging and reservoir monitoring applied to CO2 geosequestration* Curtin University].
Dou, S., Ajo-Franklin, J., Daley, T., Robertson, M., Wood, T., Freifeld, B., Pevzner, R., Correa, J., Tertyshnikov, K., & Urosevic, M. (2016). Surface orbital vibrator (SOV) and fiber-optic DAS: Field demonstration of economical, continuous-land seismic time-lapse monitoring from the Australian CO2CRC Otway site. SEG International Exposition and Annual Meeting,
Duxbury, A., White, D., Samson, C., Hall, S., Wookey, J., & Kendall, J. M. (2012). Fracture mapping using seismic amplitude variation with offset and azimuth analysis at the Weyburn CO2 storage site. *Geophysics*, *77*, 295-B306. https://doi.org/10.1190/geo2011-0075.1
Ekechukwu, G. K., & Sharma, J. (2021). Well-scale demonstration of distributed pressure sensing using fiber-optic DAS and DTS. *Scientific Reports*, *11*(1), 12505. https://doi.org/10.1038/s41598-021-91916-7
Ennis-King, J., LaForce, T., Paterson, L., Dance, T., Jenkins, C., & Cinar, Y. (2017). Interpretation of Above Zone and Storage Zone Pressure Responses to Carbon Dioxide Injection in the 2016 CO2CRC Field Test. *Energy Procedia*, *114*, 5671-5679. https://doi.org/https://doi.org/10.1016/j.egypro.2017.03.1706
Ennis-King, J., & Paterson, L. (2007). Coupling of geochemical reactions and convective mixing in the long-term geological storage of carbon dioxide. *International Journal of Greenhouse Gas Control*, *1*(1), 86-93.
Erickson, K. P., Lempp, C., & Pöllmann, H. (2015). Geochemical and geomechanical effects of scCO 2 and associated impurities on physical and petrophysical properties of Permotriassic Sandstones (Germany): an experimental approach. *Environmental earth sciences*, *74*, 4719-4743.
Espinoza, D. N., & Santamarina, J. C. (2012). Clay interaction with liquid and supercritical CO2: The relevance of electrical and capillary forces. *International Journal of Greenhouse Gas Control*, *10*, 351-362. https://doi.org/https://doi.org/10.1016/j.ijggc.2012.06.020
Espinoza, D. N., & Santamarina, J. C. (2017). CO2 breakthrough—Caprock sealing efficiency and integrity for carbon geological storage. *International Journal of Greenhouse Gas Control*, *66*, 218-229. https://doi.org/https://doi.org/10.1016/j.ijggc.2017.09.019
European Commission. (2011). *Implementation of Directive 2009/31/EC on the Geological Storage of Carbon Dioxide Guidance Document 1 CO2 Storage Life Cycle Risk Management Framework*.
European Commission. (2017). *Report from the Commission to the European Parliament and the Council on Implimentation of Directive 2009/31/EC on the Geological storage of Carbon Dioxide*.
European Parliament. (2009). Directive 2009/31/EC of the European Parliament and the Council of 23 April 2009 on the geological storage of carbon dioxide. *Official Journal of the European Union*, 114-135.
Evans, B., Rezaee, M. R., Rasouli, V., Lebedev, M., Saeedi, A., Liu, K., & Iglauer, S. (2014). Predicting CO2 injectivity properties for application at CCS sites.
Evans, D., Kingdon, A., Hough, E., Reynolds, W., & Heitmann, N. (2012). First account of resistivity borehole micro-imaging (FMI) to assess the sedimentology and structure of the Preesall Halite, NW England: Implications for gas storage and wider applications in CCS caprock assessment. *Journal of the Geological Society*, *169*, 587-592. https://doi.org/10.1144/0016-76492011-143
Evgenii Kanin, I. G., Sergei Boronin, Svetlana Zhigulskiy, Artem Penigin,Andrey Afanasyev, Dmitry Garagash, Andrei Osiptsov. (2023). CO2 storage in deep saline aquifers: evaluation of geomechanical risksusing integrated modeling workflow. *Journal of Natural Gas Science and Engineering (Pre-print)*.

Fatah, A., Mahmud, H. B., Bennour, Z., Gholami, R., & Hossain, M. (2022). Geochemical modelling of CO2 interactions with shale: Kinetics of mineral dissolution and precipitation on geological time scales. *Chemical Geology*, *592*, 120742. https://doi.org/https://doi.org/10.1016/j.chemgeo.2022.120742
Fatt, I. (1956). The network model of porous media. *Transactions of the AIME*, *207*(01), 144-181.
Fawad, M., & Mondol, N. H. (2021). Monitoring geological storage of CO2: a new approach. *Scientific Reports*, *11*(1), 5942. https://doi.org/10.1038/s41598-021-85346-8
Fischer, S., Zemke, K., Liebscher, A., Wandrey, M., & Group, C. S. (2011). Petrophysical and petrochemical effects of long-term CO2-exposure experiments on brine-saturated reservoir sandstone. *Energy Procedia*, *4*, 4487-4494.
Gamboa, D., Williams, J. D., Bentham, M., Schofield, D. I., & Mitchell, A. C. (2019). Application of three-dimensional fault stress models for assessment of fault stability for CO2 storage sites. *International Journal of Greenhouse Gas Control*, *90*, 102820.
Gammer, D. T., Owain;. (2018). *Brine Production and its Potential Impact on UK Carbon Dioxide Storage*.
Gao, C., & Gray, K. E. (2022). A coupled geomechanics and reservoir simulator with a staggered grid finite difference method. *Journal of Petroleum Science and Engineering*, *209*, 109818. https://doi.org/https://doi.org/10.1016/j.petrol.2021.109818
Gao, Y. (2013). *Reservoir Characterization of Snøhvit Field, Norwegian Barents Sea*
Gassmann, F. (1951). Uber die elastizitat poroser medien. *Vierteljahrsschrift der Naturforschenden Gesellschaft in Zurich*, *96*, 1-23.
Gaus, I., Audigane, P., André, L., Lions, J., Jacquemet, N., Durst, P., Czernichowski-Lauriol, I., & Azaroual, M. (2008). Geochemical and solute transport modelling for CO2 storage, what to expect from it? *International Journal of Greenhouse Gas Control*, *2*(4), 605-625. https://doi.org/https://doi.org/10.1016/j.ijggc.2008.02.011
GCCSI. (2016). *'Enhanced Water Recovery': Brine Extraction with CO2 Geological Storage as part of CCS*. https://www.globalccsinstitute.com/news-media/insights/enhanced-water-recovery-brine-extraction-with-co2-geological-storage-as-part-of-ccs/
Gemmer, L., Hansen, O., Iding, M., Leary, S., & Ringrose, P. (2012). Geomechanical Response to CO2 Injection at Krechba, InSalah, Algeria. *First Break*, *30*, 79-84. https://doi.org/10.3997/2214-4609.20144113
Gherardi, F., Xu, T., & Pruess, K. (2007). Numerical modeling of self-limiting and self-enhancing caprock alteration induced by CO2 storage in a depleted gas reservoir. *Chemical Geology*, *244*(1-2), 103-129.
Glubokovskikh, S., Shashkin, P., Shapiro, S., Gurevich, B., & Pevzner, R. (2023). Multiwell Fiber Optic Sensing Reveals Effects of CO 2 Flow on Triggered Seismicity. *Seismological Research Letters*, *94*(5), 2215-2230.
Golab, A., Romeyn, R., Averdunk, H., Knackstedt, M., & Senden, T. (2012). 3D characterisation of potential CO2 reservoir and seal rocks. *Australian Journal of Earth Sciences*, *60*, 1-13. https://doi.org/10.1080/08120099.2012.675889
Goldie Divko, L. M. K., M.;. (2019). *New seal capacity measurements from legacy core and cuttings - Onshore Otway Basin, Victoria*.
Gor, G. Y., Elliot, T. R., & Prévost, J. H. (2013). Effects of thermal stresses on caprock integrity during CO2 storage. *International Journal of Greenhouse Gas Control*, *12*, 300-309. https://doi.org/https://doi.org/10.1016/j.ijggc.2012.11.020
Gor, G. Y., & Prévost, J. H. (2013). Effect of CO2 Injection Temperature on Caprock Stability. *Energy Procedia*, *37*, 3727-3732. https://doi.org/https://doi.org/10.1016/j.egypro.2013.06.267
Goudarzi, A., Hosseini, S. a., Sava, D., & Nicot, J.-P. (2017). Simulation and 4D seismic studies of pressure management and CO 2 plume control by means of brine extraction and monitoring at the Devine Test Site, South Texas, USA: Original Research Article: Simulation and 4D seismic studies of pressure management and CO 2 plume control. *Greenhouse Gases: Science and Technology*, *8*. https://doi.org/10.1002/ghg.1731
Government of Western Australia: Department of Mines, I. R. a. S. (2023). *South West Hub Project.* Retrieved March 30 from https://www.dmp.wa.gov.au/South-West-Hub-CCS-1489.aspx
Grande, L., Mondol,N.M., Hopper,J., Roberts,D., Phillips, D. (2022). *Stress Drivers and Outline of Proposed Numerical Modelling Campaign*. https://www.sharp-storage-act.eu/globalassets/bilder/eksterne-prosjektsider/sharp-storage/dv1_1b_wp1_report_v1.pdf
Groot, H. d. (2011). *Quest CCS Project: Containment Risk and Uncertainty Review*.
Grude, S., Landrø, M., & Osdal, B. (2013). Time-lapse pressure–saturation discrimination for CO2 storage at the Snøhvit field. *International Journal of Greenhouse Gas Control*, *19*, 369-378.
Guglielmi, Y., Nussbaum, C., Cappa, F., De Barros, L., Rutqvist, J., & Birkholzer, J. (2021). Field-scale fault reactivation experiments by fluid injection highlight aseismic leakage in caprock analogs: Implications for CO2 sequestration. *International Journal of Greenhouse Gas Control*, *111*, 103471. https://doi.org/https://doi.org/10.1016/j.ijggc.2021.103471

Gundersen, K., Hosseini, S., Oleynik, A., & Alendal, G. (2021). Application of Deep Learning for Characterization of CO2 Leakage Based on Above Zone Monitoring Interval (AZMI) Pressure Data. *SSRN Electronic Journal*. https://doi.org/10.2139/ssrn.3818244

Gunnarsson, I., Aradóttir, E. S., Oelkers, E. H., Clark, D. E., Arnarson, M. Þ., Sigfússon, B., Snæbjörnsdóttir, S. Ó., Matter, J. M., Stute, M., Júlíusson, B. M., & Gíslason, S. R. (2018). The rapid and cost-effective capture and subsurface mineral storage of carbon and sulfur at the CarbFix2 site. *International Journal of Greenhouse Gas Control*, *79*, 117-126. https://doi.org/https://doi.org/10.1016/j.ijggc.2018.08.014

Hamling, J., Klapperich, R., Jiang, T., Yu, X., Williamson, C. (2022). Brine Extraction and Storage Test (Best): Enhancing Co2 Storage through Active Reservoir Management. 16th Greenhouse Gas Control Technologies Conference (GHGT-16), Lyon.

Han, D.-h., Nur, A., & Morgan, D. (1986). Effects of porosity and clay content on wave velocities in sandstones. *Geophysics*, *51*(11), 2093-2107. https://doi.org/10.1190/1.1442062

Hangx, S., Bakker, E., Bertier, P., Nover, G., & Busch, A. (2015). Chemical–mechanical coupling observed for depleted oil reservoirs subjected to long-term CO2-exposure–A case study of the Werkendam natural CO2 analogue field. *Earth and Planetary Science Letters*, *428*, 230-242.

Hangx, S., Pluymakers, A., Ten Hove, A., & Spiers, C. (2014). The effects of lateral variations in rock composition and texture on anhydrite caprock integrity of CO2 storage systems. *International Journal of Rock Mechanics and Mining Sciences*, *69*, 80-92.

Hangx, S., Spiers, C., & Peach, C. (2010). Creep of simulated reservoir sands and coupled chemical-mechanical effects of CO2 injection. *Journal of Geophysical Research: Solid Earth*, *115*(B9).

Hangx, S., van der Linden, A., Marcelis, F., & Bauer, A. (2013). The effect of CO2 on the mechanical properties of the Captain Sandstone: Geological storage of CO2 at the Goldeneye field (UK). *International Journal of Greenhouse Gas Control*, *19*, 609-619.

Hannon Jr, M. J., & Esposito, R. A. (2015). Screening considerations for caprock properties in regards to commercial-scale carbon-sequestration operations. *International Journal of Greenhouse Gas Control*, *32*, 213-223.

Hartog, A. H. (2017). *An introduction to distributed optical fibre sensors*. CRC press.

Harvey, S., O'Brien, S., Minisini, S., Oates, S., & Braim, M. (2021). Quest CCS facility: Microseismic system monitoring and observations. Proceedings of the 15th Greenhouse Gas Control Technologies Conference,

Haynes, A., Jager, K., Maekivi, J., Scoby-Smith, L., & Shawcross, T. (2023). Integration of the comprehensive Gorgon CO2 surveillance program for history matching of the Dupuy reservoir model. *The APPEA Journal*, *63*, S386-S390. https://doi.org/https://doi.org/10.1071/AJ22190

Heath, J. E., Lachmar, T. E., Evans, J. P., Kolesar, P. T., & Williams, A. P. (2009). Hydrogeochemical characterization of leaking, carbon dioxide-charged fault zones in east-central Utah, with implications for geologic carbon storage. *Carbon sequestration and its role in the global carbon cycle*, *183*, 147-158.

Hoffman, N. (2018). Quantifying Intraformational Seal in a Coal-Rich Sedimentary System. 14th Greenhouse Gas Control Technologies Conference Melbourne,

Hornby, B. E., Schwartz, L. M., & Hudson, J. A. (1994). Anisotropic effective-medium modeling of the elastic properties of shales. *Geophysics*, *59*(10), 1570-1583.

Horne, S. A. (2013). A statistical review of mudrock elastic anisotropy. *Geophysical Prospecting*, *61*(4), 817-826. https://doi.org/https://doi.org/10.1111/1365-2478.12036

Hou, L., Yu, Z., Luo, X., & Wu, S. (2022). Self-sealing of caprocks during CO2 geological sequestration. *Energy*, *252*, 124064. https://doi.org/https://doi.org/10.1016/j.energy.2022.124064

Hovorka, S., Meckel, T., Treviño, R., Lu, J., Nicot, J.-P., Choi, J.-W., Freeman, D., Cook, P., Daley, T., Ajo-Franklin, J., Freifeild, B., Doughty, C., Carrigan, C., Brecque, D., Kharaka, Y., Thordsen, J., Phelps, T., Yang, C., Romanak, K., & Butsch, R. (2011). Monitoring a large volume CO2 injection: Year two results from SECARB project at Denbury's Cranfield, Mississippi, USA. In (Vol. 4, pp. 3478-3485). https://doi.org/10.1016/j.egypro.2011.02.274

Hoydalsvik, H., Devaux, F., Zweigel, P., Gittins, C., Tucker, O., Seldon, L., & Neele, F. (2021). CO2 Storage Safety in the North Sea: Implications of the CO2 Storage Directive. Proceedings of the 15th Greenhouse Gas Control Technologies Conference,

Huang*, F., Juhlin, C., Han, L., Kempka, T., Norden, B., Löth, S., & Zhang, F. (2015). Application of seismic complex decomposition on thin layer detection of the CO2 plume at Ketzin, Germany. In *SEG Technical Program Expanded Abstracts 2015* (pp. 5477-5482). Society of Exploration Geophysicists.

Hunt, L. (2024). *CCS Value Written in a Bowtie*.

Hyman, J. D., Karra, S., Makedonska, N., Gable, C. W., Painter, S. L., & Viswanathan, H. S. (2015). dfnWorks: A discrete fracture network framework for modeling subsurface flow and transport. *Computers & Geosciences*, *84*, 10-19. https://doi.org/https://doi.org/10.1016/j.cageo.2015.08.001

IEAGHG. (2020). *Faults and their Significance for Large-Scale CO_2 Storage Workshop* (Technical Report 2020-03).

IEAGHG/British Geological Survey. (2019). *Interactive Design of Monitoring Programmes for the Geological Storage of CO2 (2020-01)*. IEAGHG. Retrieved 7 August from https://ieaghg.org/ccs-resources/monitoring-selection-tool
IEAGHG/DNV. (2022). *Applying ISO Standards to Geologic Storage and EOR Projects* (2022-11).
Iglauer, S., Pentland, C. H., & Busch, A. (2015). CO2 wettability of seal and reservoir rocks and the implications for carbon geo-sequestration. *Water Resources Research*, *51*(1), 729-774. https://doi.org/https://doi.org/10.1002/2014WR015553
Ingram, G. M., & Urai, J. L. (1999). Top-seal leakage through faults and fractures: the role of mudrock properties. *Geological Society, London, Special Publications*, *158*(1), 125-135.
The Storage of Carbon Dioxide (Licensing etc.) Regulations 2010, (2010). https://www.legislation.gov.uk/uksi/2010/2221/contents/made
International Energy Agency. (2022). *SCALE Act (Storing CO2 and Lowering Emissions Act)*. https://www.iea.org/policies/13193-scale-act-storing-co2-and-lowering-emissions-act#
International Standard Organisation. (2017). Carbon dioxide capture, transportation and geological storage - geological storage. In.
International Standard Organisation. (2018). SO 31000:2018 Risk Management - Guidelines. In.
Isaenkov, R., Pevzner, R., Glubokovskikh, S., Yavuz, S., Yurikov, A., Tertyshnikov, K., Gurevich, B., Correa, J., Wood, T., & Freifeld, B. (2021). An automated system for continuous monitoring of CO2 geosequestration using multi-well offset VSP with permanent seismic sources and receivers: Stage 3 of the CO2CRC Otway Project. *International Journal of Greenhouse Gas Control*, *108*, 103317.
Jacquemyn, C., Jackson, M. D., & Hampson, G. J. (2019). Surface-based geological reservoir modelling using grid-free NURBS curves and surfaces. *Mathematical Geosciences*, *51*, 1-28.
Jakobsen, M., Hudson, J. A., Minshull, T. A., & Singh, S. C. (2000). Elastic properties of hydrate-bearing sediments using effective medium theory. *Journal of Geophysical Research*, *105*, 561-577.
Jeanne, P., Rutqvist, J., Dobson, P. F., Walters, M., Hartline, C., & Garcia, J. (2014). The impacts of mechanical stress transfers caused by hydromechanical and thermal processes on fault stability during hydraulic stimulation in a deep geothermal reservoir. *International Journal of Rock Mechanics and Mining Sciences*, *72*, 149-163. https://doi.org/https://doi.org/10.1016/j.ijrmms.2014.09.005
Jenkins, C., Marshall, S., Dance, T., Ennis-King, J., Glubokovskikh, S., Gurevich, B., La Force, T., Paterson, L., Pevzner, R., & Tenthorey, E. (2017). Validating subsurface monitoring as an alternative option to Surface M&V-the CO2CRC's Otway Stage 3 Injection. *Energy Procedia*, *114*, 3374-3384.
Jin, G., & Roy, B. (2017). Hydraulic-fracture geometry characterization using low-frequency DAS signal. *The Leading Edge*, *36*, 975-980. https://doi.org/10.1190/tle36120975.1
Jin, X., Shah, S. N., Roegiers, J.-C., & Zhang, B. (2015). An integrated petrophysics and geomechanics approach for fracability evaluation in shale reservoirs. *SPE Journal*, *20*(03), 518-526.
Johnston, J. E., & Christensen, N. I. (1995). Seismic anisotropy of shales. *Journal of Geophysical Research*, *100*, 5991-6003.
Josh, M., Esteban, L., Delle Piane, C., Sarout, J., Dewhurst, D., & Clennell, M. (2012). Laboratory characterisation of shale properties. *Journal of Petroleum Science and Engineering*, *88*, 107-124.
Jreij, S., Trainor-Guitton, W., Morphew, M., & Lim Chen Ning, I. (2020). The Value of Information From Horizontal Distributed Acoustic Sensing Compared to Multicomponent Geophones Via Machine Learning. *Journal of Energy Resources Technology*, *143*, 1-21. https://doi.org/10.1115/1.4048051
Kaldi, J., Daniel, R., Tenthorey, E., Michael, K., Schacht, U., Nicol, A., Underschultz, J., & Backe, G. (2013). Containment of CO2 in CCS: Role of Caprocks and Faults. *Energy Procedia*, *37*, 5403-5410.
Kaldi, J., Daniel, R., Tenthorey, E., Michael, K., Schacht, U., Nicol, A., Underschultz, J. Backe, G. (2011). *Caprock Systems for Geological Storage of CO2*
Kampman, N., Busch, A., Bertier, P., Snippe, J., Hangx, S., Pipich, V., Di, Z., Rother, G., Harrington, J., & Evans, J. P. (2016). Observational evidence confirms modelling of the long-term integrity of CO2-reservoir caprocks. *Nature Communications*, *7*(1), 12268.
Katahara, K. W. (1996). Clay mineral elastic properties. In *SEG technical program expanded abstracts 1996* (pp. 1691-1694). Society of Exploration Geophysicists.
Keehm, Y., Mukerji, T., & Nur, A. (2004). Permeability prediction from thin sections: 3D reconstruction and Lattice-Boltzmann flow simulation. *Geophysical Research Letters*, *31*(4).
Kempka, T., De Lucia, M., & Kühn, M. (2014). Geomechanical integrity verification and mineral trapping quantification for the Ketzin CO2 storage pilot site by coupled numerical simulations. *Energy Procedia*, *63*, 3330-3338.
Khazaei, C., & Chalaturnyk, R. (2017). A Reservoir–Geomechanical Model to Study the Likelihood of Tensile and Shear Failure in the Caprock of Weyburn CCS Project with Regard to Interpretation of Microseismic Data. *Geotechncial and Geological Engineering*, *35*. https://doi.org/10.1007/s10706-017-0262-4

Khazaei, C., Hazzard, J., & Chalaturnyk, R. (2016). A discrete element model to link the microseismic energies recorded in caprock to geomechanics. *Acta Geotechnica*, *11*(6), 1351-1367. https://doi.org/10.1007/s11440-016-0489-x
Kirkham, C., Cartwright, J., James, D., & Kearney, L. (2022). Episodic venting of extreme subsalt overpressure through a thick evaporitic seal. *Marine and Petroleum Geology*, *142*, 105741. https://doi.org/https://doi.org/10.1016/j.marpetgeo.2022.105741
Kivi, I. R., Pujades, E., Rutqvist, J., & Vilarrasa, V. (2022). Cooling-induced reactivation of distant faults during long-term geothermal energy production in hot sedimentary aquifers. *Sci Rep*, *12*(1), 2065. https://doi.org/10.1038/s41598-022-06067-0
Koperna, G., Oudinot, A., McColpin, G., Liu, N., Heath, J., Wells, A., & Young, G. (2009). CO2-ECBM/storage activities at the San Juan basin's Pump Canyon test site. *SPE Annual Technical Conference and Exhibition*. https://doi.org/10.2118/124002-MS
Krooss, B. M., Leythaeuser, D., Schumacher, D., & Abrams, M. A. (1996). Molecular Diffusion of Light Hydrocarbons in Sedimentary Rocks and Its Role in Migration and Dissipation of Natural Gas. In *Hydrocarbon Migration and Its Near-Surface Expression* (Vol. 66, pp. 0). American Association of Petroleum Geologists. https://doi.org/10.1306/m66606c14
Krushin, J. T. (1997). AAPG Memoir 67: Seals, Traps, and the Petroleum System. Chapter 3: Seal Capacity of Nonsmectite Shale.
Labuz, J. F., & Zang, A. (2012). Mohr–Coulomb failure criterion. *Rock mechanics and rock engineering*, *45*, 975-979.
LaForce, T., Ennis-King, J., & Paterson, L. (2013). Magnitude and Duration of Temperature Changes in Geological Storage of Carbon Dioxide. *Energy Procedia, 37*, 4465-4472.
Landrø, M. (2001). Discrimination between pressure and fluid saturation changes from time-lapse seismic data. *Geophysics*, *66*(3), 836-844.
Langhi, L., Strand, J., & Ricard, L. (2021). Flow modelling to quantify structural control on CO2 migration and containment, CCS South West Hub, Australia. *Petroleum Geoscience*, *27*(2), petgeo2020-2094.
Li, B., Wong, R., & Milnes, T. (2014). Anisotropy in capillary invasion and fluid flow through induced sandstone and shale fractures. *International Journal of Rock Mechanics and Mining Sciences*, *65*, 129-140.
Li, Q., Li, X., Liu, G., Li, X., Cai, B., Liu, L.-C., Zhang, Z., Cao, D., & Shi, H. (2017). Application of China's CCUS Environmental Risk Assessment Technical Guidelines (Exposure Draft) to the Shenhua CCS Project. *Energy Procedia*, *114*, 4270-4278. https://doi.org/https://doi.org/10.1016/j.egypro.2017.03.1567
Lim Chen Ning, I., & Sava, P. (2018). High-resolution multicomponent distributed acoustic sensing. *Geophysical Prospecting*, *66*. https://doi.org/10.1111/1365-2478.12634
Littmann, W., & Littmann, K. (2012). Unstructured Grids for Numerical Reservoir Simulation - Using TOUGH2 for Gas Storage. *Oil Gas European Magazine*, *38*, 204-209.
Liu, F., Lu, P., Griffith, C., Hedges, S. W., Soong, Y., Hellevang, H., & Zhu, C. (2012). CO2–brine–caprock interaction: Reactivity experiments on Eau Claire shale and a review of relevant literature. *International Journal of Greenhouse Gas Control*, *7*, 153-167. https://doi.org/https://doi.org/10.1016/j.ijggc.2012.01.012
Liu, Q., Zhu, D., Jin, Z., Tian, H., Zhou, B., Jiang, P., Meng, Q., Wu, X., Xu, H., & Hu, T. (2023). Carbon capture and storage for long-term and safe sealing with constrained natural CO2 analogs. *Renewable and Sustainable Energy Reviews*, *171*, 113000.
Liu, Y., Li, H. A., & Okuno, R. (2016). Measurements and modeling of interfacial tension for CO2/CH4/brine systems under reservoir conditions. *Industrial & Engineering Chemistry Research*, *55*(48), 12358-12375.
Lohr, C. D., & Hackley, P. C. (2018). Using mercury injection pressure analyses to estimate sealing capacity of the Tuscaloosa marine shale in Mississippi, USA: Implications for carbon dioxide sequestration. *International Journal of Greenhouse Gas Control*, *78*, 375-387. https://doi.org/https://doi.org/10.1016/j.ijggc.2018.09.006
Loizzo, M., Lecampion, B., Bérard, T., Harichandran, A., & Jammes, L. (2009). Reusing O&G Depleted Reservoirs for CO2 Storage: Pros and Cons. *SPE 124317*.
Loveland, A. M. (2013). Mercury injection capillary pressure (MICP) results from outcrop samples in the Naknek Formation, Iniskin Peninsula, Alaska.
Luu, K., Schoenball, M., Oldenburg, C. M., & Rutqvist, J. (2022). Coupled hydromechanical modeling of induced seismicity from CO2 injection in the Illinois Basin. *Journal of Geophysical Research: Solid Earth*, *127*(5), e2021JB023496.
Lynch, G., & Trollope, S. W. (2001). Dolomitization, platform collapse, and reservoir development in Ordovician carbonates of Anticosti Island, Gulf of St. Lawrence.
Manzocchi, T., Walsh, J. J., Nell, P., & Yielding, G. (1999). Fault transmissibility multipliers for flow simulation models. *Petroleum Geoscience*, *5*. https://doi.org/10.1144/petgeo.5.1.53

Marbler, H., Erickson, K. P., Schmidt, M., Lempp, C., & Pöllmann, H. (2013). Geomechanical and geochemical effects on sandstones caused by the reaction with supercritical CO 2: an experimental approach to in situ conditions in deep geological reservoirs. *Environmental earth sciences*, *69*, 1981-1998.
Marsden, R. (2007). Geomechanics for reservoir management. Algeria well evaluation conference,
Masoudi, R., Jalil, M. A. A., Press, D. J., Lee, K. H., Tan, C. P., Leo, Anis, Darman, N. B., & Othman, M. (2011). IPTC 15029 An Integrated Reservoir Simulation-Geomechanical Study on Feasibility of CO 2 Storage in M 4 Carbonate Reservoir , Malaysia.
Mastalerz, M., Drobniak, A., & Hower, J. C. (2021). Controls on reservoir properties in organic-matter-rich shales: Insights from MICP analysis. *Journal of Petroleum Science and Engineering*, *196*, 107775. https://doi.org/https://doi.org/10.1016/j.petrol.2020.107775
Mateeva, A., Lopez, J., Chalenski, D., Tatanova, M., Zwartjes, P., Yang, Z., Bakku, S., Vos, K. d., & Potters, H. (2017). 4D DAS VSP as a tool for frequent seismic monitoring in deep water. *The Leading Edge*, *36*(12), 995-1000.
Matthai, S., Shao, Q., Bonneau, F. (2020). *Impact of Faults on CO2 Plume Spreading in Sand-Shale Basins: Preliminary Results from a Numeric Simulation Study of a Fault Array Produced in a Sand-Box Experiment* GHGT-15, Abu Dhabi, UAE.
Mavko, G., Mukerji, T., & Dvorkin, J. (2020). *The rock physics handbook*. Cambridge university press.
Mbia, E. N., Frykman, P., Nielsen, C. M., Fabricius, I. L., Pickup, G. E., & Sørensen, A. T. (2014). Modeling of the pressure propagation due to CO2 injection and the effect of fault permeability in a case study of the Vedsted structure, Northern Denmark. *International Journal of Greenhouse Gas Control*, *28*, 1-10.
McArdle, N., & Ackers, M. (2012). Understanding seismic thin-bed responses using frequency decomposition and RGB blending. *First Break*, *30*(12).
McColpin, G. (2009). Surface Deformation Monitoring As a Cost Effective MMV Method. *Energy Procedia*, *1*, 2079-2086. https://doi.org/10.1016/j.egypro.2009.01.271
McGrail, B. P., Schaef, H. T., Spane, F. A., Horner, J. A., Owen, A. T., Cliff, J. B., Qafoku, O., Thompson, C. J., & Sullivan, E. C. (2017). Wallula Basalt Pilot Demonstration Project: Post-injection Results and Conclusions. *Energy Procedia*, *114*, 5783-5790. https://doi.org/https://doi.org/10.1016/j.egypro.2017.03.1716
Meng, L., Zheng, J., Yang, R., Peng, S., Sun, Y., Xie, J., & Li, D. (2023). Microseismic Monitoring Technology Developments and Prospects in CCUS Injection Engineering. *Energies*, *16*(7), 3101. https://www.mdpi.com/1996-1073/16/7/3101
Merrill, M. (2013). Depositional Environment as an Indicator of Favorable Regional Sequestration Targets: Examples from the USGS CO2 Storage Resource Assessment. *Energy Procedia*, *37*, 4975-4981. https://doi.org/10.1016/j.egypro.2013.06.410
Metz, B., Davidson, O., De Coninck, H., Loos, M., & Meyer, L. (2005). *IPCC special report on carbon dioxide capture and storage*. Cambridge: Cambridge University Press.
Metz, B., O. Davidson, H. C. de Coninck, M. Loos, and L. A. Meyer. (2005). *Intergovernmental Panel on Climate Change Special Report on Carbon Capture and Storage, Prepared by Working Group III of the Intergovernmental Panel on Climate Change*. C. U. Press.
Mews, K. S., Alhubail, M. M., & Barati, R. G. (2019). A Review of Brittleness Index Correlations for Unconventional Tight and Ultra-Tight Reservoirs. *Geosciences*, *9*(7).
Michael, K., Avijegon, A., Ricard, L., Myers, M., Tertyshnikov, K., Pevzner, R., Strand, J., Hortle, A., Stalker, L., Pervukhina, M., Harris, B., Feitz, A., Pejcic, B., Larcher, A., Rachakonda, P., Freifeld, B., Woitt, M., Langhi, L., Dance, T., . . . Seyyedi, M. (2020). A controlled CO2 release experiment in a fault zone at the In-Situ Laboratory in Western Australia. *International Journal of Greenhouse Gas Control*, *99*, 103100. https://doi.org/https://doi.org/10.1016/j.ijggc.2020.103100
Moghaddam, N., Nourallah, H., Vasco, D., Samsonov, S., & Rudiger, C. (2021). Interferometric SAR Modelling of Near-Surface Data to Improve Geological Model in the Surat Basin, Australia. *Journal of Applied Geophysics, 194*.
Müller-Huber, E., Börner, F., Börner, J. H., & Kulke, D. (2018). Combined interpretation of NMR, MICP, and SIP measurements on mud-dominated and grain-dominated carbonate rocks. *Journal of Applied Geophysics*, *159*, 228-240. https://doi.org/https://doi.org/10.1016/j.jappgeo.2018.08.011
Müller, N., Ramakrishnan, T. S., Boyd, A., & Sakruai, S. (2007). Time-lapse carbon dioxide monitoring with pulsed neutron logging. *International Journal of Greenhouse Gas Control*, *1*(4), 456-472. https://doi.org/https://doi.org/10.1016/S1750-5836(07)00071-0
Mutailipu, M., Liu, Y., Jiang, L., & Zhang, Y. (2019). Measurement and estimation of CO2–brine interfacial tension and rock wettability under CO2 sub-and super-critical conditions. *Journal of colloid and interface science*, *534*, 605-617.
Myshakin, E., Saidi, W., Romanov, V., Cygan, R., & Jordan, K. (2013). Molecular Dynamics Simulations of Carbon Dioxide Intercalation in Hydrated Na-Montmorillonite. *The Journal of Physical Chemistry C*, *117*, 11028–11039. https://doi.org/10.1021/jp312589s

Nababan, B., Hutami, H., & Fatkhan, F. (2022). The Feasibility Study of Reservoir Geomechanics from Brittleness Evaluation. *Scientific Contributions Oil and Gas*, *45*, 10-20. https://doi.org/10.29017/SCOG.45.1.920
National Energy Technology Laboratory. (2023, September 26, 2023). *NETL Oversees Landmark Research To Protect Caprock Integrity at Carbon Storage Sites*. https://netl.doe.gov/node/12923
Nicol, A., Seebeck, H., Field, B., McNamara, D., Childs, C., Craig, J., & Rolland, A. (2017). Fault Permeability and CO2 Storage. *Energy Procedia*, *114*, 3229-3236. https://doi.org/https://doi.org/10.1016/j.egypro.2017.03.1454
Nishizawa, O., & Yoshino, T. (2001). Seismic velocity anisotropy in mica-rich rocks: an inclusion model. *Geophysical Journal International*, *145*(1), 19-32. https://doi.org/10.1111/j.1365-246X.2001.00331.x
Nourollah, H., Keetley, J., & O'Brien, G. (2010). Gas chimney identification through seismic attribute analysis in the Gippsland Basin, Australia. *The Leading Edge*, *29*(8), 896-901. https://doi.org/10.1190/1.3479999
Nourollah, H., & Urosevic, M. (2019). Evaluation of sealing potential near gas chimneys–the Gippsland Basin, Australia. *Journal of Applied Geophysics*, *160*, 254-263. https://doi.org/https://doi.org/10.1016/j.jappgeo.2018.11.019
Nourollah, H., Urosevic, M., & Keetley, J. (2015). Seal potential of shale sequences through seismic anisotropy: Case study from Exmouth Sub-basin, Australia. *Interpretation*, *3*, T257-T267. https://doi.org/10.1190/INT-2014-0284.1
O'Brien, G., Lisk, M., Duddy, I., Eadington, P., Cadman, S., & Fellows, M. (1996). Late Tertiary fluid migration in the Timor Sea: a key control on thermal and diagenetic histories? *The APPEA Journal*, *36*(1), 399-427.
O'Brien, G., Quaife, P., Cowley, R., Morse, M., Wilson, D., Fellows, M., & Lisk, M. (1998). Evaluating trap integrity in the Vulcan sub-basin, Timor Sea, Australia, using integrated remote-sensing geochemical technologies.
O'Brien, G., Tingate, P., Divko, L. G., Harrison, M., Boreham, C., Liu, K., Arian, N., & Skladzien, P. (2008). First order sealing and hydrocarbon migration processes, Gippsland Basin, Australia: implications for CO2 geosequestration.
O'Brien, G., & Woods, E. (1995). Hydrocarbon-related diagenetic zones (HRDZs) in the Vulcan Sub-basin, Timor Sea: recognition and exploration implications. *The APPEA Journal*, *35*(1), 220-252.
O'Brien, G., Divko, L. G., Tingate, P., Harrison, M., Hamilton, J., Liu, K., Campi, M., & Miranda, J. (2013). Basin-scale Migration-fluid Flow, Sealing, and Leakage-seepage Processes, Gippsland Basin, Australia.
O'Brien, G. W., Cowley, R., Quaife, P., & Morse, M. (2002). Characterizing hydrocarbon migration and fault-seal integrity in Australia's Timor Sea via multiple, integrated remote-sensing technologies. *Surface exploration case histories: applications of geochemistry, magnetics and remote sensing. AAPG Stud Geol*, *48*, 393-413.
Ohno, H., & Ishii, E. (2022). Effect of fault activation on the hydraulic connectivity of faults in mudstone. *Geomechanics for Energy and the Environment*, *31*, 100317. https://doi.org/10.1016/j.gete.2022.100317
Oldenburg, C. M. (2006). *Joule-Thomson Cooling Due to CO2 Injection into Natural Gas Reservoirs* Conference: TOUGH Symposium 2006, Berkeley, CA, 15-17 May2006, United States. https://www.osti.gov/biblio/898956
Oldenburg, C. M., Jordan, P. D., Nicot, J.-P., Mazzoldi, A., Gupta, A. K., & Bryant, S. L. (2011). Leakage risk assessment of the In Salah CO2 storage project: Applying the certification framework in a dynamic context. *Energy Procedia*, *4*, 4154-4161.
Paluszny, A., Graham, C. C., Daniels, K. A., Tsaparli, V., Xenias, D., Salimzadeh, S., Whitmarsh, L., Harrington, J. F., & Zimmerman, R. W. (2020). Caprock integrity and public perception studies of carbon storage in depleted hydrocarbon reservoirs. *International Journal of Greenhouse Gas Control*, *98*, 103057. https://doi.org/https://doi.org/10.1016/j.ijggc.2020.103057
Pan, P., Wu, Z., Feng, X., & Yan, F. (2016). Geomechanical modeling of CO2 geological storage: A review. *Journal of Rock Mechanics and Geotechnical Engineering*, *8*(6), 936-947. https://doi.org/https://doi.org/10.1016/j.jrmge.2016.10.002
Park, J., Viken, I., Bjørnarå, T. I., & Aker, E. (2011). CSEM data analysis for Sleipner CO2 storage. Trondheim CCS-6 Conference, June,
Partyka, G., Gridley, J., & Lopez, J. (1999). Interpretational applications of spectral decomposition in reservoir characterization. *The Leading Edge*, *18*(3), 353-360.
Payre, X., Maisons, C., Marblé, A., & Thibeau, S. (2014). Analysis of the passive seismic monitoring performance at the Rousse CO2 storage demonstration pilot. *Energy Procedia*, *63*, 4339-4357.
Peach, C. J. (1991). *Influence of deformation on the fluid transport properties of salt rocks* Faculteit Aardwetenschappen der Rijksuniversiteit te Utrecht].
Pearce, J. M., Shepherd, T.J. Kemp, S.J., Wagner, D., Rochelle, C.A., Nador, A., Baker, J., Veto, I., Toth, G., Lombardi, S., Annuziatellis, A., Ciotoil, G., Beaubien, S.E., Pauwels, H., Czernichowski-Lauriol, I., Le Nindre, Y.M., Petelet-Giraud, E., Le Guern-Marot, C., Gaus, I., Girard, J.P., Serra, H., Schroot, B., Schuttenhelm, A., Orlic, B., Hatziyannis, G., Metaxas, A., Spyridonos, E., Gale, J., Manacourt, A., Brune,

S., Hagendorf, J., Teschner, M., Faber, E., Poggenburg, J., Iliffe, J., Kroos, B.M., Alles, S., Hildenbrand, A. & Heggland, R. . (2005). *Natural Analogues for the Geological Storage of CO2*.
Pearson, S., & Kupoluyi, M. (2022). *Deliverable 5.2 - Methodology for Quantitative Modelling of CO2 Storage Containment Risks*.
Pentland, C. H., El-Maghraby, R., Iglauer, S., & Blunt, M. J. (2011). Measurements of the capillary trapping of super-critical carbon dioxide in Berea sandstone. *Geophysical Research Letters*, *38*(6).
Peters, E. J. (2012). *Advanced Petrophysics: Geology, porosity, absolute permeability, heterogeneity, and geostatistics* (Vol. 1). Greenleaf Book Group.
Pevzner, R., Collet, O., Glubokovskikh, S., Tertyshnikov, K., & Gurevich, B. (2023). Detection of a CO2 plume by time-lapse analysis of Rayleigh-wave amplitudes extracted from downhole DAS recordings of ocean microseisms. *The Leading Edge*, *42*(11), 763-772.
Pevzner, R., Glubokovskikh, S., Isaenkov, R., Shashkin, P., Tertyshnikov, K., Yavuz, S., Gurevich, B., Correa, J., Wood, T., & Freifeld, B. (2022). Monitoring subsurface changes by tracking direct-wave amplitudes and traveltimes in continuous distributed acoustic sensor VSP data. *Geophysics*, *87*(1), A1-A6.
Pevzner, R., Gurevich, B., Pirogova, A., Tertyshnikov, K., & Glubokovskikh, S. (2020). Repeat well logging using earthquake wave amplitudes measured by distributed acoustic sensors. *The Leading Edge*, *39*(7), 513-517.
Pevzner, R., Nourollah, H., & Gurevich, B. (2024). Feasibility of targeted active seismic monitoring of geological carbon storage using refracted waves. *International Journal of Greenhouse Gas Control*, *132*, 104046.
Pevzner, R., Tertyshnikov, K., Sidenko, E., & Yavuz, S. (2021). Effects of Cable Deployment Method on Das VSP Data Quality: Study at CO2CRC Otway in-situ Laboratory. 82nd EAGE Annual Conference & Exhibition,
Pitt, W. D., & Scott, G. L. (1981). *Porosity zones of lower part of San Andres Formation, east-central New Mexico*. New Mexico Bureau of Mines & Mineral Resources.
Popik, S., Pevzner, R., Bona, A., Tertyshnikov, K., Glubokovskikh, S., & Gurevich, B. (2021). Estimation of P-wave anisotropy parameters from 3D vertical seismic profile with distributed acoustic sensors and geophones for seismic imaging in the CO2CRC Otway Project. *Geophysical Prospecting*, *69*(4), 842-855.
Popik, S., Pevzner, R., Tertyshnikov, K., Popik, D., Urosevic, M., Shulakova, V., Glubokovskikh, S., & Gurevich, B. (2020). 4D surface seismic monitoring the evolution of a small CO2 plume during and after injection: CO2CRC Otway Project study. *Exploration Geophysics*, *51*(5), 570-580.
Prasun, S. a. D., Ganesh and Ganesan Krishnamurthy, Prasanna and Jennette, Benjamin and Niranjan, SC. (2021). *A Method to Assess CO2 Migration through Faults during CO2 Sequestration* 15th International Conference on Greenhouse Gas Control Technologies, GHGT-15,
Prevost, J. H. (2013). One-way versus two-way coupling in reservoir-geomechanical models. Poromechanics V: Proceedings of the Fifth Biot Conference on Poromechanics,
Raaen, A., Andrews, J., & Fintland, T. (2022). The LOP revisited. ARMA US Rock Mechanics/Geomechanics Symposium,
Rahman, M., Fawad, M., Choi, J. C., & Mondol, N. (2022). Effect of overburden spatial variability on field-scale geomechanical modeling of potential CO2 storage site Smeaheia, offshore Norway. *Journal of Natural Gas Science and Engineering*, *99*, 104453. https://doi.org/10.1016/j.jngse.2022.104453
Rahman, M., Fawad, M., Jahren, J., & Mondol, N. (2022). Top seal assessment of Drake Formation shales for CO2 storage in the Horda Platform area, offshore Norway. *International Journal of Greenhouse Gas Control*, *119*, 103700. https://doi.org/10.1016/j.ijggc.2022.103700
Rangriz Shokri, A., Chalaturnyk, R., & Nickel, E. (2019). *Non-Isothermal Injectivity Considerations for Effective Geological Storage of CO2 at the Aquistore Site, Saskatchewan, Canada*. https://doi.org/10.2118/196118-MS
Rasool, M. H., & Ahmad, M. (2023). Reactivity of Basaltic Minerals for CO2 Sequestration via In Situ Mineralization: A Review. *Minerals*, *13*(9), 1154. https://www.mdpi.com/2075-163X/13/9/1154
Raza, A., Gholami, R., Sarmadivaleh, M., Tarom, N., Rezaee, R., Bing, C. H., Nagarajan, R., Hamid, M. A., & Elochukwu, H. (2016). Integrity analysis of CO2 storage sites concerning geochemical-geomechanical interactions in saline aquifers. *Journal of Natural Gas Science and Engineering*, *36*, 224-240.
Raza, A., Glatz, G., Gholami, R., Mahmoud, M., & Alafnan, S. (2022). Carbon mineralization and geological storage of CO2 in basalt: Mechanisms and technical challenges. *Earth-Science Reviews*, *229*. https://doi.org/10.1016/j.earscirev.2022.104036
Rezaeyan, A., Tabatabaei-Nejad, S. A., Khodapanah, E., & Kamari, M. (2015). A laboratory study on capillary sealing efficiency of Iranian shale and anhydrite caprocks. *Marine and Petroleum Geology*, *66*, 817-828.
Rickett, J., Duranti, L., Hudson, T., Regel, B., & Hodgson, N. (2007). 4D time strain and the seismic signature of geomechanical compaction at Genesis. *The Leading Edge*, *26*(5), 644-647.
Ringrose, P., & Bentley, M. (2016). *Reservoir model design* (Vol. 467). Springer.
Risk and Uncertainty Assessments for Geologic Storage of CO2 - Report 670. (2023).
Risktec Solutions. (2021). *Bowtie Analysis - Carbon Storage SECURe Project*.

Rock, L., O'Brien, S., Tessarolo, S., Duer, J., Bacci, V. O., Hirst, B., Randell, D., Helmy, M., Blackmore, J., & Duong, C. (2017). The Quest CCS project: 1st year review post start of injection. *Energy Procedia*, *114*, 5320-5328.

Rohmer, J., Loschetter, A., & Raucoules, D. (2017). Chapter 8 - Global Sensitivity Analysis for Supporting History Matching of Geomechanical Reservoir Models Using Satellite InSAR Data: A Case Study at the CO2 Storage Site of In Salah, Algeria. In G. P. Petropoulos & P. K. Srivastava (Eds.), *Sensitivity Analysis in Earth Observation Modelling* (pp. 145-159). Elsevier. https://doi.org/https://doi.org/10.1016/B978-0-12-803011-0.00008-2

Rohmer, J., Pluymakers, A., & Renard, F. (2016). Mechano-chemical interactions in sedimentary rocks in the context of CO2 storage: Weak acid, weak effects? *Earth-Science Reviews*, *157*, 86-110.

Romano, V., Bigi, S., Carnevale, F., Hyman, J., Karra, S., Valocchi, A., Tartarello, M., & Battaglia, M. (2020). Hydraulic characterization of a fault zone from fracture distribution. *Journal of Structural Geology*, *135*, 104036. https://doi.org/10.1016/j.jsg.2020.104036

Romano, V., Bigia, S., Park, H., Valocchic A.J., De'Haven Hymand,J., Karra,S., Nole,M., Hammond,G., Proietti,G., Battaglia, M. (2022, 23rd - 27th October 2022). *Numerical modeling to study gas CO2 migration in a fault zone: a case scenario* GHGT-16, Lyon.

Rosenqvist, M. P., Meakins, M. W. J., Planke, S., Millett, J. M., Kjøll, H. J., Voigt, M. J., & Jamtveit, B. (2023). Reservoir properties and reactivity of the Faroe Islands Basalt Group: Investigating the potential for CO2 storage in the North Atlantic Igneous Province. *International Journal of Greenhouse Gas Control*, *123*, 103838. https://doi.org/https://doi.org/10.1016/j.ijggc.2023.103838

Røste, T., & Ke, G. (2017). Overburden 4D time shifts—Indicating undrained areas and fault transmissibility in the reservoir. *The Leading Edge*, *36*(5), 423-430.

Rucci, A., Vasco, D., & Novali, F. (2013). Monitoring the geologic storage of carbon dioxide using multicomponent SAR interferometry. *Geophysical Journal International*, *193*(1), 197-208.

Rutqvist, J., Birkholzer, J., & Tsang, C.-F. (2008). Coupled reservoir-geomechanical analysis of the potential for tensile and shear failure associated with CO2 injection in multilayered reservoir-caprock systems. *International Journal of Rock Mechanics and Mining Sciences*, *45*, 132-143. https://doi.org/10.1016/j.ijrmms.2007.04.006

Saadatpoor, E., Bryant, S. L., & Sepehrnoori, K. (2010). New trapping mechanism in carbon sequestration. *Transport in porous media*, *82*, 3-17.

Sagu, O., & Pao, W. (2013). In-situ Stress Perturbation Due to Temperature Around Borehole During Carbon Injection. *Asian Journal of Applied Sciences*, *6*, 40-49. https://doi.org/10.3923/ajaps.2013.40.49

Salimzadeh, S., Kasperczyk, D., Chen, Z., Movassagh, A., Arjomand, E., Mow, W. S., & Kear, J. (2022). Ground surface monitoring for CO2 injection and storage. *The APPEA Journal*, *62*, S492-S496. https://doi.org/https://doi.org/10.1071/AJ21105

Sarg, J. (2001). The sequence stratigraphy, sedimentology, and economic importance of evaporite–carbonate transitions: a review. *Sedimentary Geology*, *140*(1-2), 9-34.

Sarout, J., & Guéguen, Y. (2008). Anisotropy of elastic wave velocities in deformed shales: Part 1—Experimental results. *Geophysics*, *73*(5), D75-D89.

Sato, K. (2011). Value of information analysis for adequate monitoring of carbon dioxide storage in geological reservoirs under uncertainty. *International Journal of Greenhouse Gas Control - INT J GREENH GAS CONTROL*, *5*, 1294-1302. https://doi.org/10.1016/j.ijggc.2011.07.010

Sayers, C. M. (1994). P-wave propagation in weakly anisotropic media. *Geophysical Journal International*, *116*(3), 799-805.

Sayers, C. M. (2005). Seismic anisotropy of shales. *Geophysical Prospecting*, *53*(5), 667-676. https://doi.org/https://doi.org/10.1111/j.1365-2478.2005.00495.x

Schmidt-Hattenberger, C., Bergmann, P., Labitzke, T., Schröder, S., Krüger, K., Rücker, C., & Schütt, H. (2011). Monitoring of geological CO2 storage with electrical resistivity tomography (ERT): Results from a field experiment near Ketzin/Germany. International Workshop on Geoelectric Monitoring,

Schoenherr, J., Urai, J. L., Kukla, P. A., Littke, R., Schléder, Z., Larroque, J.-M., Newall, M. J., Al-Abry, N., Al-Siyabi, H. A., & Rawahi, Z. (2007). Limits to the sealing capacity of rock salt: A case study of the infra-Cambrian Ara Salt from the South Oman salt basin. *AAPG Bulletin*, *91*(11), 1541-1557.

Schulze, O., Popp, T., & Kern, H. (2001). Development of damage and permeability in deforming rock salt. *Engineering geology*, *61*(2-3), 163-180.

Shahraeeni, M. (2012). Effect of Lithological Uncertainty on the Time-lapse Pressure-saturation Inversion. 74th EAGE Conference and Exhibition incorporating EUROPEC 2012,

Shao, Q., & Matthai, S. (2020). Numerical Modelling of CO2 Migration through Faulted Storage Strata with a New Asynchronous FE-FV Compositional Simulator. *2020*(1), 1-16. https://doi.org/https://doi.org/10.3997/2214-4609.202035016

Shao, Q., Matthai, S., & Gross, L. (2018). *Efficient modelling of CO2 injection and plume spreading with discrete event simulation (DES)*.

Shell Canada Ltd. (2017). *Shell Quest Carbon Capture and Storage Project: Measurement, Monitoring and Verification Plan*.
Shell UK Ltd. (2016). *Peterhead CCS Project: Risk Management Plan & Risk Register*.
Shi, J.-Q., Durucan, S., Korre, A., Ringrose, P., & Mathieson, A. (2019). History matching and pressure analysis with stress-dependent permeability using the In Salah CO2 storage case study. *International Journal of Greenhouse Gas Control*, *91*, 102844. https://doi.org/https://doi.org/10.1016/j.ijggc.2019.102844
Shiach, G., Nolan, A., McAvoy, S., McStay, D., Prel, C., & Smith, M. (2007). Advanced feed-through systems for in-well optical fibre sensing. *Journal of Physics: Conference Series*, *76*(1), 012066. https://doi.org/10.1088/1742-6596/76/1/012066
Sidenko, E., Tertyshnikov, K., Gurevich, B., & Pevzner, R. (2022). DAS signature of reservoir pressure changes caused by a CO2 injection: Experience from the CO2CRC Otway Project. *International Journal of Greenhouse Gas Control*, *119*, 103735. https://doi.org/10.1016/j.ijggc.2022.103735
Skurtveit, E., Aker, E., Soldal, M., Angeli, M., & Wang, Z. (2012). Experimental investigation of CO2 breakthrough and flow mechanisms in shale. *Petroleum Geoscience*, *18*, 3-15. https://doi.org/https://doi.org/10.1144/1354-079311-016
Sneider, R. M., Sneider, J. S., Bolger, G. W., & Neasham, J. W. (1997). AAPG Memoir 67: Seals, Traps, and the Petroleum System. Chapter 1: Comparison of Seal Capacity Determinations: Conventional Cores vs. Cuttings.
Snippe, J., Kampman, N., Bisdom, K., Tambach, T., March, R., Maier, C., Phillips, T., Inskip, N. F., Doster, F., & Busch, A. (2022). Modelling of long-term along-fault flow of CO_2 from a natural reservoir. *International Journal of Greenhouse Gas Control*, *118*, 103666. https://doi.org/https://doi.org/10.1016/j.ijggc.2022.103666
Snippe, J., & Tucker, O. (2014). CO2 fate comparison for depleted gas field and dipping saline aquifer. *Energy Procedia*, *63*, 5586-5601.
Snæbjörnsdóttir, S.Ó., Oelkers, E.H., Mesfin, K., Aradóttir, E.S., Dideriksen, K., Gunnarsson, I., Gunnlaugsson, E., Matter, J.M., Stute, M. and Gislason, S.R., (2017) The chemistry and saturation states of subsurface fluids during the in situ mineralisation of CO2 and H2S at the CarbFix site in SW-Iceland. *International Journal of Greenhouse Gas Control, 58, pp.87-102*.
Snæbjörnsdóttir, S.Ó., Sigfússon, B., Marieni, C., Goldberg, D., Gislason, S.R. and Oelkers, E.H., (2020) Carbon dioxide storage through mineral carbonation. *Nature Reviews Earth & Environment, 1(2), pp.90-102*.
Soleymani, H., & Cranganu, C. (2013). *Carbon Dioxide Sealing Capacity: Textural or Compositional Controls?* https://doi.org/10.2172/1133113
Song, Y., Jun, S., Na, Y., Kim, K., Jang, Y., & Wang, J. (2023). Geomechanical challenges during geological CO2 storage: A review. *Chemical Engineering Journal*, *456*, 140968. https://doi.org/https://doi.org/10.1016/j.cej.2022.140968
Springer, N., & Lindgren, H. (2006). Caprock properties of the Nordland Shale recovered from the 15/9-A11 well, the Sleipner area. 8th Greenhouse Gas Control Technologies conference (GHGT-8), Trondheim,
Stalker, L., Varma, S., Van Gent, D., Haworth, J., & Sharma, S. (2013). South West Hub: a carbon capture and storage project. *Australian Journal of Earth Sciences*, *60*(1), 45-58. https://doi.org/10.1080/08120099.2013.756830
Stanek, F., Jin, G., & Simmons, J. (2022). Fracture Imaging Using DAS-Recorded Microseismic Events. *Frontiers in Earth Science*, *10*. https://doi.org/10.3389/feart.2022.907749
Stevens, S. H., & Tye, B. S. (2005). *Natural CO2 analogs for Carbon Sequestration*.
Sun, Y., Liu, J., Xue, Z., Li, Q., Fan, C., & Zhang, X. (2021). A critical review of distributed fiber optic sensing for real-time monitoring geologic CO2 sequestration. *Journal of Natural Gas Science and Engineering*, *88*, 103751. https://doi.org/https://doi.org/10.1016/j.jngse.2020.103751
Sutton, S. J., Ethridge, F. G., Almon, W. R., Dawson, W. C., & Edwards, K. K. (2004). Textural and sequence-stratigraphic controls on sealing capacity of Lower and Upper Cretaceous shales, Denver basin, Colorado. *AAPG Bulletin*, *88*(8), 1185-1206.
Tadjer, A., Hong, A., & Bratvold, R. B. (2021). A sequential decision and data analytics framework for maximizing value and reliability of CO2 storage monitoring. *Journal of Natural Gas Science and Engineering*, *96*, 104298. https://doi.org/https://doi.org/10.1016/j.jngse.2021.104298
Tao, Q., Alexander, D., & Bryant, S. L. (2013). Development and Field Application of Model for Leakage of CO2 Along a Fault. *Energy Procedia*, *37*, 4420-4427. https://doi.org/https://doi.org/10.1016/j.egypro.2013.06.347
Tenthorey, E., Feitz, A., Knackstedt, M., Dewhurst, D.N., Watson, M. (2022). The Otway CCS Fault Injection Experiment: Fault Analysis. 16th Greenhouse Gas Control Technologies Conference (GHGT-16), Lyon.
Tenthorey, E., Feitz, A., Knackstedt, M., Dewhurst, D.N., Watson, M., Richard, T., & Dewhurst, D. N. (2019). A continuous, proxy-based rock mechanical approach for developing mechanical frameworks at CO2

storage sites. *International Journal of Greenhouse Gas Control*, *85*, 36-45. https://doi.org/https://doi.org/10.1016/j.ijggc.2019.03.028
Tenthorey, E., Richard, T., & Dewhurst, D. N. (2018). Reduced CCS Operational Uncertainty Using Innovative Rock Mechanics Workflows. 14th Greenhouse Gas Control Technologies Conference Melbourne,
Tertyshnikov, K., Bergery, G., Freifeld, B., & Pevzner, R. (2020). Seasonal effects on DAS using buried helically wound cables. EAGE Workshop on Fiber Optic Sensing for Energy Applications in Asia Pacific,
Thompson, N., Andrews, J. S., Reitan, H., & Teixeira Rodrigues, N. E. (2022). Data Mining of In-Situ Stress Database Towards Development of Regional and Global Stress Trends and Pore Pressure Relationships. SPE Norway Subsurface Conference,
Thompson, N., Andrews, J. S., Wu, L., & Meneguolo, R. (2022). Characterization of the in-situ stress on the Horda platform – A study from the Northern Lights Eos well. *International Journal of Greenhouse Gas Control*, *114*, 103580. https://doi.org/https://doi.org/10.1016/j.ijggc.2022.103580
Tillner, E., Shi, J.-Q., Bacci, G., Nielsen, C. M., Frykman, P., Dalhoff, F., & Kempka, T. (2014). Coupled Dynamic Flow and Geomechanical Simulations for an Integrated Assessment of CO2 Storage Impacts in a Saline Aquifer. *Energy Procedia*, *63*, 2879-2893. https://doi.org/https://doi.org/10.1016/j.egypro.2014.11.311
Titus, Z., Heaney, C., Jacquemyn, C., Salinas, P., Jackson, M., & Pain, C. (2022). Conditioning surface-based geological models to well data using artificial neural networks. *Computational Geosciences*, *26*(4), 779-802.
Tosaya, C. A. (1982). *Acoustical properties of clay-bearing rocks*. Stanford University.
Trainor-Guitton, W., Ramirez, A., Yang, X., Mansoor, K., Sun, Y., & Carroll, S. A. (2013). Value of information methodology for assessing the ability of electrical resistivity to detect co2/brine leakage into a shallow aquifer. *International Journal of Greenhouse Gas Control*, *18*, 103-113.
Trani, M., Arts, R., Leeuwenburgh, O., & Brouwer, J. (2011). Estimation of changes in saturation and pressure from 4D seismic AVO and time-shift analysis. *Geophysics*, *76*(2), C1-C17.
Trupp, M., Ryan, S., Barranco Mendoza, I., Leon, D., & Scoby-Smith, L. (2021). Developing the world's largest CO2 Injection System–a history of the Gorgon Carbon Dioxide Injection System. Proceedings of the 15th Greenhouse Gas Control Technologies Conference,
Tucker, M. E., & Wright, V. P. (2009). *Carbonate sedimentology*. John Wiley & Sons.
Tucker, O., Holley, M., Metcalfe, R., & Hurst, S. (2013). Containment Risk Management for CO2 Storage in a Depleted Gas Field, UK North Sea. *Energy Procedia*, *37*, 4804-4817. https://doi.org/https://doi.org/10.1016/j.egypro.2013.06.390
Energy Bill [HL], (2022). https://bills.parliament.uk/publications/47229/documents/2107
Underschultz, J. (2007). Hydrodynamics and membrane seal capacity. *Geofluids*, *7*(2), 148-158.
United Kingdom Government. (2022). *Plans to bolster UK Energy security set to become law*. Retrieved 1st October from https://www.gov.uk/government/news/plans-to-bolster-uk-energy-security-set-to-become-law
United States Environmental Protection Agency. (1974). Safe Drinking Water Act 1974. In.
United States Environmental Protection Agency. (2018). *Underground Injection Control Program Class VI Implementation - Manual for UIC Program Directors*.
United States Environmental Protection Agency. (2023a). *Protecting Underground Sources of Drinking Water from Underground Injection (UIC)*. https://www.epa.gov/uic
United States Environmental Protection Agency. (2023b). *Summary of the Safe Drinking Water Act*. https://www.epa.gov/laws-regulations/summary-safe-drinking-water-act
S.799 - 117th Congress: SCALE Act (2023). https://www.govtrack.us/congress/bills/117/s799
Varre, S. B., Siriwardane, H. J., Gondle, R. K., Bromhal, G. S., Chandrasekar, V., & Sams, N. (2015). Influence of geochemical processes on the geomechanical response of the overburden due to CO2 storage in saline aquifers. *International Journal of Greenhouse Gas Control*, *42*, 138-156.
Vasylkivska, V., Dilmore, R., Lackey, G., Zhang, Y., King, S., Bacon, D., Chen, B., Mansoor, K., & Harp, D. (2021). NRAP-Open-IAM: A Flexible Open-Source Integrated-Assessment-Model for Geologic Carbon Storage Risk Assessment and Management. *Environmental Modelling & Software*, *143*, 105114. https://doi.org/10.1016/j.envsoft.2021.105114
Vavra, C., Kaldi, J., & Sneider, R. M. (1992). Geological applications of capillary pressure: A review. *AAPG Bulletin (American Association of Petroleum Geologists); (United States)*, *76:6*.
Veer, E., Van Der Waldmann, S., & Fokker, P. (2015). A coupled geochemical-transport-geomechanical model to address caprock integrity during long-term CO2 storage. ARMA US Rock Mechanics/Geomechanics Symposium,
Verdon, J., Kendall, J. M., Stork, A., Chadwick, R., White, D., & Bissell, R. (2013). Comparison of geomechanical deformation induced by megatonne-scale CO2 storage at Sleipner, Weyburn, and In Salah. *Proceedings of the National Academy of Sciences of the United States of America*, *110*. https://doi.org/10.1073/pnas.1302156110

Vilarrasa, V., & Carrera, J. (2015). Geologic carbon storage is unlikely to trigger large earthquakes and reactivate faults through which CO2 could leak. *Proc Natl Acad Sci U S A*, *112*(19), 5938-5943. https://doi.org/10.1073/pnas.1413284112
Vilarrasa, V., & Laloui, L. (2016). Impacts of thermally induced stresses on fracture stability during geological storage of CO2. *Energy Procedia*, *86*, 411-419.
Vilarrasa, V., Makhnenko, R. Y., & Laloui, L. (2017). Potential for Fault Reactivation Due to CO2 Injection in a Semi-Closed Saline Aquifer. *Energy Procedia*, *114*, 3282-3290. https://doi.org/https://doi.org/10.1016/j.egypro.2017.03.1460
Vilarrasa, V., Olivella, S., Carrera, J., & Rutqvist, J. (2014). Long term impacts of cold CO2 injection on the caprock integrity. *International Journal of Greenhouse Gas Control*, *24*, 1-13. https://doi.org/https://doi.org/10.1016/j.ijggc.2014.02.016
Vilarrasa, V., & Rutqvist, J. (2017). Thermal effects on geologic carbon storage. *Earth-Science Reviews*, *165*, 245-256. https://doi.org/https://doi.org/10.1016/j.earscirev.2016.12.011
Wang, Z., Dilmore, R., Bacon, D. H., & Harbert, W. (2021). Evaluating Probability of Containment Effectiveness at a GCS Sites using integrated assessment modeling approach with Bayesian decision Networks. *Greenhouse Gases: Science and Technology*, *11*(PNNL-SA-154995), Medium: X; Size: 360-376. https://doi.org/10.1002/ghg.2056
Warren, J. K., & Warren, J. K. (2016). Hydrocarbons and evaporites. *Evaporites: A Geological Compendium*, 959-1079.
Watson, M. (2014). Containment Risk Assessment. In P. Cook (Ed.), *Geologically Storing Carbon: Learning from the Otway Project Experience*. CSIRO.
Watson, M. N. (2012). Natural CO_2 accumulations as analogues for CO_2 geological storage and CO_2-induced diagenesis in the Otway Basin, Australia.
White, A. J., Traugott, M. O., & Swarbrick, R. E. (2002). The use of leak-off tests as means of predicting minimum in-situ stress. *Petroleum Geoscience*, *8*(2), 189-193.
White, D., Bellefleur, G., Dodds, K., & Movahedzadeh, Z. (2022). Toward improved distributed acoustic sensing sensitivity for surface-based reflection seismics: Configuration tests at the Aquistore CO2 storage site. *Geophysics*, *87*(2), P1-P14.
White, J. A., Chiaramonte, L., Ezzedine, S., Foxall, W., Hao, Y., Ramirez, A., & McNab, W. (2014). Geomechanical behavior of the reservoir and caprock system at the In Salah CO2 storage project. *Proceedings of the National Academy of Sciences*, *111*(24), 8747-8752.
White, J. C., Williams, G., & Chadwick, A. (2018). Seismic amplitude analysis provides new insights into CO2 plume morphology at the Snøhvit CO2 injection operation. *International Journal of Greenhouse Gas Control*, *79*, 313-322.
White, J. C., Williams, G., Chadwick, A., Furre, A.-K., & Kiær, A. (2018). Sleipner: The ongoing challenge to determine the thickness of a thin CO2 layer. *International Journal of Greenhouse Gas Control*, *69*, 81-95.
White, J. C., Williams, G. A., Grude, S., & Chadwick, R. A. (2015). Utilizing spectral decomposition to determine the distribution of injected CO2 at the Snøhvit Field. *Geophysical Prospecting*, *63*(5), 1213-1223.
Williams, G., & Chadwick, A. (2012). Quantitative seismic analysis of a thin layer of CO 2 in the Sleipner injection plume. *Geophysics*, *77*(6), R245-R256.
Wilson, G., Ellmauthaler, A., Seabrook, B., Maida, J., Bush, J., Leblanc, M., Dupree, J., & Uribe, M. (2020). *Topside Distributed Acoustic Sensing of Subsea Wells*. https://doi.org/10.3997/2214-4609.202070029
Worden, R. H. (2023). Value of core for reservoir and top-seal analysis for carbon capture and storage projects. *Geological Society, London, Special Publications*, *527*(1), SP527-2022-2038.
Worden, R. H., Allen, M. J., Faulkner, D. R., Utley, J. E., Bond, C. E., Alcalde, J., Heinemann, N., Haszeldine, R. S., Mackay, E., & Ghanbari, S. (2020). Lower Cretaceous Rodby and Palaeocene Lista shales: Characterisation and comparison of top-seal mudstones at two planned CCS sites, offshore UK. *Minerals*, *10*(8), 691.
Worth, K., White, D., Chalaturnyk, R., Sorensen, J., Hawkes, C., Rostron, B., Johnson, J., & Young, A. (2014). Aquistore Project Measurement, Monitoring, and Verification: From Concept to CO2 Injection. *Energy Procedia*, *63*, 3202-3208. https://doi.org/https://doi.org/10.1016/j.egypro.2014.11.345
Worth, K., White, D., Chalaturnyk, R., Sorensen, J., Hawkes, C., Rostron, B., Risk, D., Young, A., & Sacuta, N. (2017). Aquistore: Year One – Injection, Data, Results. *Energy Procedia*, *114*, 5624-5635. https://doi.org/https://doi.org/10.1016/j.egypro.2017.03.1701
Wu, L., Skurtveit, E., Thompson, N., Michie, E. A. H., Fossen, H., Braathen, A., Fisher, Q., Lidstone, A., & Bostrøm, B. (2022). Containment Risk Assessment and Management of Co2 Storage on the Horda Platform. *SSRN Electronic Journal*. https://doi.org/10.2139/ssrn.4272132
Xu, T., Apps, J. A., & Pruess, K. (2004). Numerical simulation of CO2 disposal by mineral trapping in deep aquifers. *Applied geochemistry*, *19*(6), 917-936.
Yang, G., Ma, X., Feng, T., Yu, Y., Yin, S., Huang, M., & Wang, Y. (2020). Geochemical modelling of the evolution of caprock sealing capacity at the Shenhua CCS demonstration project. *Minerals*, *10*(11), 1009.

Yielding, G., Bretan, P., & Freeman, B. (2010). Fault seal calibration: a brief review. *Geological Society, London, Special Publications*, *347*(1), 243-255.
Yielding, G., Freeman, B., & Needham, D. T. (1997). Quantitative Fault Seal Prediction1. *AAPG Bulletin*, *81*(6), 897-917. https://doi.org/10.1306/522b498d-1727-11d7-8645000102c1865d
Yilo, N. K., Weitemeyer, K., Minshull, T. A., Attias, E., Marin-Moreno, H., Falcon-Suarez, I. H., Gehrmann, R., & Bull, J. (2024). Marine CSEM synthetic study to assess the detection of CO2 escape and saturation changes within a submarine chimney connected to a CO2 storage site. *Geophysical Journal International*, *236*(1), 183-206.
Yong, W. P., Azahree, A. I., M Ali, S. S., Jaafar Azuddin, F., & M Amin, S. (2019). A New Modelling Approach to Simulate CO2 Movement and Containment Coupled with Geochemical Reactions and Geomechanical Effects for an Offshore CO2 Storage in Malaysia. SPE Europec featured at 81st EAGE Conference and Exhibition,
Zain-Ul-Abedin, M., & Henk, A. (2020). Building 1D and 3D Mechanical Earth Models for Underground Gas Storage—A Case Study from the Molasse Basin, Southern Germany. *Energies*, *13*, 5722. https://doi.org/10.3390/en13215722
Zappone, A., Rinaldi, A., Rinaldi, A. P., Grab, M., Wenning, Q., Roques, C., Madonna, C., Obermann, A., Bernasconi, S., Brennwald, M., Kipfer, R., Soom, F., Cook, P., Guglielmi, Y., Nussbaum, C., Giardini, D., Mazzotti, M., & Wiemer, S. (2021). Fault sealing and caprock integrity for CO2 storage: an in situ injection experiment.
Zemke, K., Liebscher, A., & Wandrey, M. (2010). Petrophysical analysis to investigate the effects of carbon dioxide storage in a subsurface saline aquifer at Ketzin, Germany (CO2SINK). *International Journal of Greenhouse Gas Control*, *4*(6), 990-999.
Zhang, N., Luo, Z., Chen, Z., Liu, F., Liu, P., Chen, W., Wu, L., & Zhao, L. (2023). Thermal–hydraulic–mechanical–chemical coupled processes and their numerical simulation: a comprehensive review. *Acta Geotechnica*, 1-22.
Zhang, S., Xu, Y., & Lu, P. (2022). Analysis and modeling of dolomite sealing potential. *Petro Chem Indus Intern, 5 (3), 153*, *161*.
Zhang, T., Zhang, W., Yang, R., Gao, H., & Cao, D. (2022). Analysis of available conditions for InSAR surface deformation monitoring in CCS projects. *Energies*, *15*(2), 672.
Zhang, Y., Lei, X., Hashimoto, T., & Xue, Z. (2020). In situ hydromechanical responses during well drilling recorded by fiber-optic distributed strain sensing. *Solid Earth*, *11*(6), 2487-2497. https://doi.org/10.5194/se-11-2487-2020
Zhang, Y., Lei, X., Hashimoto, T., & Xue, Z. (2021). Toward Retrieving Distributed Aquifer Hydraulic Parameters From Distributed Strain Sensing. *Journal of Geophysical Research (Solid Earth)*, *126*, e2020JB020056. https://doi.org/10.1029/2020jb020056
Zheng, F., Jahandideh, A., Jha, B., & Jafarpour, B. (2021). Geologic CO2 Storage Optimization under Geomechanical Risk Using Coupled-Physics Models. *International Journal of Greenhouse Gas Control*, *110*, 103385. https://doi.org/https://doi.org/10.1016/j.ijggc.2021.103385
Zoback, M. D. (2010). *Reservoir Geomechanics*. Cambridge University Press. https://books.google.com.au/books?id=Xx63OaM2JIIC
Zweigel, P., Vebenstad, K., Vazquez Anzola D., Lidstone, A. (2021). Containment Risk Assessment of the Northern Lights Aurora CO2 Storage Site. 15th Greenhouse Gas Control Technologies,

Appendix A.MICP Database

A-1 Mercury Porosimetry

MICP experiments are a commonly applied method for estimating capillary pressure and subsequently seal capacity.

One of the advantages of the MICP method (mercury porosimetry) is that the samples can be any shape and size (on the provision that they fit in the measurement capsule). This is advantageous as a large proportion of wells do not acquire full (conventional) core or side wall cores, and therefore, the experimental data is based on measurements performed on cuttings. The recovery of core and samples from shaly formations is particularly difficult as they can get washed/lost during drilling/percolation. Therefore, the capability of MICP measurement to be performed on cuttings is very useful in the evaluation of shale sealing capacity (Sneider et al., 1997).

In the MICP method, a highly non-wetting phase (mercury) is injected into a wetting-phase (air) soaked sample (i.e., dried sample). At each stage, the injection pressure is increased (usually up to 60,000 psi) and the equivalent mercury that has displaced the air in the pore space is recorded. The result is a table consisting of a pair of pressure/porosity or pressure/saturation figures for the sample. The convention is to assign the equivalent pressure of either 7.5% or 10% saturation (of mercury) as the capillary threshold pressure (Espinoza & Santamarina, 2017; Vavra et al., 1992).

However, a more robust technique identifies the deflection point on the MICP/saturation curve and assigns it as the representative sealing capacity (Daniel & Kaldi, 2009; Kaldi, 2011). An example is shown in Figure 92, where the cumulative increase in mercury saturation is measured against the pressure. The interpretation of the example graph is relatively straightforward where the sample has a relatively uniform pore throat distribution.

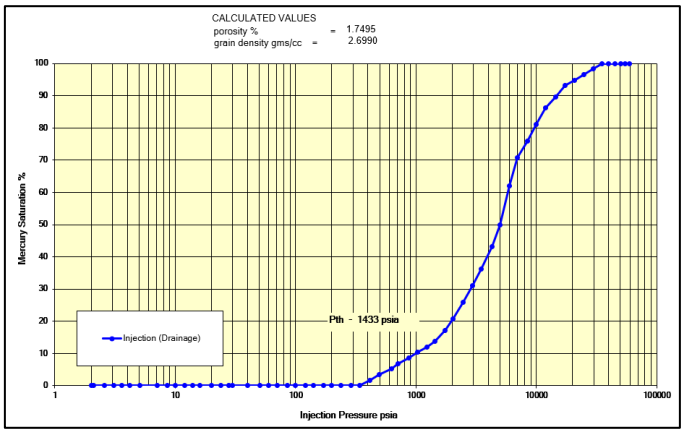

Figure 92: Example of graph measuring the capillary pressure values at each saturation level. The deflection of the curve represents the interpreted MICP value.

An example of the range of threshold pressure calculated for the same sample using three different methods is presented in Figure 93 to illustrate the range of uncertainty in MICP threshold pressure interpretation.

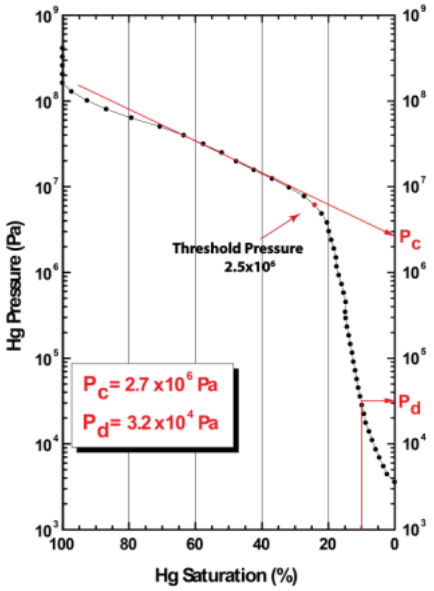

Figure 93: MICP threshold pressure calculation methods (Daniel & Kaldi, 2009; Sutton et al., 2004; Vavra et al., 1992) from (Soleymani & Cranganu, 2013)

Data from MICP measurements must be converted from mercury-air (i.e. lab conditions) to a CO_2-brine capillary pressure. This requires an understanding of the wettability (contact angle) and CO_2-brine interfacial tension as discussed in sections 4.2.2 and 4.2.3 respectively.

The equivalent radius of the pipe (pore space) can be calculated from the measured entry pressure using the Young-Laplace equation. However, it is important to remember that this radius is a calculated number and, therefore, represents a general guide to the range of the pore throat radii at entry pressure. A statistical distribution of the pore radii is generated from the experimental data (Figure 94). This graph is very useful in combination with the actual MICP measurement data. However, the extraction of statistical data such as the average, mode and median pore throat might be a misleading guide to the measured MICP value (or its calculated r_c equivalent). For example, the pore distribution can be bimodal which introduces ambiguity in the best pore-throat representative for the sealing capacity (Figure 94).

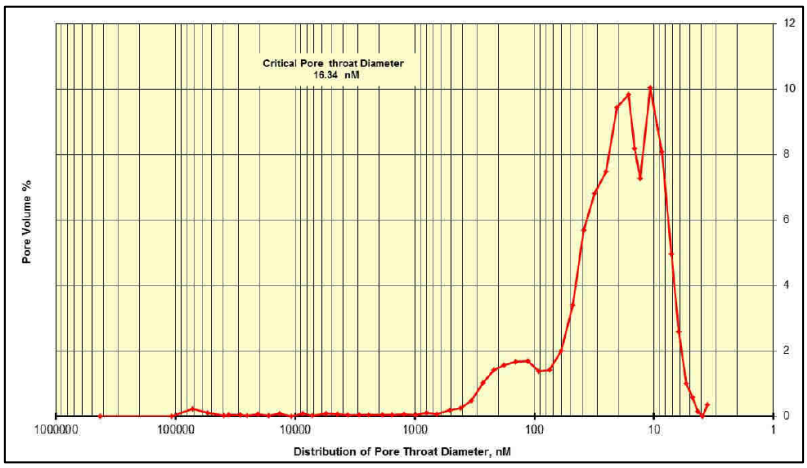

Figure 94: Example of a graph showing the statistical distribution of the pore throat size in a sample

There is limited resistance for a non-wetting fluid that is immiscible to the wetting fluid of the caprock to pass through a larger and more connected network of pores. Standard MICP tests measure the largest connected pore and assign the corresponding capillary pressure or equivalent column pressure as the sealing capacity

of the sample. MICP can result in an underestimation of the actual breakthrough pressure in systems with a non-uniform pore size distribution and cannot discriminate bedding-induced anisotropy (Espinoza & Santamarina, 2017). The MICP method is best applied to siliciclastic rocks such as shale, silts, sandstones as well as carbonates.

An example of the column height calculation based on MICP and corrected to reservoir conditions is illustrated in Figure 95, which can then be used to calculate a maximum storage volume/mass within a structural trap prior to membrane failure.

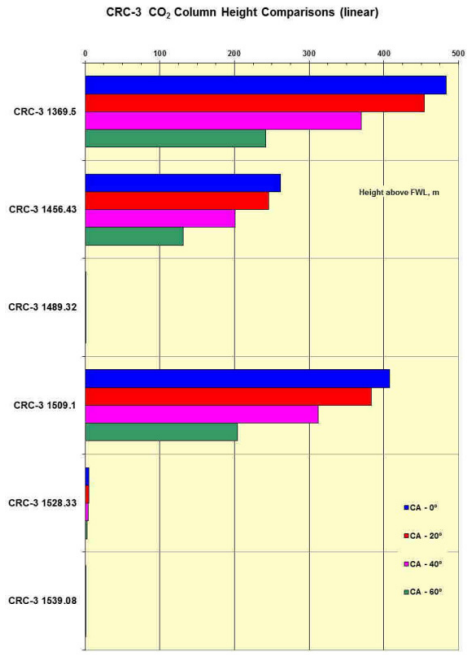

Figure 95: Seal capacity (column height) in metres (CRC-3, Otway)(Internal CO2CRC publication). The data with very small column heights (< 1 m) are from the storage formation, whilst the claystone/mudstone column heights are more than 100 m.

A-2 Challenges with MICP

Quantitative measurement of the sealing capacity for certain rock types is not straightforward using the MICP methodology (Peach, 1991). One example is MICP measurements for halite. The increase in saturation concentration tends to increase the permeability through the dissolution of the pore walls, whereas an increase in effective stress tends to diminish the radius of the flow channels. Laboratory measurement of undisturbed halite shows that their permeability is less than 10^{-22} m^2 (Cosenza et al., 1999; Schoenherr et al., 2007). Halite deforms plastically without the formation and propagation of dilating cracks as long as the state of stresses remains within the non-dilatant stress domain (Schulze et al., 2001). Such properties are integral to the development of as underground salt caverns for waste disposal (e.g., radioactive waste) or underground hydrogen storage. Unless impurities such as shale or carbonates compromise the rock strength of the salt and generate local fracturing, salt rocks can withstand and seal pressures as high as lithostatic (Schoenherr et al., 2007).

Upscaling the results from MICP analysis to achieve a model of capillary flow through a seal is clearly challenging. As mentioned previously, an MICP experiment can be performed on cuttings as well as larger samples including one inch core plugs. Quantifying the sample size required to achieve a representative MICP experiment was the subject of one study that used samples from the Eagle Ford Formation, with the authors concluding that MICP results demonstrated a strong dependence on sample size due to conformance (pore volume compression) and pore accessibility (Comisky et al., 2011). In this instance a certain sample

size (-20+35) was deemed as optimal for determining porosity in the Eagle Ford Formation. Whilst analysis of cuttings is useful, it should be supplemented and compared with core data when possible (Comisky et al., 2011).

A-3 Screening of CO_2 column heights

A conversion of the classic Sneider et al. oil column heights to supercritical CO_2 column heights for various seal-flow barrier types is provided in Table 20. It is important to re-state that this method is only applicable when assuming CO_2 storage under a membrane seal within a structural closure and an understanding of the spill points from the structure. Further, it is also predicated on the assumption that it is appropriate to apply seal threshold pressures from MICP experiments and recognise the uncertainties therein (refer to section A-2). As such, it may be a useful guide for a high-level screening assessment of multiple opportunities prior to undertaking a more detailed, site-specific screening.

Table 20: A classification guideline developed for the cap rock sealing capacity. The original guidelines are based on a 35º API oil column, but can be converted to the equivalent entry pressure, adapted from original work by (Sneider et al., 1997). A CO_2 density of 640 kg/m^3 is assumed as well as an IFT of 26 mN/m and a contact angle of 40º. Values are rounded for simplicity.

Seal-Flow Barrier Type	35^0 API Oil Column Held (m)	$scCO_2$ Column Held (m)
A*	≥1500	≥500
A	≥300-<1500	≥100-<500
B	≥150-<300	≥50-<100
C	≥30-<150	≥10<50
D	≥15-<30	≥5-<10
E	<15	<5
F	"Waste Zone Rocks"	

Previous research has resulted in the creation of a caprock MICP database (Daniel & Kaldi, 2012) focused on Australian and New Zealand hydrocarbon seals.

For this current study, regions were identified where there is either an operating GCS project or where future large-scale GCS projects are anticipated, and MICP data was collated. An excerpt from the database is provided in this section. Note that the database is dependent on data that is either publicly available or was made available based on communication with the relevant technical authors.

The regions identified for the database were:

- Otway, Australia
- Eastern Europe
- USA regional partnerships (e.g., Southeast Regional Carbon Sequestration Partnership, SECARB)
- Central West Canada
- China (e.g., Ordos, Tarim basins)

Table A- 1: MICP data for Tuscaloosa Marine Shale (Lohr & Hackley, 2018)

Sample No./ID	Country	State	Stratigraphic unit / Formation	Sample depth (m)	Air-Hg Entry Pressure (psi)
S1	USA	Mississippi	Tuscaloosa Marine Shale	10173.4–10173.65	2199
S2	USA	Mississippi	Tuscaloosa Marine Shale	10192.8–10193.05	3265
S3	USA	Mississippi	Tuscaloosa Marine Shale	12111	876
S4	USA	Mississippi	Tuscaloosa Marine Shale	12112.5	1608
S5	USA	Mississippi	Tuscaloosa Marine Shale	12116.9	709
S6	USA	Mississippi	Tuscaloosa Marine Shale	12118.45	5986
S7	USA	Mississippi	Tuscaloosa Marine Shale	12140	4398
S8	USA	Mississippi	Tuscaloosa Marine Shale	10659–10660	3991
S9	USA	Mississippi	Tuscaloosa Marine Shale	10668–10669	798
S10	USA	Mississippi	Tuscaloosa Marine Shale	10660–10661	1761
S11	USA	Mississippi	Tuscaloosa Marine Shale	10657–10658	8288
S12	USA	Mississippi	Tuscaloosa Marine Shale	10658–10659	6019
S13	USA	Mississippi	Tuscaloosa Marine Shale	10661–10662	876
S14	USA	Mississippi	Tuscaloosa Marine Shale	10654.8	962
S15	USA	Mississippi	Tuscaloosa Marine Shale	10657.2	1197
S16	USA	Mississippi	Tuscaloosa Marine Shale	10659.8	4897
S17	USA	Louisiana	Tuscaloosa Marine Shale	7273.9	7330
S18	USA	Mississippi	Tuscaloosa Marine Shale	10480–10490; 10520–10530	2960
S19	USA	Mississippi	Tuscaloosa Marine Shale	10720–10780; 10840–10870	4452
S20	USA	Mississippi	Tuscaloosa Marine Shale High Resistivity Zone	10370–10400; 10430–10460	3226
S21	USA	Mississippi	Tuscaloosa Marine Shale High Resistivity Zone	10957–10987	3226
S22	USA	Mississippi	Tuscaloosa Marine Shale High Resistivity Zone	12539.5	4380
S23	USA	Mississippi	Tuscaloosa Marine Shale High Resistivity Zone	12484.05	2660
S24	USA	Mississippi	Lower Tuscaloosa	10943	3265
S25	USA	Mississippi	Lower Tuscaloosa	10745	3652

S26	USA	Mississippi	Lower Tuscaloosa	11089	5986
S27	USA	Mississippi	Lower Tuscaloosa	12305	4398
S28	USA	Mississippi	Lower Tuscaloosa	11068	8162
S29	USA	Mississippi	Lower Tuscaloosa	14237.2	723
S30	USA	Mississippi	Lower Tuscaloosa	14231.3	4380
S31	USA	Mississippi	Lower Tuscaloosa	13090.9–13091.1	5986

Table A- 2: MICP data from the Otway Basin (Goldie Divko, 2019)

Sample No./ID	Country	Basin	Stratigraphic unit / Formation	Well/Borehole	Sample depth (m)	MICP laboratory data - Threshold pressure (psi)
1	Australia	Otway	Belfast Mudstone	Belfast-11	1326.2	2695
2	Australia	Otway	Paaratte Formation	Drik Drik-1	999.7	2194
3	Australia	Otway	Nullawarre Greensand	Sherbrook-1	1096.6	7301
4	Australia	Otway	Belfast Mudstone	Iona-4	1382.5	4095
5	Australia	Otway	Belfast Mudstone	Flaxmans-1	1815.3	9795
6	Australia	Otway	Belfast Mudstone	Flaxmans-1	1944.3	9549
7	Australia	Otway	Belfast Mudstone	Flaxmans-1	1943.1	9563
8	Australia	Otway	Flaxman Formation	Flaxmans-1	2021.4	6284
9	Australia	Otway	Belfast Mudstone	Koroit-10	1163.7	635
10	Australia	Otway	Skull Creek Mudstone	Koroit-10	1110.6	5396
11	Australia	Otway	Flaxman Formation	Cooriejong-2	871.7	5606
12	Australia	Otway	Belfast Mudstone	Nirranda-6	1678.5	5849
13	Australia	Otway	Belfast Mudstone	Nirranda-6	1633.7	4525
14	Australia	Otway	Flaxman Formation	Nirranda-3	1623.9	1142
15	Australia	Otway	Belfast Mudstone	Nirranda-3	1580.9	6208
16	Australia	Otway	Belfast Mudstone	Nirranda-3	1501.4	10067
17	Australia	Otway	Paaratte Formation	Annya-2	731.8	1784
18	Australia	Otway	Belfast Mudstone	Belfast-4	1417.3	3990
19	Australia	Otway	Paaratte Formation	Laang-1	1023.5	578
20	Australia	Otway	Belfast Mudstone	Port Campbell-2	2163.7	8792
21	Australia	Otway	Flaxman Formation	Brucknell-2	1265.5	3009
22	Australia	Otway	Flaxman Formation	Waarre-1	976.2	567
23	Australia	Otway	Waarre Formation	Waarre-1	1022.9	4045
24	Australia	Otway	Belfast Mudstone	Narrawaturk-2	1515.7	5917
25	Australia	Otway	Waarre Formation	Narrawaturk-2	1623.6	2060

26	Australia	Otway	Waarre Formation	Nullawarre-3	1557.8	90.4
27	Australia	Otway	Belfast Mudstone	Nullawarre-3	1542.2	1786
28	Australia	Otway	Paaratte Formation	Mepunga-7	1018	804
29	Australia	Otway	Paaratte Formation	Codrington-1	1095.1	2397
30	Australia	Otway	Belfast Mudstone	Port Campbell-4	1404.5	5656
31	Australia	Otway	Paaratte Formation	Werrikoo-1	947.9	785
32	Australia	Otway	Paaratte Formation	Cobboboonee-5	1768.1	397
33	Australia	Otway	Paaratte Formation	Homerton-3	1271.9	2644
34	Australia	Otway	Paaratte Formation	Yambuk-2	1233.8	825
35	Australia	Otway	Paaratte Formation	Wangoom-6	991.2	704
36	Australia	Otway	Nullawarre Greensand	Pretty Hill-1	833.3	1977
37	Australia	Otway	Eumeralla Formation	Wilkin-2	384	7.2
38	Australia	Otway	Skull Creek Mudstone	Malanganee-4	1549	4694
39	Australia	Otway	Belfast Mudstone	North Paaratte-2	1442	1201.4
40	Australia	Otway	Belfast Mudstone	Wallaby Creek-1	1420	565
41	Australia	Otway	Belfast Mudstone	Grumby-1	1599	637
42	Australia	Otway	Belfast Mudstone	Iona-6	1473	1021
43	Australia	Otway	Nullawarre Greensand (caving)	Iona-6	1485	8.19
44	Australia	Otway	Belfast Mudstone	Mylor-1	1620	446
45	Australia	Otway	Belfast Mudstone	Fenton Creek-1	1500	6.39
46	Australia	Otway	Belfast Mudstone	Iona Obs-1	1443	1914.87
47	Australia	Otway	Belfast Mudstone	Iona Obs-1	1449	5.77
48	Australia	Otway	Belfast Mudstone	Halladale-1 DW-1	1580	332.8
49	Australia	Otway	Belfast Mudstone	Dunbar-1	1470	774.69
50	Australia	Otway	Eumeralla Formation	Brucknell-2	1371.6	3257.53
51	Australia	Otway	Nullawarre Greensand	Brucknell-2	1212.5	18.4
52	Australia	Otway	Nullawarre Greensand	Mepunga-7	1040.3	346

53	Australia	Otway	Nullawarre Greensand	Nirranda-6	1576.7	6.68
54	Australia	Otway	Skull Creek Mudstone	Nirranda-6	1493.8	919.7
55	Australia	Otway	Skull Creek Mudstone	Nirranda-6	1439.8	1708
56	Australia	Otway	Paaratte Formation	Bootahpool-2	1026.8	49.8
57	Australia	Otway	Paaratte Formation	Yangery-1	828.4	1484
58	Australia	Otway	Nullawarre Greensand	Nullawarre-3	1510.6	3.48
59	Australia	Otway	Belfast Mudstone	Port Campbell-2	1627.6	7957
60	Australia	Otway	Eumeralla Formation	Mepunga-10	1827.2	12003
61	Australia	Otway	Paaratte Formation	Wangoom-2	922.3	15.3
62	Australia	Otway	Paaratte Formation	Wangoom-6	951.5	568
63	Australia	Otway	Nullawarre Greensand	Sherbrook-1	1026.5	25.56
64	Australia	Otway	Paaratte Formation	Tyrendarra-13	1263	333
65	Australia	Otway	Nullawarre Greensand	Waarre-1	932.6	13.86
66	Australia	Otway	Skull Creek Mudstone	Fergusons Hill-1	479.7	136.3
67	Australia	Otway	Nullawarre Greensand	Fergusons Hill-1	540.4	24.7
68	Australia	Otway	Belfast Mudstone	Fergusons Hill-1	616.3	417.3
69	Australia	Otway	Eumeralla Formation	Mepunga-7	1104.6	57.1
70	Australia	Otway	Eumeralla Formation	Fergusons Hill-1	1139	1077
71	Australia	Otway	Pebble Point Formation	Waarre-1	468.8	58.1
72	Australia	Otway	Eumeralla Formation	Pretty Hill-1	1410	4892
73	Australia	Otway	Pretty Hill Formation	Casterton-1	1709.9	14719
74	Australia	Otway	Eumeralla Formation	Casterton-1	616.6	4408
75	Australia	Otway	Laira Formation	Heathfield-1	1945.8	10045
76	Australia	Otway	Eumeralla Formation	Yangery-1	1318.9	53
77	Australia	Otway	Eumeralla Formation	Annya-2	805.3	3475
78	Australia	Otway	Eumeralla Formation	Mepunga-10	1829.1	10718
79	Australia	Otway	Eumeralla Formation	Laang-1	1179.9	15

Table A- 3: MICP data from organic rich Devonian shales, converted to psi (Mastalerz et al., 2021)

Country	State	Stratigraphic unit / Formation	Entry Pressure (Po, psi)	Injection P in psi @ 80% Hg saturation
USA	Ohio	New Albany Shale	61	45687
USA	Ohio	New Albany Shale	18	44527
USA	Ohio	New Albany Shale	8	44237
USA	Ohio	New Albany Shale	19	39450
USA	Ohio	New Albany Shale	56	44237
USA	Ohio	New Albany Shale	29	44962
USA	Ohio	Marcellus Shale	11	44962
USA	Ohio	Pennsylvanian Coal	11	32198
USA	Ohio	Pennsylvanian Coal	15	42641
USA	Ohio	Pennsylvanian Coal	29	44962

Table A- 4: MICP data from outcrop samples in the Naknek Formation, Alaska (from Table 1 (Loveland, 2013)). Threshold pressure is interpreted from Figure 1 of the original reference based on 10% Hg saturation criteria

Sample No./ID	Country	Location	Stratigraphic unit / Formation	Air/Mercury Capillary Entry Pressure (psia)	Injection P in psi @ 90% Hg saturation
12MAW100-51.6d	USA	Lower Cook Inlet	Naknek Formation	11.8	~30
12MAW100-105b	USA	Lower Cook Inlet	Naknek Formation	22.2	~55
12MAW105b	USA	Lower Cook Inlet	Naknek Formation	964	~3000
12MAW106-1.3b	USA	Lower Cook Inlet	Naknek Formation	59.6	~200
12MAW106-2.9b	USA	Lower Cook Inlet	Naknek Formation	964	~2400
12MAW106-4.0b	USA	Lower Cook Inlet	Naknek Formation	229	~600
12MAW114b	USA	Lower Cook Inlet	Naknek Formation	65.2	~200
12MAW114e	USA	Lower Cook Inlet	Naknek Formation	328	~800
12MAW115b	USA	Lower Cook Inlet	Naknek Formation	9.04	~35

Table A- 5: MICP data from CO2CRC wells (select data) - originally Table 6.3, from (Cook, 2014)

Sample No./ID	Country	Basin	Stratigraphic unit / Formation	Well/Borehole	Sample depth (m)	MICP laboratory data - Threshold pressure (psi)
CRC-2-930.63	Australia	Otway	Pember Mudstone	CRC-2	930.63	1410
CRC-1-933.18	Australia	Otway	Pember Mudstone	CRC-1	933.18	1436
CRC-2-1321.25	Australia	Otway	Paaratte Formation	CRC-2	1321.25	698
CRC-2-1322.73	Australia	Otway	Paaratte Formation	CRC-2	1322.73	1432
CRC-2-1323.89	Australia	Otway	Paaratte Formation	CRC-2	1323.89	2472
CRC-2-1328.89	Australia	Otway	Paaratte Formation	CRC-2	1328.89	5976
CRC-2-1330.56	Australia	Otway	Paaratte Formation	CRC-2	1330.56	2932
CRC-2-1434.7	Australia	Otway	Paaratte Formation	CRC-2	1434.7	2922
CRC-2-1448.58	Australia	Otway	Paaratte Formation	CRC-2	1448.58	1433
CRC-2-1481.46	Australia	Otway	Paaratto Formation	CRC-2	1481.46	4986
CRC-2-1485.39	Australia	Otway	Paaratte Formation	CRC-2	1485.39	85
CRC-2-1491.43	Australia	Otway	Paaratte Formation	CRC-2	1491.43	340
CRC-2-1523.1	Australia	Otway	Skull Creek Formation	CRC-2	1523.1	1426

Table A- 6: MICP data from the Lower Muschelkalk (from Table 1 and Table 2 of (Müller-Huber et al., 2018)). Dominant average pore throat size presented

Sample No./ID	Country	Basin	Stratigraphic unit / Formation	MICP rt [µm]	Lithology
R 2/1	Germany	Central European	Lower Muschelkalk	0.071	Marly/micritic Wellenkalk
R 3/1	Germany	Central European	Lower Muschelkalk	0.032	Marly/micritic Wellenkalk
R 4/1	Germany	Central European	Lower Muschelkalk	0.112	Marly/micritic Wellenkalk
R 7/1	Germany	Central European	Lower Muschelkalk	0.838	Micritic Schaumkalk
R 11/2	Germany	Central European	Lower Muschelkalk	0.662	Micritic Schaumkalk
R 14/1	Germany	Central European	Lower Muschelkalk	0.715	Oomoldic Schaumkalk
R 15/2	Germany	Central European	Lower Muschelkalk	0.795	Oomoldic Schaumkalk
R 16/1	Germany	Central European	Lower Muschelkalk	2.41	Oomoldic Schaumkalk
R 20/2	Germany	Central European	Lower Muschelkalk	3.79	Oomoldic Schaumkalk
R 21/1	Germany	Central European	Lower Muschelkalk	0.747	Oomoldic Schaumkalk

Appendix B.Monitoring Technologies (from IEAGHG 2020-01 Table 2-3)

Table B- 1: Monitoring Technologies (from IEAGHG 2020-01 Table 2-3)

Name	Description	Monitored Zone	Equipment	Pre-/Post Processing requirements	Frequency	Domain	Accuracy/ Resolution	TRL/Field Applications	General TRL Rating (DoE and Euro TRL mapping)	Coverage	Unit Costs	Risk Category	Advantages	Limitations
2D surface seismic	2D linear image for site characterization and time-lapse monitoring to survey potential changes due to CO2 injection	Surface/Near-Surface/Reservoir	Seismic sensors, source arrays, and sources (vibrator trucks/vibrator systems)	Baseline surveys, geocharacteriztion, and multiple data processing events	Frequency dependent on monitoring plan	X, Z	1 – 5m	Specialized, research oriented	5	50m-1 km	$1.0M/km	Capacity, Containment, Contingency, Mitigation	Site characterization prior to injection and time-lapse monitoring to survey potential changes due to CO2 injection. Identification of potential fractures and faults in the subsurface.	small scale faults with offsets >10 m are not detectable, lacks full surface coverage
3D surface seismic	3D data on storage and reservoir characterization and time-lapse monitoring to survey CO2 distribution and migration	Surface/Near-Surface/Reservoir	Seismic sensors, source arrays, and sources (vibrator trucks/vibrator systems)	Baseline surveys, geocharacteriztion, and multiple data processing events	Frequency dependent on monitoring plan	X,Y, indirectZ	1 – 5m	Specialized, research oriented	5	1-100 km2	$1.0M/km2	Capacity, Containment, Contingency, Mitigation	Full site characterization of overburden and storage zones. Monitor CO2 migration in the well Identification of potential fractures and faults in the subsurface.	small scale faults with offsets >10 m are not detectable, requires extensive data processing
Airborne EM	Air surveys to detect electrical conductivity variations in earth materials as indicator of CO2	Surface/Near-Surface: Soil, intermediate zones	Airplane, EM coil array	Baseline, post injection, processing & interpretation of difference	Annual or greater	XY	10-50% change, 100s sq. meters perturbations	Specialized, research oriented	5	10s-100s km2	$10K/survey	Contingency, Mitigation, Public Acceptance	Covers large area, non-invasive	Limited depth penetration to 100s of meters, requires large CO2 storage plume
Airborne spectral imaging	Air surveys to detect spectral signal vegetative stress as indicator of CO2 leakage from the ground	Atmospheric/Surface: Soil, atmosphere	Airplane survey, hyperspectral imager	Baseline, post injection, processing & interpretation of difference	Annual or greater	XY	10-50% change, 100s sq. meters	Specialized, research oriented	4	10s-100s km2	$10K/survey	Contingency, Mitigation, Public Acceptance	Covers large area, non-invasive	Natural CO2 variations, false positives
Annulus Pressure testing	Tests designed to pressure annuls space and measure pressure drop to ensure well integrity and prevent casing leaks	Near-Surface/Reservoir: Wellbore system	Pressure gauge on wellhead	Simple test	Annual	Z (well system)	Usually 5-10% pressure drop over several hours	Mature, common	8	Point	$1k/test	Contingency, Mitigation	Direct test, low-cost	Limited to well system, not continuous test
Boomer/Sparker profiling	2D sub-bottom water profiling used for site characterization and to detect changes due to injected CO2	Surface/Near-Surface/Reservoir	Vessel, source/hydrophone array, ship explosives, vessel and crew	Baseline, post injection, processing & interpretation of difference	Initial, annual or greater	X, Z	0.2 - 1m	Mature, common	7	20-750 m	$1.0M/km	Capacity, Containment, Contingency, Mitigation	Provides continuous mapping of shallow sediment layers, structural changes due to CO2 migration and leakage, high peak frequencies and large bandwidth for higher resolution	Limited tow capability, high voltage/high current, boomer plates are large and constrain towing
Borehole EM	Images changes in electrical resistivity signal from induction source and receiver array due to saturation changes between wells or shallow soil zone	Surface/Near-Surface/Reservoir	At least two wells with string array of electrodes attached to well casing	Baseline, post injection, processing & interpretation of difference	Continuous, annual or greater	XZ (interwell)	10-50% change, square meter resolution	Specialized, research oriented	5	200-1000 m (interwell)	$200k/km	Capacity, Containment	Focused on reservoir zone, more accurate than some other seismic methods, lower processing	Only covers interwell cross section zone, subject to interpretation, requires high CO2 saturation, non-conductive pipe
Borehole ERT	Images changes in electrical resistivity signal between 2 electrodes due to saturation changes between wells or shallow soil zone	Surface/Near-Surface/Reservoir	Electric source, downhole receiver array, at least 2 wells	Baseline, post injection, processing & interpretation of difference	Annual or greater	XZ (interwell)	10-50% change, square meter resolution	Specialized, research oriented	5	100 m (interwell)	$200k/km	Capacity, Containment	Focused on reservoir zone, more accurate than some other seismic methods, lower processing	Only covers interwell cross section zone, requires closely spaced wells, permanent installation, subject to interpretation, requires high CO2 saturation, non-conductive pipe
Bubble stream chemistry	Measures dissolved gases and chemistry of water to detect potential CO2	Surface/Near-Surface: Ground water and seafloor	Vessel or team of sampling units, samples, laboratory testing	Baseline and continuous sampling	Initial and continuous	XYZ	ppm	Mature, common	8	Specified zones and depths	$10K/test	Containment, Contingency, Mitigation	Provides dissolved gas and other chemistry of specific zones of interest. Can determine minor and major leakage.	Frequent sampling is needed to monitor containment of CO2 . Does not measure over an entire area so several samples from different locations are necessary for analysis.
Bubble stream detection	High frequencies used to measure seafloor and create acoustic images of seafloor to determined potential pits created by CO2 leakage	Surface: Seafloor	Vessel, echosounders, processing	Baseline, post injection, processing & interpretation of difference	Initial, annual or greater	X Z	1-5m	Mature	7	50 m	$750k/km	Containment, Contingency, Mitigation	Detailed high images created of seafloor which can detect deformation changes and density changes due to CO2	Extensive seafloor mapping required in order to example baseline and repeat data. Minor leaks can go undetec+B16:O17ted due to resolution of technology
Casing Inspection logs	Downhole survey of well materials for indication of defects	Surface/Near-Surface/Reservoir: Wellbore system	Caliper, flux, sonic, EM, or noise logging tool	Processing and interpretation of results	Annual or greater	Z (well system)	+/- 1 m within well	Mature, common	8	Well	$10k/well	Containment	Straight forward test, can show precursors of corrosion, failure	Periodic test, well must be shut-in, interupts operations
Casing pressure monitoring	Monitoring pressure on casing annulus for casing leaks	Surface/Near-Surface/Reservoir: Wellbore system	Annulus pressure system and pressure gauge	Direct monitoring	Continuous	Z (well system)	0.01 Mpa	Mature, common	8	Well	$10k/well	Containment	Direct test, low-cost, often regulatory requirement	Limited to well system, does not provide location of defect
Cement bond logging	Acoustic log that provides evaluation of cement/casing to measure well integrity and zone isolation	Surface/Near-Surface/Reservoir: Wellbore system	Wireline vendor and service rig	Baseline, post injection, processing	Initial, annual or greater	Z (cement/casin g)	3 cm	Mature, common	8	15 cm	$10k/well	Containment	Simple quantitative method for analyzing cement quality and inferring compressive strength	Limited to only evaluating cement bonding to the casing. Does not provide imaging between cement and formation. Does not evaluate low density cement.
Corrosion Monitoring (well materials)	Inspection and/or corrosion tickets in wells to detect any corrosion of well materials	Surface/Near-Surface/Reservoir: Wellbore system	Coupons, mechanical, ultrasonic, and electromagnetic tools	Interpretation of results	Annual or greater	Z (well system)	+/- 1 m within well	Mature, common	4	Well	$10k/well	Containment	Straight forward test, can show precursors of corrosion, failure	Periodic test, well must be shut-in, interupts operations
Crosswell Seismic	Inter-well seismic profiling to measure structural changes due to CO2 injection	Surface/Near-Surface/Reservoir: Between wellbores	Wireline vendor, service rig, source and receiver arrays	Baseline survey, processing of periodic surveys to show difference	Yearly	X, Z	1 – 5m	Specialized, research oriented	5	0.5-1 km	$200k/km	Capacity, Containment, Contingency, Mitigation	Subsurface monitoring of injection of CO2 plumes. Estimate rock and fluid properties. Identification of potential fractures and faults in the subsurface.	Source strength is limited by the distance between wellbores. Presence of gas in the well can reduce detection of CO2 . Geologic complexity and noise interferences can degrade seismic data. The maximum distance between wells is dependent on casing.
Distributed Acoustic Sensing	Laser light pulses from permeant downhole fiber optic cables seismic profiling that measures reservoir and caprocks to determine structural changes due to CO2 injection and reservoir integrity	Surface/Near-Surface/Reservoir: Proximal to wellbore	Vendor, fiber optics, permeant onsite data acquisition	Continuous	Continuous	XYZ	10m	Specialized, research oriented	5	4-5 km (depending on receivers)	$500K Well	Capacity, Containment, Mitigation	Provides continuous monitoring of the well site and can be used to detect changes due to CO2 injection	A large amount of data is produced from this technology and requires extensive and costly processing. Can cause integrity issues if not installed correctly
Distributed Temperature Sensing	Linear fiber optic cables that measures changes in temperature to detect/monitor temperature indicators of CO2	Surface/Near-Surface/Reservoir: Proximal to wellbore	Vendor, fiber optics, permeant onsite data acquisition	Continuous	Continuous	XYZ	0.01 - 0.05 °C	Specialized, research oriented	5	3 km	$500K Well	Containment, Mitigation	Provides continuous temperature monitoring and migration CO2	A large amount of data is produced from this technology and requires extensive and costly processing. Can cause integrity issues if not installed correctly
Downhole fluid chemistry	Provides fluid chemistry from reservoir zones to determine CO2 migrations and analyze reservoir conditions	Reservoir	Wireline/slickline vendor with bailer, laboratory services	Baseline and regular repeat sampling, laboratory testing	Initial and quarterly to annual	X (Target Interval)	ppm for entire reservoir interval	Mature, common	8	Entire sampled interval	$10k/well	Containment, Contingency, Mitigation	Formation fluids can be collected directly from the zone of interest	Fluid sampling in high risk wells is a potential hazard, fluid around sampler may be in two-phase condition, mechanical failure of sampler due to pressures and fluid present
Downhole pressure/temperature	Continuous temperature and pressure measurements to monitor reservoir integrity and CO2 migration	Reservoir	Wireline/slickline vendor with bailer, laboratory services	Direct monitoring	Continuous	X (Target Interval)	+/- 0.25 °C 0.005 °C	Mature, common	8	25 cm	$10k/well	Injectivity, Containment, Contingency, Mitigation	Continuous inplace monitoring, batteries can potentially last up to a year	Gaskets can corrode over time and cause gauge malfunctioning,

Name	Description	Monitored Zone	Equipment	Pre-/Post Processing requirements	Frequency	Domain	Accuracy/ Resolution	TRL/Field Applications	General TRL Rating (DoE and Euro TRL mapping)	Coverage	Unit Costs	Risk Category	Advantages	Limitations
Ecosystems studies	Survey of vegetation for stress or damage caused by CO2 leakage	Atmospheric/Surface: Soil, atmosphere	Visual survey, inspection, flyover of CO2 storage area	Baseline survey, regular repeat surveys	Quarterly to Annual	XY	Indirect, sq. meters	Mature, common	7	Km2s	$1000s/km2	Contingency, Mitigation, Public Acceptance	Low impact technology, non-invasive, simple	Requires significant CO2 migration to detect leakage, not suitable for areas without vegetation, qualitative
Eddy covariance	Measurement of air flow and CO2 concentrations to detect CO2 leakage at the surface	Atmosphere	Stationary or mobile observation towers	Baseline, post injection, processing & interpretation of difference	Continuous	XY	umol/m2*s	Specialized, research oriented	8	100 sq meters to sq kilometers	$10,000s/ point	Contingency, Mitigation, Public Acceptance	Low impact technology, non-invasive, can cover wide areas, high visibility	Natural CO2 variations, false positives, sensitive to humidity, temperature
Electric Spontaneous Potential	Measures mineral and clay compositions, and can show porosity mineralogical changes near wellbore which can be used to indicate potential wellbore integrity	Reservoir: Wellbore	Wireline vendor and service rig	Baseline, well schematics and geochemistry, post injection, processing & interpretation of difference	Initial and quarterly to annual	X, Z (wellbore)	±6%	Mature, common	5	30 - 40 cm	$60k/well	Capacity, Containment	Measures mineral and clay compositions, and can show porosity mineralogical changes near wellbore which can be used to indicate potential wellbore integrity	high clay and salinities are necessary for optimal functionality of the tool
Fluid geochemistry	Fluid measurements to determine rock-CO2 interactions, monitor CO2 migration and storage integrity/breach of CO2	Reservoir: Wellbore	Wireline vendor and service rig	Baseline and regular repeat sampling, laboratory testing	Initial and quarterly to annual	X (Target Interval)	ppm for entire reservoir interval	Mature, common	8	Entire sampled interval	$20k/well	Capacity, Containment, Contingency, Mitigation	Formation fluids can be collected directly from the zone of interest or at the wellhead to analyze multiple zones of interest and	Fluid sampling in high risk wells is a potential hazard, fluid around sampler may be in two-phase condition, mechanical failure of sampler due to pressures and fluid present
Geophysical Density Logs	Measures wellbore densities to determine lithology and potential, changes and identifies CO2 breakthrough and is used to analyze wellbore integrity	Surface/Near-Surface/Reservoir: Wellbore	Wireline vendor and service rig	Baseline survey	Initial	X, Z	1 g/cm^{3}	Mature, common	5	25 cm	$50k/well	Capacity, Containment	Measures densities to determine lithology changes near wellbore which can be used to indicate potential wellbore integrity	susceptible to borehole rugosity/washouts and types of drilling muds. Erroneous lithology data due to averages between drastically different density lithology changes
Geophysical Pulse Neutron Capture logs	Measures wellbore fluid saturation (oil/gas/water), changes and identifies CO2 breakthrough and is used to analyze wellbore integrity	Surface/Near-Surface/Reservoir: Wellbore	Wireline vendor and service rig	Baseline, well schematics and geochemistry, post injection, processing & interpretation of difference	Initial and quarterly to annual	X, Z (wellbore)	±6%	Mature, common	5	30 - 40 cm	$50k/well	Capacity, Containment	Fluid saturation of cased wells, porosity indicator, can show porosity changes near wellbore which can be used to indicate potential wellbore integrity	Fluid behind casing, cannot differentiate between various gases, high porosities and salinities are necessary for optimal functionality of the tool
Global Positioning System	Satellite technique that provides epochs with displacement measurements for ground deformation related to CO2 storage	Surface/Near-Surface	Receiver, GPS antenna, power supply, pseudolites, pressure gauges, and satellite system	Baseline survey, periodic surveys	Monthly-Yearly	X,Y, indirect	mm-scale	Mature, research oriented	7	10s-100s km2	$1k/km2	Containment, Mitigation, Public Acceptance	Measures displacement in proximity or area of CO2 reservoir	Temporal sampling may be limited, land use and access, atmospheric effects, satellite orbit coverage
Ground penetrating radar	Geophysical method that processes reflection of high freq. radio waves to image features in the shallow subsurface	Surface/Near-Surface: Shallow soil and groundwater	GPR system (source/cart, data logger, software) and/or crosswell groundwater wells	Baseline survey, operational survey, post-injection, processing/interpretation of raw GPR results	Yearly	XZ (shallow GW)	Indicator of CO2 through CO2 desaturation	Mature, moderately common	8	km2s	$10,000s/km2	Contingency, Mitigation, Public Acceptance	Low impact technology, non-invasive	Requires significant CO2 migration to detect leakage, may be subject to interpretation bias, not suitable for low CO2 levels, limited to ~15 m depth, certain sediments affect accuracy
Groundwater monitoring	Sampling and analysis of shallow groundwater wells for indicators of CO2 leakage and/or brine displacement	Surface/Near-Surface: Shallow groundwater quality	Shallow gw wells, sampling equipment, lab analysis	Baseline samples, interpretation of gw quality indicators,	Monthly-Yearly	Z (shallow GW)	mg/L or greater	Mature, common	8	km2s	$1000s/event	Containment, Contingency, Mitigation, Public Acceptance	Direct monitoring of groundwater resources, high visibility monitoring, easy to communicate to stakeholders, understandable results	Relies on indicators of CO2 (pH, anions, cations, alk., TDS), false positives, needs good baseline data, may require significant CO2 migration to detect leakage
High resolution acoustic imaging	Acoustic full-waveform sonic to measures and images structural features and changes that occur due to CO2 injection	Reservoir: Wellbore	Wireline vendor and service rig	Baseline survey, regular repeat surveys	Frequency dependent on monitoring plan	X, Z (wellbore)	15 cm	Mature, moderately common	5	3 m	$50K/well	Containment, Contingency, Mitigation	Direct imaging and monitoring of borehole structures and changes due to CO2 injection	susceptible to borehole rugosity/washouts which will create poor quality images.
Land EM	Electrical resistivity signals used to measure from induction source and receiver array due to CO2 saturation between wells or shallow soil zone	Surface/Near-Surface/Reservoir: Reservoir or soil	At least two wells with string array of electrodes attached to well casing	Baseline, post injection, processing & interpretation of difference	Continuous, annual or greater	XZ (interwell)	10-50% change, square meter resolution	Specialized, research oriented	5	200-1000 m (interwell)	$100ks/survey	Capacity, Containment, Contingency	Focused on reservoir zone, more accurate than some other seismic methods, lower processing	Only covers interwell cross section zone, subject to interpretation, requires high CO2 saturation, non-conductive pipe
Land ERT	Electrical resistivity measurements to determine changes in structure and water saturations due to CO2 injection	Surface/Near-Surface/Reservoir: Ground water and subsurface	Seismic sensors, source arrays, and sources (vibrator trucks/vibrator systems)	Baseline surveys, geocharacteriztion, and multiple data processing events	Frequency dependent on monitoring plan	X, Z	1 – 5m	Specialized, research oriented	5	Dependent on arrays, lithology, and depth of investigation	$100ks/survey	Capacity, Containment, Contingency	Site characterization prior to injection and time-lapse monitoring to survey potential changes due to CO2 injection. Identification of potential fractures and faults in the subsurface.	small scale faults feature offsets >10 m are not detectable, lacks full surface coverage
Long-term downhole pH	Optical sensors in casing that measures chemical changes due to CO2 changes	Surface/Near-Surface/Reservoir: Wellbore	Vendor, fiber optics, permeant onsite data acquisition	Continuous	Continuous	X,Z	.01 unit	Specialized, research oriented	5	30 - 40 cm	$100K/well	Containment, Contingency, Mitigation	Provides continuous pH monitoring and migration CO2, works in highly saline waters, good for high pressure and temperature environments	This is a near wellbore technology and provides data within specified installation zone.
Microseismic/Seismic Activity Monitoring	Passive technique for monitoring and identifying downhole fractures and microseismic events	Surface/Near-Surface/Reservoir: Reservoir and above	Borehole geophones, monitoring station, solar charge panels, strong-motion-sensor	Baseline survey, analysis of data to estimate location of seismic event	Continuous	X, Y, Z seismic activity	500m	Mature, moderately common	7	5-20 km2	$250K/km2	Containment, Contingency	Can monitor fracture properties from downhole, surface to subsurface. Time-lapse monitoring to survey migration of CO2 plumes. Identification of potential fractures and faults in the subsurface.	Moderate changes in dip perturbation or velocity changes can cause errors in velocity models. Low and high frequency signals can affect mechanism inversion.
Multibeam echo sounding	Sonar emitted by a vessel that measures distances and topography of the seafloor to determine surface changes due to CO2	Surface/Near-Surface/Reservoir: Seafloor	Vessel, sonic source, hydrophones, antenna	Baseline, post injection, processing & interpretation of difference	Initial, annual or greater	X, Y Z	0.2 - 1m	Mature	7	20-750 m	$250K/m2	Containment, Contingency	Provides continuous mapping of shallow sediment layers, structural changes due to CO2 migration and leakage	Minor deformation is not detected due to resolution limitations.
Multicomponent surface seismic	3D compressive and shear waves use to measure fluid changes and structural monitoring to survey CO2 distribution and migration	Surface/Near-Surface/Reservoir: Reservoir and above	Seismic sensors, source arrays, and sources (vibrator trucks/vibrator systems)	Baseline surveys, geocharacteriztion, and multiple data processing events	Frequency dependent on monitoring plan	X,Y, indirect	1 – 5m	Specialized, research oriented	7	Dependent on arrays, lithology, and depth of investigation	$750K/km	Containment, Contingency	Full site characterization of overburden and storage zones. Monitor CO2 migration in the well Identification of potential fractures and faults in the subsurface.	small scale faults with offsets >10 m are not detectable, requires extensive data processing
Non dispersive IR gas analysers	Gas meter that measures CO2 concentrations in air based on IR spectroscopy	Atmosphere	Gas meter, data logger system	None	Continuous	XY	PPM	Mature, common	8	100 sq meters	$100s/pt	Containment, Contingency, Public Acceptance	Direct measurements, simple technology, high visibility, easy to communicate	Natural CO2 variations, false positives
Operational Monitoring	CO2 injection flow rates, pressure, temperature, density, composition monitoring	Reservoir	Gauges and flowmeters	Direct measurements	Continuous	Point	0.1 psi, BBL/Min	Mature, common	8	Point	$10k/pt	Capacity, Injectivity	Monitor injection performance for pressure drops and flow variations	Limited to injection well
Produced Gas/Fluid Analysis	Gas/fluid sampling & analysis to determine CO2 interactions, monitor CO2 migration and storage integrity	Reservoir: Wellbore	Coriolis meter, laboratory testing	Baseline and regular repeat sampling, laboratory testing	Initial and quarterly to annual	X (Target Interval)	ppm for entire reservoir interval	Mature, common	8	Entire sampled interval	$20k/well	Containment, Contingency, Mitigation	Formation samples can be collected directly from the zone of interest or at the wellhead to analyze multiple zones of interest	Fluid sampling in high risk wells is a potential hazard, fluid around sampler may be in two-phase condition, mechanical failure of sampler due to pressures and fluid present
Satellite interferometry/INSAR	Satellite-based technique that provides topographic images of site surface area to measure surface deformation	Surface/Near-Surface	Satellite, reflector stations	Baseline survey, multiple satellite passes for survey verification	Monthly-Yearly	X,Y, indirect	mm-scale	Mature, research oriented	5	10s-100s km2	$10k/km2	Containment, Contingency,	Monitoring injection of CO2 in the subsurface at carbon sequestration test sites.	Level terrain, minimal land use, atmospheric effects, and satellite orbit coverage
Seabottom EM	Images changes in electrical resistivity signal from induction source and receiver array measures surface changes due to CO2	Surface/Near-Surface	Vessel, source and several receiver strings	Baseline, post injection, processing & interpretation of difference	Continuous, annual or greater	XYZ	10-50% change, square meter resolution	Mature, common	7	20-750 m	$500K/km	Containment, Contingency	Provides continuous mapping of seafloor structural changes due to CO2 migration and leakage, high peak frequencies and large bandwidth for higher resolution	Limited tow capability, high voltage/high current and constrain towing

Name	Description	Monitored Zone	Equipment	Pre-/Post Processing requirements	Frequency	Domain	Accuracy/ Resolution	TRL/Field Applications	General TRL Rating (DoE and Euro TRL mapping)	Coverage	Unit Costs	Risk Category	Advantages	Limitations
Seabottom gas sampling	Sampling at the sediment-seawater interface to measure density changes due to CO2	Surface/Near-Surface: Sediment/water Interval	Sampling units, samples, laboratory testing	Baseline and continuous sampling	Initial and continuous	X	ppm	Mature, common	7	Specified intervals	$20k/survey	Containment, Contingency, Mitigation,	Provides dissolved gas and other chemistry of specific zones of interest. Can determine minor and major leakage.	Frequent sampling is needed to monitor containment of CO2 . Does not measure over an entire area so several samples from different locations are necessary for analysis.
Seawater chemistry	Measures temperature, pressure and chemistry of water to detect changes due to CO2	Surface/Near-Surface: Seafloor	Vessel or team of sampling units, samples, laboratory testing	Baseline and continuous sampling	Initial and continuous	Point	ppm	Mature, common	7	Specified zones and depths	$20k	Containment, Contingency, Mitigation	Provides dissolved gas and other chemistry of specific zones of interest. Can determine minor and major leakage.	Frequent sampling is needed to monitor containment of CO2 . Does not measure over an entire area so several samples from different locations are necessary for analysis.
Sidescan sonar	Sonar emitted from autonomous underwater vehicles that measure distances and topography of the seafloor to determine surface changes due to CO2	Surface/Near-Surface: Seafloor	Vessel, AUV, echosounders	Baseline, post injection, processing & interpretation of difference	Initial, annual or greater	X, Y Z	0.2 - 1m	Mature	7	20-750 m	$500K/km	Containment, Contingency	Provides continuous mapping of shallow sediment layers, structural changes due to CO2 migration and leakage, high peak frequencies and large bandwidth for higher resolution	Minor deformation is not detected due to resolution limitations.
Single well EM	Images changes in electrical resistivity signal from induction source and receiver array due to CO2 saturation proximal well or shallow soil zone	Surface/Near-Surface/Reservoir: Reservoir or soil	One well with string array of electrodes attached to well casing	Baseline, post injection, processing & interpretation of difference	Continuous, annual or greater	XZ (interwell)	10-50% change, square meter resolution	Specialized, research oriented	5	200-1000 m (interwell)	$100ks/survey	Capacity, Containment, Contingency	Focused on reservoir zone, more accurate than some other seismic methods, lower processing	Only covers interwell cross section zone, subject to interpretation, requires high CO2 saturation, non-conductive pipe
Soil gas concentrations	Monitoring of soil gas composition todetect increases in CO2 levels or other indicators of CO2 leakage	Surface/Near-Surface: Shallow soil zone	Soil gas monitoring points, gas collection equipment, analytical lab services	Baseline, post injection, processing & interpretation of difference	Monthly-annual	XY	PPM	Mature, common	7	100 sq meters to sq kilometers	$1,000s/pt	Containment, Contingency, Mitigation,	Direct measurements, simple technology, high visibility, easy to communicate	Natural CO2 variations, false positives
Surface gas flux	Monitoring CO2 flux and chemistry as indicator of CO2 leakage from reservoir	Surface/Near-Surface: Shallow soil zone	Gas flux chambers, gas collection equipment, analytical lab services	Baseline, post injection, processing & interpretation of difference	Monthly-annual	XY	mmol/m2/s	Mature, common	7	100 sq meters to sq kilometers	$1,000s/pt	Public Acceptance Containment, Contingency, Mitigation	Direct measurements, simple technology, high visibility, easy to communicate	Natural CO2 variations, false positives
Surface gravimetry	Surface survey of gravimetric changes caused by CO2 storage	Reservoir	Gravity survey system or permanent gravity stations	Baseline, post injection, processing & interpretation of difference	Annual or greater	XY	10-50% change	Mature, research oriented	8	10s-100s km2	$1000s/km2	Capacity, Containment	Low impact technology, non-invasive, can cover wide areas, high visibility	Low resolution, requires large volumes of CO2, subject to interpretation
Surface Safety/Gas Meters	CO2 gas meters near surface equipment to monitor releases	Atmosphere	CO2 gas meters	None	Continuous	XY	PPM	Mature, common	8	100 sq meters	$1,000s/pt	Containment, Contigency, Mitigation	Direct measurements, simple technology, high visibility, easy to communicate	Limited to injection site, only provides notice of large equipment failures
Tiltmeters	Inclinometer technology which measures deviation from horizontal and vertical plane	Surface/Near-Surface	Tiltmeter and Monitoring Station	Baseline survey, periodic surveys	Continuous	X,Y, indirect	microradian	Mature, research oriented	7	1-50 km2	$1k/km2	Containment, Contingency, Mitigation	Measure surface deformation in proximity to injection sites	Land access, data collection, spurious changes due to temperature and rainfall
Tracers	Introduction of PFT tracers into injection stream and monitoring in soil gas points for indications of leakage	Atmospheric/Surface: Soil, atmosphere	Soil gas monitoring points, gas collection equipment, analytical lab services	None	Monthly-Annual	XY	Parts per trillion as indicator	Specialized, research oriented	8	100 sq meters to sq kilometers	$10,000s/pt	Containment, Contingency, Public Acceptance	Direct measurements, simple technology, high visibility, easy to communicate	Requires careful sampling, false positives possible, requires significant CO2 migration to detect leakage
Vertical seismic profiling (VSP)	Seismic profiling that images reservoir and caprocks to determine saturation changes due to CO2 injection	Surface/Near-Surface/Reservoir: Proximal to wellbore	Wireline vendor, service rig, source and receiver arrays	Baseline survey, processing of periodic surveys to show difference	Yearly	X, Z	10 – 30m	Specialized, research oriented	5	0.5-1 km	$1.0M/km	Capacity, Containment	Site characterization prior to injection and time-lapse monitoring to survey migration of CO2 plumes. Identification of potential fractures and faults in the subsurface.	Presence of hydrocarbons or high salinity. Must verify that potential historical sites are not damaged during logging. 450 m distance limitation.
Water bottom sediment sampling	Sampling at the seabed sediment for geochemical indicators of CO2	Surface/Near-Surface: Sediment/water Interval	Sampling units, samples, laboratory testing	Baseline and continuous sampling	Initial and continuous	X	ppm	Mature, common	8	Specified intervals	$20k	Containment, Contingency, Mitigation	Provides dissolved gas and other chemistry of specific zones of interest. Can determine minor and major leakage.	Frequent sampling is needed to monitor containment of CO2 . Does not measure over an entire area so several samples from different locations are necessary for analysis.

CO2CRC
Level 3, 289 Wellington Parade South
East Melbourne, Victoria 3002
PO Box 24121, Melbourne, Victoria 3001
p: +61 3 8595 9600
e: info@CO2crc.com.au
www.co2crc.com.au

Partners

CO2CRC acknowledges and appreciates the strong relationships it has with industry, community, government, research organisations, and agencies in Australia and around the world

Industry

Beach Energy

BHP

BP

Chevron Australia

ConocoPhillips

Eni

ExxonMobil

Global CCS Institute

INPEX

J-POWER

KIGAM

LETA

Santos

Sahara Group

Shell Australia

TotalEnergies

Woodside Energy

Government

Australian Government: Department of Education

Australian Government: Department of Industry, Science and Resources

CarbonNet Project

Coal Innovation NSW

NSW: Department of Planning and Environment

Victoria: Department of Jobs, Skills, Industry and Regions

Research

Australian National University

CSIRO

Curtin University

Deakin University

Federation University Australia

Geoscience Australia

Helmholtz Centre Potsdam – GFZ German Research Centre for Geosciences

Lawrence Berkeley National Laboratory (LBNL)

Monash University

Stanford University

The Research Institute of Innovative Technology for the Earth (*RITE*)

University of Adelaide

University of Cambridge

University of Edinburgh

University of Melbourne

University of NSW

University of Wollongong

UK CCS Research Centre

Associate

National Energy Resources Australia (NERA)

IEA Greenhouse Gas R&D Programme

ieaghg.org
+44 (0)1242 802911
mail@ieaghg.org

IEAGHG, Pure Offices, Cheltenham Office Park,
Hatherley Lane, Cheltenham, GL51 6SH, UK

IEAGHG